

**Identification of susceptibility targets of bacterial
leaf blight and development of genome edited rice
lines with increased resistance**

Von der Naturwissenschaftlichen Fakultät
der Gottfried Wilhelm Leibniz Universität Hannover

zur Erlangung des Grades
Doktorin der Naturwissenschaften (Dr. rer. nat.)

genehmigte Dissertation

von

Stefanie Mücke, M.Sc.

2020

Referent: Prof. Dr. rer. nat. Jens Boch
Korreferent: Prof. Dr. rer. hort. Edgar Maiß
Tag der Promotion: 14.09.2020

Zusammenfassung

Pflanzenpathogene *Xanthomonas oryzae* Bakterien infizieren Reis und verursachen hohe Ernteverluste, die eine sichere Lebensmittelversorgung gefährden. *Transcription activator-like effectors* (TALEs) sind Hauptvirulenzfaktoren dieser Pathogene und manipulieren die Genexpression des Wirts zu Gunsten der Infektion. Mithilfe des Programms AnnoTALE können TALEs Klassen zugeordnet werden, die eine enge Verwandtschaft der TALEs zeigen und auf ein mögliches gemeinsames Zielgen hinweisen. Eine Analyse von 34 asiatischen *Xanthomonas oryzae* pv. *oryzae* (Xoo)-Stämmen enthüllte insgesamt 45 TALE-Klassen und einen Basissatz aus 10 TALE Kernklassen, die in mehr als 80% der Stämme vorkommen.

Eine Kombination aus computerbasierten TALE-Zielgen-Vorhersagen und Transkriptomdaten von infiziertem Reis resultierte in 61 TALE-Zielgenkandidaten für die drei selektierten Xoo-Stämme. Repräsentative TALEs dieser Stämme wurde nachgebaut und in einen Xoo-Stamm eingebracht, der keine TALE-Gene trägt, um die Korrelation zwischen einzelnen TALEs und spezifischen, induzierten Genen zu prüfen. Für 13 Reisgene konnte eine TALE-spezifische Induktion nach Infektion nachgewiesen werden. Durch den Einsatz von Reporterassays konnten direkte Interaktionen zwischen den TALEs und ihren Zielpromotoren gezeigt werden. Durch diese neu identifizierten Zielgene konnte eine konvergente Evolution zwischen Xoo und den reispathogenen *Xanthomonas oryzae* pv. *oryzicola* aufgedeckt werden, welche mehr gemeinsame Zielgene besitzen als zuvor angenommen und diese mit verschiedenen TALEs adressieren.

Einzelne TALEs hatten keinen großen Einfluss auf die Virulenz von Xoo in *gain-of-function*-Assays, aber mehrere TALE-Klassen manipulieren vermutlich den Salicylsäurehaushalt, der Xoo-Resistenz in Reis kontrolliert. Reispflanzen wurden mithilfe von CRISPR/Cas9 verändert, um Zielgene auszuknocken oder mehrere TALE-Bindestellen in Zielpromotoren zu mutieren. Initiale Ergebnisse deuten auf eine reduzierte Virulenz von Wildtyp Xoo-Stämmen auf Reispflanzen hin, in denen 7 TALE-Bindestellen von Zielpromotoren mutiert wurden, die in dieser Arbeit identifiziert wurden.

Zusammengefasst konnte ein detailliertes Bild von TALE-manipulierten Pflanzenprozessen etabliert werden, dass unser Verständnis von *Xanthomonas oryzae*-Virulenz signifikant erweitert. Zusätzlich wurde der Grundstein für die Entwicklung neuer Resistenzen gelegt, um diese wichtigen Reiskrankheiten zu bezwingen.

Schlagerworte: Weißblättrigkeit des Reis, Pflanzenbiotechnologie, Pflanzengenetik

Abstract

Phytopathogenic *Xanthomonas oryzae* bacteria infect rice and cause severe harvest loss, which challenges the stable food supply. Transcription activator-like effectors (TALEs) are major virulence factors of these pathogens and manipulate the host gene expression to benefit infection. With the help of the AnnoTALE tool, TALEs can be assigned into classes, which represent closely related TALEs that likely activate the same gene. Analyzing the TALome diversity of 34 Asian *Xanthomonas oryzae* pv. *oryzae* (*Xoo*) strains revealed a total of 45 TALE classes and a common core set of 10 TALE classes present in more than 80% of strains.

Combining computational TALE target gene predictions and transcriptomics data of infected rice produced 61 likely TALE target genes for three selected *Xoo* strains. Representative TALEs of these strains were reconstructed and introduced into a naturally TALE-free *Xoo* strain to verify the correlation between individual TALEs and specific induced genes. 13 genes were shown to be TALE-dependently induced upon infection in rice. Using reporter assays, direct interaction between TALEs and their corresponding target promoters could be demonstrated. These newly identified target genes unveiled convergent evolution between *Xoo* and rice-pathogenic *Xanthomonas oryzae* pv. *oryzicola*, which share more common target genes addressed by different TALE classes than previously believed.

Individual TALEs did not have a strong influence on virulence in gain-of-function assays but several TALE classes might be linked to salicylic acid manipulation, which controls *Xoo* resistance reactions. Rice plants were edited using CRISPR/Cas9 to knockout target genes or mutate multiple TALE binding sites in target promoters. Initial results indicate reduced virulence of wild type *Xoo* strains on rice plants with 7 mutated TALE binding sites in TALE target promoters identified in this thesis.

Taken together, a detailed picture of TALE-induced plant processes could be established that significantly expands understanding of *Xanthomonas oryzae* virulence strategies. Additionally, the groundwork was laid to facilitate the development of novel resistances to overcome this important rice disease.

Key words: bacterial leaf blight of rice, plant biotechnology, plant genetics

Acknowledgements

I want to thank everybody that helped and supported me during my time in the lab and the writing of this thesis.

Especially, I want to thank Prof. Dr. Jens Boch for the opportunity to be a PhD student in his group and to work on this fascinating topic as well as the inspiring discussions and guidance.

Additionally, I want to thank Dr. Jan Grau and Annett for their help with all matters of bioinformatics and the good cooperation in general.

In general, I want to thank the whole department of plant biotechnology for the wonderful atmosphere, great cake and irreplaceable memories. A special thanks belongs to Beate and the other technicians that made experiments on such big scales possible.

I want to thank Jana, Sebastian, Caro and Maren for silly jokes, uplifting talks and scientific guidance when I needed them most. Your friendship means more to me than you know.

Sebastian, thank you for believing in me when I didn't and for your patience and support throughout the rough patches, long nights and lost weekends – they would have been so much worse without you and your food delivery.

Finally, I want to thank Thosa IT for providing me with the hardware needed to write this thesis, Jana and my Mom for proofreading as well as Prof. Dr. Traud Winkelmann, Prof. Dr. Edgar Maiß and Prof. Dr. Jens Boch for agreeing to be referees.

Table of contents

Zusammenfassung.....	I
Abstract	II
Acknowledgements	III
Table of contents.....	IV
List of figures	VIII
List of tables	IX
List of abbreviations.....	XI
1. Introduction	1
1.1. The phytopathogenic genus <i>Xanthomonas</i>	1
1.2. The arms race between pathogens and their hosts	2
1.2.1. Salicylic acid – defense system against <i>Xanthomonas</i>	3
1.2.2. The type-III-secretion system and <i>Xanthomonas</i> outer proteins	3
1.3. Transcription activator-like effectors	5
1.3.1. Form and function.....	5
1.3.2. The TALE code and DNA binding properties.....	7
1.3.3. Golden TALE Technology and designer TALEs	9
1.3.4. TALE nomenclature	10
1.3.5. Predicting TALE target genes	11
1.4. Virulence and resistance	11
1.4.1. TALEs as virulence factors.....	11
1.4.2. TALEs and resistance genes	12
1.5. Genome editing and designer resistance alleles.....	13
1.5.1. The rise of user-friendly genome editing tools.....	14
1.5.2. Double-strand breaks and repair mechanisms	16
1.5.3. Practical applications of genome editing in plants.....	17
1.6. Objectives of this thesis.....	18
2. Material and Methods	19
2.1. Materials.....	19
2.1.1. Bacterial strains	19
2.1.2. Media and additives	19
2.1.3. Buffers and solutions.....	20
2.1.4. Oligonucleotides.....	21
2.1.5. sgRNAs.....	26
2.1.6. Vectors and plasmids	28
2.1.7. Plant material	36
2.2. Methods.....	37
2.2.1. DNA work	37

2.2.1.1.	Plasmid isolation	37
2.2.1.2.	DNA amplification via polymerase chain reaction	37
2.2.1.3.	Agarose gel electrophoresis	38
2.2.1.4.	Gel extraction of DNA.....	38
2.2.1.5.	Restriction digest	38
2.2.1.6.	Blunt-end cloning into pUC57 & pUC57G	39
2.2.1.7.	Golden Gate cloning.....	39
2.2.1.7.1.	Generating new vectors with Golden Gate cloning.....	39
2.2.1.7.2.	Golden TALE Technology	40
2.2.1.7.3.	Cloning in the MoClo system.....	41
2.2.1.8.	Transformation of bacteria.....	41
2.2.1.8.1.	Transformation of electrocompetent cells	41
2.2.1.8.2.	Transformation of chemically competent cells	42
2.2.1.9.	DNA sequencing.....	42
2.2.2.	RNA work	42
2.2.2.1.	RNA isolation from rice	42
2.2.2.2.	cDNA synthesis.....	42
2.2.2.3.	Quantitative real-time PCR	42
2.2.3.	Protein work.....	43
2.2.3.1.	Quantitative GUS assay	43
2.2.3.2.	GUS staining.....	44
2.2.3.3.	Bradford assay	44
2.2.3.4.	Protein isolation of <i>Xanthomonas</i>	44
2.2.3.5.	SDS-PAGE	44
2.2.3.6.	Western Blot analysis	45
2.2.4.	Plant work.....	45
2.2.4.1.	<i>Agrobacterium</i> -mediated transient expression in <i>N. benthamiana</i>	45
2.2.4.2.	HR assay in <i>N. benthamiana</i>	45
2.2.4.3.	Inoculation of rice with <i>Xanthomonas</i>	45
2.2.4.4.	Leaf clipping assay.....	46
2.2.4.5.	Bacterial growth assay.....	46
2.2.4.6.	Salicylic acid assay	46
2.2.4.7.	Sterile culture of rice seedlings.....	47
2.2.4.8.	Protoplast isolation	47
2.2.4.9.	Protoplast transformation	47
2.2.4.10.	Protoplast esculin uptake assay	48
2.2.4.11.	Dexamethasone induction <i>in planta</i>	48
2.2.4.12.	<i>Agrobacterium</i> -mediated stable transformation of rice callus.....	48

2.2.4.13.	Detection of transgenes and mutations in rice	50
3.	Results	51
3.1.	Understanding Asian <i>Xoo</i> TALEs	51
3.1.1.	TALome diversity in Asian <i>Xoo</i> strains	51
3.1.2.	Construction of analogues to natural TALEs	56
3.1.3.	Analysis of truncated TALEs	59
3.1.3.1.	Truncated TALEs and gene induction	59
3.1.3.2.	Can truncated TALEs suppress Bs4 resistance reactions?	61
3.2.	Identifying target genes for <i>Xoo</i> TALEs	63
3.2.1.	Prediction of TALE target genes in rice	63
3.2.2.	Validation of TALE-dependent target gene induction	67
3.2.3.	Differentiating direct and indirect TALE targets	71
3.2.4.	Convergent evolution of TALEs in rice-pathogenic <i>Xanthomonas</i> species ...	73
3.3.	Impact of individual TALEs on virulence	76
3.3.1.	Influence of single TALEs on lesion length in rice	76
3.3.2.	Impact of individual TALEs on bacterial growth <i>in planta</i>	78
3.3.3.	Collaborative effects of TALEs on virulence.	79
3.4.	TALE-dependent phenotypic changes in rice based on target gene function	80
3.4.1.	Adapting TALEs to the versatile MoClo Cloning system	81
3.4.2.	TALEs and cell membrane transporters	83
3.4.2.1.	Establishing rice protoplasts for TALE research	83
3.4.2.2.	<i>SWEET</i> -inducing TALEs and esculin uptake	86
3.4.3.	TalAQ and the <i>OsDOX-1</i> phenotype	88
3.4.3.1.	Potential flavanol synthase function of <i>OsDOX-1</i>	88
3.4.3.2.	<i>DOX</i> genes and suppression of immunity	90
3.4.3.3.	The influence of TalAQ on salicylic acid content in rice	92
3.4.4.	Rice with inducible TALEs	94
3.5.	Mutating TALE target genes in rice	98
3.5.1.	TALE target gene knockouts	99
3.5.2.	Mutating TALE binding sites in rice	103
3.5.3.	TT03 rice plants have decreased TALE-mediated expression during <i>Xoo</i> and <i>Xoc</i> infection	109
3.5.4.	Impact of TT03 mutations on <i>Xoo</i> and <i>Xoc</i> virulence	110
4.	Discussion	113
4.1.	The TALome of Asian <i>Xoo</i> is well understood	113
4.1.1.	Spatiotemporal diversity of sequenced Asian <i>Xoo</i> strains	114
4.2.	Solving <i>Xoo</i> infection mechanisms one TALE at a time	115
4.2.1.	General modes of action among phytopathogens emerge	115

4.2.1.1.	Coerced nutrient supply.....	116
4.2.1.1.1.	Sugar in the xylem	117
4.2.1.1.2.	Circumventing phosphate starvation.....	118
4.2.1.1.3.	Manipulating the nitrogen regulon	119
4.2.1.1.4.	The enigma of silicon nutrition.....	120
4.2.1.1.5.	<i>Xanthomonas</i> and nutrient flow	121
4.2.1.2.	Hormonal imbalances make plants vulnerable	122
4.2.1.2.1.	SA – the bane of biotrophs existence.....	122
4.2.1.2.2.	ABA – the enemy of my enemy is my friend.....	124
4.2.1.2.1.	Other hormonal manipulations	125
4.2.1.3.	TALEs specialize in transcription manipulation	126
4.2.1.3.1.	Nested transcription factors	126
4.2.1.3.2.	Modulating transcription machinery and transcripts	127
4.2.1.4.	Tearing down walls.....	128
4.2.1.4.1.	Getting rid of pectin	128
4.2.1.4.2.	Confusing the guards.....	129
4.2.1.5.	Waste management.....	130
4.2.2.	Convergent evolution – connections are unveiled	131
4.2.3.	Temporal hierarchy of type III effectors	132
4.2.4.	TALEs with no known target gene	133
4.3.	A new approach to TALE research	133
4.3.1.	Growth phenotypes – an outdated system?	134
4.3.2.	Tailored phenotype assays.....	134
4.3.2.1.	Observing molecular functions	135
4.3.2.2.	Altered target gene expression	136
4.4.	Resistance breeding – hopes and limits	136
4.4.1.	Durable resistance and trade-off	137
4.4.1.1.	Cost of virulence and executor R genes	137
4.4.1.2.	Partial resistance and the cost of durability.....	137
4.4.1.3.	Novel ideas and technologies	138
4.4.2.	Sustainability and loss of susceptibility.....	139
4.4.2.1.	Creating less susceptible rice lines based on identified TALE boxes..	139
4.4.2.2.	TALE evolution and the arms race of breeding.....	140
	References.....	XIV
	Curriculum vitae	XXXIX
	List of publications	XL

List of figures

Figure 1: Overview of the genus <i>Xanthomonas</i>	2
Figure 2: Zigzag model of immune responses of plants.....	4
Figure 3. Schematic overview of TALEs.	6
Figure 4. TALE repeat structure and aberrant repeats.	7
Figure 5. Overview of Golden TALE Technology Cloning Kit.	9
Figure 6. Schematic overview of common genome editing tools and their mechanisms.	15
Figure 7. Overview of TALE clusters for all sequenced Asian <i>Xoo</i> strains.	53
Figure 8. TALE class abundance and cluster affiliation.....	55
Figure 9. Western Blot analysis of Roth X1-8 strains with artificial TALEs.....	58
Figure 10. Analysis of gene induction capability of truncated TALEs.....	60
Figure 11. Influence of truncated TALEs on Bs4 function.....	62
Figure 12. Prediction of rice target genes for TALEs from PX083, PX0142 and ICMP 3125 ^T	64
Figure 13. Induction of target rice gene expression upon infection with <i>Xoo</i> strains.	68
Figure 14. TALE boxes of rice target gene promoters.....	69
Figure 15. TalAO shifts the transcriptional start of <i>OsPHO1;3</i>	71
Figure 16. TALEs directly induce expression of target rice promoters in reporter studies in <i>N. benthamiana</i>	72
Figure 17. Overview of convergent evolution of TALEs.....	74
Figure 18. New shared TALE targets of <i>Xoo</i> and <i>Xoc</i>	75
Figure 19. Impact of single TALEs on disease severity measured by lesion length.	77
Figure 20. Influence of individual TALEs on bacterial growth <i>in planta</i>	78
Figure 21. Collaborative impact of selected TALEs on virulence.	80
Figure 22. Adapting the Golden TALE Technology Cloning Kit to the MoClo system.....	81
Figure 23. Cloning of pUC57G, pMC176 and pOS01.....	82
Figure 24. Establishing fluorescence markers to identify transformed rice protoplasts. .	84
Figure 25. Visualizing protoplasts transformed with TALE expression constructs.	85
Figure 26. Esculin uptake assays in rice protoplasts.	87
Figure 27. AtDMR6 and the rice <i>DOX</i> genes.	88
Figure 28. The apigenin biosynthesis pathway.	89
Figure 29. Influence of TalAQ3 on defense-associated gene expression in rice.....	91
Figure 30. Changes in salicylic acid content in rice during infection with <i>Xoo</i>	93
Figure 31. Cloning of DEX-inducible TALEs for rice transformation.....	95

Figure 32. pMC173 enables DEX-inducible <i>tGFP</i> expression in <i>N. benthamiana</i>	96
Figure 33. <i>tGFP</i> fluorescence in pMC173 transgenic rice leaves.	97
Figure 34. Cloning of CRISPR/Cas9 genome editing constructs.	98
Figure 35. Overview of TALE target gene knockout constructs.....	99
Figure 36. KO1 facilitates mutations in <i>OsLsi1</i>	100
Figure 37. KO5 facilitates deletion of <i>OsPHO1;3</i>	102
Figure 38. Overview of TALE box mutation constructs.	103
Figure 39. TT04 causes inheritable mutations.	104
Figure 40. TT02 facilitates TALE box mutations in susceptibility genes in rice.	105
Figure 41. TT03 causes mutations in newly identified TALE boxes.....	107
Figure 42. Changes in TALE boxes of PX0142, PX099 and CFBP2286 in T0 TT03 #09.	108
Figure 43. TT03 #09 progeny has reduced TALE-mediated expression in mutated loci.	110
Figure 44. Xoo and Xoc symptom formation on TT03 plants.....	111
Figure 45. TT03 mutations make rice less susceptible to PX0142 and PX099.	111
Figure 46. Modes of action for TALEs in rice.....	116
Figure 47. Postulated enzymatic functions of AtDMR6.....	123
Figure 48. Schematic overview of the ubiquitination machinery.....	130

List of tables

Table 1. Used bacterial strains.....	19
Table 2. Used media and their composition.....	19
Table 3. Antibiotics and concentrations.	20
Table 4. Used buffers and solutions.	20
Table 5: List of used oligo nucleotides.	21
Table 6. Evaluation of sgRNAs.	27
Table 7. List of used vectors.....	28
Table 8. List of used plasmids.....	29
Table 9. Overview of excitation and emission maxima of fluorescent markers and corresponding filters.	48
Table 10. Specialized media for <i>Agrobacterium</i> -mediated transformation of rice callus.	49
Table 11. Summary of culturing conditions for <i>Agrobacterium</i> -mediated transformation of rice callus.	50
Table 12. General features of completely sequenced Asian Xoo strains.....	51

Table 13. RVD composition of artificial TALEs and their <i>Xoo</i> strains of origin.....	57
Table 14. List of potential TALE target genes in rice for PX083, PX0142 and ICMP 3125 ^T	65
Table 15. List of hand-selected potential TALE target genes in rice for PX083, PX0142 and ICMP 3125 ^T	67
Table 16. Differences in TALEs inducing <i>OsDOX-1</i>	73
Table 17. Variations of TalAL in strains with more than one copy.....	76

List of abbreviations

16K TMP	16K transmembrane protein
2,5-DHBA	2,5-dihydroxybenzoic acid
A	adenine
aa	amino acid
ABA	abscisic acid
ADT	arogenate dehydratase
AEJ	alternative end joining
AIM	<i>Agrobacterium</i> infiltration medium
Avr	avirulence protein
Bp	base pairs
BSA	bovine serum albumin
C	cytosine
C4H	cinnamate 4-hydroxylase
cDNA	complementary DNA
CDS	coding sequence
CFU	colony forming units
CHI	chalcone isomerase
CHS	chalcone synthase
CRISPR	clustered regularly interspaced short palindromic repeats
CRR	central repeat region
crRNA	crispr RNA
CTM	C-terminal region
DAMP	damage-associated molecular pattern
DEX	dexamethasone
DMR6	downy mildew resistant 6
DMSO	dimethyl sulfoxide
DNA	deoxyribonucleic acid
DOX	dioxygenase
dpi	days post inoculation
DSB	double-strand break
E1	ubiquitin-activating enzyme
E2	ubiquitin-conjugating enzyme
E3	ubiquitin ligase
EDTA	ethylenediaminetetraacetic acid
ET	ethylene
ETI	effector-triggered immunity
fwd	forward
G	guanine
GFP	green fluorescent protein
GOI	gene of interest
GR	glucocorticoid receptor
GUS	β -glucuronidase
HD	histidine-aspartate RVD
HDR	homology directed repair
HLS1	hookless 1

hpi	hours post inoculation
HR	hypersensitive response
Hrp	hypersensitive response and pathogenicity
i.e.	id est (that is)
ICS	isochorismate synthase
iTALE	interfering TALE
JA	jasmonic acid
Kbp	kilo base pair
KO	knockout
LB	lysogeny broth
LOX	lipoxygenase
mC	methylated cytosine
MES	2-(N-morpholino)ethanesulfonic acid
mRFP	monomeric red fluorescent protein
mRNA	messenger RNA
MS	Murashige-Skoog
MU	4-methylumbelliferone
MUG	4-methylumbelliferyl- β -D-glucuronid
N	unspecified nucleotide
N*	asparagine only RVD
NG	asparagine-glycine RVD
NHEJ	non-homologous end joining
NI	asparagine-isoleucine RVD
NLR	nucleotide-binding leucine rich repeat domain containing protein
NLS	nuclear localization signal
NN	asparagine-asparagine RVD
NS	asparagine-serine RVD
NTM	N-terminal region
OD	optical density
PAL	phenylalanine ammonia lyase
PAM	protospacer adjacent motive
PAMP	pathogen-associated molecular pattern
PAT1	phosphoribosyl anthranilate transferase 1
PCR	polymerase chain reaction
PEG	polyethylene glycol
PIP	plant-inducible promoter
PR1a	pathogenesis-related protein 1a
PSA	peptone sucrose agar
PTI	pathogen-triggered immunity
pv.	pathovar
qRT-PCR	quantitative real-time PCR
R gene	resistance gene
Rev	reverse
RNA	ribonucleic acid
rpm	revolutions per minute
RVD	repeat variable diresidue
SA	salicylic acid

SAR	systemic acquired resistance
SDS-PAGE	sodium dodecyl sulfate-polyacrylamide gel electrophoresis
sgRNA	single guide RNA
SNP	single-nucleotide polymorphism
ssp.	subspecies
SWEET	sugar will eventually be exported transporter
T	thymine
TALE	transcription activator-like effector
TALEN	TALE nuclease
tGFP	turbo GFP
TPK	tyrosine protein kinase
tracrRNA	trans-activating crisper RNA
truncTALE	truncated TALE
TSS	transcriptional start site
TT	TALE target box
TTSS	type III secretion system
TU	transcriptional unit
UAS	upstream activating sequence
UTR	untranslated region
v/v	volume per volume
w/v	weight per volume
WAK	wall-associated kinase
<i>Xac</i>	<i>Xanthomonas citri</i> pv. <i>citri</i>
<i>Xam</i>	<i>Xanthomonas axonopodis</i> pv. <i>manihotis</i>
<i>Xcc</i>	<i>Xanthomonas campestris</i> pv. <i>campestris</i>
<i>Xcm</i>	<i>Xanthomonas citri</i> pv. <i>malvacearum</i>
<i>Xcv</i>	<i>Xanthomonas campestris</i> pv. <i>vesicatoria</i>
X-Gluc	5-bromo-4-chloro-3-indolyl β -D-glucuronide
<i>Xoc</i>	<i>Xanthomonas oryzae</i> pv. <i>oryzicola</i>
<i>Xoo</i>	<i>Xanthomonas oryzae</i> pv. <i>oryzae</i>
Xop	<i>Xanthomonas</i> outer protein
YEB	yeast extract broth
ZFN	zinc finger nuclease

1. Introduction

In contrast to their inorganic environment, plants contain enormous amounts of energy in form of macromolecules and therefore are attractive targets for a variety of phytopathogenic nematodes, viruses, fungi and bacteria. The infestation of important crops is of special interest to researchers, because bacterial phytopathogens alone cause around 1 billion dollars in yield loss annually (Martins *et al.*, 2018). Even though these numbers are high, the successful colonization of plants is the exception rather than the rule. Plants have evolved multiple mechanisms to combat intruders and shield themselves. Therefore, only a few pathogens have found ways to undermine these defenses.

Once a crop is infected with phytopathogenic bacteria, most options of pest control take a big toll on the environment. In the past, copper-based sprays and antibiotics were used to manage diseases, but resistant strains emerged quickly (Ritchie and Dittapongpitch, 1991). Instead, infection should be prevented by using non-infected seeds, good agricultural practices and resistant cultivars. How pathogens are able to overcome plant defenses is a central question in breeding resistant crop varieties.

1.1. The phytopathogenic genus *Xanthomonas*

Xanthomonas ssp. are rod-shaped γ -proteobacteria that infect virtually all economically important crops (Martins *et al.*, 2018). Most species of *Xanthomonas* are subdivided into pathovars (pv.) according to their host plants and colonization strategies. *Xanthomonas* ssp. infect monocotyledonous and dicotyledonous plants and display different tissue preferences (Ryan *et al.*, 2011). Vascular pathovars cause wilting and rot by clogging xylem vessels with extracellular polysaccharides and high numbers of bacteria in late stages of the infection (Figure 1; Yadeta and Thomma, 2013). Mesophyllic pathovars typically elicit necrotic and chlorotic lesions of leaves, which can later spread to fruits and other organs (Figure 1; Ryan *et al.*, 2011).

Rice-infecting *Xanthomonas* species are the most serious bacterial disease of rice. Bacterial leaf blight creates harvest losses of up to 50% and is caused by *Xanthomonas oryzae* pv. *oryzae* (*Xoo*) (Liu *et al.*, 2014). The causal agent of bacterial leaf streak of rice, *X. oryzae* pv. *oryzicola* (*Xoc*), has a less severe impact with up to 32% in yield loss, but it is emerging as an important global rice disease (Liu *et al.*, 2014). *Xoo* and *Xoc* differ in their tissue preferences and modes of infection. While *Xoc* enters the plant through stomata and wounds to colonize the parenchyma tissue locally, *Xoo* invades through hydathodes and wounds to infect the xylem vessels and spreads through the vasculature

(Ou, 1985; Noda and Kaku, 1999; Niño-Liu *et al.*, 2006; White and Yang, 2009). *Xoo* strains are subdivided in Asian and African strains, which differ significantly in their virulence factor composition.

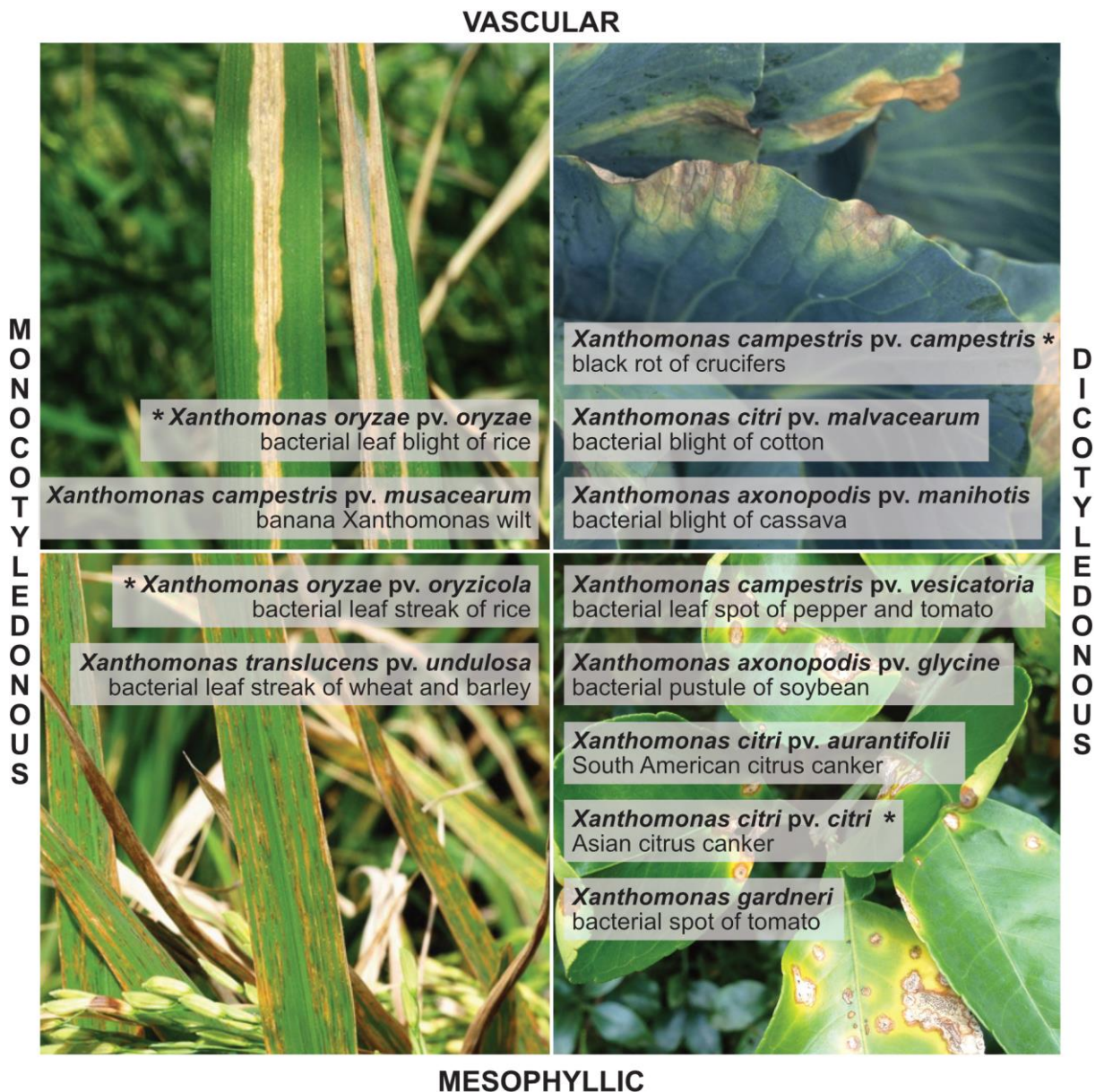


Figure 1: Overview of the genus *Xanthomonas*. Representative *Xanthomonas* species and their corresponding disease are depicted and sorted by tissue preferences and by monocotyledonous or dicotyledonous host plant. The typical symptoms of one disease each are shown and the causal agents are marked with stars. Pictures of symptoms originate from Nancy Castilla, undated; Sparks *et al.* undated; Holmes, 2010 and Salinas, 2017.

1.2. The arms race between pathogens and their hosts

Plants have developed constitutive and inducible mechanisms to defend themselves against colonization by bacteria. The constitutive basal defense is based on the recognition of substances that occur during infections. These so-called pathogen-associated molecular patterns (PAMPs) are conserved parts of bacterial cells like lipopolysaccharides, the elongation factor EF-Tu and flagellin, or debris of host

components (DAMPs) like degraded plant cell walls (Jones and Dangl, 2006; Zipfel, 2014). Plants can recognize PAMPs or DAMPs and will trigger defense responses that cumulate in the release of antimicrobial substances (i.e. phytoalexins) and the fortification of cell walls by callose deposition (Wu *et al.*, 2014; Büttner, 2016). This PAMP-triggered immunity (PTI) enables the plant to prevent infection (Wu *et al.*, 2014; Büttner, 2016). The recognition of PAMPs will further lead to the release of stress signals in form of phytohormones (i.e. salicylic acid) that spread through the plant and induce the expression of resistance-associated genes, creating systemic acquired resistance (SAR) to prepare for subsequent attacks (Klessig *et al.*, 2018).

1.2.1. Salicylic acid – defense system against *Xanthomonas*

Salicylic acid (SA) is a phenolic phytohormone that is involved in pathogen response. SA was specifically shown to be a major contributor in *Xoo* resistance in rice (Tamaoki *et al.*, 2013). SA accumulation is associated with PTI and SAR (Klessig *et al.*, 2018). The effectiveness of SA against biotrophic pathogens was attributed to the SA-dependent inhibition of auxin signaling, which benefits pathogen growth by loosening cell walls through expansin production (Wang *et al.*, 2007; Ding *et al.*, 2008). Recently, SA accumulation was shown to be connected to accumulation of biochemical components associated with *Xoo* resistance (i.e. lignin and pectin) (Thanh *et al.*, 2017; Shasmita *et al.*, 2019). Exogenous application of SA on rice lead to priming against *Xoo*, which was met with increased HR after subsequent infection (Thanh *et al.*, 2017; Shasmita *et al.*, 2019).

1.2.2. The type-III-secretion system and *Xanthomonas* outer proteins

In order to infect plants successfully, pathogens have to prevent the plants PTI response. Therefore, many phytopathogenic bacteria possess transport systems to manipulate the host plant. The type-III-secretion system (TTSS) enables the transport of proteins from bacterial cells directly into the host cytosol (Portaliou *et al.*, 2016). The TTSS components are encoded by the *hrp* (hypersensitive response and pathogenicity) gene cluster that is not expressed constitutively, but is induced after the perception of an unknown apoplastic elicitor (Wengelnik *et al.*, 1996). A two-component regulatory system is responsible for this perception. While the sensor kinase HpaS was found to be involved in *hrp* gene expression in *X. campestris* pv. *campestris* (*Xcc*), homologs in other *Xanthomonas* ssp. have not been reported, yet (Li *et al.*, 2014). The associated response regulator HrpG is well known in most *Xanthomonas* species and is responsible for activating the transcriptional regulator HrpX (Wengelnik *et al.*, 1996). HrpX, in turn,

induces the expression of the *hrp* gene clusters by binding to a specific regulatory element, the plant-inducible promoter (PIP) box (Koebnik *et al.*, 2006).

This cascade leads to the assembly of the basal secretion apparatus of the TTSS, which spans both membranes of the gram-negative bacteria (Portaliou *et al.*, 2016). Afterwards, the basal secretion apparatus secretes the components of the secretion pilus, which penetrates the cell wall (Weber *et al.*, 2005). Finally, the translocon protein, which integrates into the host cell membrane, is secreted to form a full TTSS (Büttner *et al.*, 2002). Now, the TTSS will start to translocate effector proteins into the host cell. Most of these effectors are called *Xanthomonas* outer proteins (Xops) and they are responsible for suppressing PAMP recognition and manipulating host signaling to benefit infection (Büttner, 2016). Both, *Xoo* and *Xoc* rely on the TTSS to translocate a plethora of effector proteins for infection (White and Yang, 2009).

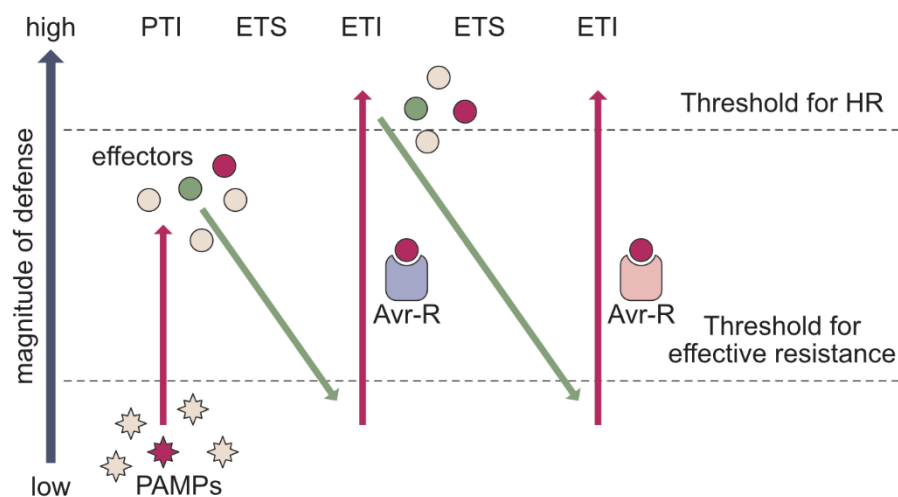


Figure 2: Zigzag model of immune responses of plants.

In this overview, the magnitude of plant defense responses is shown in relation to pathogen perception and manipulation. Plants detect pathogen-associated molecular patterns (PAMPs, diamonds) to trigger PAMP-triggered immunity (PTI). Adapted pathogens deliver effectors (circles) that can interfere with PTI (green), resulting in effector-triggered susceptibility (ETS). Some effectors (red; Avr) can get recognized by a resistance protein (R), activating effector-triggered immunity (ETI). ETI is more drastic than PTI and leads to the induction of hypersensitive reaction (HR). In response, pathogens adapt effectors to suppress ETI. This cycle of adaptation is ongoing in nature. This overview was based on Jones and Dangl (2006).

As a countermeasure, plants have evolved resistance genes that enable the detection of effector proteins. The resulting resistance is called effector-triggered immunity (ETI) (Jones and Dangl, 2006; van Schie and Takken, 2014; Büttner, 2016). There are two common ways to perceive an effector protein. Either they are directly bound by a receptor or their function is detected by guarding their targets to detect manipulations (Dangl and Jones, 2001; Jones and Dangl, 2006). The guard mechanism is found more often, because it can detect the activity of structurally different effector proteins with similar activities (Jones and Dangl, 2006; Khan *et al.*, 2016). After the perception of an effector

protein, a rapid localized cell death is initiated (Morel and Dangl, 1997; Jones and Dangl, 2006). This so-called hypersensitive reaction (HR) is accompanied by the dispersal of antimicrobial substances and in particular, reactive oxygen species (Morel and Dangl, 1997; Balint-Kurti, 2019). The ETI reaction is more severe in comparison to PTI and aims to kill the intruding pathogens at a higher cost (Morel and Dangl, 1997; Balint-Kurti, 2019). Traditionally, effectors inducing ETI were called avirulence proteins (Avr).

As a response to ETI, pathogens can lose or modify recognized effectors or evolve ETI-suppressing effectors. This arms race between pathogens and host is often described as a zigzag model (Figure 2; Jones and Dangl, 2006).

1.3. Transcription activator-like effectors

The genus *Xanthomonas* possesses a special type of effectors, the transcription activator-like effectors (TALEs), which activate expression of host genes to support infection (Boch and Bonas, 2010). After translocation into the host cell via the TTSS, TALEs are transported into the cell nucleus, where they bind to target promoter regions to induce expression (Van den Ackerveken *et al.*, 1996; Gu *et al.*, 2005; Kay *et al.*, 2007).

1.3.1. Form and function

TALEs have a unique structure composed of an N-terminal region (NTM), a central repeat region (CRR) and a C-terminal region (CTM) (Figure 3; Boch *et al.*, 2009). The NTM contains the TTSS signal that marks TALEs for translocation into the host cell and a non-sequence specific DNA-binding domain (Szurek *et al.*, 2002; Gao *et al.*, 2012; Schreiber *et al.*, 2015). The CTM contains two functional nuclear localization signals (NLS) that enable import into the host nucleus and an acidic activation domain, which is needed for efficient transcription initiation (Van den Ackerveken *et al.*, 1996; Zhu *et al.*, 1998; Yang *et al.*, 2000; Szurek *et al.*, 2001). The CRR contains up to 33.5 repeats of typically 34 amino acids and is responsible for recognizing and binding the target sequence in the promoter (Figure 3; Boch *et al.*, 2009; Moscou and Bogdanove, 2009). The last repeat is usually only 20 amino acids long and is referred to as a half repeat (Herbers *et al.*, 1992). Each repeat can recognize one base in the DNA in a sequential fashion (Boch *et al.*, 2009; Moscou and Bogdanove, 2009). Two hypervariable residues in each repeat at position 12 and 13 control the base specificity and are called RVD (repeat variable diresidue) (Boch *et al.*, 2009; Moscou and Bogdanove, 2009).

TALEs bind DNA loosely with their NTM and slide along the DNA in an extended superhelical pitch to find their corresponding target sequence (Mak *et al.*, 2012; Cuculis *et al.*, 2015). Upon finding their target sequence, TALEs transition into a compressed

superhelical pitch and interact with the major groove of the double helix (Mak *et al.*, 2012; Cuculis *et al.*, 2015). The repeats form a helix-loop-helix structure, exposing the RVD towards the DNA bases (Figure 4A; Mak *et al.*, 2012). The 13th residue of a repeat directly binds the corresponding base of the leading DNA strand and the 12th amino acid stabilizes the repeat array by connecting repeats (Deng *et al.*, 2012; Mak *et al.*, 2012). The NTM is able to bind DNA generally. It contains degenerated repeats forming similar structures, which cause TALEs to favor an initial thymine immediately before their target sequence (Deng *et al.*, 2012; Gao *et al.*, 2012; Mak *et al.*, 2012). After binding the target sequence (TALE box), it is hypothesized that TALEs recruit the transcription initiation complex by interacting with the transcription initiation factor IIA α and γ subunits (Yuan *et al.*, 2016; Huang *et al.*, 2017; Ma *et al.*, 2018).

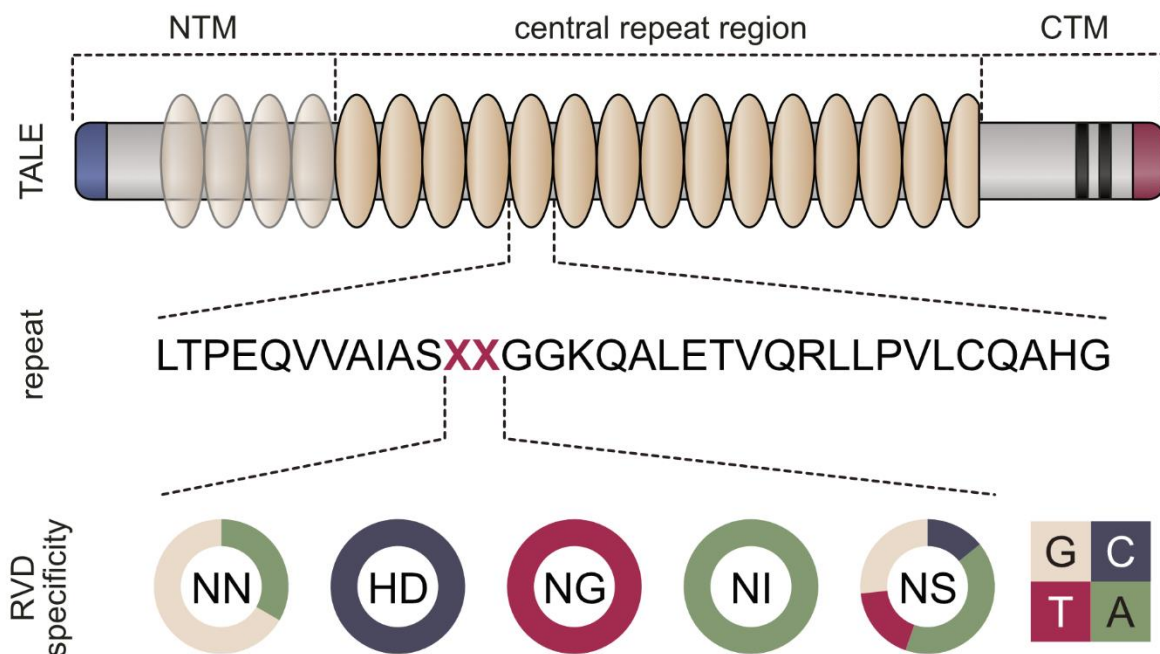


Figure 3. Schematic overview of TALEs.

Transcription activator-like effectors (TALEs) have a modular structure. The N-terminal region (NTM) contains a type-III-secretion and translocation signal (blue) and a degenerated repeat structure that generally binds DNA and specifically an initial thymine. The C-terminal region (CTM) contains an acidic activation domain (red) to activate transcription and two nuclear localization signals (black). The central repeat region is a DNA binding domain made up of 34 amino acid repeats. The last repeat consists of only 20 amino acids. Each repeat binds one DNA base and the base specificity is determined by the repeat variable diresidue (RVD), which consists of the 12th and 13th amino acid (represented by red XX). The five most common RVDs and their base specificities are shown.

TALEs are able to shift the transcription start site and generally, transcription starts 40-60 bp downstream of their binding region, but the exact transcription start site likely depends on the relative position of other promoter elements (Hummel *et al.*, 2012; Streubel *et al.*, 2017). Recently, it was reported that TALEs can induce transcription

bidirectionally, but no examples of biological importance in nature have been described, yet (Hummel *et al.*, 2012; Streubel *et al.*, 2017).

1.3.2. The TALE code and DNA binding properties

The base specificity of RVDs was first unraveled by studying the *Xanthomonas campestris* pv. *vesicatoria* (*Xcv*) TALE AvrBs3, which has 17.5 repeats and was shown to bind a core region of 18 bp (Boch *et al.*, 2009). The proposed binding sequences of TALEs derived from their RVD sequences were cloned into a minimal promoter and specific TALE-dependent reporter gene activation was shown (Boch *et al.*, 2009). Taken together, these findings cracked the TALE code of RVD-DNA binding. HD (histidine, aspartate) binds cytosine, NI (asparagine, isoleucine) binds adenine and NG (asparagine, glycine) binds thymine (Boch *et al.*, 2009; Moscou and Bogdanove, 2009). The interaction of other

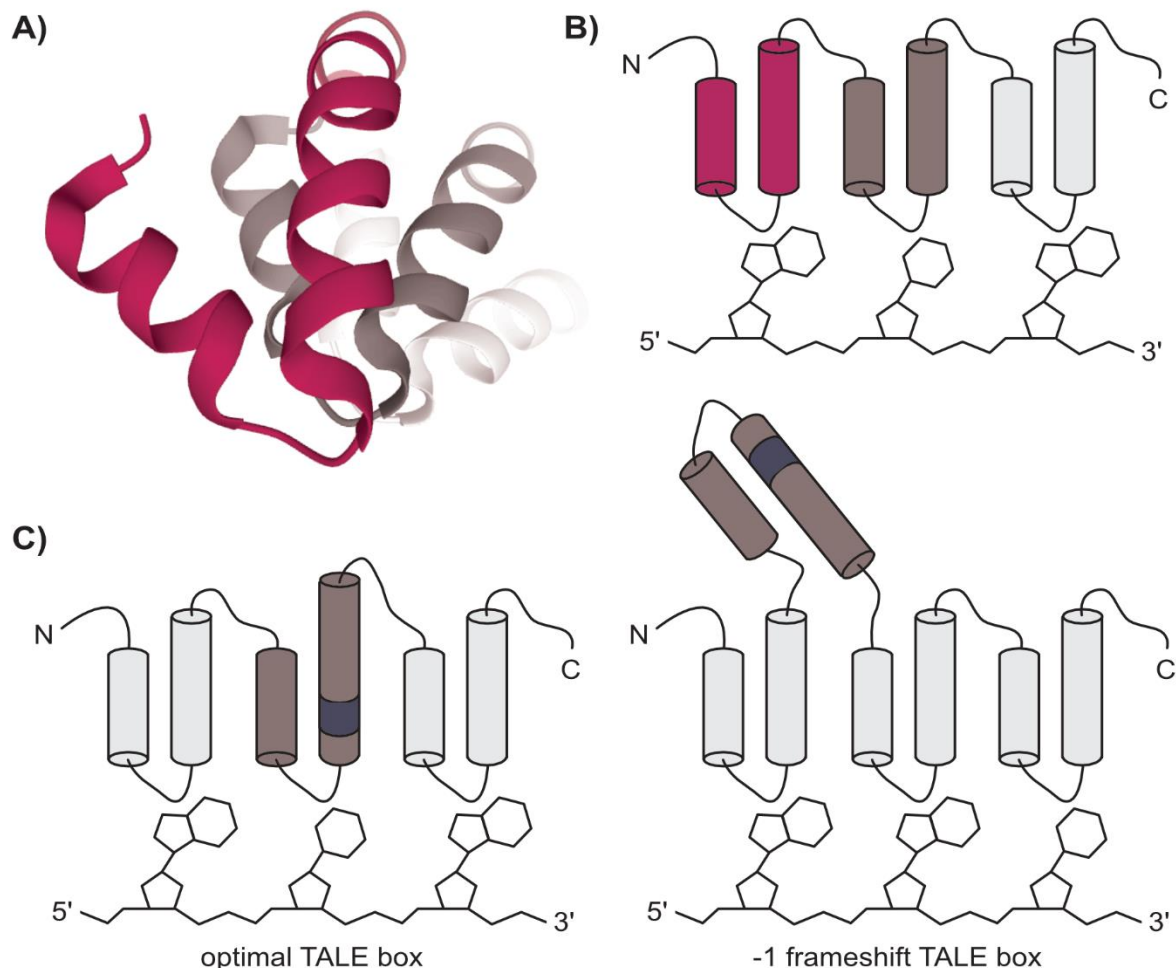


Figure 4. TALE repeat structure and aberrant repeats.

A) 3D model of three repeats, which are distinguished by color. The model was created on the Research Collaboratory for Structural Bioinformatics Protein Data Bank with Mol* using the structure 4HPZ based on TALE structure published by Gao *et al.*, 2012 (Berman *et al.*, 2000; Sehnal *et al.*, 2018). B) Schematic view of standard repeat array. C) Schematic view of repeat array containing an aberrant repeat with a duplication (blue). Aberrant repeats are hypothesized to loop out of the repeat array, if a -1 bp frameshift occurs in the TALE box. This overview is based on Richter *et al.*, 2014.

RVDs with DNA is more flexible, as NN (asparagine, asparagine) can bind both purine bases and NS (asparagine and serine) permits all four DNA bases (Boch *et al.*, 2009; Moscou and Bogdanove, 2009). Simultaneously, bioinformatic analyses of known TALE and target promoter pairs identified hypothetical specificities for 15 RVDs (Figure 3; Moscou and Bogdanove, 2009). Following these discoveries, all possible RVDs were tested for their DNA specificity in a systematic fashion (Yang *et al.*, 2014; Juillerat *et al.*, 2015; Miller *et al.*, 2015).

RVDs interact differently with DNA bases. Strong RVDs like HD and NN form hydrogen bonds with the bases and stabilize overall TALE binding, while weak RVDs like NG and NI connect to bases with van der Waals forces (Mak *et al.*, 2012; Streubel *et al.*, 2012). TALEs need a sufficient amount of strong RVDs, usually two or three, to bind their target DNA and activate transcription efficiently (Streubel *et al.*, 2012). DNA binding is further stabilized by increasing the number of repeats in general, which saturates at about 18 repeats (Rinaldi *et al.*, 2017). TALEs can exhibit TALE activity on TALE boxes containing mismatches between RVDs and DNA bases. The longer the TALE, the more mismatches can be tolerated (Rinaldi *et al.*, 2017).

Additionally, repeats of unusual length have been discovered. The most common variant is a 33 amino acid long repeat, which misses the 13th amino acid. These RVDs are marked with an asterisk (N*, H*) and result in a shortened RVD loop that favors pyrimidine bases (Streubel *et al.*, 2012; Rinaldi *et al.*, 2017). N* and other repeats missing the 13th amino acid were further shown to recognize methylated cytosine (mC), which is an important epigenetic marker (Valton *et al.*, 2012; Zhang *et al.*, 2017a). Contrarily, HD is sensitive to mC enabling the distinction of methylated and unmethylated DNA with TALEs using the right RVD composition (Valton *et al.*, 2012; Zhang *et al.*, 2017a).

Other repeats of unusual length contain deletions or duplications in the first or second helix of the repeat and are named aberrant repeats (Figure 4). Aberrant repeats of 30, 39/40 and 42 amino acids were shown to facilitate the binding of TALE boxes containing frameshifts (Richter *et al.*, 2014). Usually, a frameshift in the TALE box leads to an increased number of mismatches for the TALE, but aberrant repeats are able to disengage from the repeat array to accommodate 1 bp deletions by looping out (Figure 4B; Richter *et al.*, 2014).

1.3.3. Golden TALE Technology and designer TALEs

The modular structure of the DNA binding domain of TALEs allows for the design of custom DNA binding specificities. Therefore, many researchers created cloning systems to generate custom TALEs (Cermak *et al.*, 2011; Geißler *et al.*, 2011; Sander *et al.*, 2011; Zhang *et al.*, 2011; Sanjana *et al.*, 2012; Sakuma *et al.*, 2013; Schmid-Burgk *et al.*,

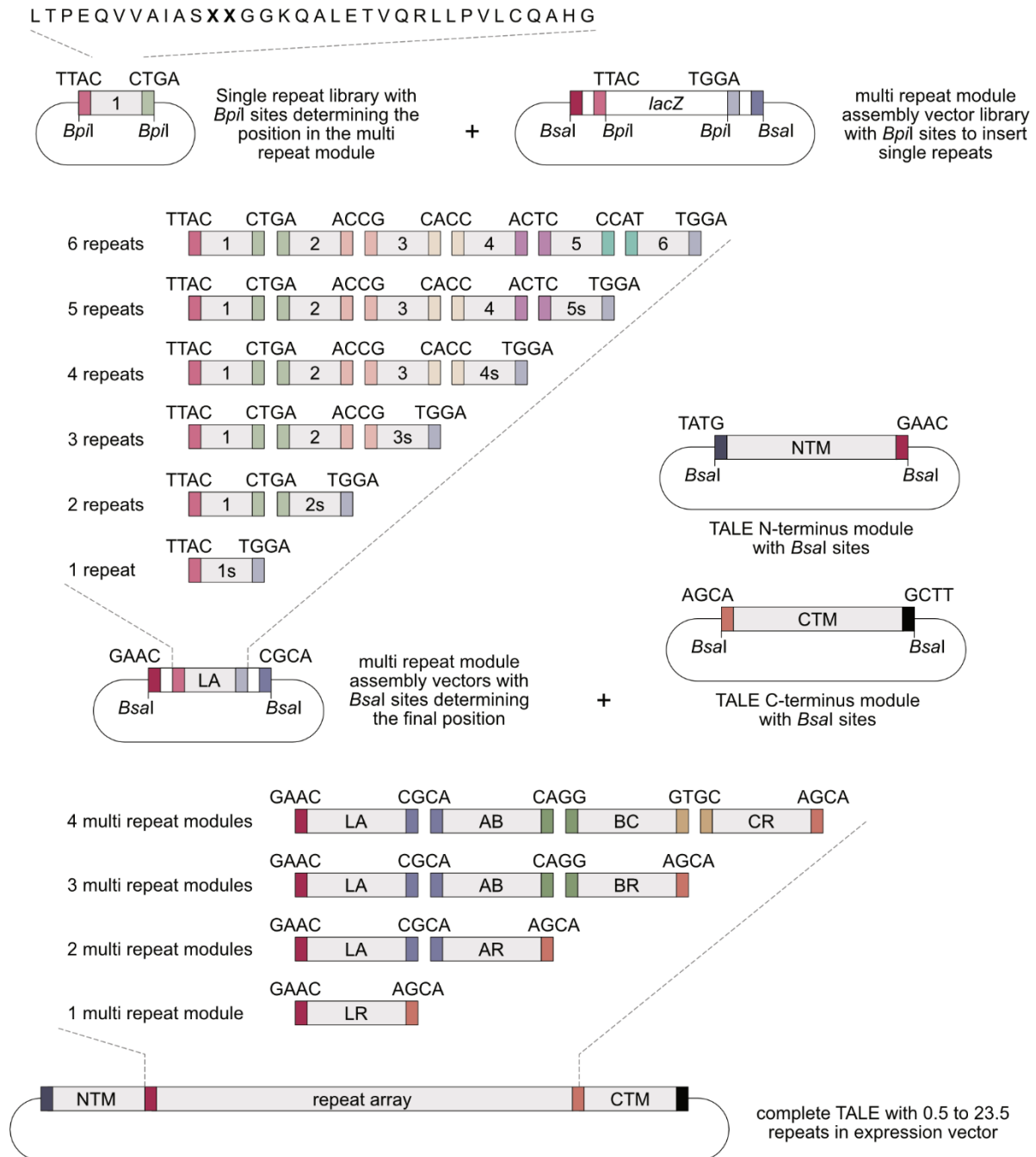


Figure 5. Overview of Golden TALE Technology Cloning Kit.

Single repeat modules have flanking *Bpil* sites determining their position in the multi repeat modules assembled in the first cloning step. In order to create multi repeat modules with less than six repeats, “stop repeats” (1s - 5s) can be employed. Up to four multi repeat modules can be combined with the TALE N-terminal region (NTM) and the C-terminal region (CTM) in the second cloning step using their flanking *Bsal* sites.

2013). Our group generated the Golden TALE Technology Cloning Kit that is based on Golden Gate Cloning (Figure 5; Geißler *et al.*, 2011). The TALEs were separated into three basic units: the NTM, the CTM and the repeat array. The repeat array was further subdivided into so called multi repeat modules that consist of up to six single repeats. In order to clone a custom TALE, two cloning steps are necessary.

Single repeat modules are available in a repeat library and have flanking *Bpil* sites determining their position in the multi repeat modules assembled in the first cloning step. In order to create multi repeat modules with less than six repeats, “stop repeats” can be employed. Assembly vectors for multi repeat modules contain flanking *Bsal* sites that determine the order of the multi repeat modules in the repeat array. They are labeled according to their flanking regions from L (left)-A up to C-R (right). As many as four multi repeat modules can be combined with the NTM and CTM in the second cloning step creating TALEs with up to 23.5 repeats (Figure 5).

The Golden TALE Technology Cloning Kit enables the creation of custom TALEs that can be used to analyze TALE functions, induce expression of genes of interest and might even help cure diseases (Geißler *et al.*, 2011; Geissler *et al.*, 2015).

1.3.4. TALE nomenclature

Especially *Xoo* and *Xoc* carry a lot of TALEs with up to 19 and 29 genes, respectively (Booher *et al.*, 2015; Wilkins *et al.*, 2015). At the start of this thesis, the full genomic sequences of ten *Xoc* strains and five Asian *Xoo* strains were published and two additional sequences of *Xoo* PX0142 and ICMP 3125^T were available in our group (Lee *et al.*, 2005; Ochiai *et al.*, 2005; Salzberg *et al.*, 2008; Booher *et al.*, 2015; Wilkins *et al.*, 2015; Grau *et al.*, 2016). Traditionally, TALEs were named based on their locus in the bacterial genome. The clusters of *TALE* genes were numbered starting from the origin of replication and the *TALE* genes inside the clusters were differentiated by letters (i.e. Tal2c). As plant-pathogenic *Xanthomonas* species contain hundreds of transposable elements and fragments thereof (*Xoo* PX099: 267 complete, 683 fragments), they are prone to genomic rearrangements (Salzberg *et al.*, 2008). Variations in the order of TALEs in between strains were common, which lead to completely unrelated TALEs with identical names and identical TALEs with different names (Salzberg *et al.*, 2008; Grau *et al.*, 2016). Additionally, *Xoo* TALEs with known pathogenicity or avirulence functions have historically been given different names: PthXo# or AvrXa#, respectively.

The proposed TALE nomenclature of our group utilizes the AnnoTALE program to establish TALE classes, which are represented by a two-letter code and based on similarity of the

repeat regions of TALEs (Grau *et al.*, 2016). Additionally, each member of the TALE class will get a unique allele number (i.e. TalAB14). This nomenclature helps to identify TALEs with identical target genes, which simplifies the assessment of new strains.

1.3.5. Predicting TALE target genes

The prediction of perfect binding sequences of natural TALEs from RVDs is very easy. Nevertheless, the tolerance for mismatches and the flexibility of some permissive RVDs allow for targeting patterns that are more complex. Therefore, multiple TALE target prediction programs were created by researchers (Doyle *et al.*, 2012; Grau *et al.*, 2013; Pérez-Quintero *et al.*, 2013). The first program Target Finder predicted target genes based on naturally occurring RVD-nucleotide association of known pairings and ranked results based on mismatch frequencies (Doyle *et al.*, 2012). This was further optimized in Talvez, which extrapolates specificities of rare RVDs based on common RVDs with the same 13th amino acid (Pérez-Quintero *et al.*, 2013). Additionally, Talvez is weighting mismatches based on their position in the TALE, tolerating more mismatches near the CTM (Pérez-Quintero *et al.*, 2013).

Our group helped create TALgetter, which predicts the 100 most likely TALE targets in a given genome based on RVD specificities and efficiencies (Grau *et al.*, 2013). The RVD specificities were learned using pairings of TALEs and TALE boxes with information on functionality of the pairing. The RVD efficiencies revealed in Streubel 2012 are implemented by adding an importance term to different RVDs (Grau *et al.*, 2013). Recently, a new prediction tool called PrediTALe was introduced with the help of our group (Erkes *et al.*, 2019). PrediTALe is based on large amounts of quantitative data on TALE target gene activation, which enables the incorporation of more specific parameters. PrediTALe considers dependencies between adjacent RVDs, dependencies between the first RVD and position 0 of the TALE box, positional effects of mismatches and for the first time, aberrant repeats and frame-shift tolerance (Erkes *et al.*, 2019).

1.4. Virulence and resistance

TALEs can have very different effects on virulence. Especially in *Xoo* and *Xoc*, contributions to infection seem to vary greatly. While a few TALEs are major virulence factors and are essential for infection, the deletion of most TALEs has no visible effect and some TALEs even trigger resistance reactions (Cernadas *et al.*, 2014; Ji *et al.*, 2016).

1.4.1. TALEs as virulence factors

The most well-known TALE targets are the clade III *SWEET* genes, which are necessary for *Xoo* virulence (Streubel *et al.*, 2013). *SWEET* transporters bidirectionally transport sugars

across cell membranes (Chen *et al.*, 2010, 2012). They contribute to pollen nutrition, nectar secretion, phloem loading as well as seed filling and are presumed to provide nutrients for pathogens (Chen *et al.*, 2010, 2012; Zhou *et al.*, 2015; Jeena *et al.*, 2019). At present, three members of the rice *SWEET* gene family were shown to be induced by Asian and African *Xoo* TALEs. *OsSWEET11* is induced by the TALE PthXo1 (also known as TalBX), *OsSWEET13* is addressed by PthXo2 (TalAM) and *OsSWEET14* is targeted by PthXo3 (TalBH), TalC (TalBS), AvrXa7 (TalAC) and Tal5 (TalDK) (Yang and White, 2004; Yang *et al.*, 2006; Antony *et al.*, 2010; Römer *et al.*, 2010; Yu *et al.*, 2011; Streubel *et al.*, 2013; Zhou *et al.*, 2015). *X. citri* pv. *malvacearum* (*Xcm*) and *X. axonopodis* pv. *manihotis* (*Xam*) infecting cotton and cassava, respectively, are also relying on *SWEET* gene induction for virulence (Cohn *et al.*, 2014; Cox *et al.*, 2017). This indicates that *SWEET* genes are a central virulence hub for *Xanthomonas* infections of different plants.

Additionally, TALEs target transcription factors. In rice, Asian *Xoo* strains induce the bZIP transcription factor *OsTFX1* with PthXo6 (TalAR) (Sugio *et al.*, 2007). In pepper, *Xcv* causes hypertrophy of leaf cells by activating the expression of bHLH transcription factor UPA20 with AvrBs3 (Kay *et al.*, 2007).

Despite the huge amount of *TALE* genes per strain in *Xoc*, only one *TALE* virulence target is known to date. The putative sulfate transporter *OsSULTR3;6* is induced by Tal2g (TalBF) to expand lesions and promote bacterial exudation (Cernadas *et al.*, 2014).

PthXo7 (TalBM) of *Xoo* was described as a virulence factor under certain conditions. This *TALE* induces the general transcription initiation factor *OsTFIIAγ1*, which contributes to virulence on the rice variety IRBB5 containing the *xa5* resistance gene (Sugio *et al.*, 2007). The *xa5* resistance prevents *TALE*s from interacting with the basal transcription machinery due to mutations in *OsTFIIAγ5* (Iyer and McCouch, 2004; Huang *et al.*, 2016; Yuan *et al.*, 2016). By expressing the paralog *OsTFIIAγ1*, PthXo7 can restore normal *TALE* function (Sugio *et al.*, 2007).

While the number of identified *TALE*s rises steadily, only very few *TALE*s have known target genes. Full genome sequences and full *TALomes* of *Xoo* are an important tool to start identifying more *TALE* target genes.

1.4.2. TALEs and resistance genes

The specific mode of action of *TALE*s has resulted in specialized resistance genes. These so-called executor resistance (R) genes have a *TALE* box in their promoter and act as a trap. If the *TALE*s is active in the host cell, the executor R gene is expressed and causes rapid cell death (Gu *et al.*, 2005; Liu *et al.*, 2007; Wu *et al.*, 2008a; Tian *et al.*, 2014;

Wang *et al.*, 2015). Well-known examples of executor R genes against Xoo TALEs in rice are *Xa7*, *Xa10*, *Xa23* and *Xa27*. In general, known executor R genes are not related and their physiological function is often unknown, except for *Xa10* and *Xa23*. *Xa10* and *Xa23* share sequence similarities and are both localized to the endoplasmic reticulum, where they cause calcium depletion (Tian *et al.*, 2014; Wang *et al.*, 2015, 2017b).

Xa7 recognizes the SWEET-inducing TALE AvrXa7 (TalAC), which is a major virulence factor (Yang *et al.*, 2000, 2006; Zhang *et al.*, 2015). *Xa10*, *Xa23* and *Xa27* recognize the TALEs AvrXa10 (TalBJ), AvrXa23 (TalAQ) and AvrXa27 (TalAO), respectively, (Wu *et al.*, 2008a; Tian *et al.*, 2014; Wang *et al.*, 2015). In pepper, the executor R gene *Bs3* recognizes the TALEs AvrBs3 of *Xcv* and AvrHah1 of *X. gardneri*, which are both needed for symptom formation (Römer *et al.*, 2007; Schornack *et al.*, 2008).

At the beginning of this thesis, only one resistance gene was known, that could recognize TALEs based on their structure and not their function. The tomato resistance gene *Bs4* is a nucleotide-binding leucine rich repeat domain containing (NLR) protein recognizing TALEs in a dose-dependent manner and shows different levels of sensitivity for specific TALEs of *Xcv* and *Xcc* (Schornack *et al.*, 2004, 2005; Kay *et al.*, 2005).

Another common mechanism by the plant to evade infection involves the natural mutation of TALE boxes in the promoters of susceptibility genes. The crop varieties with point mutations coinciding with TALE boxes had an evolutionary advantage, because they were less susceptible. In rice, the *xa13* resistance has mutations in the *OsSWEET11* promoter, *xa41* affects TALE boxes in the *OsSWEET14* promoter and *xa25* is caused by changes in the *OsSWEET13* promoter (Yang *et al.*, 2006; Hutin *et al.*, 2015b; Zhou *et al.*, 2015). It was hypothesized that many TALEs have evolutionarily countered this by binding near the TATA boxes of plant promoters, which are highly conserved and less likely to permit mutations (Grau *et al.*, 2013).

1.5. Genome editing and designer resistance alleles

At the beginning of this thesis, researchers had mutated TALE boxes in the promoters of *OsSWEET14* to create less susceptible variants in rice (Li *et al.*, 2012). These precise changes in the genomes of plants were accomplished by using genome editing tools (Li *et al.*, 2011). Genome editing tools contain a DNA-binding domain specifying the target sequence and a nuclease domain introducing the double-strand breaks (DSBs) into the DNA to provoke mutations. DSBs will be repaired by the cell repair mechanisms. Eventually, the repeated introduction of DSBs will lead to a mutation as the repair mechanisms sometimes fail to repair the DNA perfectly and are hindered by DNA bound

genome editing tools (Brinkman *et al.*, 2018). This enables precise and efficient modification of DNA at a desired locus.

1.5.1. The rise of user-friendly genome editing tools

The concept of creating targeted DSBs has been pursued for a long time. The biggest obstacle was the lack of customizable DNA binding domains for precision. The first effective tools utilized the zinc finger domain of eukaryotic transcription factors (Kim *et al.*, 1996; Urnov *et al.*, 2010). DNA-binding zinc fingers can form a small structural motif with an α -helix whose amino acids interact with three to four specific bases in the major groove of DNA (Miller *et al.*, 1985; Wolfe *et al.*, 2000). The amino acid composition of the α -helix can alter the specificity of the zinc finger for different sets of three bases (Wolfe *et al.*, 2000). The combination of multiple zinc fingers into arrays enables researchers to create customizable DNA-binding domains that are only restricted by available zinc finger specificities. The construction of zinc finger arrays is further complicated by the overlapping of binding sites of neighboring zinc fingers in the array and interactions between neighboring zinc fingers (Wolfe *et al.*, 2000).

In order to create a genome editing tool, zinc finger arrays were fused to an endonuclease. The type IIS restriction enzyme *FokI* has two separate domains for recognizing its target sequence and DNA cleavage (Li *et al.*, 1992). The unspecific DNA cleavage domain of *FokI* was fused to zinc finger arrays to create zinc finger nucleases (ZFNs) (Figure 6A; Kim *et al.*, 1996; Urnov *et al.*, 2010). As *FokI* naturally forms dimers to create DSBs, ZFNs were used in inverted pairs to enable *FokI* domain dimerization (Bitinaite *et al.*, 1998). The usage of ZFN pairs also increased the specificity of the DSBs, as both ZFNs had to bind to create the cut (Urnov *et al.*, 2010).

After the TALE code was deciphered, a new, fully customizable DNA-binding domain was available (Boch *et al.*, 2009). In order to transform TALEs into TALE nucleases (TALEN), some adjustments needed to be made. The NTM and CTM of TALEs were shortened to minimize the size of the TALEN (Miller *et al.*, 2011). This minimalistic TALE was fused to the DNA cleavage domain of *FokI* to create TALEN (Christian *et al.*, 2010; Cermak *et al.*, 2011; Li *et al.*, 2011; Miller *et al.*, 2011). TALEN were used in pairs similar to ZFNs and quickly dominated the genome editing field because of their versatility (Figure 6B). The first mutations in TALE boxes in the *OsSWEET14* promoter were created with TALEN (Li *et al.*, 2012).

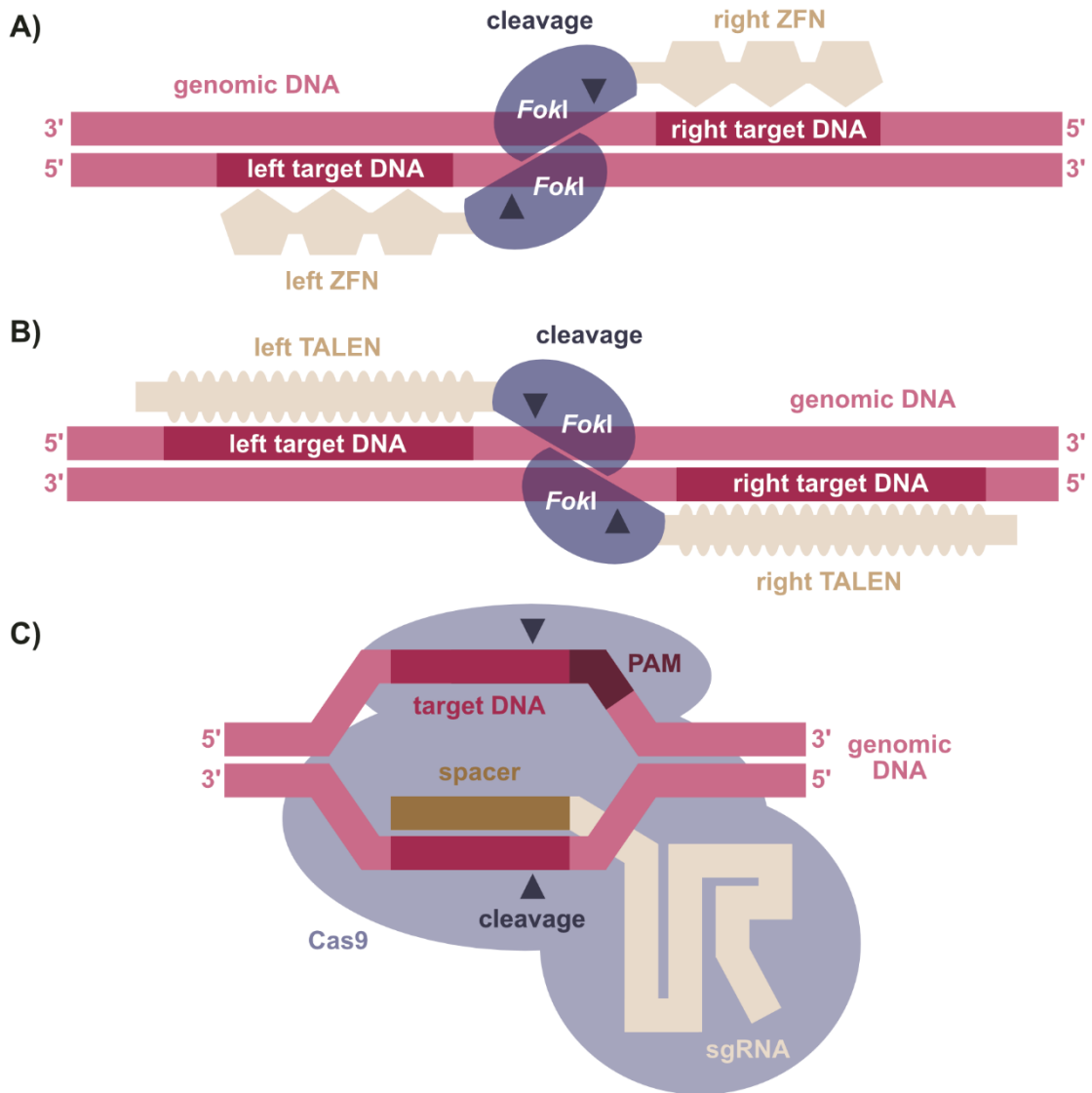


Figure 6. Schematic overview of common genome editing tools and their mechanisms.

Genome editing tools are able to bind the desired target DNA (red) with a customizable DNA-binding domain (yellow) and create double-strand breaks with an endonuclease (blue). A) Zinc finger nucleases (ZFNs) are used in pairs, because the *FokI* nuclease domains must dimerize to create a staggered double-strand break between both target DNA regions. The left and right target DNA are recognized by arrays of zinc finger domains, each binding three bases. B) TALE nucleases (TALEN) are also utilizing *FokI* domains and create similar double-strand breaks in pairs. The left and right target DNA are recognized by TALE repeat arrays with one repeat recognizing one base. C) The Cas9 endonuclease contains two nuclease domains that cut both strands of DNA independently and create a blunt-end cut in the target DNA. The target DNA is recognized by the integrated sgRNA, which binds the target DNA by base pairing. The target DNA will only be cut, if the protospacer adjacent motif (PAM) is recognized by Cas9.

Shortly after the development of TALEN, a new tool emerged that was perceived as even more user-friendly. The clustered regularly interspaced short palindromic repeats (CRISPR)/Cas9 system is based on the adaptive immune system of bacteria, which identifies foreign DNA by matching it with memorized short DNA fragments of previous infections (Brouns *et al.*, 2008; Bhaya *et al.*, 2011). The identification is based on simple complementary DNA-RNA base pairing and leads to DNA cleavage (Bhaya *et al.*, 2011). The spacers in the CRISPR array encode these memorized DNA fragments and are

transcribed into the crRNA that binds to a tracrRNA (van der Oost *et al.*, 2014). The crRNA-tracrRNA complex is incorporated into the Cas9 protein to form a functioning nuclease. The region of the spacer binds to the target DNA and the two nuclease domains of Cas9 create a DSB in the target DNA (Brouns *et al.*, 2008; Bhaya *et al.*, 2011). In order to prevent the CRISPR/Cas9 system from cutting the CRISPR array, a safety mechanism exists. Cas9 will only cut the target DNA, if the spacer region of the target DNA has a protospacer adjacent motive (PAM) at the 3' end (Jinek *et al.*, 2012; Anders *et al.*, 2014). PAMs may vary between Cas9 proteins of different species, but the most commonly used SpCas9 of *Streptococcus pyogenes* has a 5'-NGG PAM (Sternberg *et al.*, 2014).

In order to use the CRISPR/Cas9 system as a genome editing tool, the crRNA and the tracrRNA are usually fused to create a single guide RNA (sgRNA) (Jinek *et al.*, 2012; Jiang *et al.*, 2013). Supplementing the Cas9 protein with sgRNAs with designed spacers enables the specific targeting of Cas9 to any desired target DNA adjacent to a PAM (Figure 6C). The spacer region of sgRNAs is usually 20 bp long and the target DNA is cut between the 17th and 18th base of the spacer (Jinek *et al.*, 2012). The CRISPR/Cas9 system will often also cut imperfect target sequences with lower efficiency and mismatched bases close to the PAM have a higher impact on efficiency (Jinek *et al.*, 2012; Fu *et al.*, 2013). Additionally, the sequence of spacers has an impact on efficiency (Doench *et al.*, 2014, 2016; Wang *et al.*, 2014a). The reasons for sequence preferences in the spacer are still unknown, but interactions between Cas9 and the spacer were hypothesized to contribute to the differences (Nishimasu *et al.*, 2014).

Because the target DNA is defined by small sgRNAs, the delivery of multiple sgRNAs simultaneously is not hindering the delivery of the tool. Therefore, the CRISPR/Cas9 system is uniquely able to handle a multiplexing approach that targets many genomic regions simultaneously.

1.5.2. Double-strand breaks and repair mechanisms

Genome editing tools are able to repeatedly introduce DSBs at the same location (Brinkman *et al.*, 2018). Because these genomic DSBs can be lethal, they will be repaired by the eukaryotic cell to preserve the integrity of the genome (Puchta, 2005). There are two major repair mechanisms known in eukaryotes: non-homologous end joining (NHEJ) and homology directed repair (HDR) (Ceccaldi *et al.*, 2016).

HDR repairs DSBs based on a repair template that requires sequence homology of at least 75 bp (Schmidt *et al.*, 2019). HDR is a lot less common than NHEJ and can only

occur in cell cycle phases after the synthesis of sister chromatids, which can be used as the repair template (Ceccaldi *et al.*, 2016; Schmidt *et al.*, 2019).

NHEJ repairs DSBs by blunt-end ligation independently of sequence homology (Ceccaldi *et al.*, 2016; Schmidt *et al.*, 2019). This process can occur in most cell cycle phases and is the most common repair mechanism in higher eukaryotes (Ceccaldi *et al.*, 2016). Because of the indiscriminate ligation of DNA ends, it can lead to mutations and was shown to create small deletions or insertions at DSB sites as well as big deletions, inversions and chromosomal translocations between multiple DSBs (Ceccaldi *et al.*, 2016; Schmidt *et al.*, 2019). The knockout of NHEJ components has led to the discovery of multiple alternative end joining (AEJ) mechanisms (McVey and Lee, 2008; Wu *et al.*, 2008b). AEJ mechanisms often rely on microhomologies in DSB repair (Schmidt *et al.*, 2019). Microhomologies are commonly defined to be 3 to 20 bp long and can be identified after DSB repair has occurred and deletions are flanked by homologous sequences.

Genome editing utilizes the error-prone nature of NHEJ to create mutations in genes of interest and other genomic regions (Schmidt *et al.*, 2019). HDR can be used to create specific changes by providing a designed repair template including desired changes (Schmidt *et al.*, 2019).

1.5.3. Practical applications of genome editing in plants

The use of genome editing to improve crop traits has been widespread. The most common technique is the knockout of undesirable traits. Notable examples include the knockouts of negative regulators for yield in rice resulting in increased grain weight and the knockout of *Wx1* in corn to change the composition of starch (Waltz, 2016; Xu *et al.*, 2016). The so-called waxy corn created by DuPont Pioneer was approved by the United States regulatory system and will be commercially available soon (Waltz, 2016). The creation of low-gluten wheat using CRISPR/Cas9 multiplexing might also hold great potential for people with celiac disease in the future (Sánchez-León *et al.*, 2018). Novel approaches aim to use genome editing to accelerate the domestication of wild crop varieties or to use CRISPR/Cas9 as a defense mechanism against plant pathogenic viruses similar to its original function (Ali *et al.*, 2015; Li *et al.*, 2018).

Another important field is the improvement of abiotic and biotic stress tolerance in crop plants. One of the most successful efforts to increase the tolerance to abiotic stress in crops to date is the creation of plants with reduced accumulation of toxic heavy metals. The knockout of different transporters in rice with affinity to cadmium or arsenic

decreased heavy metal accumulation (Tang *et al.*, 2017; Wang *et al.*, 2017a). At the forefront of biotic stress tolerance are the knockout of *MLO* alleles in wheat to increase powdery mildew resistance and the mutation of TALE boxes in rice to improve *Xoo* resistance using TALEN (Li *et al.*, 2012; Wang *et al.*, 2014b).

1.6. Objectives of this thesis

TALEs have been intensively researched since their code has been broken. Especially *Xoo* strains, which harbor up to 20 *TALE* genes, have been sequenced in recent years. Even though the amount of known TALEs has grown a lot, the target genes of very few TALEs is known. In this thesis, a better understanding of the diversity of TALEs in different *Xoo* strains was to be gained by comparing 34 fully sequenced strains. This new information was to be used to identify more TALE target genes of the many TALEs without known function. Specifically, the TALE target genes of *Xoo* strains PX083, PX0142 and ICMP 3125^T were to be investigated. TALE targets were to be identified by bioinformatic and transcriptomic analyses.

Additionally, the impact of TALEs on virulence was to be examined to connect TALE target genes with a virulence function. To this end, new methods were to be established to identify potential influences on virulence by TALEs and their target genes. These efforts should focus on target gene specific functions like transport capabilities or hormone balance manipulations as well as general changes in virulence.

Finally, rice lines with mutated target genes should be created to further analyze their function and impact on virulence. Genome editing was to be performed using CRISPR/Cas9 to mutate up to 8 target genes or their promoters simultaneously.

2. Material and Methods

2.1. Materials

2.1.1. Bacterial strains

In this thesis, *E. coli* strain OneShot® Top10 was used to multiply plasmids and generally incubated at 37 °C. The *A. tumefaciens* strain GV3101 was used for transient expression in *N. benthamiana* and EHA105 was used to transform rice calli. Several *Xoo* strains were utilized for infection studies in rice. Both, *A. tumefaciens* and *Xoo* were cultured at 28 °C.

Table 1. Used bacterial strains.

strain	characteristics	reference
<i>Escherichia coli</i>		
OneShot ® Top10	F- <i>mcr A</i> Δ(<i>mrr-hsd RMS-mcr BC</i>) φ80 <i>dlac ZΔM15Δ lacX74 recA1 araD139 Δ(araleu)7697 galU galK rpsL endA1 nupG</i>	Thermo Fisher Scientific Inc./Waltham, United States of America
<i>Agrobacterium tumefaciens</i>		
GV3101	C58, rifampicin resistance; Ti plasmid: pMP90 (pTIC58 Δ T-DNA) gentamycin resistance, gene for nopaline synthesis	Van Larebeke <i>et al.</i> , 1974; Koncz and Schell, 1986
EHA105	C58, rifampicin resistance; Ti plasmid: pEHA105 (pTIBo542 Δ T-DNA) gentamycin resistance, succinamopine	Hood <i>et al.</i> , 1993
<i>Xanthomonas oryzae pv. oryzae</i>		
PX099	rifampicin resistance	Salzberg <i>et al.</i> , 2008
PX083	rifampicin resistance	Grau <i>et al.</i> , 2016
PX0142	rifampicin resistance	Mücke <i>et al.</i> , 2019
ICMP 3125 ^T	rifampicin resistance	Mücke <i>et al.</i> , 2019
Roth X1-8	rifampicin resistance	Triplett <i>et al.</i> , 2011

2.1.2. Media and additives

Table 2. Used media and their composition.

Media	composition	usage
LB medium (lysogeny broth)	1% (w/v) tryptone 0.5% (w/v) yeast extract 1% (w/v) NaCl pH 7.5	Incubation <i>E. coli</i>
YEB medium (yeast extract broth)	0.5% (w/v) beef extract 0.1% (w/v) yeast extract 0.5% (w/v) peptone 0.5% (w/v) sucrose 0.05% (w/v) MgSO ₄ pH 7.2	Incubation of <i>A. tumefaciens</i>
AIM (<i>Agrobacterium</i> infiltration medium)	10 mM MES; pH 5.4 10 mM MgCl ₂ 150 μM acetosyringone	Inoculation of <i>A. tumefaciens</i>
PSA medium (peptone sucrose agar)	1% (w/v) peptone 1% (w/v) sucrose 0.1% (w/v) glutamic acid pH 7.0	Incubation of <i>Xoo</i>
½ MS medium (Murashige-Skoog)	2% (w/v) MS salts 1% (w/v) sucrose pH 5.7	Sterile culture of rice

The utilized media to cultivate bacteria and plants are described in Table 2. In order to create solid media, the recipes were adjusted to contain 1.5% (w/v) agar. The addition of antibiotics was used to cultivate under selective pressure. The used antibiotics and their concentrations are displayed in Table 3. All media were stored at 4 °C until use.

Table 3. Antibiotics and concentrations.

antibiotics	concentration
Ampicillin	100 µg/ml in solid media 50 µg/ml in liquid media
Carbenicillin	100 µg/ml
Cycloheximide	50 µg/ml
Gentamycin	20 µg/ml
Hygromycin	50 µg/ml
Kanamycin	100 µg/ml (<i>A. tumefaciens</i>) 25 µg/ml (<i>E. coli</i>)
Rifampicin	100 µg/ml
Spectinomycin	30 µg/ml

2.1.3. Buffers and solutions

The compositions of used buffers and solutions are described in Table 4.

Table 4. Used buffers and solutions.

Buffer / solution	composition
DNA analysis	
Agarose gel	1% (w/v) agarose In 1x TAE 0.005% (v/v) Midori Green
1x TAE	40 mM Tris 1 mM EDTA 20 mM acetic acid pH 8.8
5x loading dye	15% Ficoll 400 Orange G
Protein analysis	
4x Lämmli	0.25 M Tris-HCl (pH 6.8) 40% (v/v) glycerol 8% (w/v) SDS 10% (v/v) β-mercaptoethanol Bromophenol blue
1x TANK	25 mM Tris 0.1% (w/v) SDS 250 mM glycine
1x TBST	10 mM Tris-HCl (pH 7.5) 0.5% (v/v) Tween 150 mM NaCl
Towbin buffer	48 mM Tris 20% (v/v) methanol 39 mM glycine 0.04% (w/v) SDS
Separation gel (10%)	10% (v/v) acrylamide 0.001% (w/v) SDS 0.001% (v/v) TEMED 375 mM Tris-HCl (pH 8.8) 0.01% (w/v) APS
Stacking gel	6% (v/v) acrylamide 0.001% (w/v) SDS 0.001% (v/v) TEMED 125 mM Tris-HCl (pH 6.8) 0.01% (w/v) APS
Blocking solution	5% (w/v) milk powder In 1x TBST 3% (w/v) BSA fraction 5
ECL solution	100 mM Tris-HCl (pH 8.5) 1.25 mM luminol 0.225 mM p-coumaric acid 0.3% (v/v) H ₂ O ₂
GUS assay	
GUS extraction buffer	50 mM sodium phosphate (pH 7.0) 0.1% (w/v) SDS 10 mM β-mercaptoethanol 10 mM EDTA (pH 8.0) 0.1% Triton X-100
GUS staining solution	10 mM sodium phosphate (pH 7.0) 1 mM potassium ferricyanide 0.1% Triton X-100 10 mM EDTA (pH 8.0) 1 mM potassium ferrocyanide 0.1% X-Gluc

Buffer / solution	composition	
Protoplastation		
W5 solution	2 mM MES (pH 5.7) 154 mM NaCl	125 mM CaCl ₂ 5 mM KCl
WI solution	4 mM MES (pH 5.7) 0.5 M mannitol	20 mM KCl
MMG solution	4 mM MES (pH 5.7) 0.4 M mannitol	15 mM MgCl ₂
PEG solution	40% (w/v) PEG4000 0.2 M mannitol	100 mM CaCl ₂
Cell wall-dissolving enzyme solution	20 mM MES (pH 5.7) 1.5% (w/v) cellulase R10 0.75% (w/v) macerozyme R10 0.6 M mannitol	10 mM KCl 10 mM CaCl ₂ 0.1% (w/v) BSA

2.1.4. Oligonucleotides

The sequences of all utilized oligo nucleotides are listed in Table 5 in combination with a short description of the application.

Table 5: List of used oligo nucleotides.

Oligo name	Sequence	Description
Extension of the Golden TALE Technology Kit		
lacIII-D-F_JB	TTTGCAATGCACTGTGCCAGGCGCATGGCCTTACAAGTC TTCCTTGTCTGTAAGCGG	AV DE
lacIII-E-R-SM	TTTGCAATGTCATGGCACAGCACCGGCAACAGCCGC	AV DE
lacIII-E-F-SM	TTTGCAATGCAGCCAGGCGCATGGCCTTACAAGTC	AV EF & ER
lacIII-R-R-JB	TTTGCAATGTCATGCTCTCCAAAGTCTTCGCCCAATA	AV ER & FR
lacIII-F-F-SM	TTTGCAATGCAGCGGCTGTTGCCGGTGCTGTGCCAGGC GCATGGCC	AV FR
lacIII-F-R-SM	TTTGCAATGTCACCGCTGCACCGTCTCCAAAGTCTT	AV EF
Hax-N-F	TTTGGTCTCATATGGATCCCATTCTCGCGC	NTM TaIAI
Hax-N-R	TTTGGTCTCAGTTCAGGGGGGCACCCGTCAG	NTM TaIAI
Hax34-C-F	TTTGGTCTCAAGCATTGTTGCCAGTTATCTC	CTM TaIAI3 & AI4
AI3-Cws-R/SM	TTTGGTCTCAAAGCTCAGGACCGTTTACGTCTGCT	CTM TaIAI3
AI4-Cws-R/SM	TTTGGTCTCAAAGCTCAATCATGCGATTTCTCTTCC	CTM TaIAI4
BoxAI3/SM	TTTGGTCTCACACCTACTTTTCCCGCTCACGCTTCTTCT TGTATATAACTTTGTCC	TaIAI box opt
BoxAI-1/SM	TTTGGTCTCACACCTACTTTTCCCGCTCACGCTTCTTCTT GTATATAACTTTGTCC	TaIAI box -1
Bs4Pr-GG_R/AR	TTTGGTCTCACCTTAGATTCGATTAATAAATAAATTGTATG	TaIAI boxes
qRT-PCR TALE targets		
Aktin neu RT F/JS	TGTGTGTGACAATGGAAGTGGC	Actin
Aktin neu RT 1 R/JS	GAGTCCAACACGATACCAGTTG	Actin
11N3_alternativ_F2/JS	CTACCTGGCCCCACTGC	OsSWEET14
11N3_alternativ_R/JS	GTGCGCACCACCAGCC	OsSWEET14
Os03g03034_F3	CACGGCTTCTCCAGGTGCTCA	OsDOX-1
Os03g03034_R3	TTCTGTCTTCTGTGATACCAGCACT	OsDOX-1
Os04g05050_F3	CTCTCCAAGTGCAGCCGACGG	OsPLL4
Os04g05050_R3	GCGGTTGCCCTGGCTGTTGA	OsPLL4
Os06g29790_F3	TCCTCCACGGAGATCAGTCCCT	OsPHO1;3
Os06g29790_R3	ACAGAAGCTCACGGATGGCGG	OsPHO1;3
OsHen1_qrt_F/MR	TATGCCAGACCAATGCTGAAGTG	OsHEN1
OsHen1_qrt_R/MR	GATTGCCCTCGACAAGCTTGG	OsHEN1
OsTFIIAy_qrt_F/MR	GCCACCTTCGAGCTGTACCG	OsTFIIAy1

Oligo name	Sequence	Description
OsTFIIAy_qRT_R/MR	TACTCTTCTTTAGTCTCCAGCAATTTG	OsTFIIAy1
OsTFX1_qRT-F/MR	TTACCATGGCGAGGTGGCC	OsTFX1
OsTFX1_qRT-R1/MR	CGGCCCTCTCCTTCCTGAG	OsTFX1
qRT_Aquap_F1/SM	CATCGCCGACTTCTTCCTC	OsLsi1
qRT_Aquap_R1/SM	ATATCGCTCCGGTGAAGTGC	OsLsi1
qRT_FBX109_F4/SM	TGGATCGGCAAGACACACGA	OsFBX109
qRT_FBX109_R4/SM	GTCGCGAGGTCGAGGGATAC	OsFBX109
qRT_HLS_F2/SM	GGCAATGGCAGGGAGATCAT	OsHLS1
qRT_HLS_R2/SM	GTCCGGAAGTTGGAGTAGCC	OsHLS1
qRT_PTR2_F3/SM	GATCGCCGTGAACCTGGTCA	OsNPF6.3
qRT_PTR2_R3/SM	TAGAGCGCCAGGTACAGCAC	OsNPF6.3
qRT_WAK51_F2/SM	GCTCTCATGGATACGAAGTAACC	OsWAK51
qRT_WAK51_R2/SM	ATACCGTTCCATGACCTCCTTGG	OsWAK51
qRT_Dehyd_F3/SM	ATGGGAACGCACGGCAC	OsRAB21
qRT_Dehyd_R3/SM	GTGCCGGTGGTCATCCC	OsRAB21
Os8N3 RT Chu F/JS	AGTCGACGGGAGGGTACAG	OsSWEET11
Os8N3 RT R/JS	TTCGGGTACATGACGTAGGG	OsSWEET11
Os04g49194_F1/SM	GTCATCGCCGAGATTGCTCA	OsDOX-2
Os04g49194_R1/SM	TTGAACTGTGCCGGATTAGAGG	OsDOX-2
qRT_Os01g50370_MPK4_F2/SM	GATCAAGTCATTGGCGTGCC	OsMAP3K.4
qRT_Os01g50370_MPK4_R2/SM	GCGCAGACTTTATCCGACG	OsMAP3K.4
Cloning TALE target promoters for GUS assays		
1000bpFlavo_F	TTTGGTCTCACACCCTCTATGCGACATCCTATATAG	OsDOX-1
1000bpFlavo_R	TTTGGTCTCACCTTGCCGCGGTACACACACACAAC	OsDOX-1
1000bpPhos_F	TTTGGTCTCACACCTAGGACAAGTAGTACTACTC	OsPHO1;3
1000bpPhos_R	TTTGGTCTCACCTTGGGAGAGGTGTACTTATACG	OsPHO1;3
P_Aquap_F/SM	TTTGGTCTCTCACCCATTATTGTAATGTCACCTTTGCAA	OsLsi1
P_Aquap_R/SM	TTTGGTCTCTCCTTTTCTGACGCTCTATCTAGCTG	OsLsi1
P_HEN1_F/SM	TTTGGTCTCTCACCATTTTATTGGATGCATGCATTGTATTTA	OsHEN1
P_HEN1_R/SM	TTTGGTCTCTCCTTCAAACGCCCAAAAAAAAAACAACAAAA	OsHEN1
P_HLS_F/SM	TTTGGTCTCTCACCCGCCATACCAATATTTTAGCGTTA	OsHLS1
P_HLS_R/SM	TTTGGTCTCTCCTTGTATATATGCCCGGTGATTGG	OsHLS1
P_OsFBX109neuF/SM	TTTGGTCTCTCACCGTGCCACACACCCTCTAC	OsFBX109
P_OsFBX109neuR/SM	TTTGGTCTCTCCTTAGCCGGACCACCGACAAC	OsFBX109
P_OsPTR2neuF/SM	TTTGGTCTCTCACCTACAGTAACTCAATTCCATCTAT	OsNPF6.3
P_OsPTR2neuR/SM	TTTGGTCTCTCCTTCTTCTCTCTCTCTCTCTCTCTC	OsNPF6.3
P_PectLy_F/SM	TTTGGTCTCTCACAAAAATACAGTAATTAGTTGCAGGACA	OsPLL4
P_PectLy_R/SM	TTTGGTCTCTCCTTTGCTCCCGCGCCTCGAC	OsPLL4
P_TFIIA_F/SM	TTTGGTCTCTCACCGAATGATAAACTTTAATAGTTAATTT GC	OsTFIIAy1
P_TFIIA_R/SM	TTTGGTCTCTCCTTCGATGATCGAATATCGATCCC	OsTFIIAy1
P_TFX1_F/SM	TTTGGTCTCTCACCATATAGGCTTATAGAAGCACACC	OsTFX1
P_TFX1_R/SM	TTTGGTCTCTCCTTGGCTGTTTTCGCTTGTAGT	OsTFX1
P_WAK51_F/SM	TTTGGTCTCTCACCTGAAACTTGAGGGACTAAATTAATA	OsWAK51
P_WAK51_R/SM	TTTGGTCTCTCCTTGCCAGTATATATGGAGATGTATTG	OsWAK51
Adapting TALEs into the MoClo system		
GentR_F/SM	TTTGGTCTCTTATGTTACGCAGCAGCAACGAT	pUC57G
GentR_R/SM	TTTGGTCTCTACAGTTAGGTGGCGGTACTTGGG	pUC57G
pUC57G_F/SM	TTTGGTCTCTCATACTCTCCTTTTCAATATTATTG	pUC57G
pUC57G_R/SM	TTTGGTCTCTCTGTCAGACCAAGTTACTCATAT	pUC57G
pUC57G_SapI_F/SM	TTTGGTCTCTACTTCCGCTTCCCTCGCTCAC	pUC57G

Oligo name	Sequence	Description
pUC57G_SapI_R/SM	TTTGGTCTCTAAGTGCGCCAATACGCAAACCG	pUC57G
Lvl1DummyCDS_F/SM	TTTGGTCTCTAATGGAAGAGCCAATACGCAAACCGCCTCTC	pOS01
Lvl1DummyCDS_R/SM	TTTGGTCTCTAAGCGAAGAGCTATAAACGCAGAAAGGCC CAC	pOS01
ReceiverTALE_F/SM	TTTGCTCTTCTAATGAGAGACCCAATACGCAAACCGCCTC TC	pMC176
ReceiverTALE_R/SM	TTTGCTCTTCTAAGCAGAGACCTATAAACGCAGAAAGGCC CAC	pMC176
qRT-PCR for DOX function assays		
Os09g19734_F/SM	GGTTTGACTGCCAGTCCTGT	ICS
Os09g19734_R/SM	GTCGAGAGTGTGCTGGGTAC	ICS
Os03g17730_F/SM	CCCCTCCTCCTCCTCCTC	ADT
Os03g17730_R/SM	GGCAACCTTGAGCCCCTC	ADT
Os05g25640_F/SM	TCATGTTTCGACCGCCGTTT	C4H
Os05g25640_R/SM	GGTTGATCTCGCCCTCCTC	C4H
Os11g32650_F/SM	CACATGGTCGAGCTCAAGGA	CHS
Os11g32650_R/SM	CATCTTGGCGAGCTGGTAGT	CHS
Os02g21520_F/SM	ATTGCTCAATCGGCGTTGAC	CHI
Os02g21520_R/SM	TCGAGGGTTCAAGCCAAGTT	CHI
Os02g41630_F/SM	CATCTACGGCGTCACCACC	OsPAL
Os02g41630_R/SM	GAACCAGGTCACCGGACG	OsPAL
Os03g03450_F/SM	AAGGGCGAGACCTACGAAGA	OsPAT1
Os03g03450_R/SM	AACACCCACCTCATTGACACA	OsPAT1
Os08g39840_F/SM	ACGATCATAGCGTCGTCACC	OsLOX
Os08g39840_R/SM	GGAGGTCATTCTCCGGTAGC	OsLOX
Os07g03710_F/SM	CTTCGTGGACCCGCACAA	OsPR1a
Os07g03710_R/SM	ACCACCTGCGTGTAGTGC	OsPR1a
Os05g25770qRT_F2/SM	CAGAGCGAGGTCACCTGC	OsWRKY45
Os05g25770qRT_R2/SM	GCCGATGTAGGTGACCCTG	OsWRKY45
cloning sgRNAs		
sgKO_001_F_SB	GTTGGAGAAGCCTGAGCAACTGGG	sgK0001
sgKO_001_R_SB	AAACCCAGTTGCTCAGGCTTCTC	sgK0001
sgKO_002_F_SB	GTTGCAACTCGAGAACAACTCCA	sgK0002
sgKO_002_R_SB	AAACTGGAGTTTGTCTCGAGTTG	sgK0002
sgKO_003_F_SB	GTTGCACTGCTGCTTCGTACACGC	sgK0003
sgKO_003_R_SB	AAACGCGTGTACGAAGCAGCAGTG	sgK0003
sgKO_004_F_SB	GTTGGGCAGAGACTGATGCACAAG	sgK0004
sgKO_004_R_SB	AAACCTTGTGCATCAGTCTCTGCC	sgK0004
sgKO_005_F_SB	GTTGTTATAGTAGTAATCCCCCG	sgK0005
sgKO_005_R_SB	AAACCGGGGGGATTACTACTATAA	sgK0005
sgKO_006_F_SB	GTTGGGGCAACTACGTGCGCCCCG	sgK0006
sgKO_006_R_SB	AAACCGGGGCGCACGTAGTTGCC	sgK0006
sgKO_007_F_SB	GTTGCTTCAACCGAGAACTACGG	sgK0007
sgKO_007_R_SB	AAACCCGTAGTTTCTCGGTTGAAG	sgK0007
sgKO_008_F_SB	GTTGTGATTGATTACTATTCCAA	sgK0008
sgKO_008_R_SB	AAACTTGAATGAGTAATCAATCA	sgK0008
sgKO_017_F_SB	GTTGGGGAGAGGTGTACTIONTATACG	sgK0017
sgKO_017_R_SB	AAACCGTATAAGTACACCTCTCCC	sgK0017
sgKO_018_F_SB	GTTGGCAGTGGTAGTGTGTCTCAA	sgK0018
sgKO_018_R_SB	AAACTTGAGACACACTACCACTGC	sgK0018
sgKO_019_F_SB	GTTGTATATAGATGTAGAATACAG	sgK0019
sgKO_019_R_SB	AAACCTGTATTCTACATCTATATA	sgK0019
sgKO_020_F_SB	GTTGAAGATCGAATACTAATCTCG	sgK0020

Oligo name	Sequence	Description
sgKO_020_R_SB	AAACCGAGATTAGTATTCGATCTT	sgK0020
sgKO_029_F_SB	GTTGAAACGCAGGTGAGAGTGAGA	sgK0029
sgKO_029_R_SB	AAACTCTCACTCTCACCTGCGTTT	sgK0029
sgKO_030_F_SB	GTTGGGCGACGCGTGGGACTACCG	sgK0030
sgKO_030_R_SB	AAACCGGTAGTCCCACGCGTCGCC	sgK0030
sgKO_031_F_SB	GTTGACGTACGTGTGTACCAAGCG	sgK0031
sgKO_031_R_SB	AAACCGCTTGGTACACACGTACGT	sgK0031
sgKO_032_F_SB	GTTGATTGTACTGATGAAGCCG	sgK0032
sgKO_032_R_SB	AAACCGGCTTCATCAGTGACAAT	sgK0032
sgKO_037_F_SB	GTTGAGCACGTAGTTACTGCAGTG	sgK0037
sgKO_037_R_SB	AAACCACTGCAGTAACTACGTGCT	sgK0037
sgKO_038_F_SB	GTTGCTCGCTCCCTCAAACGTCGT	sgK0038
sgKO_038_R_SB	AAACACGACGTTTGAGGGAGCGAG	sgK0038
sgKO_039_F_SB	GTTGGAAAAAACCCTAAAGGCCTA	sgK0039
sgKO_039_R_SB	AAACTAGGCCTTTAGGGTTTTTTC	sgK0039
sgKO_040_F_SB	GTTGTGAAGAGTGACACATGTTTG	sgK0040
sgKO_040_R_SB	AAACCAAACATGTGTCCTCTTCA	sgK0040
sgKO_041_F_SB	GTTGACACATCCAACGCTGCCTAT	sgK0041
sgKO_041_R_SB	AAACATAGGCAGCGTTGGATGTGT	sgK0041
sgKO_042_F_SB	GTTGTCTCCAAGGGTACTTGTGGG	sgK0042
sgKO_042_R_SB	AAACCCACAAGTACCCTTGAGAGA	sgK0042
sgKO_043_F_SB	GTTGAAGCGCCTAGCGCCCTAGCA	sgK0043
sgKO_043_R_SB	AAACTGCTAGGGCGCTAGGCGCTT	sgK0043
sgKO_044_F_SB	GTTGACATGTAATAACCACTAAGC	sgK0044
sgKO_044_R_SB	AAACGCTTAGTGGTTATTACATGT	sgK0044
sgKO_045_F_SB	GTTGACCGGCACCGTCGAGCTCAT	sgK0045
sgKO_045_R_SB	AAACATGAGCTCGACGGTGCCGGT	sgK0045
sgKO_046_F_SB	GTTGGGCACCGTCGAGCTCATCGG	sgK0046
sgKO_046_R_SB	AAACCCGATGAGCTCGACGGTGCC	sgK0046
sgKO_047_F_SB	GTTGAAGCTACTACCGAACATCG	sgK0047
sgKO_047_R_SB	AAACCGATGTTCCGGTAGTAGCTT	sgK0047
sgKO_048_F_SB	GTTGAATGGTGAATCTTCTTGAG	sgK0048
sgKO_048_R_SB	AAACCTCCAAGAAGATTCACCATT	sgK0048
sgKO_049_F_SB	GTTGCAACTACCTCCACAACGCGT	sgK0049
sgKO_049_R_SB	AAACACGCGTTGTGGAGGTAGTTG	sgK0049
sgKO_050_F_SB	GTTGGCCGAATCGAACTCCCCCGG	sgK0050
sgKO_050_R_SB	AAACCCGGGGGAGTTTCGATTCGGC	sgK0050
sgKO_051_F_SB	GTTGTTCCTGAATCATACTGGAA	sgK0051
sgKO_051_R_SB	AAACTTCCAGTATGATTCAGTGAA	sgK0051
sgKO_052_F_SB	GTTGGGAATGGTGAACCTTTTGGG	sgK0052
sgKO_052_R_SB	AAACCCAAAAGTTTCACCATTCC	sgK0052
sgRNA2g1_F_MR	GTTGCGATCAACAAGGAGAGGCTA	sgTT001
sgRNA2g1_R_MR	AAACTAGCCTCTCCTTGTGATCG	sgTT001
sgRNA-AP1_F_MR	GTTGGGTGAAGTGGGGTTTAGGGA	sgTT002
sgRNA-AP1_R_MR	AAACTCCCTAAACCCCACTTACC	sgTT002
sgRNA-Ax71_F pMGE_MR	GTTGTATATAAACCCCTCCAACC	sgTT005
sgRNA-Ax71_R_MR	AAACGGTTGGAGGGGTTTATATA	sgTT005
sgRNA-BX1_F_MR	GTTGTTTTGGTGGTGTACAGTAGG	sgTT007
sgRNA-BX1_R_MR	AAACCTACTGTACACCACCAAAA	sgTT007
sgRNA-TC1_F_MR	GTTGAGGGCATGCATGTCAGCAGC	sgTT008
sgRNA-TC1_R_MR	AAACGCTGCTGACATGCATGCCCT	sgTT008
sgTT009_sgRNA-AR2_F_SB	GTTGAGGAGGCGATGGGTTGGTGA	sgTT009
sgTT009_sgRNA-AR2_R_SB	AAACTACCAACCCATCGCCTCCT	sgTT009

Oligo name	Sequence	Description
sgTT010_sgRNA-AQ2_F_SB	GTTGCGGGGGGAGAGGGGCCGGAT	sgTT010
sgTT010_sgRNA-AQ2_R_SB	AAACATCCGGCCCCTCTCCCCCG	sgTT010
sgTT011_sgRNA-BM2_F_SB	GTTGGGAAGGGAGGAGGGGATTG	sgTT011
sgTT011_sgRNA-BM2_R_SB	AAACCAAATCCCCTCCTCCCTCC	sgTT011
sgTT012_sgRNA-AB1_F_SB	GTTGGAGCTTAGTATAAATCGGCG	sgTT012
sgTT012_sgRNA-AB1_R_SB	AAACCGCCGATTTATACTAAGCTC	sgTT012
sgTT013_sgRNA-AD1_F_SB	GTTGCCCTCCATAGTACGCGCGCG	sgTT013
sgTT013_sgRNA-AD1_R_SB	AAACCGCGCGCTACTATGGAGGG	sgTT013
sgTT014_sgRNA-AE1_F_SB	GTTGGCATAGTAGATTCTCTCCCT	sgTT014
sgTT014_sgRNA-AE1_R_SB	AAACAGGGGAGAGAATCTACTATGC	sgTT014
sgTT015_sgRNA-AH1_F_SB	GTTGCTCCTCCGGCTTATAAATGG	sgTT015
sgTT015_sgRNA-AH1_R_SB	AAACCCATTATAAGCCGGAGGAG	sgTT015
sgTT016_sgRNA-AV1_F_SB	GTTGCTGAGCAACTGGGAGGTGGC	sgTT016
sgTT016_sgRNA-AV1_R_SB	AAACGCCACCTCCCAGTTGCTCAG	sgTT016
sgTT017_sgRNA-AL1_F_SB	GTTGTAGGGAGATCGAGCTAGCTA	sgTT017
sgTT017_sgRNA-AL1_R_SB	AAACTAGCTAGCTCGATCTCCCTA	sgTT017
sgTT018_sgRNA-AO1_F_SB	GTTGACTGGGGAGAGGCTAGCTAG	sgTT018
sgTT018_sgRNA-AO1_R_SB	AAACCTAGCTAGCCTCTCCCCAGT	sgTT018
sgTT019_F_SB	GTTGCTAGCCCTCCCACACACAGC	sgTT019
sgTT019_R_SB	AAACGCTGTGTGTGGGAGGGCTAG	sgTT019
sgTT020_F_SB	GTTGTATGATCTGCCACAAAGTGA	sgTT020
sgTT020_R_SB	AAACTCACTTTGTGGCAGATCATA	sgTT020
sgTT021_F_SB	GTTGATTGCACATCAATGTCATCG	sgTT021
sgTT021_R_SB	AAACCGATGACATTGATGTGCAAT	sgTT021
sgTT025_F_SB	GTTGTTGTCATGGTCTATCGAGGG	sgTT025
sgTT025_R_SB	AAACCCCTCGATAGACCATGACAA	sgTT025
sgTT026_F_SB	GTTGAGGGTGGTGTGTTAATTTG	sgTT026
sgTT026_R_SB	AAACCAAATTAACACACCACCCT	sgTT026
sgTT029_F_SB	GTTGACACATCCAACGCTGCCTAT	sgTT029
sgTT029_R_SB	AAACATAGGCAGCGTTGGATGTGT	sgTT029
sgTT030_F_SB	GTTGACTACGCCACAGGCATCGG	sgTT030
sgTT030_R_SB	AAACCCGATGCCTGTGGGCGTAGT	sgTT030
sgTT031_F_SB	GTTGGACGAGGCCAAAGGACGCGA	sgTT031
sgTT031_R_SB	AAACTCGCGTCTTTGGCCTCGTC	sgTT031
Detection of KO and TT mutations in rice		
SB_OsNIP_AF	ACAAAATCTGAATCCCCGTCGA	K01 <i>OsLsi1</i>
SB_OsNIP_AR	GGTGAGGAGGGAAGAAGTCG	K01 <i>OsLsi1</i>
SB_OsNIP_BR	ACGGAATGATAACGCACATGC	K01 <i>OsLsi1</i>
SB_OsPHO1.1_A_F	CGACGAGAGTTGACAGGAGGAGG	K05 <i>OsPHO1;3</i>
SB_OsPHO1.1_A_R	TCGGGCACAAGCTGGCCCTC	K05 <i>OsPHO1;3</i>
SB_OsPHO1.1_B_R	CTGGGATGGTGTGTTGCAGTTTTTCTTG	K05 <i>OsPHO1;3</i>
SB_TFIIA_F	GCAGTATGCATTGACCAGGTC	TT02 <i>OsTFIIAγ1</i>
SB_TFIIA_R	AGATCGGCATGCAAAGGCT	TT02 <i>OsTFIIAγ1</i>
SB_SulfTr_F	GGAGATCGAACGGTGCCTT	TT02 <i>OsSULTR3;6</i>
SB_SulfTr_R	GGAGCGGAGGAAGGGAAC	TT02 <i>OsSULTR3;6</i>
SB_OsHEN1_F	GGGATGTCGAGCGAGCAG	TT02 <i>OsHEN1</i>
SB_OsHEN1_R	CCGCTAACGTTAACAAGAAGGC	TT02 <i>OsHEN1</i>
SB_OsTFX1_F	ACTACTCGCGCAAGTCAAGT	TT02 <i>OsTFX1</i>
SB_OsTFX1_R	TGGTAGGCTTGGAGGTGAGA	TT02 <i>OsTFX1</i>
SB_SWEET14_F	AGCTAGCAGATTGGCACTTTCT	TT02 <i>OsSWEET14</i>
SB_SWEET14_R	GCCCAGGGATGCTGAAGAG	TT02 <i>OsSWEET14</i>
SB_SWEET11_F	ACACTGAGTGGTCATACGTGTC	TT02 <i>OsSWEET11</i>
SB_SWEET11_R	TGGTTGCATGCTTTACCTGC	TT02 <i>OsSWEET11</i>

Oligo name	Sequence	Description
DOX_500_F_SM	ACAGAGATCGAACACACGG	TT02 & 3 <i>OsDOX-1</i>
DOX_500_R_SM	GACCTGGGAGACGAGCTTG	TT02 & 3 <i>OsDOX-1</i>
FBX_500_F_SM	ATTCAATGTGACACGCAAGATCA	TT03 <i>OsFBX109</i>
SB_OsFBXneu_R	CAACAACACTACCTCCACAACGC	TT03 <i>OsFBX109</i>
SB_OsNPF_F	TAGTCCCACGCGTCGCCAG	TT03 <i>OsNPF6.3</i>
SB_OsNPF_R	GCAGTGAGTGCCCTGATCCAGG	TT03 <i>OsNPF6.3</i>
SB_PecLy_F	GGCGGGAGGTTTAGTACGAGACG	TT03 <i>OsPLL4</i>
SB_PecLy_R	GCCCTGGAACGGGACGGATC	TT03 <i>OsPLL4</i>
SB_Dehyd_F	ATGCCGGCGGTGCCCATCTG	TT03 <i>OsRAB21</i>
SB_Dehyd_R	CGCAGCGTTCAGGCCCATGAG	TT03 <i>OsRAB21</i>
SB_Aqua_R	GGGAAGAAGTCGGCGATGGCC	TT03 <i>OsLsi1</i>
SB_Aqua_F	CGGCCAATGCTGATCCGACAACG	TT03 <i>OsLsi1</i>
SB_PhosTr_F	GTGCGCGGGCTACCTTCCTAG	TT03 <i>OsPHO1;3</i>
SB_PhosTr_R	GCCTCTCTCACCTTGACAGGTC	TT03 <i>OsPHO1;3</i>
SB_16ktrans_F	ACGACGATCCCGACCTCGAACCC	TT04 <i>16K TMP</i>
SB_16ktrans_R	CGTGACCCAAATCGGCACGACG	TT04 <i>16K TMP</i>
SB_TyrProtK_F	CGTCGCTGTGGGAGGAGGTG	TT04 <i>TPK</i>
SB_TyrProtK_R	GGGTCTACAGCTTACCTGTGGG	TT04 <i>TPK</i>
SB_OsWAK51_F	CCGGCGGCGAAAGAAGCCCA	TT04 <i>OsWAK51</i>
SB_OsWAK51_R	TGCGCTGCCTATCATCCATGGCC	TT04 <i>OsWAK51</i>
SB_HLS_F	CGTACGCTTTCCCGTTGCTCTGTG	TT04 <i>OsHLS1</i>
SB_HLS_R	CGCCGCTGCTCTGCACACA	TT04 <i>OsHLS1</i>
other		
qRT_GVG_F/SM	GGTGGGGATCCAATTCAGCA	qRT-PCR GVG
qRT_GVG_R/SM	TGGTATCGCCTTTGCCATT	qRT-PCR GVG
pSKX1_EV_F/SM	TATGGCAGGAGCT	Cloning pSKX1 ev
pSKX1_EV_R/SM	CACCAGCTCCTGC	Cloning pSKX1 ev
M13F	GTA AACGACGGCCAG	sequencing
M13R	CAGGAAACAGCTATGAC	sequencing
Assembly seq F	ATGATATATTTTATCTTG	sequencing
Assembly seq R	GCTCACATGTTCTTCTCCTGC	sequencing
seq rep rev	GGGCGAGATAACTGGGCAAC	sequencing
OcSTer_F	GAGATATGCGAGAAGCCTATGATCG	transgene check
OCSTer_R	GACGCCAATACTCAACTCAAGG	transgene check

2.1.5. sgRNAs

The designed sgRNAs for genome editing applications were evaluated using the Deskgen online tool. Deskgen was designed to predict the most efficient sgRNAs in any given DNA sequence and gives them a score between 1 and 100. As the genome of rice is available in the Deskgen database, potential off targets will also be provided. The Deskgen scores and potential off targets are depicted in Table 6.

Table 6. Evaluation of sgRNAs.

mismatches:	coding off targets				non-coding off targets				Deskgen score	target gene	TALE classes
	0	1	2	3	0	1	2	3			
sgK0001	0	0	0	1	0	0	0	1	72	<i>OsLsi1</i>	AL, AV
sgK0002	0	0	0	0	0	0	0	2	68	<i>OsLsi1</i>	AL, AV
sgK0003	0	0	0	0	0	0	0	1	66	<i>OsLsi1</i>	AL, AV
sgK0004	0	0	0	2	0	0	0	2	59	<i>OsLsi1</i>	AL, AV
sgK0005	0	0	0	0	0	0	0	0	74	<i>OsDOX-1</i>	AQ, BR
sgK0006	0	0	0	1	0	0	0	2	60	<i>OsDOX-1</i>	AQ, BR
sgK0007	0	0	0	0	0	0	0	0	82	<i>OsDOX-1</i>	AQ, BR
sgK0008	0	0	0	0	0	0	0	2	64	<i>OsDOX-1</i>	AQ, BR
sgK0017	0	0	0	0	0	0	0	1	71	<i>OsPHO1;3</i>	AO
sgK0018	0	0	0	0	0	0	0	1	66	<i>OsPHO1;3</i>	AO
sgK0019	0	0	0	0	0	0	0	5	67	<i>OsPHO1;3</i>	AO
sgK0020	0	0	0	0	0	0	0	1	67	<i>OsPHO1;3</i>	AO
sgK0029	0	0	0	0	0	0	0	14	61	<i>OsNPF6.3</i>	AE
sgK0030	0	0	0	0	0	0	0	1	62	<i>OsNPF6.3</i>	AE
sgK0031	0	0	0	0	0	0	0	1	73	<i>OsNPF6.3</i>	AE
sgK0032	0	0	0	0	0	0	0	2	66	<i>OsNPF6.3</i>	AE
sgK0037	0	0	0	0	0	0	0	0	74	<i>OsHLS1</i>	BA
sgK0038	0	0	0	0	0	0	0	1	58	<i>OsHLS1</i>	BA
sgK0039	0	0	0	0	0	0	0	0	64	<i>OsHLS1</i>	BA
sgK0040	0	0	0	0	0	0	0	4	70	<i>OsHLS1</i>	BA
sgK0041	0	0	0	0	0	0	0	1	52	<i>OsWAK51</i>	ES
sgK0042	0	0	0	0	0	0	0	1	64	<i>OsWAK51</i>	ES
sgK0043	0	0	0	0	0	0	0	0	49	<i>OsWAK51</i>	ES
sgK0044	0	0	0	0	0	0	0	0	58	<i>OsWAK51</i>	ES
sgK0045	0	0	0	0	0	0	0	2	69	<i>OsFBX109</i>	AD
sgK0046	0	0	0	0	0	0	0	1	63	<i>OsFBX109</i>	AD
sgK0047	0	0	0	1	0	0	0	1	57	<i>OsFBX109</i>	AD
sgK0048	0	0	0	0	0	0	0	3	63	<i>OsFBX109</i>	AD
sgK0049	0	0	0	11	0	0	2	6	56	<i>OsPLL4</i>	AB
sgK0050	0	1	9	82	0	1	9	86	51	<i>OsPLL4</i>	AB
sgK0051	0	0	0	0	0	0	0	1	73	<i>OsPLL4</i>	AB
sgK0052	0	0	0	0	0	0	0	0	61	<i>OsPLL4</i>	AB
sgTT001 ^A	0	0	0	1	0	0	0	6	49	<i>OsSULTR3;6</i>	BF
sgTT002 ^A	0	0	0	1	0	0	1	5	53	<i>OsHEN1</i>	AP
sgTT005 ^A	0	0	0	0	0	0	0	3	57	<i>OsSWEET14</i>	AC, BH
sgTT007 ^A	0	0	0	0	0	0	0	11	65	<i>OsSWEET11</i>	BX
sgTT008 ^A	0	0	0	1	0	0	0	6	51	<i>OsSWEET14</i>	BS
sgTT009 ^A	0	0	0	0	0	0	0	11	55	<i>OsTFX1</i>	AR, DI
sgTT010 ^{AB}	0	0	0	1	0	0	1	89	46	<i>OsDOX-1</i>	AQ, BR
sgTT011 ^A	0	1	1	1	0	2	9	50	42	<i>OsTFIIAy1</i>	BM
sgTT012 ^B	0	0	0	0	0	0	0	0	63	<i>OsPLL4</i>	AB
sgTT013 ^B	0	0	0	0	0	0	0	2	61	<i>OsFBX109</i>	AD
sgTT014 ^B	0	0	0	0	0	0	0	1	64	<i>OsNPF6.3</i>	AE
sgTT015 ^B	0	0	0	0	0	0	0	0	63	<i>OsRAB21</i>	AH
sgTT016 ^B	0	0	0	0	0	0	0	0	52	<i>OsLsi1</i>	AV
sgTT017 ^B	0	0	0	0	0	0	1	3	51	<i>OsLsi1</i>	AL

mismatches:	coding off targets				non-coding off targets				Deskgen score	target gene	TALE classes
	0	1	2	3	0	1	2	3			
sgTT018 ^B	0	0	0	1	0	0	0	6	67	<i>OsPHO1;3</i>	AO
sgTT019 ^C	0	0	0	0	0	0	0	3	57	<i>OsHLS1</i>	BA
sgTT020 ^C	0	0	0	0	0	0	0	3	63	<i>OsHLS1</i>	BA
sgTT021 ^C	0	0	0	0	0	0	0	2	72	<i>OsWAK51</i>	ES
sgTT025 ^C	0	0	0	0	0	0	0	0	64	<i>TPK</i>	BV
sgTT026 ^C	0	0	0	0	0	0	0	4	56	<i>TPK</i>	BV
sgTT029 ^C	0	0	0	0	0	0	0	1	51	<i>OsWAK51</i>	ES
sgTT030 ^C	0	0	0	0	0	0	0	1	63	<i>16K TMP</i>	BG
sgTT031 ^C	0	0	0	2	0	0	0	15	63	<i>16K TMP</i>	BG

^A sgRNA is used in TT02 construct, ^B sgRNA is used in TT03 construct, ^C sgRNA is used in TT04 construct

2.1.6. Vectors and plasmids

The utilized vector backbones of this thesis are listed in Table 7 and corresponding plasmids with a description of their inserts are depicted in Table 8.

Table 7. List of used vectors.

name	description	reference
Assembly vectors (AV LA – FR)	Assembly vectors of TALE multi repeat modules: <i>Bsal</i> – repeat border – <i>Bpil lacZ Bpil</i> – repeat border – <i>Bsal</i> , kanamycin resistance	Geißler et al., 2011
pAGM8031	MoClo level M assembly vector: backbone derived from pBIN19 & pUC19, LB – <i>Bpil lacZ Bpil</i> – RB, spectinomycin resistance	Weber et al., 2011
pGWB3GG	transient gene expression in plant by <i>Agrobacterium</i> -mediated transformation (promoter analysis): pGWB3 backbone; <i>Bsal lacZ Bsal</i> , <i>uidA</i> CDS, <i>nos</i> ter, kanamycin resistance	Nakagawa et al., 2007
pICH47732	MoClo level 1 vector position 1: backbone derived from pBIN19 & pUC19, LB – <i>Bpil Bsal lacZ Bsal</i> <i>Bpil</i> – RB, ampicillin resistance	Weber et al., 2011
pICH47742	MoClo level 1 vector position 2: backbone derived from pBIN19 & pUC19, LB – <i>Bpil Bsal lacZ Bsal</i> <i>Bpil</i> – RB, ampicillin resistance	Weber et al., 2011
pICH47751	MoClo level 1 vector position 3: backbone derived from pBIN19 & pUC19, LB – <i>Bpil Bsal lacZ Bsal</i> <i>Bpil</i> – RB, ampicillin resistance	Weber et al., 2011
pSKA2	transient gene expression in plant by <i>Agrobacterium</i> -mediated transformation: pVM_BGW backbone, LB- 35S pro, NTM_eGFP, <i>Bsal ccdB Bsal</i> - RB, spectinomycin resistance	Sabiene Thieme
pSKX1	gene expression in <i>Xanthomonas</i> : pBBR1MCS-5 backbone, lac pro, <i>Bsal ccdB Bsal</i> , CTM_FLAG; gentamycin resistance	Streubel et al., 2013
pUC57	Cloning vector for <i>E. coli</i> : pUC19 backbone, <i>lacZ</i> with multiple cloning site ampicillin resistance	Yanisch- Perron et al., 1985
pUC57G	Cloning vector for <i>E. coli</i> : pUC19 backbone, <i>lacZ</i> with multiple cloning site, no <i>SapI</i> sites, gentamycin resistance	This thesis
sgRNA vectors (MoM1 – MoM8E)	MoClo compatible vector for sgRNA cloning: pUC57 backbone; <i>OsU6</i> pro, <i>Bsal ccdB Bsal</i> , sgRNA backbone for <i>SpCas9</i> , ampicillin resistance	Jana Streubel

Table 8. List of used plasmids.

plasmid name	description	backbone ¹	origin ²
Construction of TALEs ³			
pRH*5(34)	single Rep. Pos. 5, RVD H*, 34aa	pUC57	SM
pRHD3(36)	single Rep. Pos. 3, RVD HD, 36aa	pUC57	SM
pRN*3(39)	single Rep. Pos. 3, RVD N*, 39aa	pUC57	SM
pRNS1(36)	single Rep. Pos. 1, RVD NS, 36aa	pUC57	SM
pNTMXooAG4	NTM Xoo TalAG4 (PX083)	pUC57	CS
pCTAOws	CTM Xoo TalAO3 (PX083)	pUC57	MR
pLAAA2	first multiple repeat module for TalAA15	AV LA	SM
pABAA2	second multiple repeat module for TalAA15	AV AB	SM
pBCAA2	third multiple repeat module for TalAA15	AV BC	SM
pCRAA2	fourth multiple repeat module for TalAA15	AV CR	SM
pLAAB2	first multiple repeat module for TalAB16	AV LA	SM
pABAB2	second multiple repeat module for TalAB16	AV AB	SM
pBRAB2	third multiple repeat module for TalAB16	AV BR	SM
pLAAD5	first multiple repeat module for TalAD23	AV LA	SM
pABAD5	second multiple repeat module for TalAD23	AV AB	SM
pBCAD5	third multiple repeat module for TalAD23	AV BC	SM
pCRAD5	fourth multiple repeat module for TalAD23	AV CR	SM
pLAAE4	first multiple repeat module for TalAE15	AV LA	SM
pABAE4	second multiple repeat module for TalAE15	AV AB	SM
pBRAE4	third multiple repeat module for TalAE15	AV BR	SM
pLAAF1	first multiple repeat module for TalAF17	AV LA	SM
pABAF1	second multiple repeat module for TalAF17	AV AB	SM
pBRAf1	third multiple repeat module for TalAF17	AV BR	SM
pLAAG2	first multiple repeat module for TalAG15	AV LA	SM
pABAG2	second multiple repeat module for TalAG15	AV AB	SM
pBCAG2	third multiple repeat module for TalAG15	AV BC	SM
pCRAG2	fourth multiple repeat module for TalAG15	AV CR	SM
pLAAH2	first multiple repeat module for TalAH12	AV LA	SM
pABAH2	second multiple repeat module for TalAH12	AV AB	SM
pBCAH2	third multiple repeat module for TalAH12	AV BC	SM
pCRAH2	fourth multiple repeat module for TalAH12	AV CR	SM
pLAAI3	first multiple repeat module for TalAI3	AV LA	SM
pABAI3	second multiple repeat module for TalAI3	AV AB	SM
pABAI3-34	second multiple repeat module for TalAI3 with aberrant repeat substituted with 34aa	AV AB	SM
pBCAI3	third multiple repeat module for TalAI3	AV BC	SM
pCRAI3	fourth multiple repeat module for TalAI3	AV CR	SM
pLAAL11	first multiple repeat module for TalAL11	AV LA	SM
pABAL11	second multiple repeat module for TalAL11	AV AB	SM
pBRAL11	third multiple repeat module for TalAL11	AV BR	SM
pLAAN2	first multiple repeat module for TalAN15	AV LA	SM
pABAN2	second multiple repeat module for TalAN15	AV AB	SM
pBCAN2	third multiple repeat module for TalAN15	AV BC	SM
pCRAN2	fourth multiple repeat module for TalAN15	AV CR	SM
pLAAO3	first multiple repeat module for TalAO16	AV LA	SM
pABAO3	second multiple repeat module for TalAO16	AV AB	SM
pBRAO3	third multiple repeat module for TalAO16	AV BR	SM
pLAAP3	first multiple repeat module for TalAP15	AV LA	SM
pABAP3	second multiple repeat module for TalAP15	AV AB	SM
pBCAP3	third multiple repeat module for TalAP15	AV BC	SM
pCRAP3	fourth multiple repeat module for TalAP15	AV CR	SM

plasmid name	description	backbone ¹	origin ²
pLAAQ3	first multiple repeat module for TalAQ3	AV LA	SM
pABAQ3	second multiple repeat module for TalAQ3	AV AB	SM
pBCAQ3	third multiple repeat module for TalAQ3	AV BC	SM
pCDAQ3	fourth multiple repeat module for TalAQ3	AV CD	SM
pDRAQ3	fifth multiple repeat module for TalAQ3	AV DR	SM
pLAAR3	first multiple repeat module for TalAR3	AV LA	SM
pABAR3	second multiple repeat module for TalAR3	AV AB	SM
pBCAR3	third multiple repeat module for TalAR3	AV BC	SM
pCRAR3	fourth multiple repeat module for TalAR3	AV CR	SM
pLAAS3	first multiple repeat module for TalAS3	AV LA	SM
pABAS3	second multiple repeat module for TalAS3	AV AB	SM
pBCAS3	third multiple repeat module for TalAS3	AV BC	SM
pCDAS3	fourth multiple repeat module for TalAS3	AV CD	SM
pDRAS3	fifth multiple repeat module for TalAS3	AV DR	SM
pLABA1	first multiple repeat module for TalBA8	AV LA	SM
pABBA1	second multiple repeat module for TalBA8	AV AB	SM
pBRBA1	third multiple repeat module for TalBA8	AV BR	SM
pLABH2	first multiple repeat module for TalBH2	AV LA	SM
pABBH2	second multiple repeat module for TalBH2	AV AB	SM
pBCBH2	third multiple repeat module for TalBH2	AV BC	SM
pCDBH2	fourth multiple repeat module for TalBH2	AV CD	SM
pDRBH2	fifth multiple repeat module for TalBH2	AV DR	SM
pLABJ2	first multiple repeat module for TalBJ2	AV LA	SM
pABBJ2	second multiple repeat module for TalBJ2	AV AB	SM
pBRBJ2	third multiple repeat module for TalBJ2	AV BR	SM
pLABK2	first multiple repeat module for TalBK2	AV LA	SM
pABBK2	second multiple repeat module for TalBK2	AV AB	SM
pBCBK2	third multiple repeat module for TalBK2	AV BC	SM
pCRBK2	fourth multiple repeat module for TalBK2	AV CR	SM
pLABM2	first multiple repeat module for TalBM2	AV LA	SM
pABBM2	second multiple repeat module for TalBM2	AV AB	SM
pBCBM2	third multiple repeat module for TalBM2	AV BC	SM
pCRBM2	fourth multiple repeat module for TalBM2	AV CR	SM
pLABX1	first multiple repeat module for TalBX1	AV LA	SM
pABBX1	second multiple repeat module for TalBX1	AV AB	SM
pBCBX1	third multiple repeat module for TalBX1	AV BC	SM
pCRBX1	fourth multiple repeat module for TalBX1	AV CR	SM
pLACA1	first multiple repeat module for TalCA1	AV LA	SM
pABCA1	second multiple repeat module for TalCA1	AV AB	SM
pBRCA1	third multiple repeat module for TalCA1	AV BR	SM
pLACK1	first multiple repeat module for TalES1	AV LA	SM
pARCK1	second multiple repeat module for TalES1	AV AR	SM
pLACL1	first multiple repeat module for TalET1	AV LA	SM
pABCL1	second multiple repeat module for TalET1	AV AB	SM
pBCCL1	third multiple repeat module for TalET1	AV BC	SM
pCDCL1	fourth multiple repeat module for TalET1	AV CD	SM
pDECL1	fifth multiple repeat module for TalET1	AV DE	SM
pERCL1	sixth multiple repeat module for TalET1	AV ER	SM
TALs for expression in <i>Xanthomonas</i> ³			
pSM013	TalAA15 with natural RVDs and Xoo NTM/CTM	pSKX1	SM
pSM014	TalAB16 with natural RVDs and Xoo NTM/CTM	pSKX1	SM
pnTXAD5	TalAD23 with natural RVDs and Xoo NTM/CTM	pSKX1	SM
pnTXAE4	TalAE15 with natural RVDs and Xoo NTM/CTM	pSKX1	SM

plasmid name	description	backbone ¹	origin ²
pSM015	TalAF17 with natural RVDs and Xoo NTM/CTM	pSKX1	SM
pSM016	TalAG15 with natural RVDs and Xoo NTM/CTM	pSKX1	SM
pnTXAH1	TalAH12 with natural RVDs and Xoo NTM/CTM	pSKX1	SM
pSM026	TalAL11 with natural RVDs and Xoo NTM/CTM	pSKX1	SM
pSM018	TalAN15 with natural RVDs and Xoo NTM/CTM	pSKX1	SM
pSM019	TalAO16 with natural RVDs and Xoo NTM/CTM	pSKX1	SM
pSM020	TalAP15 with natural RVDs and Xoo NTM/CTM	pSKX1	SM
pSM021	TalAQ3 with natural RVDs and Xoo NTM/CTM	pSKX1	SM
pnTXAR3	TalAR3 with natural RVDs and Xoo NTM/CTM	pSKX1	SM
pnTXAS3	TalAS3 with natural RVDs and Xoo NTM/CTM	pSKX1	SM
pSM022	TalBA8 with natural RVDs and Xoo NTM/CTM	pSKX1	SM
pnTXBH2	TalBH2 with natural RVDs and Xoo NTM/CTM	pSKX1	SM
pnTXBJ2	TalBJ2 with natural RVDs and Xoo NTM/CTM	pSKX1	SM
pnTXBK2	TalBK2 with natural RVDs and Xoo NTM/CTM	pSKX1	SM
pSM023	TalBM2 with natural RVDs and Xoo NTM/CTM	pSKX1	SM
pSM024	TalBX1 with natural RVDs and Xoo NTM/CTM	pSKX1	SM
pSM025	TalCA1 with natural RVDs and Xoo NTM/CTM	pSKX1	SM
pnTXDO1	TalES1 with natural RVDs and Xoo NTM/CTM	pSKX1	SM
pnTXDP1	TalET1 with natural RVDs and Xoo NTM/CTM	pSKX1	SM
Full TALEs for expression in <i>Agrobacterium</i>³			
pnTAAB2	TalAB16 with natural RVDs and Hax3 NTM/CTM	pSKA2	SM
pnTAAD5	TalAD23 with natural RVDs and Hax3 NTM/CTM	pSKA2	SM
pnTAAE4	TalAE15 with natural RVDs and Hax3 NTM/CTM	pSKA2	SM
pnTAAH1	TalAH12 with natural RVDs and Hax3 NTM/CTM	pSKA2	SM
pnTAAL1	TalAL11 with natural RVDs and Hax3 NTM/CTM	pSKA2	SM
pnTAAO3	TalAO16 with natural RVDs and Hax3 NTM/CTM	pSKA2	CS
pnTAAAP3	TalAP15 with natural RVDs and Hax3 NTM/CTM	pSKA2	SM
pnTAAQ3	TalAQ3 with natural RVDs and Hax3 NTM/CTM	pSKA2	CS
pnTAAR3	TalAR3 with natural RVDs and Hax3 NTM/CTM	pSKA2	SM
pnTAAS3	TalAS3 with natural RVDs and Hax3 NTM/CTM	pSKA2	SM
pnTABA1	TalBA8 with natural RVDs and Hax3 NTM/CTM	pSKA2	SM
pnTABH2	TalBH2 with natural RVDs and Hax3 NTM/CTM	pSKA2	SM
pnTABJ2	TalBJ2 with natural RVDs and Hax3 NTM/CTM	pSKA2	SM
pnTABK2	TalBK2 with natural RVDs and Hax3 NTM/CTM	pSKA2	SM
pnTABM2	TalBM2 with natural RVDs and Hax3 NTM/CTM	pSKA2	SM
pnTADO1	TalES1 with natural RVDs and Hax3 NTM/CTM	pSKA2	SM
pnTADP1	TalET1 with natural RVDs and Hax3 NTM/CTM	pSKA2	SM
pCS007	Artificial TALE TalD1 with Hax3 NTM/CTM	pSKA2	CS
pCS008	Artificial TALE TalD2 with Hax3 NTM/CTM	pSKA2	CS
pCS036	TalBR1 with natural RVDs and Hax3 NTM/CTM	pSKA2	CS
pT473	TalBL1 with natural RVDs and Hax3 NTM/CTM	pSKA2	SB
pT393	TalAV1 with natural RVDs and Hax3 NTM/CTM	pSKA2	SB
Analysis of truncated TALEs			
pPNTM	Pseudo NTM TalAI3	pUC57	SM
pPCTM_WS	Pseudo CTM TalAI3 with stop	pUC57	SM
pCTMAI4ws	Pseudo CTM TalAI4 with stop	pUC57	SM
pnTAAI3	TalAI3 with Hax3 NTM; Hax3CTM	pSKA2	SM
pnTAAI3_PC	TalAI3 with Hax3 NTM; pseudo CTM AI3	pSKA2	SM
pnTAAI3_PN	TalAI3 with pseudo NTM; Hax3 CTM	pSKA2	SM
pnTAAI3_PNPC	TalAI3 with pseudo NTM; pseudo CTM AI3	pSKA2	SM
pSM001	TalAI3 with Hax3 NTM; CTM AI4	pSKA2	SM
pSM002	TalAI3 with pseudo NTM; CTM AI4	pSKA2	SM

plasmid name	description	backbone ¹	origin ²
pSM003	TalAI3 with Hax3 NTM; CTM AI4; aberrant repeat substituted with 34aa	pSKA2	SM
pSM004	TalAI3 with pseudo NTM; CTM AI4; aberrant repeat substituted with 34aa	pSKA2	SM
pSM005	TalAI3 with Hax3 NTM; Hax3 CTM; aberrant repeat substituted with 34aa	pSKA2	SM
pSM006	TalAI3 with Hax3 NTM; pseudo CTM AI3; aberrant repeat substituted with 34aa	pSKA2	SM
pSM007	TalAI3 with pseudo NTM; Hax3 CTM; aberrant repeat substituted with 34aa	pSKA2	SM
pSM008	TalAI3 with pseudo NTM; pseudo CTM AI3; aberrant repeat substituted with 34aa	pSKA2	SM
pBoxAI3	optimal box for TalAI3	pGWB3GG	SM
pBoxAI3-1	box for TalAI3 -1 at pos. 4	pGWB3	SM
pHax3	TALE Hax3	pSKA2	HS
pBoxHax3	box for TALE Hax3	pGWB3GG	HS
pArtBs4	TALE ArtBs4	pSKA2	JS
p35S:GUS	positive control; GUS under 35S promoter	pGWB3GG	HS
pVSF200::avrBs4	TALE AvrBs4 under 35S promoter; CTM FLAG	n/a	ST
pVTSB::Bs4	genomic Bs4 under natural promoter	n/a	ST
pGWB20::Bs4	genomic Bs4 under 35S promoter; CTM 10x Myc	n/a	ST
TALE target promoters for GUS assays			
pFNSI-1	1000 bp upstream ATG of OsDOX-1 Os03g03034	pGWB3GG	CS
pOsSWEET14	1000 bp upstream ATG of OsSWEET14	pGWB3GG	JS
pPHO1;3	1000 bp upstream ATG of OsPHO1;3 Os06g29790	pGWB3GG	CS
pSM038	1000 bp upstream ATG of Os03g51760 (OsFBX109)	pGWB3GG	SM
pSM039	1000 bp upstream ATG of Os08g05910 (OsNPF6.3)	pGWB3GG	SM
pSM049	1000 bp upstream ATG of Os09g29820 (OsTFX1)	pGWB3GG	SM
pSM050	1000 bp upstream ATG of Os01g73890 (OsTFIIAγ1)	pGWB3GG	SM
pSM051	1000 bp upstream ATG of Os07g06970 (OsHEN1)	pGWB3GG	SM
pSM052	1000 bp upstream ATG of Os02g51110 (OsLsi1)	pGWB3GG	SM
pSM053	1000 bp upstream ATG of Os04g05050 (OsPLL4)	pGWB3GG	SM
pSM054	1000 bp upstream ATG of Os11g26790 (OsRAB21)	pGWB3GG	SM
pSM055	1000 bp upstream ATG of Os03g55530 (OsHLS1)	pGWB3GG	SM
pSM056	1000 bp upstream ATG of Os04g43730 (OsWAK51)	pGWB3GG	SM
pPR58	1000 bp upstream ATG of OsDOX-2 Os04g49149	pGWB3GG	SB
Adapting TALEs into the MoClo system			
pMC167	Xoo NTM MoClo compatible	pUC57	SB
pMC168	Xoo CTM MoClo compatible	pUC57	SB
pOS01	dummy cassette <i>mRFP</i> as lvl 0 CDS module for MoClo; can be switched out with pMC176 content using <i>SapI</i>	pUC57G	OS
pMC2	<i>ZmUbi</i> promoter 2kb Fragment + leader Intron 5'UTR	pUC57	JS
pICH44300	<i>act2</i> terminator + 3'UTR	n/a	PP
pMC190	Expression plasmid with <i>mRFP</i> dummy to be switched out with <i>SapI</i> (<i>ZmUbi</i> pro; <i>mRFP</i> dummy; <i>act2</i> ter)	pICH47742	SM
pOS02	full TALE CDS MoClo compatible for TalAB16	pMC176	OS
pOS03	full TALE CDS MoClo compatible for TalAD23	pMC176	OS
pOS04	full TALE CDS MoClo compatible for TalAE15	pMC176	OS
pOS05	full TALE CDS MoClo compatible for TalAL11	pMC176	OS
pOS06	full TALE CDS MoClo compatible for TalA016	pMC176	OS
pOS07	full TALE CDS MoClo compatible for TalAP15	pMC176	OS
pOS08	full TALE CDS MoClo compatible for TalAQ3	pMC176	OS
pOS09	full TALE CDS MoClo compatible for TalAR3	pMC176	OS

plasmid name	description	backbone ¹	origin ²
pOS10	full TALE CDS MoClo compatible for TalBA8	pMC176	OS
pOS11	full TALE CDS MoClo compatible for TalBH2	pMC176	OS
pOS12	full TALE CDS MoClo compatible for TalBM2	pMC176	OS
pOS13	full TALE CDS MoClo compatible for TalES1	pMC176	OS
pUbiTalAE15	<i>ZmUbi</i> pro; full TalAE15; <i>act2</i> ter; lvl 1 pos. 2	pICH47742	SM
pUbiTalAL11	<i>ZmUbi</i> pro; full TalAL11; <i>act2</i> ter; lvl 1 pos. 2	pICH47742	SM
pUbiTalAO16	<i>ZmUbi</i> pro; full TalAO16; <i>act2</i> ter; lvl 1 pos. 2	pICH47742	SM
pUbiTalBH2	<i>ZmUbi</i> pro; full TalBH2; <i>act2</i> ter; lvl 1 pos. 2	pICH47742	SM
Protoplast assays			
pICH51288	double 35S with omega leader 5'UTR	n/a	PP
pICSL80005	CDS of <i>turboGFP</i> (<i>tGFP</i>) codon-optimized for plants	n/a	PP
pICSL80007	CDS of <i>mCherry</i>	n/a	PP
pICH41421	3'UTR + <i>nos</i> terminator	n/a	PP
pICH50881	MoClo level M end-link 2	n/a	MC
ptGFP	<i>d35S</i> pro; <i>tGFP</i> ; <i>nos</i> ter – lvl 1 pos.1	pICH47732	SM
pmCherry	<i>d35S</i> pro; <i>mCherry</i> ; <i>nos</i> ter– lvl 1 pos.1	pICH47732	SM
pZmUbi::mCherry	<i>ZmUbi</i> pro; <i>mCherry</i> ; <i>nos</i> ter– lvl 1 pos.1	pICH47732	SM
pnTGBH2	lvl M: pos.1 (<i>d35S</i> pro; <i>tGFP</i> ; <i>nos</i> ter) + pos. 2 (<i>ZmUbi</i> pro; full TalBH2; <i>act2</i> ter)	pAGM8031	SM
Cloning DEX-inducible TALEs			
pICH41308	CDS hygromycin resistance	n/a	PP
pICH41432	3'UTR + <i>ocs</i> terminator	n/a	PP
pJOG641	GVG CDS	n/a	EM
pJOG644	Fusion of GAL4UAS and 35S minimal promoter	n/a	EM
pICSL30008	6x HA	n/a	PP
pICH50892	MoClo level M end-link 3	n/a	MC
pMC170	<i>d35S</i> pro; <i>hygR</i> CDS; <i>ocs</i> ter – lvl 1 pos.1	pICH47732	OS
pMC171	<i>ZmUbi</i> pro; GVG CDS; <i>nos</i> ter – lvl 1 pos.2	pICH47742	OS
pMC172	<i>GAL4uas</i> pro; 6xHA; <i>tGFP</i> CDS; <i>act2</i> ter – lvl 1 pos.3	pICH47751	OS
pMC173	lvl M: pMC170 + pMC171 + pMC172	pAGM8031	OS
pMC175	inducible vector with <i>mRFP</i> dummy to be switched out with <i>SapI</i> (<i>GALuas</i> pro;6xHA; <i>mRFP</i> dummy; <i>act2</i> ter)	pICH47751	OS
pOS14	<i>GALuas</i> pro; full TalAB16; <i>act2</i> ter - lvl 1 pos. 3	pICH47751	OS
pOS15	<i>GALuas</i> pro; full TalAD23; <i>act2</i> ter - lvl 1 pos. 3	pICH47751	OS
pOS16	<i>GALuas</i> pro; full TalAE15; <i>act2</i> ter - lvl 1 pos. 3	pICH47751	OS
pOS17	<i>GALuas</i> pro; full TalAL11; <i>act2</i> ter - lvl 1 pos. 3	pICH47751	OS
pOS18	<i>GALuas</i> pro; full TalAO16; <i>act2</i> ter - lvl 1 pos. 3	pICH47751	OS
pOS19	<i>GALuas</i> pro; full TalAP15; <i>act2</i> ter - lvl 1 pos. 3	pICH47751	OS
pOS20	<i>GALuas</i> pro; full TalAQ3; <i>act2</i> ter - lvl 1 pos. 3	pICH47751	OS
pOS21	<i>GALuas</i> pro; full TalAR3; <i>act2</i> ter - lvl 1 pos. 3	pICH47751	OS
pOS22	<i>GALuas</i> pro; full TalBA8; <i>act2</i> ter - lvl 1 pos. 3	pICH47751	OS
pOS23	<i>GALuas</i> pro; full TalBH2; <i>act2</i> ter - lvl 1 pos. 3	pICH47751	OS
pOS24	<i>GALuas</i> pro; full TalBM2; <i>act2</i> ter - lvl 1 pos. 3	pICH47751	OS
pOS25	<i>GALuas</i> pro; full TalES1; <i>act2</i> ter - lvl 1 pos. 3	pICH47751	OS
pDEXAB16	lvl M: pMC170 + pMC171 + pOS14 (TalAB16)	pAGM8031	SM
pDEXAD23	lvl M: pMC170 + pMC171 + pOS15 (TalAD23)	pAGM8031	SM
pDEXAE15	lvl M: pMC170 + pMC171 + pOS16 (TalAE15)	pAGM8031	SM
pDEXAL11	lvl M: pMC170 + pMC171 + pOS17 (TalAL11)	pAGM8031	SM
pDEXAO16	lvl M: pMC170 + pMC171 + pOS18 (TalAO16)	pAGM8031	SM
pDEXAP15	lvl M: pMC170 + pMC171 + pOS19 (TalAP15)	pAGM8031	SM
pDEXAQ3	lvl M: pMC170 + pMC171 + pOS20 (TalAQ3)	pAGM8031	SM
pDEXAR3	lvl M: pMC170 + pMC171 + pOS21 (TalAR3)	pAGM8031	SM
pDEXBA8	lvl M: pMC170 + pMC171 + pOS22 (TalBA8)	pAGM8031	SM

plasmid name	description	backbone ¹	origin ²
pDEXBH2	lvl M: pMC170 + pMC171 + pOS23 (TalBH2)	pAGM8031	SM
pDEXBM2	lvl M: pMC170 + pMC171 + pOS24 (TalBM2)	pAGM8031	SM
pDEXES1	lvl M: pMC170 + pMC171 + pOS25 (TalES1)	pAGM8031	SM
Construction of genome editing constructs			
psgKO_001MoM1	sgK0001 - lvl 0 pos.1 for monocot sgRNA array	MoM1	JC
psgKO_001MoM2	sgK0001 - lvl 0 pos.2 for monocot sgRNA array	MoM2	JC
psgKO_002MoM3	sgK0002 - lvl 0 pos.3 for monocot sgRNA array	MoM3	JC
psgKO_002MoM4	sgK0002 - lvl 0 pos.4 for monocot sgRNA array	MoM4	JC
psgKO_003MoM5	sgK0003 - lvl 0 pos.5 for monocot sgRNA array	MoM5	JC
psgKO_003MoM6	sgK0003 - lvl 0 pos.6 for monocot sgRNA array	MoM6	JC
psgKO_004MoM7	sgK0004 - lvl 0 pos.7 for monocot sgRNA array	MoM7	JC
psgKO_004MoM8E	sgK0004 - lvl 0 pos.8 for monocot sgRNA array	MoM8E	JC
psgKO_005MoM1	sgK0005 - lvl 0 pos.1 for monocot sgRNA array	MoM1	JC
psgKO_005MoM2	sgK0005 - lvl 0 pos.2 for monocot sgRNA array	MoM2	JC
psgKO_006MoM3	sgK0006 - lvl 0 pos.3 for monocot sgRNA array	MoM3	JC
psgKO_006MoM4	sgK0006 - lvl 0 pos.4 for monocot sgRNA array	MoM4	JC
psgKO_007MoM5	sgK0007 - lvl 0 pos.5 for monocot sgRNA array	MoM5	JC
psgKO_007MoM6	sgK0007 - lvl 0 pos.6 for monocot sgRNA array	MoM6	JC
psgKO_008MoM7	sgK0008 - lvl 0 pos.7 for monocot sgRNA array	MoM7	JC
psgKO_008MoM8E	sgK0008 - lvl 0 pos.8 for monocot sgRNA array	MoM8E	JC
psgKO_017MoM1	sgK0017 - lvl 0 pos.1 for monocot sgRNA array	MoM1	JC
psgKO_017MoM2	sgK0017 - lvl 0 pos.2 for monocot sgRNA array	MoM2	JC
psgKO_018MoM3	sgK0018 - lvl 0 pos.3 for monocot sgRNA array	MoM3	JC
psgKO_018MoM4	sgK0018 - lvl 0 pos.4 for monocot sgRNA array	MoM4	JC
psgKO_019MoM5	sgK0019 - lvl 0 pos.5 for monocot sgRNA array	MoM5	JC
psgKO_019MoM6	sgK0019 - lvl 0 pos.6 for monocot sgRNA array	MoM6	JC
psgKO_020MoM7	sgK0020 - lvl 0 pos.7 for monocot sgRNA array	MoM7	JC
psgKO_020MoM8E	sgK0020 - lvl 0 pos.8 for monocot sgRNA array	MoM8E	JC
psgKO_029MoM1	sgK0029 - lvl 0 pos.1 for monocot sgRNA array	MoM1	JC
psgKO_029MoM2	sgK0029 - lvl 0 pos.2 for monocot sgRNA array	MoM2	JC
psgKO_030MoM3	sgK0030 - lvl 0 pos.3 for monocot sgRNA array	MoM3	JC
psgKO_030MoM4	sgK0030 - lvl 0 pos.4 for monocot sgRNA array	MoM4	JC
psgKO_031MoM5	sgK0031 - lvl 0 pos.5 for monocot sgRNA array	MoM5	JC
psgKO_031MoM6	sgK0031 - lvl 0 pos.6 for monocot sgRNA array	MoM6	JC
psgKO_032MoM7	sgK0032 - lvl 0 pos.7 for monocot sgRNA array	MoM7	JC
psgKO_032MoM8E	sgK0032 - lvl 0 pos.8 for monocot sgRNA array	MoM8E	JC
psgKO_037MoM1	sgK0037 - lvl 0 pos.1 for monocot sgRNA array	MoM1	JC
psgKO_037MoM2	sgK0037 - lvl 0 pos.2 for monocot sgRNA array	MoM2	JC
psgKO_038MoM3	sgK0038 - lvl 0 pos.3 for monocot sgRNA array	MoM3	JC
psgKO_038MoM4	sgK0038 - lvl 0 pos.4 for monocot sgRNA array	MoM4	JC
psgKO_039MoM5	sgK0039 - lvl 0 pos.5 for monocot sgRNA array	MoM5	JC
psgKO_039MoM6	sgK0039 - lvl 0 pos.6 for monocot sgRNA array	MoM6	JC
psgKO_040MoM7	sgK0040 - lvl 0 pos.7 for monocot sgRNA array	MoM7	JC
psgKO_040MoM8E	sgK0040 - lvl 0 pos.8 for monocot sgRNA array	MoM8E	JC
psgKO_041MoM1	sgK0041 - lvl 0 pos.1 for monocot sgRNA array	MoM1	JC
psgKO_041MoM2	sgK0041 - lvl 0 pos.2 for monocot sgRNA array	MoM2	JC
psgKO_042MoM3	sgK0042 - lvl 0 pos.3 for monocot sgRNA array	MoM3	JC
psgKO_042MoM4	sgK0042 - lvl 0 pos.4 for monocot sgRNA array	MoM4	JC
psgKO_043MoM5	sgK0043 - lvl 0 pos.5 for monocot sgRNA array	MoM5	JC
psgKO_043MoM6	sgK0043 - lvl 0 pos.6 for monocot sgRNA array	MoM6	JC
psgKO_044MoM7	sgK0044 - lvl 0 pos.7 for monocot sgRNA array	MoM7	JC
psgKO_044MoM8E	sgK0044 - lvl 0 pos.8 for monocot sgRNA array	MoM8E	JC
psgKO_045MoM1	sgK0045 - lvl 0 pos.1 for monocot sgRNA array	MoM1	JC

plasmid name	description	backbone ¹	origin ²
psgKO_045MoM2	sgK0045 - lvl 0 pos.2 for monocot sgRNA array	MoM2	JC
psgKO_046MoM3	sgK0046 - lvl 0 pos.3 for monocot sgRNA array	MoM3	JC
psgKO_046MoM4	sgK0046 - lvl 0 pos.4 for monocot sgRNA array	MoM4	JC
psgKO_047MoM5	sgK0047 - lvl 0 pos.5 for monocot sgRNA array	MoM5	JC
psgKO_047MoM6	sgK0047 - lvl 0 pos.6 for monocot sgRNA array	MoM6	JC
psgKO_048MoM7	sgK0048 - lvl 0 pos.7 for monocot sgRNA array	MoM7	JC
psgKO_048MoM8E	sgK0048 - lvl 0 pos.8 for monocot sgRNA array	MoM8E	JC
psgKO_049MoM1	sgK0049 - lvl 0 pos.1 for monocot sgRNA array	MoM1	JC
psgKO_049MoM2	sgK0049 - lvl 0 pos.2 for monocot sgRNA array	MoM2	JC
psgKO_050MoM3	sgK0050 - lvl 0 pos.3 for monocot sgRNA array	MoM3	JC
psgKO_050MoM4	sgK0050 - lvl 0 pos.4 for monocot sgRNA array	MoM4	JC
psgKO_051MoM5	sgK0051 - lvl 0 pos.5 for monocot sgRNA array	MoM5	JC
psgKO_051MoM6	sgK0051 - lvl 0 pos.6 for monocot sgRNA array	MoM6	JC
psgKO_052MoM7	sgK0052 - lvl 0 pos.7 for monocot sgRNA array	MoM7	JC
psgKO_052MoM8E	sgK0052 - lvl 0 pos.8 for monocot sgRNA array	MoM8E	JC
psgTT001MoM1	sgTT001 - lvl 0 pos.1 for monocot sgRNA array	MoM1	JC
psgTT002MoM2	sgTT002 - lvl 0 pos.2 for monocot sgRNA array	MoM2	JC
psgTT009MoM3	sgTT009 - lvl 0 pos.3 for monocot sgRNA array	MoM3	JC
psgTT010MoM4	sgTT010 - lvl 0 pos.4 for monocot sgRNA array	MoM4	JC
psgTT005MoM5	sgTT005 - lvl 0 pos.5 for monocot sgRNA array	MoM5	JC
psgTT011MoM6	sgTT011 - lvl 0 pos.6 for monocot sgRNA array	MoM6	JC
psgTT007MoM7	sgTT007 - lvl 0 pos.7 for monocot sgRNA array	MoM7	JC
psgTT008MoM8E	sgTT008 - lvl 0 pos.8 for monocot sgRNA array	MoM8E	JC
psgTT012MoM1	sgTT012 - lvl 0 pos.1 for monocot sgRNA array	MoM1	JC
psgTT013MoM2	sgTT013 - lvl 0 pos.2 for monocot sgRNA array	MoM2	JC
psgTT014MoM3	sgTT014 - lvl 0 pos.3 for monocot sgRNA array	MoM3	JC
psgTT015MoM5	sgTT015 - lvl 0 pos.5 for monocot sgRNA array	MoM5	JC
psgTT016MoM6	sgTT016 - lvl 0 pos.6 for monocot sgRNA array	MoM6	JC
psgTT017MoM7	sgTT017 - lvl 0 pos.7 for monocot sgRNA array	MoM7	JC
psgTT018MoM8E	sgTT018 - lvl 0 pos.8 for monocot sgRNA array	MoM8E	JC
psgTT019MoM1	sgTT019 - lvl 0 pos.1 for monocot sgRNA array	MoM1	JC
psgTT020MoM2	sgTT020 - lvl 0 pos.2 for monocot sgRNA array	MoM2	JC
psgTT021MoM3	sgTT021 - lvl 0 pos.3 for monocot sgRNA array	MoM3	JC
psgTT029MoM4	sgTT029 - lvl 0 pos.4 for monocot sgRNA array	MoM4	JC
psgTT025MoM5	sgTT025 - lvl 0 pos.5 for monocot sgRNA array	MoM5	JC
psgTT026MoM6	sgTT026 - lvl 0 pos.6 for monocot sgRNA array	MoM6	JC
psgTT030MoM7	sgTT030 - lvl 0 pos.7 for monocot sgRNA array	MoM7	JC
psgTT031MoM8E	sgTT031 - lvl 0 pos.8 for monocot sgRNA array	MoM8E	JC
psgKOar001	Lvl 1 pos. 3 - sgRNA array K01 (2x sgK0001; 2x sgK0002; 2x sgK0003; 2x sgK0004)	pICH47751	JC
psgKOar002	Lvl 1 pos. 3 - sgRNA array K02 (2x sgK0005; 2x sgK0006; 2x sgK0007; 2x sgK0008)	pICH47751	JC
psgKOar005	Lvl 1 pos. 3 - sgRNA array K05 (2x sgK0017; 2x sgK0018; 2x sgK0019; 2x sgK0020)	pICH47751	JC
psgKOar008	Lvl 1 pos. 3 - sgRNA array K08 (2x sgK0029; 2x sgK0030; 2x sgK0031; 2x sgK0032)	pICH47751	JC
psgKOar010	Lvl 1 pos. 3 - sgRNA array K010 (2x sgK0037; 2x sgK0038; 2x sgK0039; 2x sgK0040)	pICH47751	JC
psgKOar011	Lvl 1 pos. 3 - sgRNA array K011 (2x sgK0041; 2x sgK0042; 2x sgK0043; 2x sgK0044)	pICH47751	JC
psgKOar012	Lvl 1 pos. 3 - sgRNA array K012 (2x sgK0045; 2x sgK0046; 2x sgK0047; 2x sgK0048)	pICH47751	JC

plasmid name	description	backbone ¹	origin ²
psgKOar013	Lvl 1 pos. 3 - sgRNA array KO13 (2x sgK0049; 2x sgK0050; 2x sgK0051; 2x sgK0052)	pICH47751	JC
psgTTar002	Lvl 1 pos. 3 - sgRNA array TT02 (sgTT001; sgTT002; sgTT005; sgTT007; sgTT008; sgTT009; sgTT010; sgTT011)	pICH47751	JC
psgTTar003	Lvl 1 pos. 3 - sgRNA array TT03 (sgTT010; sgTT012; sgTT013; sgTT014; sgTT015; sgTT016; sgTT017; sgTT018)	pICH47751	JC
psgTTar004	Lvl 1 pos. 3 - sgRNA array TT04 (sgTT019; sgTT020; sgTT021; sgTT025; sgTT026; sgTT029; sgTT030; sgTT031)	pICH47751	JC
pICH87633	<i>nos</i> promoter + 5'UTR	n/a	PP
pMC38	<i>nos</i> pro; <i>hygR</i> CDS; <i>ocs</i> ter - lvl 1 pos. 1	pICH47732	SM
pMC64	<i>ZmUbi</i> pro; <i>SpCas9</i> with intron CDS; <i>tGFP</i> ; <i>nos</i> ter - lvl 1 pos.2	pICH47742	JS
psgKOfi_001	lvl M: pMC38 + pMC64 + psgKOar001	pAGM8031	JC
psgKOfi_002	lvl M: pMC38 + pMC64 + psgKOar002	pAGM8031	JC
psgKOfi_005	lvl M: pMC38 + pMC64 + psgKOar005	pAGM8031	JC
psgK0008_final	lvl M: pMC38 + pMC64 + psgKOar008	pAGM8031	SM
psgKOfi_010	lvl M: pMC38 + pMC64 + psgKOar010	pAGM8031	JC
psgKOfi_011	lvl M: pMC38 + pMC64 + psgKOar011	pAGM8031	JC
psgKOfi_012	lvl M: pMC38 + pMC64 + psgKOar012	pAGM8031	JC
psgKOfi_013	lvl M: pMC38 + pMC64 + psgKOar013	pAGM8031	JC
psgTTfi002	lvl M: pMC38 + pMC64 + psgTTar002	pAGM8031	JC
psgTTfi003	lvl M: pMC38 + pMC64 + psgTTar003	pAGM8031	JC
psgTTfi004	lvl M: pMC38 + pMC64 + psgTTar004	pAGM8031	JC
other			
pSM041	small ORF instead of <i>ccdB</i> ; pSKX1 "empty vector"	pSKX1	SM

¹ plasmids with unknown backbones are marked with n/a

² CS Claudia Schwietzer; EM Extended MoClo Parts Kit (Gantner *et al.*, 2018); JC John Connolly; JS Jana Streubel; HS Heidi Scholze; MC MoClo Toolkit (Weber *et al.*, 2011; Werner *et al.*, 2012); MR Maik Reschke; PP MoClo Plant Parts Kit (Engler *et al.*, 2014); SB Sebastian Becker; SM Stefanie Mücke; ST Sabine Thieme; OS Olivia Sierra

³ assigned TALE names changed after the initial cloning of these plasmids; description contains current and published names

2.1.7. Plant material

In this thesis, *Nicotiana benthamiana* plants were used for *Agrobacterium*-mediated transient expression of reporter constructs. *N. benthamiana* plants were grown in the green house at 26 – 28 °C, 65% relative humidity and a 16 h light period.

The *Oryza sativa* variety Nipponbare was used for infection experiments and phenotype assessments of Xoo. The plants were grown in the green house at 25 – 28 °C during the 16 h light period and 22 – 24 °C at night. The relative humidity was 65% and the substrate was composed of 50% "Klaasmann Substrat 1" and 50% gardening earth for rhododendron plants.

The rice variety Kitaake was utilized for *Agrobacterium*-mediated transformation and subsequent assessments. The plants were either grown in the green house as described

for variety Nipponbare or grown in sterile culture on ½ MS medium in an incubation cabinet at 28°C and 16 h light.

2.2.Methods

2.2.1. DNA work

2.2.1.1. Plasmid isolation

The isolation of plasmid DNA was done according to user manuscripts using the QIAprep Spin Miniprep Kit (QIAGEN GmbH/Hinden, Germany) for regular use and CompactPrep Plasmid Midi Kit (QIAGEN GmbH/Hinden, Germany) for samples with the need of high DNA concentrations in large volumes. The elution was done with 50 µl dH₂O (QIAprep Spin Miniprep Kit) and 200 µl dH₂O (CompactPrep Plasmid Midi Kit).

2.2.1.2. DNA amplification via polymerase chain reaction

The PCR (polymerase chain reaction) is a method to amplify DNA fragments (Saiki *et al.*, 1988). For normal purposes, the KAPA Taq polymerase (Merck KGaA/Darmstadt, Germany) was used. The Taq polymerase of *Thermus aquaticus* has an elongation speed of about 1 kbp per minute. If the DNA is to be used for cloning or sequencing purposes, a polymerase with proofreading function should be used. The proof-reading Fusion polymerase can generate 1 kbp in 15-30 sec (Thermo Fisher Scientific Inc./Waltham, United States of America). The reactions were mixed according to the user manuals:

KAPA Taq polymerase:

18.5 µl	dH ₂ O
2.5 µl	10x KAPA Taq buffer
0.5 µl	10 mM dNTPs
1 µl	10 µM forward primer
1 µl	10 µM reverse primer
0.1 µl	5 U/µl KAPA Taq
1 µl	Template DNA

Phusion polymerase:

13.4 µl	dH ₂ O
4 µl	5x Phusion HF/GC buffer
0.4 µl	10 mM dNTPs
0.5 µl	10 µM forward primer
0.5 µl	10 µM reverse primer
0.2 µl	2 U/µl Phusion
1 µl	Template DNA

The reactions were put in a thermal cycler with a heated lid (Analytik Jena AG/Jena, Germany). The program was selected as followed:

Steps:	KAPA Taq:		Fusion:	
Initial denaturation	95 °C	3 min	98 °C	30 sec
Denaturation	95 °C	30 sec	98 °C	10 sec
Annealing	X °C	30 sec	-	-
Elongation	72 °C	Y min	72 °C	Z min
Final elongation	72 °C	5 min	72 °C	5 min
Hold	10 °C	∞	10 °C	∞

The annealing temperature X is dependent on the used primers, the elongation time Y is to be calculated based on amplicon size (1 kbp/min) and the elongation time Z is dependent on the complexity of the template DNA and should be calculated for plasmid DNA with 1 kbp/15 sec and for genomic DNA with 1 kbp/30 sec.

2.2.1.3. Agarose gel electrophoresis

The agarose gel electrophoresis is used to separate DNA fragments according to their size. The common usage required 1% (w/v) agarose in 1x TAE buffer (Table 4) and 3 µl MIDORI Green per 100 ml agarose gel. The electrophoresis was done using Sub-Cell Modell 96 or 192 Cell (Bio-Rad Laboratories Inc./Hercules, United States of America). MIDORI Green can make DNA visible under UV light and the ChemiDoc Imaging System (Bio-Rad Laboratories Inc./Hercules, United States of America) was used for detection. The size of DNA fragments was assessed with the help of GeneRuler 1 kb Plus DNA Ladder (Thermo Fisher Scientific Inc./Waltham, United States of America).

2.2.1.4. Gel extraction of DNA

The extraction of DNA out of agarose gels was done by cutting out the region of interest with a scalpel. The excised piece of gel was treated according to the user manual of the utilized GeneJET Gel Extraction Kit (Thermo Fisher Scientific Inc./Waltham, United States of America). The elution was done using 20 µl dH₂O.

2.2.1.5. Restriction digest

The sequence specific digest of isolated plasmids was done using appropriate restriction enzymes. The utilized buffers, reaction temperature and enzyme concentrations were chosen according to manufacturer recommendations. The restriction enzymes were purchased at Thermo Fisher Scientific Inc./Waltham, United States of America and New England Biolabs Inc./Ipswich, United States of America. The amount of digested DNA was usually 1 µg and digest reactions were incubated for mostly 1 h. The results of restriction digests were analyzed using agarose gel electrophoresis.

2.2.1.6. Blunt-end cloning into pUC57 & pUC57G

Cloning fragments into pUC57 or pUC57G was done using the blunt-end cutting restriction enzyme *Sma*I, which has a recognition site in the multiple cloning site of pUC57 and pUC57G. The fragment was amplified via PCR, analyzed with an agarose gel electrophoresis, the appropriate fragment size was excised, and the DNA was extracted. The reaction was performed as followed:

Reaction mix:		Thermal cycler program:	
5 µl	Elution of Gel Extraction	25 °C	1 h
1 µl	10x CutSmart Buffer	10 °C	∞
1 µl	10 mM ATP		
1 µl	pUC57(G) (50 ng/µl)		
1 µl	<i>Sma</i> I (20 U/µl)		
1 µl	T4 ligase (5 U/µl)		

Afterwards, the reaction product was used to transform *E. coli*. Selected colonies were cultured, plasmids were isolated, checked with a restriction digest and sequenced using the M13_F or M13_R primers.

2.2.1.7. Golden Gate cloning

The Golden Gate cloning method (Engler *et al.*, 2008) is based on the specific properties of type IIS restriction enzymes, which cut DNA outside of their recognition site. This enables the design of specific DNA overhangs that can be created by these enzymes, which do not have requirements for their cutting sites. The cloning method combines several fragments, which are flanked by type IIS recognition sites in a fashion that permits scar-free assembly according to the designed overhangs. This method can be used in a cutligation, which simultaneously contains restriction enzymes and ligase in one reaction, because the final product does not contain restriction enzyme recognition sites.

2.2.1.7.1. Generating new vectors with Golden Gate cloning

The generation of new vector backbones, like pUC57G, was done by Golden Gate cloning. The appropriate parts of the backbone were amplified from donor vectors using specific primers with flanking *Bsa*I sites, analyzed via agarose gel electrophoresis and the selected PCR fragments were extracted out of the gel. These PCR fragments were assembled in a cutligation in the thermal cycler (Analytik Jena AG/Jena, Germany):

Reaction mix:		Thermal cycler program:		
4 µl	10x CutSmart Buffer	37 °C	20 min	30x
4 µl	10 mM ATP	16 °C	20 min	
10 µl	Elution of fragment 1	65 °C	10 min	
10 µl	Elution of fragment 2	10 °C	∞	
10 µl	Elution of fragment 3			
1 µl	<i>Bsa</i> I (20 U/µl)			
1 µl	T4 ligase (5 U/µl)			

Afterwards, the reaction product was used to transform *E. coli*. Selected colonies were cultured, plasmids were isolated, checked with a restriction digest.

2.2.1.7.2. Golden TALE Technology

TALEs were assembled in two steps using the Golden TALE Technology, which utilizes the Golden Gate cloning principles. Single repeat modules have flanking *Bpil* sites determining their position in the multi repeat modules assembled in the first cloning step. In order to create multi repeat modules with less than six repeats, “stop repeats” (1s - 5s) can be employed. The cutligation was performed in a thermal cycler (Analytik Jena AG/Jena, Germany):

Reaction mix (20 µl):		Thermal cycler program:		
2 µl	10x Buffer Green	37 °C	10 min	30x
2 µl	10 mM ATP	16 °C	10 min	
1 µl	per used repeat module (50 ng/µl)	65 °C	10 min	
1 µl	Assembly vector (50 ng/µl)	10 °C	∞	
1 µl	<i>Bpil</i> (20 U/µl)			
1 µl	T4 ligase (5 U/µl)			
add	dH ₂ O			

Afterwards, the reaction product was used to transform *E. coli*. Selected colonies were cultured, plasmids were isolated, checked with a *Bsa*I restriction digest and sequenced using the Assembly_seq_R primer. Subsequently, the intended multi repeat modules as well as TALE NTM and CTM were assembled into the final vector. The cutligation was performed in a thermal cycler (Analytik Jena AG/Jena, Germany):

Reaction mix (20 μ l):		Thermal cycler program:	
2 μ l	10x CutSmart Buffer	37 °C	10 min
2 μ l	10 mM ATP	16 °C	10 min
1 μ l	per multi repeat module (50 ng/ μ l)	65 °C	10 min
1 μ l	final vector (50 ng/ μ l)	10 °C	∞
1 μ l	NTM module (50 ng/ μ l)		
1 μ l	CTM module (50 ng/ μ l)		
1 μ l	<i>Bsa</i> I (20 U/ μ l)		
1 μ l	T4 ligase (5 U/ μ l)		
add	dH ₂ O		

Afterwards, the reaction product was used to transform *E. coli*. Selected colonies were cultured, plasmids were isolated, checked with a *Stu*I & *Aat*II double restriction digest.

2.2.1.7.3. Cloning in the MoClo system

The MoClo system (Weber *et al.*, 2011; Engler *et al.*, 2014) utilizes Golden Gate cloning mechanisms to create a unified system of cloning vectors to assemble transcriptional units (TUs) from standardized building blocks. Therefore, several sets of cloning vectors are established: level 0 vectors contain the standardized building blocks for TUs like promoters, tags, CDS and terminators. Level 0 vectors have standardized overhangs to guarantee flawless assemblies and all modules are free of the utilized type IIS restriction enzyme sites. Level 0 modules are assembled into level 1 vectors using *Bsa*I. The flanking regions of level 1 vectors contain *Bpi*I sites that enable the creation of constructs with multiple TUs and additionally, T-DNA borders for use in *Agrobacterium*. Multiple level 1 TUs can be combined into level 2 or level M vectors, both containing T-DNA borders as well. In this thesis, level M vectors were used to create complex constructs with *Bpi*I.

2.2.1.8. Transformation of bacteria

2.2.1.8.1. Transformation of electrocompetent cells

The transformation of electrocompetent cells was done using the electroporation method with 2 μ l of plasmid DNA and 50 μ l of electrocompetent bacterial cells (*E. coli*, *A. tumefaciens* or *Xoo*). The cooled electroporation cuvette (gap width 1 mm) was filled with the reaction mix and put in the MicroPulser Electroporator (Bio-Rad Laboratories Inc./Hercules, United States of America) on program Ec2 (U = 2500 V; R = 200 Ω). Afterwards, the bacterial cells were put in 500 μ l of the appropriate liquid media and

incubated for 1 h at the right temperature. Finally, the bacterial suspension was plated on selective media and incubated accordingly (Table 2, Table 3).

2.2.1.8.2. Transformation of chemically competent cells

50 µl of chemically competent *E. coli* cells per reaction were thawed on ice. Up to 20 µl of plasmid DNA or cloning reaction products were mixed with the cells gently and incubated on ice for 30 min. Afterwards, the tube was put in an Eppendorf ThermoMixer C Dry Block Heating and Cooling (Eppendorf AG/Hamburg, Germany) at 42°C for 1 min. Subsequently, 250 µl liquid LB medium was added and the reaction was incubated at 37°C for 1 h. Finally, the bacterial suspension was plated on selective media and incubated over night at 37°C (Table 2, Table 3).

2.2.1.9. DNA sequencing

Sequencing of PCR products and plasmids was done by an external lab of the service provider SeqLab (Microsynth SeqLab GmbH/Göttingen, Germany). The send in samples contained 3 µl of the sequencing primer (10 mM) and 12 µl of template DNA (~1 µg total).

2.2.2. RNA work

2.2.2.1. RNA isolation from rice

To be analyzed plant material was harvested into a safe lock tube containing 2 metal balls, frozen in liquid nitrogen and stored at -80°C. The tissue was disrupted using the TissueLyser II (QIAGEN GmbH/Hinden, Germany). The total RNA was isolated using the RNeasy Mini Kit (QIAGEN GmbH/Hinden, Germany) and the elution was done with 40 µl RNase-free dH₂O. The isolated RNA was measured photometrically with the Spark M10 multimode microplate reader (Tecan Group Ltd./Männedorf, Switzerland). RNA was stored at -80°C.

2.2.2.2. cDNA synthesis

2 µg of the isolated total RNA per sample was transcribed into complementary DNA (cDNA) using the Maxima First Strand cDNA synthesis Kit (Thermo Fisher Scientific Inc./Waltham, United States of America) according to the user guide. The reaction was incubated in a thermal cycler with a heated lid (Analytik Jena AG/Jena, Germany) according to user guidelines and the reaction product was diluted with 20 µl RNase-free dH₂O to a final concentration of about 50 ng cDNA / µl. cDNA was stored at -20°C.

2.2.2.3. Quantitative real-time PCR

The quantitative real-time PCR (qRT-PCR) was done using the ABsolute Blue QPCR Mix (Thermo Fisher Scientific Inc./Waltham, United States of America) according to the user

guide. The 20 µl reactions including 4 µl of a 1:8 dilution of template cDNA (~25 ng) were run in a CFX Connect Real-Time PCR Detection System (Bio-Rad Laboratories Inc./Hercules, United States of America). Each sample was run as two technical replicates. The cDNA was replaced with water in negative controls.

The specificity of primer pairs was checked using a melting curve of the final PCR product. The amplification efficiency for each primer pair was analyzed using a standard curve plot of a dilution series. cDNA amounts were normalized using actin as a reference gene. The fold change induction was calculated using the $\Delta\Delta C_t$ method (Livak and Schmittgen, 2001). The fold change of the gene of interest (GOI) was calculated:

$$\text{fold change} = \frac{\text{primer efficiency (GOI)}^{\text{Ct value (reference)} - \text{Ct value (sample)}}}{\text{primer efficiency (actin)}^{\text{Ct value (reference)} - \text{Ct value (sample)}}$$

2.2.3. Protein work

2.2.3.1. Quantitative GUS assay

The quantitative GUS assay was performed as described in Boch *et al.* (2009). In short, *N. benthamiana* was inoculated with *Agrobacterium* strains carrying GUS reporter constructs and corresponding TALEs. Two days after the inoculation, two leaf disks (7 mm diameter) per inoculation spot were harvested into a safe lock tube containing ceramic beads and frozen in liquid nitrogen. The tissue was disrupted using the TissueLyser II (QIAGEN GmbH/Hinden, Germany). 300 µl of GUS extraction buffer were added to each sample and mixed vigorously. The suspension was centrifuged for 5 min at 4°C and 14.000 rpm. 200 µl of the supernatant were transferred into 96-well plates and centrifuged again for 5 min at 4°C and 14.000 rpm. 10 µl of the supernatant were mixed with 90 µl of GUS extraction buffer (Table 4) containing 5 mM MUG (4-methylumbelliferyl-β-D-glucuronid) and incubated at 37°C for 60 – 90 min. Each sample was done in technical duplicates. After the incubation period, 10 µl of the mix was added to 90 µl of 0.2 M sodium carbonate to stop the reaction. The β-glucuronidase hydrolyzed MUG into the fluorescent MU (4-methylumbilliferone). The MU fluorescence (excitation 360 nm; emission 465 nm) of the samples was measured in the Spark M10 multimode microplate reader (Tecan Group Ltd./Männedorf, Switzerland). The GUS activity was assessed using a standard plot curve with MU standard solutions and the samples were normalized to the total protein concentration assessed by Bradford assay.

2.2.3.2. GUS staining

Leaf disks for qualitative GUS staining were harvested in parallel to the samples for the quantitative GUS assay. Histochemical staining was performed using 5-bromo-4-chloro-3-indolyl β -D-glucuronide (X-Gluc) as a substrate. X-Gluc is hydrolyzed by β -glucuronidase and the product will turn blue with exposure to oxygen. The leaf disks were submerged in GUS staining solution (Table 4) and vacuum infiltrated with a needleless syringe. The suspension was incubated overnight at 37°C and afterwards leaf disks were destained using 96% ethanol.

2.2.3.3. Bradford assay

The determination of the protein concentration in a given sample was done using the Bradford assay. 10 μ l of a 1:10 dilution of the samples were mixed with 70 μ l dH₂O and 20 μ l Roti-Quant (Carl Roth GmbH/Karlsruhe, Germany) and incubated for 20 min at room temperature. Afterwards, the absorption of each sample at 595 nm was checked using the Spark M10 multimode microplate reader (Tecan Group Ltd./Männedorf, Switzerland). The assessment of the protein concentration was done using a standard curve plot with BSA (bovine serum albumin) standard solutions.

2.2.3.4. Protein isolation of *Xanthomonas*

The appropriate *Xanthomonas* strains were cultured in selective PSA liquid media (Table 2) overnight. The optical density at 600 nm was measured and the equivalent of 1 ml of an OD₆₀₀ = 0.2 suspension was harvested. The suspension was centrifuged at full speed for 2 min and supernatant was removed. 70 μ l of 4x Lämmli (Table 4) was added and the samples were incubated at 98°C for 10 min in the ThermoMixer C (Eppendorf AG/Hamburg, Germany). Samples were stored at -20°C.

2.2.3.5. SDS-PAGE

The separation of protein by their molecular weight was done using a sodium dodecyl sulfate polyacrylamide gel electrophoresis (SDS-PAGE). The gels were comprised of a 4% stacking gel and a 10% separation gel (Table 4). Usually, 15 μ l of samples was loaded on the gels and the size of separated proteins was assessed using the PageRuler Prestained Protein Ladder (Thermo Fisher Scientific Inc./Waltham, United States of America). The electrophoresis was done using the Mini-PROTEAN Tetra Vertical Electrophoresis Cell (Bio-Rad Laboratories Inc./Hercules, United States of America) and 1x TANK buffer (Table 4).

2.2.3.6. Western Blot analysis

After an SDS-PAGE, the separated proteins were transferred to a nitrocellulose membrane via semidry blot in a Trans-Blot Turbo Transfer System (Bio-Rad Laboratories Inc./Hercules, United States of America) utilizing Towbin buffer (Table 4). After the transfer, the membrane was blocked for 30 min in blocking solution (Table 4), washed in 1x TBST (Table 4) and afterwards, the membrane was incubated with the primary antibody (dilution 1:10.000) at 4°C overnight. The next day, the membrane was washed in 1 x TBST three times for 10 min and then the membrane was incubated with the appropriate secondary antibody (dilution 1:10.000) at room temperature for 1 h. Finally, the membrane was washed again in 1 xTBST three times for 10 min. In order to detect the signals of the secondary antibody, the membrane is incubated in ECL solution (Table 4) for 1 min and detection was done using the ChemiDoc Imaging System (Bio-Rad Laboratories Inc./Hercules, United States of America).

2.2.4. Plant work

2.2.4.1. *Agrobacterium*-mediated transient expression in *N. benthamiana*

The expression of genes in *N. benthamiana* was done transiently using *A. tumefaciens*. The appropriate *A. tumefaciens* strains, which contained plasmids with the desired construct, were cultured on selective YEB plates at 28°C for two days (Table 2). Afterwards, the strains were resuspended in AIM media (Table 4) and the optical density was adjusted to 0.8 at 600 nm using the spectrophotometer Ultrospec 3000 (Pharmacia Biotech/Uppsala, Sweden). The adjusted bacterial suspensions were mixed 1:1 in the appropriate combinations or 1:1 with AIM as negative controls. These mixtures were inoculated into *N. benthamiana* using a needleless syringe.

2.2.4.2. HR assay in *N. benthamiana*

In order to check for an HR, *N. benthamiana* was inoculated with *A. tumefaciens* strains carrying appropriate constructs. Strains were adjusted to an optical density (600 nm) of 0.8 and mixed in different combinations. Strains were either inoculated as a mixture or with 6 h delay between overlapping inoculation spots. 7 days post inoculation (dpi) whole leaves were harvested, destained in 96% ethanol at 60°C for a week and pressed. HR can be detected as browning regions on destained leaves.

2.2.4.3. Inoculation of rice with *Xanthomonas*

The appropriate *Xanthomonas* strains were cultured on selective PSA media for 2 – 3 days, resuspended in 10 mM MgCl₂ and adjusted to an optical density of 0.5 at 600 nm.

The inoculation was done using a needleless syringe and the inoculated rice plants were usually 4 weeks old. 6 inoculation spots per 5 cm (starting 1 cm behind the leaf tip) of the second and third true leaves were done. The harvest for RNA isolation was usually done after 48 h and harvest for phenotypic evaluation were usually done after 6 days.

2.2.4.4. Leaf clipping assay

The appropriate *Xanthomonas* strains were cultured on selective PSA media for 2 – 3 days, resuspended in 10 mM MgCl₂ and adjusted to an optical density of 0.2 at 600 nm. The infected rice plants were usually 4 weeks old. Scissors were dipped into the bacterial suspension and 1 cm of the tip of the third true leaf was cut off. The leaves were harvested after 14 days for phenotypic evaluation.

2.2.4.5. Bacterial growth assay

In order to evaluate bacterial growth of *Xanthomonas* in rice, infections were done with the leaf clipping method. 14 days after infection, leaves were harvested and separated into two 5 cm long pieces (0 - 5 cm and 5 - 10 cm after the clipping site). The samples were put in safe lock tubes with two metal balls and the tissue was disrupted at room temperature using the TissueLyser II (QIAGEN GmbH/Hinden, Germany). 1 ml of 10 mM MgCl₂ was added to each sample and a dilution series with 1:1, 1:10, 1:100, 1:1000, 1:10.000 and 1:100.000 in 10 mM MgCl₂ was prepared for each sample. 50 µl of each dilution for each sample was plated on selective PSA plates containing rifampicin and cycloheximide. The colony forming units (CFU) were calculated after three days.

2.2.4.6. Salicylic acid assay

In order to determine the salicylic acid concentration of infected and not infected rice leaves, the samples were harvested at different time intervals as described for each experiment. The spectrophotometric evaluation of salicylic acid content was done as described in Warriar *et al.* (2013). In short, the samples were collected in safe lock tubes with 2 metal balls and frozen in liquid nitrogen. The tissue was disrupted using the TissueLyser II (QIAGEN GmbH/Hinden, Germany) and samples were incubated in dH₂O (1 ml / 50 mg plant tissue) at 50°C for 10 min and 600 rpm shaking using the ThermoMixer C (Eppendorf AG/Hamburg, Germany). Afterwards, samples were centrifuged for 10 min at full speed. 100 µl of the supernatant were mixed with 2750 µl dH₂O and 150 µl of a 2% (w/v) FeCl₃ solution. The salicylic acid and FeCl₃ create a purple complex that was detected at 540 nm using the spectrophotometer Ultrospec 3000 (Pharmacia Biotech/Uppsala, Sweden). The amount of salicylic acid was estimated using a standard curve plot with salicylic acid standard solutions.

2.2.4.7. Sterile culture of rice seedlings

Rice seeds were dehulled with a hand mill and incubated in 70% ethanol for 1 min. Supernatant was removed and seeds are incubated in 6% sodium hypochlorite for 30 min with gentle shaking in intervals of 5 min. The supernatant was removed and seeds were washed three times with sterile water. Seeds were put on ½ MS media for sterile culture (Table 2).

2.2.4.8. Protoplast isolation

The isolation of rice protoplasts from stems and sheaths was done as described in Shan *et al.* (2014). In short, rice seedlings (~7 plants per desired transformation) were grown in sterile culture for two weeks, cut into small strips with a razor blade and incubated in 0.6 M mannitol for 10 min in the dark. Strips were transferred into filter-sterilized cell wall-dissolving enzyme solution (Table 4) and vacuum (~400 mmHg) was applied for 30 min in the dark. Afterwards, the strips were incubated in the cell wall-dissolving enzyme solution for 6 h with gentle shaking (70 rpm) in the dark at room temperature. After digestion, W5 buffer (Table 4) was added gently mixed with the suspension. Protoplasts were separated from the strips by filtering the suspension through a 40 µm nylon mesh. The strips were washed 5 more times with W5 buffer and all collected filtrate was transferred into round-bottomed centrifugation tubes. The filtrate was centrifuged at 250 g for 3 min at room temperature in a swinging bucket rotor and the supernatant was removed. Protoplasts were resuspended in a smaller volume of W5 and centrifuged again at 250 g for 3 min at room temperature. The supernatant was removed and protoplasts were finally resuspended in MMG solution (Table 4). The protoplast concentration can be checked with a hemocytometer under a microscope.

2.2.4.9. Protoplast transformation

The transformation of protoplasts after their isolation was done according to Shan *et al.* (2014). In short, 40 µl of plasmid DNA (~ 20 µg) were gently mixed with 200 µl isolated protoplasts and 220 µl PEG solution (Table 4) by gentle tapping. The mixture is incubated for 20 min in the dark and afterwards the transformation process was stopped by adding 880 µl W5 buffer and inverting of the tube. The suspension was centrifuged at 250 g for 3 min at room temperature and the supernatant was removed. The protoplasts are resuspended in 2 ml WI buffer (Table 4) and transferred into a 6-well plate. The transformed protoplasts are incubated at room temperature in the dark for usually 24 h. Finally, transformation efficiency is tested by checking the fluorescence of the transformation markers under the fluorescence microscope Nikon Eclipse Ti

(Nikon/Tokyo, Japan). The utilized filters for the different fluorescent markers are listed in Table 9.

Table 9. Overview of excitation and emission maxima of fluorescent markers and corresponding filters.

marker	excitation peak	emission peak	filter	excitation	emission
esculin	367 nm	454 nm	DAPI	390±18 nm	460±60 nm
tGFP	482 nm	502 nm	GFP	469±35 nm	525±39 nm
mCherry	587 nm	610 nm	TexasRed	559±34 nm	639±69 nm

2.2.4.10. Protoplast esculin uptake assay

The protoplast-esculin assay was performed as described in Rottmann *et al.* (2018). In short, rice protoplasts were isolated and transformed with appropriate constructs as described before. 24 h after transformation the protoplasts were transferred into W5 buffer containing 1 mM esculin and incubated for 40 min in the dark. The supernatant was removed and protoplasts were resuspended in W5 buffer and analyzed under the fluorescence microscope Nikon Eclipse Ti (Nikon/Tokyo, Japan).

2.2.4.11. Dexamethasone induction *in planta*

The induction of DEX-inducible expression constructs was performed in transiently transformed *N. benthamiana* plants and stable transformants in rice. In *N. benthamiana*, induction was performed 24 h after the inoculation of corresponding *Agrobacterium* strains. The inoculation spots were coated with a 10 µM DEX solution using a paintbrush. Transformed rice plants were coated with a 30 µM DEX solution containing 0.01% Tween20 with a paintbrush. 24 h after induction, samples were harvested for further analysis (e.g. microscopy).

2.2.4.12. *Agrobacterium*-mediated stable transformation of rice callus

The stable transformation of rice calli with *Agrobacterium* was done as described in Sallaud *et al.* (2003). An overview of required specialized media and a summary of culturing conditions are provided in Table 10 and Table 11, respectively.

In short, rice seeds were sterilized and put on callus-inducing media for 3 weeks and then calli are transferred on multiplication media for two more weeks. Appropriate *Agrobacterium* strains were precultured on selective YEB plates. The calli (200 per transformation) were co-cultured with the *Agrobacterium* strain at an optical density (600 nm) of 0.1 in co-culturing liquid media for 10 min with gentle shaking. Calli are dried of with sterile Whatman paper and transferred to co-culturing solid media for 3 days. Afterwards, calli are transferred to selective media multiple times to eliminate residual *Agrobacteria* and select for transformed selection markers in rice for about 5 weeks.

Finally, calli are put on regeneration media for 4 weeks and regenerated plants are grown in sterile culture for 3 weeks before they are explanted into soil in the green house.

Table 10. Specialized media for *Agrobacterium*-mediated transformation of rice callus.

Specialized media	Composition ¹	
NB basic	2.83 g/l KNO ₃ 463 mg/l (NH ₄) ₂ SO ₄ 400 mg/l KH ₂ PO ₄ 165 mg/l (CaCl ₂) x 2 H ₂ O 185 mg/l (MgSO ₄) x 7 H ₂ O 37.2 mg/l Na ₂ EDTA 27.8 mg/l (FeSO ₄) x 7 H ₂ O 100 mg/l myo-inositol 500 mg/l proline 500 mg/l glutamine 300 mg/l casein hydrolysate	10 mg/l (MnSO ₄) x H ₂ O 3 mg/l H ₃ BO ₃ 2 mg/l (ZnSO ₄) x 7 H ₂ O 0.75 mg/l KI 0.25 mg/l (Na ₂ MoO ₄) x 2 H ₂ O 0.025 mg (CuSO ₄) x 5 H ₂ O 0.025 mg/l (CoCl ₂) x 6 H ₂ O 1 mg/l niacin 1 mg/l pyridoxine 10 mg/l thiamine
R2 basic	4 g/l KNO ₃ 330 mg/l (NH ₄) ₂ SO ₄ 312 mg/l (NaH ₂ PO ₄) x H ₂ O 246 mg/l (MgSO ₄) x 7 H ₂ O 146 mg/l (CaCl ₂) x 2 H ₂ O 1.8 mg/l Na ₂ EDTA 12.5 mg/l (FeSO ₄) x 7 H ₂ O	1.6 mg/l (MnSO ₄) x H ₂ O 2.83 mg/l H ₃ BO ₃ 2.2 mg/l (ZnSO ₄) x 7 H ₂ O 0.125 mg/l (Na ₂ MoO ₄) x 2 H ₂ O 0.2 mg (CuSO ₄) x 5 H ₂ O 1 mg/l thiamine
NB-I	NB basic + 30 g/l saccharose pH 5.8	2.5 mg/l 2,4-D 2.6 g/l phytagel
R2-CL	R2 basic + 10 g/l glucose pH 5.2	2.5 mg/l 2,4-D 100 µM acetosyringone
R2-CS	R2 basic + 10 g/l glucose 7 g/l agarose	2.5 mg/l 2,4-D 100 µM acetosyringone pH 5.2
R2-S	R2 basic + 30 g/l saccharose 2.5 mg/l 2,4-D 400 mg/l cefotaxime	100 mg/l vancomycin 50 mg/l hygromycin 7 g/l agarose pH 6
NB-S	NB basic + 30 g/l saccharose 2.5 mg/l 2,4-D 400 mg/l cefotaxime	100 mg/l vancomycin 50 mg/l hygromycin 7 g/l agarose pH 6
PRN-S	NB basic + 30 g/l saccharose 100 mg/l cefotaxime 100 mg/l vancomycin 50 mg/l hygromycin	5 mg/l abscisic acid 2 mg/l 6-benzylaminopurine 1 mg/l naphthalene acetic acid 7 g/l agarose pH 5.8
RN-S	NB basic + 30 g/l saccharose 50 mg/l hygromycin 2 mg/l BAP	1 mg/l ANA 4.5 g/l phytagel pH 5.8

¹ 2,4-D - 2,4-dichlorophenoxyacetic acid

Table 11. Summary of culturing conditions for *Agrobacterium*-mediated transformation of rice callus.

step	media	conditions	duration
Callus induction	NB-I	28°C, dark	17 – 26 days
Multiplication	NB-I	28°C, dark	7 – 14 days
Co-culture (liquid)	R2-CL	Room temperature	10 min
Co-culture (solid)	R2-CS	25°C, dark	3 days
Selection 1	R2-S	28°C, dark	7 – 15 days
Selection 2	NB-S	28°C, dark	15 – 20 days
Selection 3	PRN-S	28°C, dark	7 – 10 days
Regeneration	RN-S	28°C, first 24 h dark, then 12 h light & 12 h dark	3 - 4 weeks
Plant growth	½ MS	28°C, 12 h light / 12 h dark	3 weeks

2.2.4.13. Detection of transgenes and mutations in rice

Rice plants that were regenerated from transformed callus were tested as soon as they were explanted into soil. The testing was done using the REExtract-N-Amp Plant PCR Kit (Merck KGaA/Darmstadt, Germany) according to user guidelines. In short, plant material (leaf disk 5 mm diameter) is harvested and incubated in extraction solution at 95°C for 10 min. Dilution solution is added and the supernatant can directly be used as a template for a specialized PCR and has to be stored at 4°C.

Reaction mix:

5 µl	REExtract-N-Amp PCR ReadyMix
2 µl	Extraction supernatant
0.4 µl	forward primer (10 mM)
0.4 µl	reverse primer (10 mM)
2.2 µl	dH ₂ O

Thermal cycler program:

95°C	2 min	35x
95°C	30 sec	
X°C	30 sec	
72°C	Y min	
72°C	5 min	
10°C	∞	

Alternatively, genomic DNA was isolated from rice using the innuPREP Plant DNA Kit (Analytik Jena AG/Jena, Germany). In short, plant material (4 cm of leaf) was harvested in a safe lock tube with 2 metal balls, frozen in liquid nitrogen and the tissue was disrupted using the TissueLyser II (QIAGEN GmbH/Hinden, Germany). The SLS protocol of the user manual was applied accordingly and eluted genomic DNA was used in a PCR using the Fusion polymerase.

The stable transformation of rice was confirmed by agarose gel electrophoresis of the PCR product of a PCR with primers amplifying the ocs terminator of the hygromycin resistance cassette present in all constructs. In order to identify possible mutations in the GOI, appropriate primers were chosen and the PCR product was analyzed in a gel electrophoresis, extracted from the gel and send for sequencing with the special “PCR product” treatment.

3. Results

3.1. Understanding Asian Xoo TALEs

3.1.1. TALome diversity in Asian Xoo strains

In order to decipher the full virulence arsenal of Xoo, full genome sequences are essential. At the beginning of this thesis, only 5 Asian Xoo genomes were published. Two more strains, PXO142 and ICMP 3125^T were sequenced in our group (Table 12). At present, a total of 34 Asian Xoo strains were sequenced, which were isolated between 1965 and 2014 (Lee *et al.*, 2005; Ochiai *et al.*, 2005; Salzberg *et al.*, 2008; Wilkins *et al.*, 2015; Grau *et al.*, 2016; Quibod *et al.*, 2016; Carpenter *et al.*, 2018; Chien *et al.*, 2019; Zheng *et al.*, 2019; Mücke *et al.*, 2019; Oliva *et al.*, 2019). These strains were isolated in Japan (2 strains), Korea (3 strains), the Philippines (18 strains), Thailand (1 strain) and Taiwan (2 strains) as well as China (6 strains) and India (2 strains) (Table 12). China and India are the two countries with the highest bacterial leaf blight occurrence. In order to utilize these new resources in this thesis, the TALE genes of the remaining 29 strains, which were not yet analyzed, were annotated using the AnnoTALE prediction pipeline (Grau *et al.*, 2016). The strains had an average of 17 TALE genes with YC11 having the least (12 TALEs) and PXO602 having the most (20 TALEs). The 569 TALE genes of all 34 strains were assigned into a total of 45 TALE classes (Figure 7).

Table 12. General features of completely sequenced Asian Xoo strains.

Strain ¹	TALE genes	Genome size (Mbp)	GC content (%)	PacBio coverage	Sampling country (year) ²	Reference
HuN37	18	4.92	63.7	150x	China (2003)	Zheng <i>et al.</i> 2019
ICMP 3125^T	17	4.99	63.7	170x	India (1965)	Mücke <i>et al.</i> 2019
IX-280	18	4.96	63.7	164x	India (2012)	Carpenter <i>et al.</i> 2018
JL25	15	4.90	63.7	150x	China (2003)	Zheng <i>et al.</i> 2019
JL28	10	4.70	63.7	150x	China (2003)	Zheng <i>et al.</i> 2019
JL33	16	4.90	63.7	150x	China (2003)	Zheng <i>et al.</i> 2019
JP01	17	4.95	63.7	150x	Japan (n/a)	Zheng <i>et al.</i> 2019
JW11089	17	5.01	63.7	248x	South Korea (n/a)	Oliva <i>et al.</i> 2019
KACC 10331³	13	4.94	63.7	-	Korea (n/a)	Lee <i>et al.</i> 2005
KX085 ³	16	4.98	63.7	189x	South Korea (n/a)	Oliva <i>et al.</i> 2019
MAFF 311018	17	4.94	63.7	-	Japan (n/a)	Ochiai <i>et al.</i> 2005
PX061	18	4.97	63.7	233x	Philippines (1973)	Oliva <i>et al.</i> 2019
PX071	19	4.91	63.7	102x	Philippines (1974)	Quibod <i>et al.</i> 2016

Strain ¹	TALE genes	Genome size (Mbp)	GC content (%)	PacBio coverage	Sampling country (year) ²	Reference
PX079	16	5.03	63.7	150x	Philippines (1975)	Zheng <i>et al.</i> 2019
PX083	18	5.03	63.7	170x	Philippines (1976)	Grau <i>et al.</i> 2016
PX086	18	5.02	63.7	200x	Philippines (1977)	Booher <i>et al.</i> 2015
PX099	19	5.24	63.6	200x	Philippines (1980)	Salzberg <i>et al.</i> 2008, Booher <i>et al.</i> 2015
PX0142	19	4.99	63.7	376x	Philippines (1981)	Mücke <i>et al.</i> 2019
PX0145	18	5.04	63.7	121x	Philippines (1982)	Quibod <i>et al.</i> 2016
PX0211	17	5.03	63.7	183x	Philippines (1989)	Quibod <i>et al.</i> 2016
PX0236	16	4.97	63.7	146x	Philippines (1989)	Quibod <i>et al.</i> 2016
PX0282	15	4.96	63.7	268x	Philippines (1990)	Quibod <i>et al.</i> 2016
PX0364	16	4.90	63.7	176x	Philippines (n/a)	Oliva <i>et al.</i> 2019
PX0404	18	4.91	63.7	221x	Philippines (n/a)	Oliva <i>et al.</i> 2019
PX0421	17	4.91	63.7	76x	Philippines (1994)	Oliva <i>et al.</i> 2019
PX0513	17	4.92	63.7	98x	Philippines (1994)	Oliva <i>et al.</i> 2019
PX0524	17	4.95	63.7	152x	Philippines (1994)	Quibod <i>et al.</i> 2016
PX0563	18	4.94	63.7	173x	Philippines (1998)	Quibod <i>et al.</i> 2016
PX0602	20	4.95	63.7	191x	Philippines (2006)	Quibod <i>et al.</i> 2016
ScYc-b	14	4.87	63.7	150x	China (2003)	Zheng <i>et al.</i> 2019
SK2-3	18	4.93	63.7	156x	Thailand (2008)	Carpenter <i>et al.</i> 2018
XF89b	17	4.97	63.7	-	Taiwan (1987)	Chien <i>et al.</i> 2019
XM9	17	4.92	63.7	963x	Taiwan (1986)	Chien <i>et al.</i> 2019
YC11	12	4.87	63.7	150x	China (2014)	Zheng <i>et al.</i> 2019

¹ *Xanthomonas oryzae* type strain is indicated by a superscript T and the sequenced strains available at the beginning of the thesis are shown in bold.

² Strains with unknown collection date are marked with (n/a).

Four identified TALE classes have a prominent member that has previously been described in the context of resistance reactions, i.e. AvrXa7 (TalAC), AvrXa10 (TalBJ), AvrXa23 (TalaAQ) and AvrXa27 (TalaAO), and six more contain an important virulence factor – PthXo1 (TalBX), PthXo2 (TalaM), PthXo3 (TalBH), PthXo6 (TalaR), PthXo7 (TalBM), and PthXo8 (TalaP) (Yang and White, 2004; Sugio *et al.*, 2007; Streubel *et al.*, 2013; Cernadas *et al.*, 2014; Tian *et al.*, 2014; Wang *et al.*, 2015; Mücke *et al.*, 2019). Notably, most strains have mutated TALE genes with truncated N- and C-terminal regions that should not bind to DNA or activate gene expression. The strains had an average of 2.3 truncated TALE genes. These genes seem to fall into two different categories: TALE

TALE genes are represented by arrows indicating their relative orientation in the genome. All TALEs are assigned into classes by AnnoTALE and named accordingly. Previously established TALE clusters are specified at the top and cluster affiliation of individual TALE genes is shown by color. *TALE* genes without functional N- or C-terminal regions are depicted in white with a colored outline according to TALE cluster assignment. If AnnoTALE was unable to assign a TALE class, the gene is marked with a question mark. Strains with genomic rearrangements around the origin are shown in reverse complement to simplify the view and are marked with “rev”.

genes, which cannot fulfill the typical TALE functions because of frame shifts or *TALE* genes belonging to TALE classes, which consist exclusively of TALEs with truncated N- and C-terminal regions (TalAI, TalAW, TalDR and TalFS).

To evaluate the TALome diversity for Asian Xoo strains, the TALE classes were assigned to three abundance categories depending on how frequently they occur. Core TALE classes were defined as being present in more than 80% of strains, intermittent TALE classes in 20–80% of strains, and rare TALE classes in less than 20% of strains (Mücke *et al.*, 2019). The analysis counts how many strains contain at least one member of the TALE class, regardless of functionality. In total, there are 10 core, 11 intermittent and 24 rare TALE classes (Figure 8). The strains contain on average 9.2 core TALEs, 6.2 intermittent TALEs and 1.3 rare TALEs. Interestingly, the class TalAA has an unusually high rate of *TALE* genes with frame shift mutations, which occur in seven of the 31 strains. This could be an indication, that TalAA is no longer beneficial on current rice cultivars and is lost. Alternatively, TalAA could also have negative effects on infection due to a plant resistance and is negatively selected. In contrast, the TALE class TalAL is present with two members of the TALE class per genome in five strains from the Philippines. This indicates a potential diversification of TalAL to bind different versions of the same promoter. Alternatively, the diversification of TalAL might be driven by the induction of a beneficial second target gene and subsequent optimization to induce both targets efficiently. The twelve TALEs TalBT1, TalBZ1, TalDS1, TalDT1, TalDU1, TalEQ1, TalES1, TalET1, TalFT1, TalFV1, TalFW1 and TalFX1 are unique and have no other TALE class members in any other strain, so far.

The previously described TALE clusters T-I to T-IX were annotated and an overview of all 34 strains and their *TALE* genes in the corresponding TALE clusters was generated (Figure 7; Grau *et al.*, 2016). Six of the unique *TALE* genes are located in cluster T-II. In fact, the TALE clusters T-I to T-III contain the majority of rare TALE classes and are highly diverse in their composition. Therefore, these clusters have the highest potential for new TALEs to be discovered in the future. On the contrary, T-VIII and T-IX are highly conserved in their TALE class content and contain a high amount of core TALEs. The consistency of

these clusters suggests that the TALEs in these clusters play an important role in *Xoo* infection.

The most likely common binding sites for all 45 TALE classes were generated with AnnoTALE and aligned with Clustal Omega to gain insight in the relationships between TALE classes (Grau *et al.*, 2016; Madeira *et al.*, 2019). The resulting phylogenetic tree was visualized using iTol and TALE class abundance and common TALE cluster affiliation for each TALE class are shown in Figure 8 (Letunic and Bork, 2019). Apparently, some very rare TALE classes, including half of the unique TALEs, are closely related to more common TALE classes with known target genes. These closely related TALE classes are located in the same genomic locus in different strains and appear mutually exclusive (Figure 7).

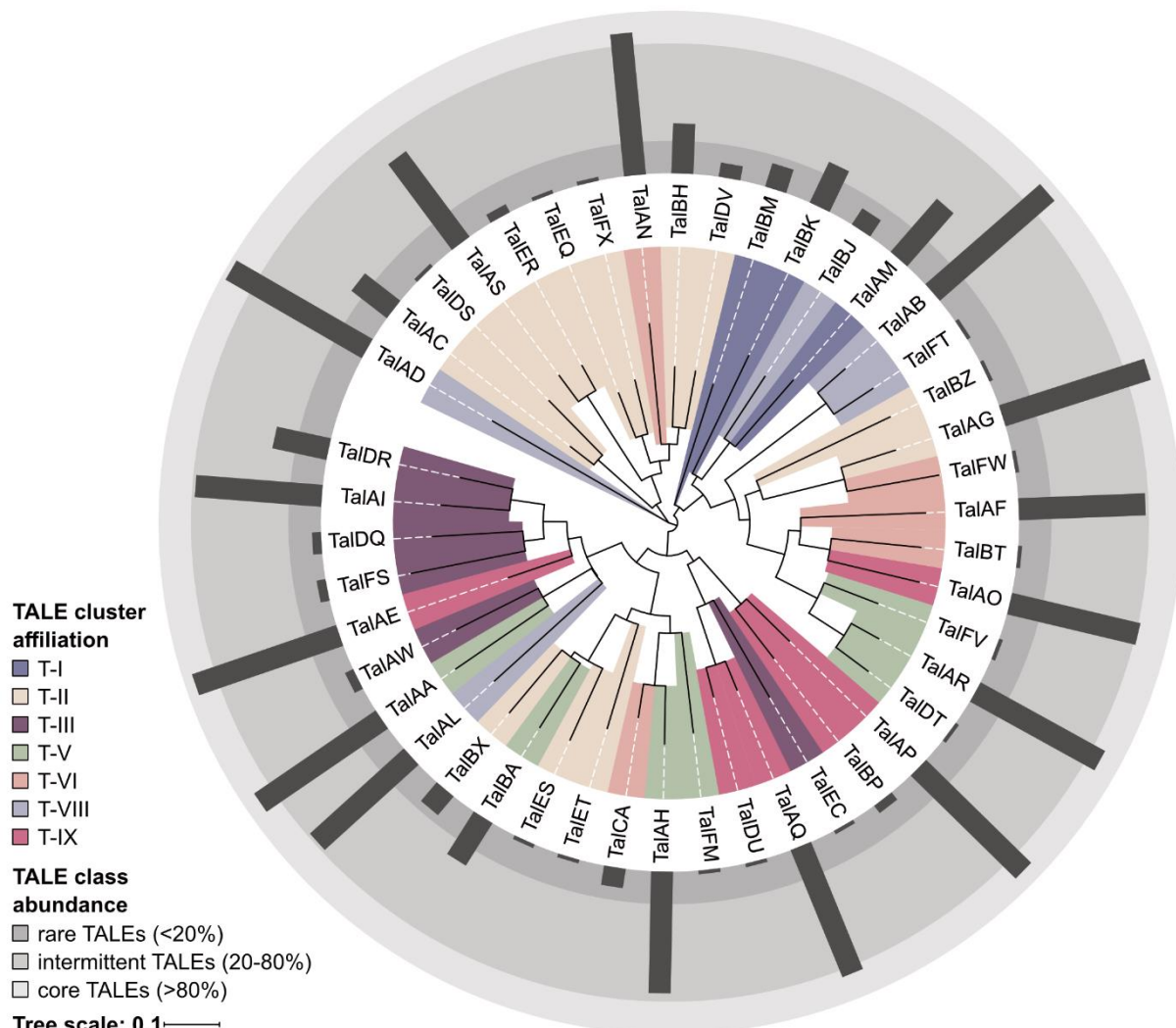


Figure 8. TALE class abundance and cluster affiliation.

A phylogenetic tree of all 45 Asian *Xoo* TALE classes was created by aligning the most likely common binding sequences of each TALE class with Clustal Omega and visualization was done using iTol. Most common TALE cluster affiliations of each TALE class are represented by the colored background of the respective branches. The abundance of each TALE class in Asian *Xoo* strains is shown as a radial bar diagram and the three assigned abundance categories are depicted as different shades of gray.

These TALE class pairs include classes with known virulence functions: TalAP & TalBP and TalAR & TalDT & TalFV, which contains two unique TALEs related to a core TALE class. Especially TalAR and its partners are very close, as both TalDT and TalFV only miss a single repeat each in comparison to TalAR, whereas TalBP misses three consecutive repeats compared to TalAP. Evidently, these deletions triggered a separate classification by AnnoTALE, as this can have a significant impact on TALE binding specificity. These changes might be adaptations to deletions in the target promoter in certain rice cultivars, because normal TALEs cannot accommodate frame shifts in their binding region (Richter and Boch, 2013). The daTALbase tool was used to find natural variations in the target genes for TalAR (*OsTFX1*) and TalAP (*OsHEN1*), but no variants that would favor the rare TALE classes were found (Pérez-Quintero *et al.*, 2018).

Additionally, there is also a closely related TALE pair containing a TALE class that triggers resistance in certain rice cultivars: TalAQ & TalDU (Wang *et al.*, 2015). TalDU has a deletion of one repeat compared to TalAQ and could be an adjustment to avoid the activation of a plant resistance gene. Both, the plant resistance gene *Xa23* and the potentially beneficial target gene *OsFNS* of TalAQ can probably not be activated by TalDU. A lot of the TALE classes present in cluster T-II are closely related. Especially interesting is the 40aa aberrant repeat N* shared by the TALE classes TalBH, TalDV, TalAC, TalDS, TalEQ and TalFX, suggesting a common origin. Additionally, TalAS and TalER have a 40aa aberrant repeat NN, which differs only by one amino acid from the 40aa aberrant repeat N* shared by a lot of other members of the cluster. Aberrant repeats with a length of 40aa are present exclusively in these classes and cannot be found in any other known Xoo TALEs.

Similarly, a lot of TALE classes of TALE cluster T-III are closely related, especially the four TALE classes containing truncated TALEs exclusively (TalAI, TalAW, TalDR and TalFS). TalAI, TalAW, TalDR and TalDQ also share the 28aa aberrant repeat NG. The aberrant length of 28aa repeats cannot be found in any other TALE class in Xoo.

These findings suggest that a focus on target genes of highly abundant TALE classes will have the best chances of creating resistant rice, because they are present in most strains and rare TALE genes are often only a variation of a common TALE class. The new categorization of TALE class abundance will simplify this process.

3.1.2. Construction of analogues to natural TALEs

In order to understand the Xoo infection, a knowledge of target host genes benefitting this infection is necessary. Upon infection, a typical Xoo strain transfers around 17 TALEs

and 23 Xops into the host cell, which responds with a multitude of transcriptional changes (Midha *et al.*, 2017; Mücke *et al.*, 2019). This complex natural interaction can make it difficult to pinpoint target genes for individual TALEs.

Therefore, expression vectors of single TALEs needed to be created using the Golden TALE Technology Cloning Kit (Figure 5; Geißler *et al.*, 2011). At the beginning of this thesis, this Kit contained the repeat modules for the most common RVDs and could build a TALE with up to 23.5 repeats. These options were not sufficient to accommodate the diversity in RVDs, differences in N- and C-terminal regions or the length of up to 33.5 repeats found in *Xoo* TALEs. Additionally, new aberrant repeats were found in *Xoo*, which were not available at all.

Table 13. RVD composition of artificial TALEs and their *Xoo* strains of origin.

TALE	repeat number	RVD sequence ¹																	Xoo strain of origin		
AA15	19.5	NI NN	HG NG	NS	HG	HG	HD	NS	NG	HD	NN	NG	HG	NG	HD	HG	HD	HD	NI	ICMP 3125 ^T	
AB16	17.5	NI	HG	NI	NI	NI	NN	HD	NS	NN	NS	NN	HD	NN	NI	HD	NN	NS	NG	ICMP 3125 ^T	
AD23	23.5	NN NN	HD NN	NS NN	NG NN	HD NN	NN HD	N*	NI	HD	NS	HD	NN	HD	NN	HD	NN	NN	NN	PX0142	
AE15	12.5	NI	NN	NI	HG	HG	NV	HG	HD	HG	HD	HD	HD	NG						ICMP 3125 ^T	
AF17	15.5	NI	NN	NN	NI	NI	NI	HD	NS	HG	NN	NN	NN	NI	NI	HG	HD			ICMP 3125 ^T	
AG15	20.5	NI N*	NG NS	NN NG	NG	NK	NG	NI	NN	NI	NN	NI	NN	NS	NG	NS	NN	NI		PX0142	
AH12	19.5	NI HD	N* NG	NI	NS	NN	NG	NN	NS	N*	NS	NN	NS	N*	HD	HG	HD	NI	HD	PX0142	
AL11	17.5	NI	NS	HD	NG	NS	NN	HD	N*	NN	NN	NI	NG	HD	NG	HD	HD	HD	NG	PX0142	
AN15	20.5	NI NN	N* NI	NI NG	HG	NI	NI	NS	HD	NN	HD	NS	NG	SS	HD	NI	NI	NN	NI	PX0142	
A016	16.5	NI	NN	N*	NG	NS	NN	NN	NN	NI	NN	NI	N*	HD	HD	NI	NG	NG		PX0142	
AP15	19.5	HD NG	HD NG	HD	NG	N*	NN	HD	HD	N*	NI	NI	NN	HD	HI	ND	HD	NI	HD	PX0142	
AQ3	26.5	HD NN	HD HD	NN HI	NN ND	NS HD	NG HG	HD NN	S* HG	HD N*	NG N*	N*	HD	HD	HD	N*	NN	<u>NI</u>		PX083	
AR3	22.5	NI HD	H* N*	NI NS	NN NI	NN NG	NN	NN	HD	NI	NN	HG	HD	NI	N*	NS	NI	NI		PX083	
AS3	26.5	NI NN	HG NN	NI HD	NI NS	HG NN	HD HD	NN N*	HD NS	HD N*	HD N*	NI	NI	NN	NI	HD	HD	HD	HG	PX083	
BA8	15.5	NI	NS	HD	HG	NS	NN	HD	H*	NG	NN	NN	HD	HD	NG	HD	NG			ICMP 3125 ^T	
BH2	28.5	NI NN	HG NS	NI NI	HG NN	NI NG	NI NN	HD NN	HD N*	HD NS	HD N*	HD	HD	HD	NG	HD	<u>N*</u>	NI	HD	HD	PX0142
BJ2	15.5	NI	H*	NI	HG	NI	NI	NN	HD	NI	HD	NN	HG	NS	N*	HD	N*			PX083	
BK2	21.5	NI HD	HG HD	NI NG	NN NG	NI NG	NN HD	NI	<u>HD</u>	HD	NS	<u>NS</u>	HD	NI	NI	HD	NG	HD		PX0142	
BM2	21.5	NI HD	NG HD	NI NG	NI N*	N* NN	NN HD	HD HD	N*	NI	NI	NI	NG	HD	HG	NN	NS	NN		ICMP 3125 ^T	

TALE	repeat number	RVD sequence ¹	Xoo strain of origin
BX1	23.5	<u>NN</u> <u>HD</u> <u>NI</u> <u>HG</u> <u>HD</u> <u>NG</u> <u>N*</u> <u>HD</u> <u>HD</u> <u>NI</u> <u>NG</u> <u>NG</u> <u>NI</u> <u>HD</u> <u>NG</u> <u>NN</u> <u>NG</u> <u>NI</u> NI NI NI N* NS N*	PX099
CA1	16.5	NI N* NI NS NN NG NN HD HD HD NG HD NS HD N* NS NG	PX083
ES1	11.5	<u>NN</u> <u>HD</u> <u>NI</u> <u>HG</u> <u>HD</u> <u>NG</u> <u>N*</u> <u>HD</u> <u>NI</u> <u>N*</u> <u>NS</u> <u>N*</u>	ICMP 3125 ^T
ET1	33.5	<u>NI</u> <u>H*</u> <u>NN</u> <u>HD</u> <u>H*</u> <u>NG</u> <u>NN</u> <u>NN</u> <u>HD</u> <u>HD</u> <u>NG</u> <u>HD</u> <u>NI</u> <u>HD</u> <u>HG</u> <u>NS</u> <u>NI</u> <u>HG</u> N* NN HD NI NG HG NN NN HD NS NN HD N* NI NI N*	ICMP 3125 ^T

¹TalAQ3, TalBH2, TalBK2 have repeats with 42, 40 and 36 amino acids, respectively, that are underlined.

Nine additional RVD varieties were created in cooperation with Maik Reschke and new aberrant repeats were created by Sebastian Becker to facilitate a construction of the most accurate representation of natural TALEs possible. The new N- and C-terminal modules of the *Xoo* TALEs were created from TalAG4 and TalAO3, respectively, by Maik Reschke. The truncated N-terminal region observed in the TALE classes present in TALE cluster T-III was amplified from TalAI3 and cloned to create a new alternative N-terminal module. Simultaneously, the two versions of truncated C-terminal regions presented by these TALEs were amplified from TalAI3 and TalAI4 to create alternative C-terminal modules. The set of multi repeat assembly vectors (LA to CR) was also expanded up to FR allowing a maximum length of 41.5 repeats per TALE.

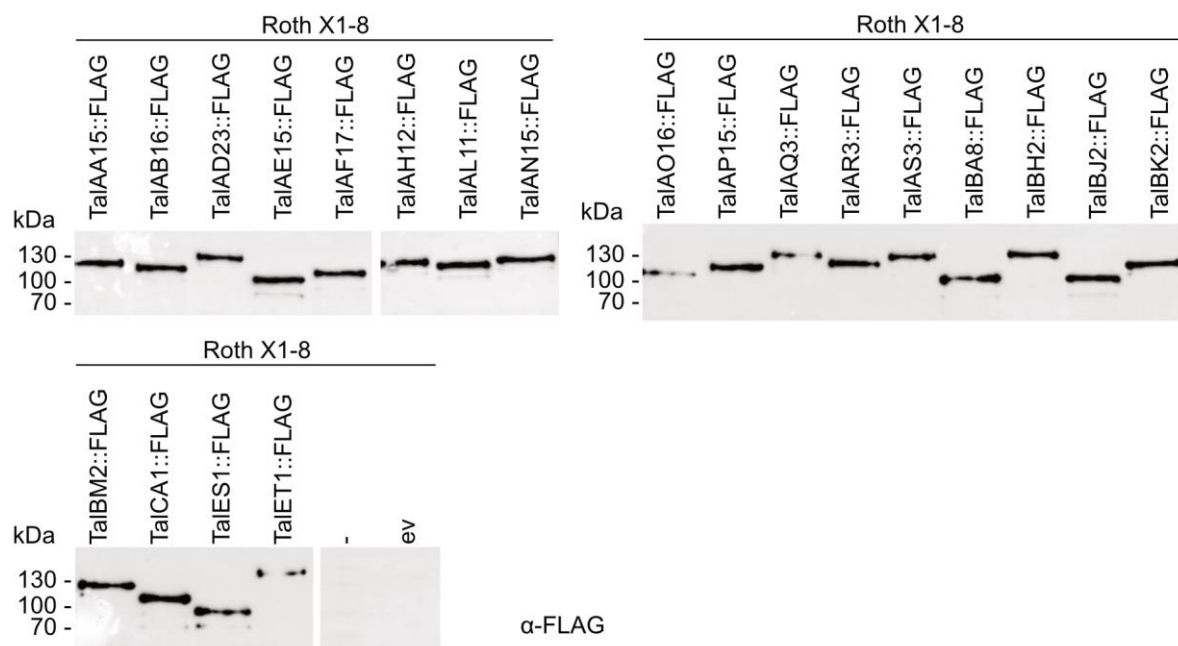


Figure 9. Western Blot analysis of Roth X1-8 strains with artificial TALEs.

Derivatives of the *Xoo* strain Roth X1-8 containing TALE::FLAG expression constructs were harvested from liquid culture, the whole protein content was separated on SDS gels and transferred on nitrocellulose membranes. Protein synthesis of TALEs was detected using α -FLAG primary antibody from mouse and α -mouse secondary antibody coupled with horseradish peroxidase. ev – empty vector

In total, TALEs representing 23 TALE classes were constructed and cloned in the *Xanthomonas*-compatible expression vector pSKX1 (Table 7) and most are also available

in the *Agrobacterium*-compatible expression vector pSKA2 (Table 13, Table 7). These TALE classes span all 10 core TALE classes, seven intermittent TALE classes and six rare TALE classes. The selection was chosen based on the availability of the strain of origin and the abundance of the TALE class according to the knowledge at the start of the thesis.

The American *Xoo* strain Roth X1-8, which naturally does not contain any TALEs, was used as a tool to study the impact of individual TALEs (Grau *et al.*, 2016; Mücke *et al.*, 2019). Therefore, Roth X1-8 was transformed with the pSKX1 derivatives containing the 22 TALEs representing the TALomes of PX083, PX0142 and ICMP 3125^T. The synthesis of these TALEs could be verified for 21 of those strains via Western Blot detecting a C-terminal FLAG tag (Figure 9). Roth X1-8 strains transformed with expression constructs for TalAG15 were repeatedly showing Western Blot signals of the wrong protein size and were not pursued further. The PthXo2-like TALE class TalBK was transferred to the project of Sebastian Becker and was not further analyzed in this thesis.

This advanced tool set can now be used to study these 21 *Xoo* TALEs and their function.

3.1.3. Analysis of truncated TALEs

The truncated TALEs of TALE cluster T-III have highly conserved changes in their N- and C-terminal regions, which suggests a specific purpose. In order to understand the purpose of these truncated TALEs, basic functionality tests were conducted.

3.1.3.1. Truncated TALEs and gene induction

The truncated TALEs all have two deletions in their N-terminal region and display two versions of C-terminal regions with one or two deletions represented by TalAI3 and TalAI4, respectively (Figure 10A). Both variants have lost the activation domain and retained one NLS. TALEs without activation domain were shown to still have residual gene activation activity and a single NLS should be sufficient for transport into the nucleus (Szurek *et al.*, 2001). Therefore, the capability of truncated TALEs to induce gene expression was tested.

Chimeras containing either normal or truncated N-terminal regions and normal, TalAI3-like or TalAI4-like C-terminal regions were created to determine the effect of the different deletions (Figure 10B). These chimeras all had the RVD composition of TalAI3 – with the 28aa aberrant repeat NG or with a normal 34aa NG. To test the gene activation ability of these TALEs, *A. tumefaciens* was transformed with the chimeras cloned into pSKA2. Additionally, a reporter construct was designed that has the GUS gene *uidA* under a minimal promoter containing a TALE box with a perfect fit for TalAI3 (Figure 10C).

Because aberrant repeats are known to loop out and to not participate in DNA binding, a second reporter with a one base deletion in the TalAI3 box at the position of the aberrant repeat was created. *A. tumefaciens* were also transformed with the reporter constructs and co-inoculated with *A. tumefaciens* carrying the TALE chimeras into *N. benthamiana*.

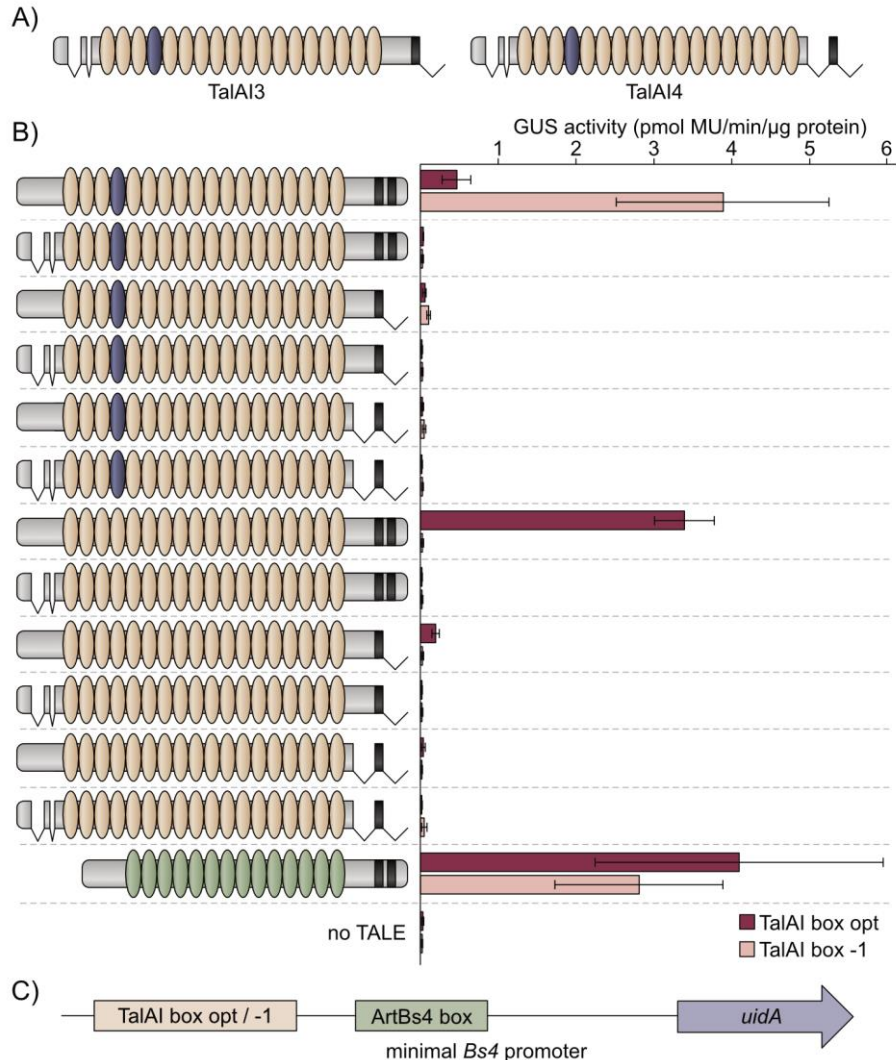


Figure 10. Analysis of gene induction capability of truncated TALEs.

Xoo strains contain truncated TALEs that display deletions in their N- and C-terminal regions in specific patterns. (A) Schematic overviews of TalAI3 and TalAI4 are depicted as representatives for the two existing variations. Repeats with aberrant length of 28aa are colored blue and NLS are black. (B) Chimeras of TALEs containing normal and truncated N- and C-terminal regions were created. Each chimera has the RVD composition of TalAI3 with an aberrant repeat or with a normal repeat instead, as indicated by color. Gene induction capability of these chimeras was tested by co-inoculating *A. tumefaciens* strains containing a chimera with a GUS reporter construct under a minimal promoter with a TALE box for TalAI3 into *N. benthamiana* (C). Each chimera was tested with two reporter constructs, one containing an optimal TALE box (opt) and one containing a 1 bp deletion at the position of the aberrant repeat (-1). ArtBs4 (green) was used as a positive control for both reporter constructs. Samples were harvested 2 dpi and a quantitative GUS assay was performed.

The samples were harvested after two days and a quantitative GUS assay was performed (Figure 10B). Only the TALEs with normal N- and C-terminal regions were able to induce the reporter gene efficiently. The TALE with the aberrant repeat strongly favored the -1

TALE box whereas the TALE with exclusively normal repeats could only induce the reporter with the perfect TALE box. The TaIAI3-like C-terminal region showed residual activity in combination with the normal N-terminal region, but not with the truncated N-terminal region. Interestingly, chimeras with a normal C-terminal region were unable to induce the reporters if they contained a truncated N-terminal region. The TALE ArtBs4 can bind in the minimal promoter of both constructs and was used as positive control to show the ability of both reporter constructs to be induced.

These findings suggest that the truncated N-terminal region and the TaIAI4-like C-terminal region result in complete loss of gene induction ability. The TaIAI3-like C-terminal region reduces the activity to less than 10%. In nature, the truncated TALEs always contain a truncated N-terminal region and therefore, should not be involved in gene induction at all.

Shortly after these experiments, two papers were published confirming that truncated TALEs do not bind to DNA (Ji *et al.*, 2016; Read *et al.*, 2016). Read *et al.* (2016) focused on TaIAI4-like TALEs and found that they suppress the resistance gene *Xo1*, which acts as an NLR protein and recognizes normal TALE structure. TaIAI4-like TALEs were therefore named interfering TALEs (iTALEs). Ji *et al.* (2016) discovered the resistance gene *Xa1*, which is also an NLR protein that recognizes full length TALEs. They found that truncated TALEs (truncTALEs)– both TaIAI3-like (truncTALE type A) and TaIAI4-like (truncTALE type B) - can suppress *Xa1*.

3.1.3.2. Can truncated TALEs suppress Bs4 resistance reactions?

Xo1 and *Xa1* are the first described resistance genes in rice that recognize TALEs by their structure and not their gene activation (Ji *et al.*, 2016; Read *et al.*, 2016). Similarly, tomato contains the well-known resistance gene *Bs4*, which is an NLR protein recognizing TALEs in a dose-dependent manner and shows different levels of sensitivity for various TALEs (Schornack *et al.*, 2005). Because the functions of *Xo1*, *Xa1* and *Bs4* seem similar, the effect of truncated TALEs on *Bs4* activity were analyzed.

Therefore, *A. tumefaciens* strains containing expression vectors for *Bs4* and the corresponding TALE *AvrBs4* were provided by the Ulla Bonas group from the Martin-Luther-Universität Halle/Wittenberg. Co-inoculation of *A. tumefaciens* carrying *Bs4* and *AvrBs4* expression constructs will lead to a hypersensitive reaction in *N. benthamiana*, which will trigger a rapid cell death (Schornack *et al.*, 2005). To analyze the ability of the truncated TALEs to interfere with *AvrBs4* recognition by *Bs4*, *A. tumefaciens* strains

carrying a truncated TALE, *AvrBs4* and *Bs4* were mixed 1:1:1 and inoculated into *N. benthamiana* (Figure 11A).

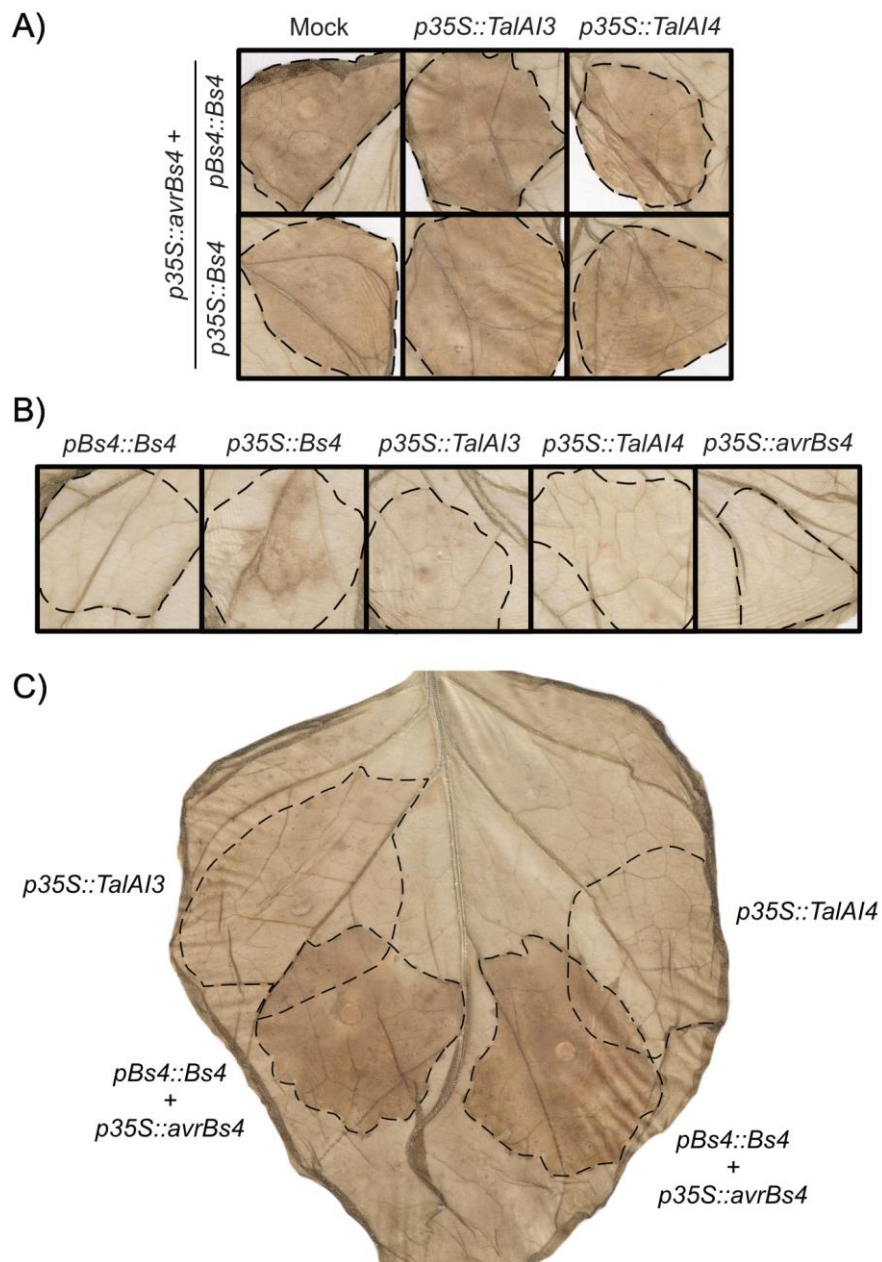


Figure 11. Influence of truncated TALEs on *Bs4* function.

N. benthamiana was inoculated with *A. tumefaciens* carrying expression constructs for the truncated TALEs TalAI3 or TalAI4, AvrBs4 and *Bs4* under different promoters. *A. tumefaciens* containing truncated TALEs, AvrBs4 and *Bs4* were adjusted to an optical density of 0.8. A) The strains were mixed 1:1:1 and inoculated. B) The strains were mixed with inoculation medium 1:2 and inoculated. C) The strains containing truncated TALEs were mixed with inoculation medium 1:2 and inoculated. 6 hpi the strains carrying AvrBs4 and *Bs4* were mixed with inoculation medium 1:1:1 and inoculated in an overlapping manner. 7 dpi leaves were harvested and destained in 96% ethanol and pressed. Inoculation spots are indicated by dashed lines.

There was no noticeable influence of either truncated TALE on *Bs4* activity, because HR development was unaffected compared to the mock control. None of the used *A. tumefaciens* strains elicited an HR on their own, suggesting that the observed HR was truly a display of *Bs4* function (Figure 11B). Because strong overexpression of *Bs4* under

a 35S promoter triggered residual responses, *Bs4* under the natural *Bs4* promoter was used for further experiments.

In order to evaluate the ability of truncated TALEs to prevent *AvrBs4* recognition by binding to *Bs4* first, a staggered inoculation was performed. *A. tumefaciens* strains carrying the truncated TALEs were inoculated first and six hours later, *A. tumefaciens* containing *AvrBs4* and *Bs4* were inoculated in the same area (Figure 11C). The presence of truncated TALEs had no impact on HR.

Under the tested conditions, truncated TALEs did not have any effect on *Bs4* activity. As the function of truncated TALEs in the *Xoo*-rice interaction had been solved by Read *et al.* 2016 and Ji *et al.* 2016, no further experiments were conducted on truncated TALEs.

3.2. Identifying target genes for *Xoo* TALEs

After gaining insight into the diversity of TALomes in *Xoo*, the target genes of TALE classes were analyzed *in silico* and *in vivo* to understand the potential impact of individual TALEs on infection and to identify promising susceptibility genes in rice.

3.2.1. Prediction of TALE target genes in rice

The analysis of target genes was focused on three *Xoo* strains: PX083, PX0142 and ICMP 3125^T. First, target genes were predicted *in silico* using the TALgetter tool (Grau *et al.*, 2013). To this end, the promoterome of the sequenced rice cultivar Nipponbare was defined as 300 bp upstream and 200 bp downstream of transcriptional start sites and scanned for TALE binding sites. These restrictions were used because this region was deemed most promising for TALE binding regions in the past (Grau *et al.*, 2013). The TALgetter tool will present the top 100 target sequences for each analyzed TALE. All 54 TALEs of the three strains were evaluated and a total of 2938 unique potential target genes were predicted, of which 325 were identified for all three strains (Figure 12A).

In parallel, actual changes in rice gene expression upon infection with these strains were analyzed by Maik Reschke, who inoculated Nipponbare with PX083, PX0142, ICMP 3125^T or a mock control and harvested the plants after 24 h for subsequent RNA-seq analysis. This relatively early harvest time was used to obtain primary TALE targets and minimize secondary effects. The processing of the resulting RNA-seq data was done in cooperation with Jan Grau. The expression of genes was compared in infected and uninfected tissue and a threshold of 1.5-fold induction ($0.585 \log_2$ fold change) was implemented to identify induced genes during infection. The analysis revealed 436, 361 and 415 induced rice genes during infections with PX083, PX0142 and ICMP 3125^T, respectively. 71 of those genes were induced in all three infections (Figure 12A).

Expression data and *in silico* predictions complement each other and a combination of both approaches provides highly likely TALE target genes. The combination resulted in 33, 17 and 28 potential target genes for PX083, PX0142 and ICMP 3125^T, respectively (Figure 12B, Table 14). Four target genes were predicted and induced in infections with all three strains: the published targets *OsHEN1* and *OsTFX1* for TalAP and TalAR, respectively, as well as the new target genes *OsFBX109* and *OsPHO1;3* for TalAD and TalAO, respectively (Sugio *et al.*, 2007; Cernadas *et al.*, 2014; Mücke *et al.*, 2019). These analyses cumulated in a total of 61 highly likely TALE target genes in Nipponbare. This drastic reduction of candidate genes makes experimental validation of these genes feasible.

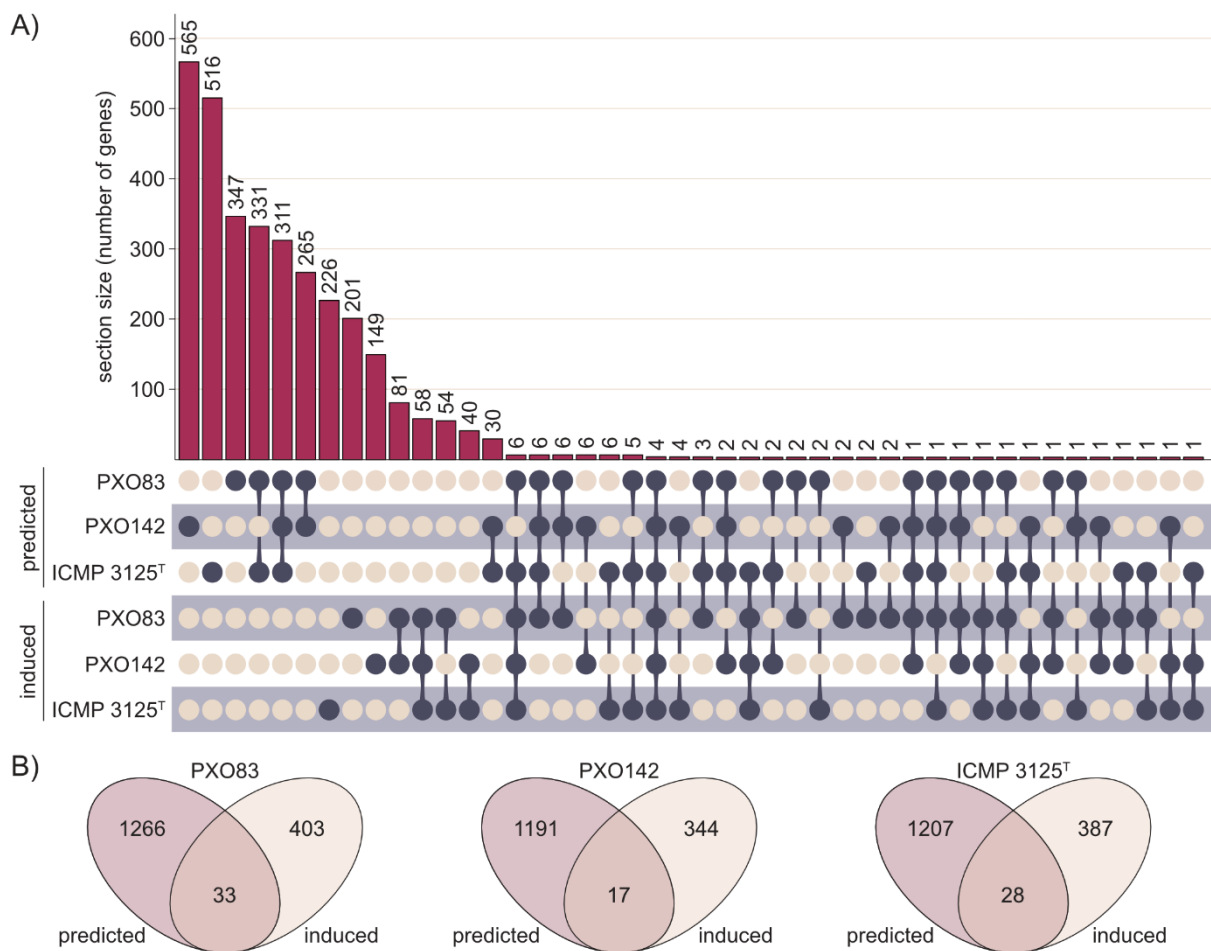


Figure 12. Prediction of rice target genes for TALEs from PX083, PX0142 and ICMP 3125^T.

(A) Three sets of genes predicted to be target genes for the Xoo strains PX083, PX0142 and ICMP 3125^T in rice by AnnoTALE (predicted) and three sets of genes that were induced upon infection of rice with the same Xoo strains (induced) were analyzed using the UpSet tool (Lex *et al.*, 2014). UpSet identifies intersections between sets and plots them as a matrix. Each row corresponds to one set of genes and each column corresponds to one intersection between sets. Dots are either empty (yellow) or filled (dark blue), which indicates that the set is part of the intersection. The number of genes that are part of the intersection are shown above in a bar diagram. (B) Venn diagrams depicting intersections between predicted and induced gene sets for the Xoo strains separately.

Table 14. List of potential TALE target genes in rice for PX083, PX0142 and ICMP 3125^T

Locus ID ^{1,2}	Annotated function ³	Log2fold change	Strain	TALE	Rank	Position TALE box (bp)
Os01g40290	expressed protein	1.894	ICMP 3125 ^T	AA15	1	268
		0.737	PX083	AA5	1	268
Os08g35400	Hypothetical protein	0.837	ICMP 3125 ^T	AA15	41	229
Os06g37410	Helix-loop-helix DNA-binding domain containing protein	0.735	PX083	AA5	58	98
Os09g30250	OsSub58 – putative subtilisin homologue	0.645	ICMP 3125 ^T	AA15	2	157
Os04g05050	pectate lyase precursor (OsPLL4)	2.221	ICMP 3125 ^T	AB16	49	178
		1.621	PX083	AB5	51	178
Os03g09150	pumilio-family RNA binding repeat domain containing protein	2.181	PX083	AB5	91	268
Os09g24400	Conserved hypothetical protein	1.206	PX0142	AB17	9	98
Os10g02840	O-methyltransferase	0.750	PX083	AB5	82	107
		0.638	ICMP 3125 ^T	AB16	80	107
Os04g19960	Retrotransposon protein	1.700	PX083	AC5	33	263
Os08g05960	Expressed protein	1.231	PX083	AC5	50	287
Os03g51760	OsFBX109 - F-box domain containing protein	2.734	ICMP 3125 ^T	AD22	16	101
		1.914	PX083	AD5	39	101
		1.368	PX0142	AD23	37	101
Os08g37250	patatin	1.161	PX083	AD5	87	297
Os01g50650	Retrotransposon protein	0.772	PX083	AD5	90	50
Os07g42834	Retrotransposon protein	0.665	PX083	AD5	55	63
Os07g31250	OsWAK69 receptor-like cytoplasmic kinase	0.606	PX0142	AD23	39	240
Os02g04830	Retrotransposon, centromere-specific	1.151	ICMP 3125 ^T	AE15	10	269
Os12g13300	Expressed protein	0.987	PX083	AE4	71	351
Os05g51390	Uncharacterized protein PA4923	0.655	PX083	AE4	92	256
Os10g32690	Expressed protein	0.794	PX083	AF4	13	41
Os03g61980	Cytochrome P450	0.594	PX083	AF4	79	285
Os01g02950	Expressed protein	0.803	PX083	AG4	57	65
Os04g21860	Transposon protein	0.665	PX083	AG4	60	125
Os01g42790	Xylem cysteine proteinase 2 precursor	0.611	PX083	AG4	13	268
Os11g26790	Dehydrin (OsRAB21)	1.695	ICMP 3125 ^T	AH11	1	455
		1.087	PX0142	AH12	30	455
Os03g40610	cytochrome P450	0.600	PX0142	AH12	1	142
Os02g05390	retrotransposon protein	0.673	PX0142	AL12	64	235
Os06g29790	phosphate transporter 1 - OsPHO1;3	1.902	ICMP 3125 ^T	A015	42	31
		0.833	PX0142	A016	2	31
		0.690	PX083	A03	44	31
Os02g40410	expressed protein	1.657	ICMP 3125 ^T	A015	21	117
		0.653	PX083	A03	23	117
Os10g38120	Cytochrome P450	0.707	PX083	A03	30	163
Os07g06970	HEN1	1.398	PX083	AP3	1	301
		0.824	PX0142	AP15	1	301
		0.687	ICMP 3125 ^T	AP14	1	301

Locus ID ^{1,2}	Annotated function ³	Log2fold change	Strain	TALE	Rank	Position TALE box (bp)
<u>Os02g21700</u>	STE MEKK ste11 MAP3K.8	0.691	PX083	AP3	2	217
Os08g38020	bZIP transcription factor domain containing protein	0.646	PX083	AP3	11	338
Os09g24590	expressed protein	0.640	ICMP 3125 ^T	AP14	80	180
<u>Os03g03034</u>	flavonol synthase/flavanone 3-hydroxylase (OsDOX-1)	1.295	ICMP 3125 ^T	AQ14	26	315
Os03g46110	LTPL94 - protease inhibitor	1.181	PX083	AQ3	11	315
		0.976	PX083	AQ3	72	237
		2.825	PX083	AR3	1	269
<u>Os09g29820</u>	bZIP transcription factor domain containing protein (OstFX1)	2.819	ICMP 3125 ^T	AR13	2	269
		2.272	PX0142	AR14	1	269
Os03g61070	expressed protein	1.283	ICMP 3125 ^T	AR13	70	182
Os11g30360	expressed protein	0.921	PX0142	AR14	92	16
<u>Os10g28240</u>	calcium-transporting ATPase, plasma membrane-type	0.918	ICMP 3125 ^T	AR13	12	248
Os03g62830	nuclear antigen	0.894	PX0142	AS12	33	389
<u>Os05g15630</u>	membrane associated DUF588 domain containing protein	0.610	PX083	AS3	32	215
		3.815	ICMP 3125 ^T	BA8	1	263
Os02g06670	retrotransposon protein	2.739	PX083	BA2	1	263
		2.942	PX083	BA2	41	267
Os07g09020	argonaute	1.781	ICMP 3125 ^T	BA8	39	267
		2.917	ICMP 3125 ^T	BA8	68	261
Os11g42950	expressed protein	2.011	PX083	BA2	70	261
Os09g07460	kelch repeat protein	0.746	ICMP 3125 ^T	BA8	27	311
<u>Os03g55530</u>	HLS	0.684	ICMP 3125 ^T	BA8	3	312
Os02g49350	plastocyanin-like domain containing protein	5.163	PX0142	BH2	18	269
Os03g09150	pumilio-family RNA binding repeat domain containing protein	2.530	PX0142	BH2	5	266
<u>Os11g31190</u>	nodulin MtN3 family protein (OsSWEET14)	2.514	PX0142	BH2	1	267
<u>Os01g19330</u>	MYB family transcription factor	0.950	PX0142	BH2	22	265
Os08g05960	Expressed protein	0.666	PX0142	BH2	73	285
Os11g44950	Glycosyl hydrolase family 3 protein	0.586	PX083	BJ2	27	266
Os04g43800	phenylalanine ammonia-lyase	0.735	PX0142	BK2	49	268
Os08g04800	triacylglycerol lipase like protein	1.898	ICMP 3125 ^T	BM2	66	245
<u>Os01g73890</u>	transcription initiation factor IIA gamma chain	1.079	ICMP 3125 ^T	BM2	2	270
<u>Os04g49970</u>	U-box	0.973	ICMP 3125 ^T	BM2	67	259
Os06g49860	methyltransferase	0.899	ICMP 3125 ^T	BM2	55	248
Os06g09350	expressed protein	0.833	ICMP 3125 ^T	BM2	74	239
Os11g36880	retrotransposon protein	0.809	PX083	CA1	93	126
<u>Os04g43730</u>	OsWAK51 receptor-like protein kinase	5.762	ICMP 3125 ^T	ES1	60	279
Os06g03710	DELLA protein SLR1	1.591	ICMP 3125 ^T	ES1	34	447

¹ target genes that were identified for more than one strain are shown in bold

² target genes that were further analyzed are underlined in red

³ target gene names differing from annotated function are added in brackets

3.2.2. Validation of TALE-dependent target gene induction

In order to validate candidate target genes, the impact of individual TALEs on target gene expression was evaluated. Therefore, the Roth X1-8 strains carrying single TALE expression constructs were utilized because these strains can be directly compared to the wild type Roth X1-8 to assess the effect of the TALE.

The rice variety Nipponbare was inoculated with the 20 Roth X1-8 derivatives containing TALE expression constructs and the wild type strains Roth X1-8, PX083, PX0142 and ICMP 3125^T. Leaf samples were harvested after 48 h and total RNA was isolated for qRT-PCR analysis. The expression of candidate target genes was compared to the gene expression in plants inoculated with inoculation medium.

17 candidate target genes were picked by educated guess from Table 14 as indicated and their expression was checked via qRT-PCR in appropriate samples. As no candidate target genes were found in the combinatorial prediction for TalAN and TalET, genes induced less than 1.5-fold were selected manually. The same procedure was performed for the classes TalAE, TalAF, TalAL, TalBJ and TalCA, as the candidate target genes were not promising because of their function or number of mismatches in the predicted TALE boxes. Six of these manually selected genes were analyzed via qRT-PCR as well (Table 15).

Table 15. List of hand-selected potential TALE target genes in rice for PX083, PX0142 and ICMP 3125^T

Locus ID	Annotated function ¹	Log2fold change	Strain	TALE	Rank	Position TALE box (bp)
Os01g50370	STE_MEKK_ste11_MAP3K.4	0.274	PX083			
		0.140	PX0142	TalAN	1	269
		0.450	ICMP 3125 ^T			
Os01g63510	homeobox domain containing protein	0.578	PX083	TalCA	4	265
Os02g51110	aquaporin protein (OsLsi1)	0.091	PX0142	TalAL	1	329
Os08g05910	peptide transporter PTR2 (OsNPF6.3)	0.366	PX083			
		0.215	PX0142	TalAE	1	231
		0.503	ICMP 3125 ^T			
Os09g30130	CSLE6 - cellulose synthase-like family E	0.106	PX083	TalBJ	19	185
Os12g24320	ATPase 3	0.307	PX083		17	
		0.293	PX0142	TalAF	17	143
		0.004	ICMP 3125 ^T		31	

¹ target gene names differing from annotated function are added in brackets

In total, the TALE-dependent induction of 13 out of 23 tested target genes could be validated with qRT-PCR (Figure 13). All 13 target genes were induced significantly in a comparison between Roth X1-8 with or without the corresponding TALE with p-values below 0.05. Four TALE targets were known previously: OsSWEET14 (Os11g31190),

OsHEN1 (Os07g06970), *OsTFIIA γ 1* (Os01g73890), and *OsTFX1* (Os09g29820) are induced by TALE classes TalBH, TalAP, TalBM and TalAR, respectively (Sugio *et al.*, 2007; Streubel *et al.*, 2013; Cernadas *et al.*, 2014). Five TALE targets were only hypothesized to be TALE targets before and are now experimentally confirmed: *OsLsi1* (Os02g51110), *OsPHO1;3* (Os06g29790), *OsNPF6.3* (Os08g05910), *OsMAP3K.4* (Os01g50370) and *OsFNS* (Os03g03034) are addressed by TALE classes TalAL, TalAO, TalAE, TalAN and TalAQ, respectively (Grau *et al.*, 2013; Cernadas *et al.*, 2014). Finally, four identified TALE targets have not been described before: *OsPLL4* (Os04g05050), *OsWAK51* (Os04g43730), *OsHLS1* (Os03g55530) and *OsFBX109* (Os03g51760) are manipulated by TALE class TalAB, TalES, TalBA, and TalAD. The target genes *OsLsi1* of TalAL, *OsNPF6.3* of TalAE and *OsMAP3K.4* of TalAN were picked manually because they were ambiguous in the RNA-seq experiment at 24 hours post inoculation (hpi). Interestingly, they were clearly induced in the qRT-PCR experiment at 48 hpi. This observation suggests that some TALEs might have a delayed effect within the host cell that is more pronounced at 48 hpi than at 24 hpi.

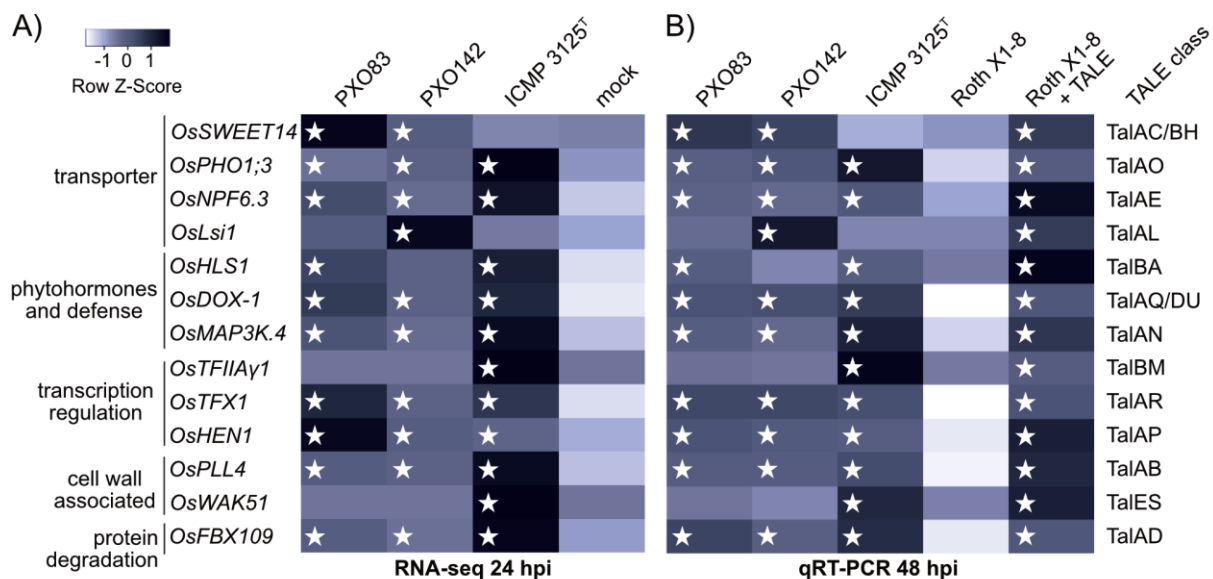


Figure 13. Induction of target rice gene expression upon infection with Xoo strains.

Unclustered heat maps were created using Heatmapper and rice gene expression is displayed via row Z-scores. Individual rice genes are labeled with their gene name and putative function (left). The right column indicates TALE classes with target boxes in the respective rice promoters. White stars mark the presence of a TALE class member in the different Xoo strains. (A) TALE-mediated gene induction analyzed via RNA-seq with RNA sampled 24 h after inoculation (hpi) of Nipponbare. Z-scores were assigned to arithmetic means of resulting RNA-seq reads of the three replicates and displayed in shades of blue. (B) Gene induction level analyzed via qRT-PCR with RNA sampled 48 h after inoculation of Nipponbare. The wild type Xoo strain Roth X1-8 does not contain any TALEs. Z-scores of relative RNA abundance were assigned to arithmetic means of two biological replicates using \log_{10} fold changes of gene expression in samples compared to mock treatment and displayed in shades of blue. Actin was used as a reference gene.

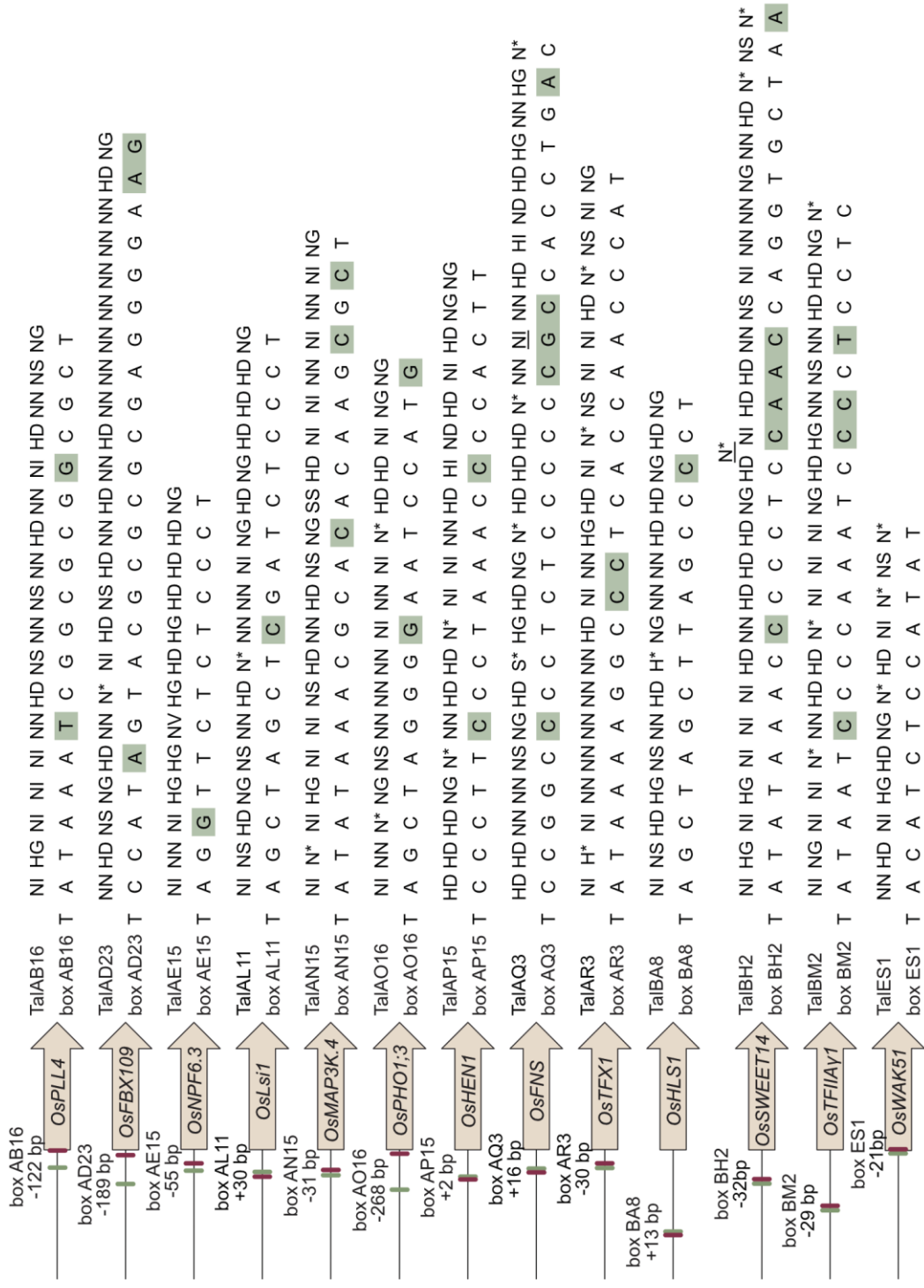


Figure 14. TALE boxes of rice target gene promoters. TALE target genes in rice cultivar Nipponbare with 1,000 bp upstream of their ATGs are shown schematically on the left and labeled with their locus identifiers. Locations of TALE boxes are indicated by green boxes and positions relative to the annotated transcription start site (red box) are noted. RVD sequences of natural TALEs analyzed in this study are lined up with the sequences of best fitting target boxes. Mismatches between RVDs and TALE boxes are highlighted green. TalAQ3 and TalBH2 have a repeat with 42 and 39 amino acids, respectively. Such repeats of aberrant length can either insert into the repeat array or loop out to accommodate 1 bp shorter target sequences. Aberrant repeats are underlined.

The TALE boxes in the promoters of these 13 genes match well to the RVD sequences of the corresponding TALEs (Figure 14). Previous findings suggest that TALEs can tolerate mismatches depending on their length and RVD composition (Rinaldi et al., 2017). This is

reflected well in the newly discovered TALE boxes, which have an average mismatch rate of 11%. The shortest TALE TalES1 fits the TALE box perfectly and the longest TALE TalBH2 tolerates 6 mismatches.

The location of TALE boxes varies greatly with TalES1 binding 21 bp upstream of the *OsWAK51* start codon and TalBA8 binding 635 bp upstream of the *OsHLS1* start codon. The position of TALE boxes in relation to the transcriptional start is more predictable, as TALE boxes are 55 bp upstream on average (Figure 14). This distance is consistent with the findings that TALEs typically determine the onset of transcription in a distance of 40 – 60 bp after their binding site (Streubel *et al.*, 2017).

The TALE boxes of TalAB16, TalAD23 and TalAO16 are located unusually far upstream of the natural transcriptional start site of their respective target genes. This could lead to a shift of the transcriptional start site (TSS). The TalAO16 box (-268 bp) is located furthest from the natural transcriptional start of its target gene *OsPHO1;3* and the effect is visible in the RNA-seq data of rice tissue infected with *Xoo* strains carrying a member of the class TalAO (Figure 15; Mücke *et al.*, 2019). The annotated TSS of *OsPHO1;3* does not seem to be used in any tested samples. In control rice plants, which were inoculated with 10 mM MgCl₂, *OsPHO1;3* transcripts were detected starting 93 bp downstream of the annotated TSS, which is also downstream of the annotated start codon (Figure 15B). In infected rice plants, *OsPHO1;3* transcripts were detected between 129 bp and 188 bp upstream of the annotated TSS (Figure 15B). This supports the previous findings suggesting TALEs can influence the transcriptional start site and it is a strong indicator that the difference in gene expression of *OsPHO1;3* is dependent on TalAO (Streubel *et al.*, 2017). Furthermore, *OsPHO1;3* contains three possible start codons, which are all in frame of the annotated CDS without stop codons in between. The annotated start codon is located in the middle, surrounded by an ATG 96 bp downstream and an ATG 63 bp upstream (Figure 15C). Therefore, it is possible that TalAO-mediated induction of *OsPHO1;3* transcription shifts the TSS and also leads to an altered CDS (Figure 15C).

The gene induction in rice infected with the Asian *Xoo* wild type strains was in accordance with the presence and absence of a member of the corresponding TALE class. This reaffirms that TALE class affiliation is a reliable indicator of shared target genes and the identification of a target gene for one member of the class will likely apply to the rest of the class members.

At the beginning of this thesis, six TALE classes with a total of 105 TALEs had known target genes. The identification of TALE-dependently induced genes in this thesis could

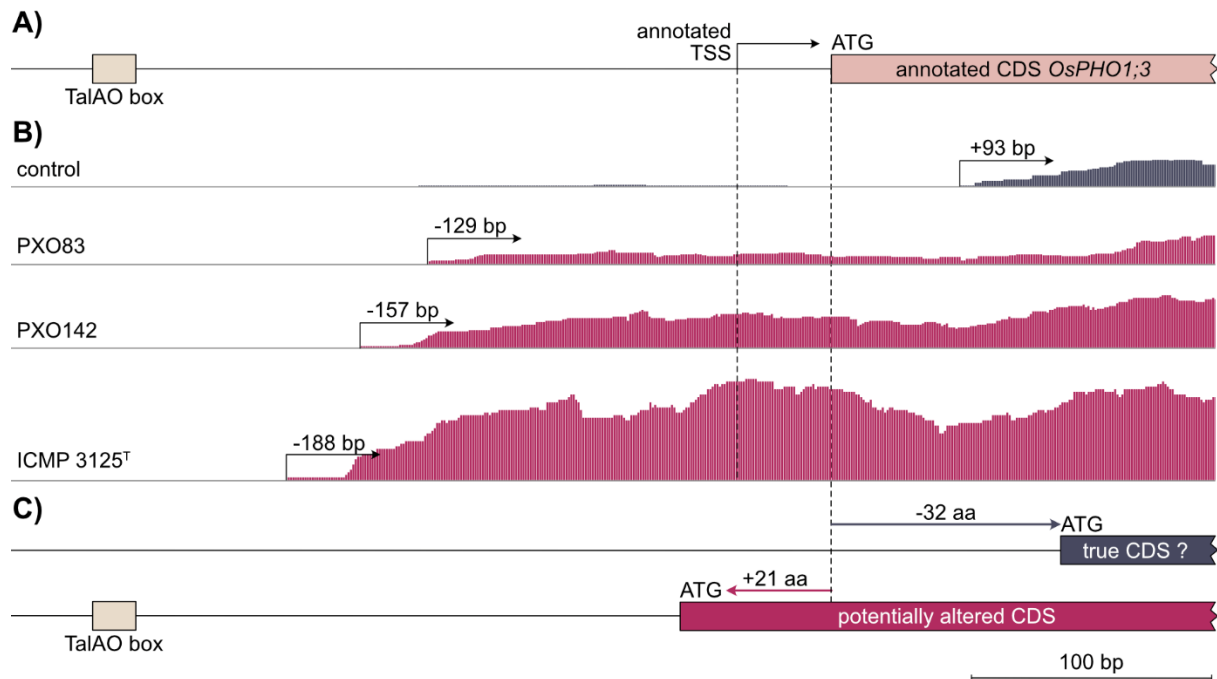


Figure 15. TalAO shifts the transcriptional start of *OsPHO1;3*.

A) True to scale overview of the *OsPHO1;3* locus with annotated transcriptional start site (TSS), start codon (ATG) and coding sequence (CDS) as well as the TalAO box. B) Coverage of RNA-seq reads of this locus. RNA-seq was performed with RNA sampled of Nipponbare 24 h after inoculation with *Xoo* strains PXO83, PXO142 or ICMP 3125^T (red) as well as control plants inoculated with 10 mM MgCl₂ (blue). Differences in TSS positions compared to annotation are indicated in base pairs (bp). C) Alternative start codons. Two hypothetical, alternative CDS are depicted with in frame alternative start codons. The difference in CDS length compared to annotation is depicted in amino acids (aa).

expand this to 14 TALE classes containing 339 TALEs. Furthermore, before this thesis the target genes of only two core TALE classes, TalAR and TalAP, were known (Sugio *et al.*, 2007; Cernadas *et al.*, 2014). At present, the potential target genes of eight core TALE classes are known: TalAR, TalAP, TalAD, TalAN, TalAB, TalAO, TalAQ and TalAE. This leaves only the target genes of core TALE classes TalAA and TalAG to be uncovered.

3.2.3. Differentiating direct and indirect TALE targets

Even though most identified target genes possess a suitable TALE box in their promoter region, the TALE-dependent gene induction is not a reliable indicator of direct promoter binding by the TALE. Therefore, the distinction between direct and indirect TALE targets needs to be made. Direct induction of target genes involves direct binding of the TALE to the promoter whereas indirect induction occurs, if the TALE is influencing target gene expression through secondary effects like the manipulation of regulatory genes without directly binding the promoter.

Therefore, the interaction between TALEs and their corresponding target gene promoters was analyzed in a transient system in *N. benthamiana*. Changing the system to a dicotyledonous plant minimizes the chances of TALEs influencing the promoters indirectly. TALEs can probably not create the same secondary effects by binding to native

promoters in *N. benthamiana* and rice, because they should be sufficiently different. Additionally, the ability of *N. benthamiana* regulatory systems to influence rice promoters should be limited. In order to observe an induction of target gene promoters, a GUS reporter assay was used. The target promoters were defined as 1,000 bp upstream of the start codon, amplified from Nipponbare DNA and cloned in front of the coding sequence of *uidA* into pGWB3GG. Reporter constructs were created for twelve of the 13 target genes (Figure 16). The interaction of *OsMAP3K.4* and *TalAN15* could not be analyzed due to time constraints. *A. tumefaciens* strains containing the reporter construct and strains carrying the corresponding TALEs in pSKA2 were co-inoculated into *N. benthamiana* (Figure 16C). The samples were harvested 2 dpi and used to perform qualitative and quantitative GUS assays.

All twelve tested TALEs can increase the GUS activity of their corresponding reporter constructs significantly, suggesting they can bind directly to their target promoters (Figure

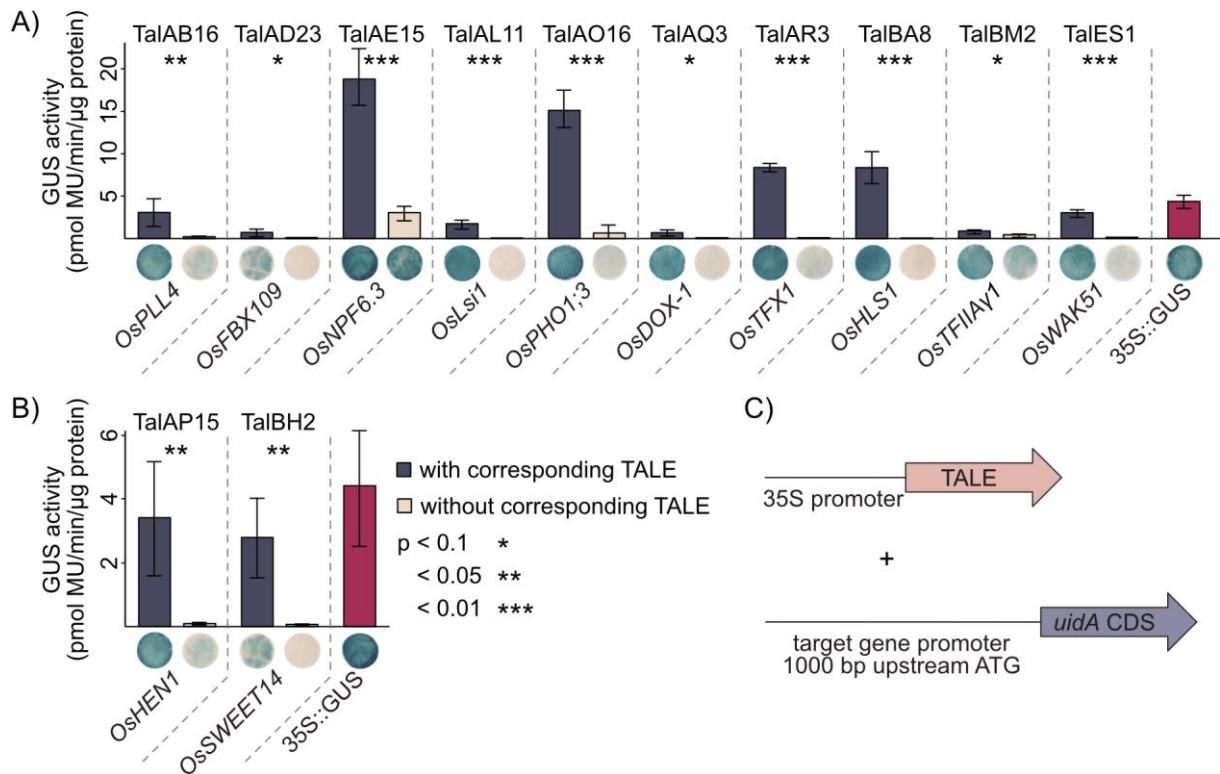


Figure 16. TALEs directly induce expression of target rice promoters in reporter studies in *N. benthamiana*. (A+B) 1,000 bp upstream of the ATGs of putative TALE target genes were amplified from rice cultivar Nipponbare DNA and cloned in front of the coding sequence of the *uidA* reporter gene. Artificial TALEs were assembled with RVD sequences shown in Figure 14 and Hax3 N- and C-terminal regions under control of a 35S promoter. *A. tumefaciens* strains delivering the reporter constructs and strains delivering the TALE expression constructs were co-inoculated into *N. benthamiana* leaves and β-glucuronidase measurements were performed 2 dpi. Experiments were performed three times with samples obtained as described above. Error bars represent standard deviation between triplicates. The statistical significance between samples with and without corresponding TALEs is indicated by p-values resulting from an unpaired t-test. The TALE Hax3 is used as a negative control in samples labeled without corresponding TALE. Histochemical GUS staining of leaf disks and quantitative GUS activity measurements were done in parallel from the same plants. (C) Schematic overview of experimental setup.

16 A+B). Most combinations of reporter constructs with their corresponding TALEs display an increase of 10- to 100-fold in GUS activity. *OsNPF6.3* and *OsTFIIAγ1* show less than 10-fold induction, while *OsLsi1* and *OsHLS1* display an increase of GUS activity of more than 100-fold. The GUS activity in samples containing reporter constructs paired with the incompatible TALE Hax3 is very low indicating that the reporter constructs are not expressed in the absence of a matching TALE. *OsNPF6.3* (Os08g05910) is the only promoter with relatively strong GUS activity even without a corresponding TALE, but the presence of TalAE15 leads to a significant increase in GUS activity, nonetheless. These findings suggest that all twelve tested target genes are direct TALE targets in rice.

In summary, the significant increase in verified TALE target genes in rice refines the understanding of the infection process and provides a multitude of potential resistance sources by interfering with susceptibility gene activation.

3.2.4. Convergent evolution of TALEs in rice-pathogenic *Xanthomonas* species

Key virulence targets that are important for a successful infection are often addressed by multiple virulence factors across pathogen species and host plants (van Schie and Takken, 2014). One of the best-studied examples of such a convergent evolution for TALE targets are *SWEET* genes. *SWEET* genes in rice, cassava and cotton are induced by different TALEs from different *Xanthomonas* strains (Yang and White, 2004; Cohn *et al.*, 2014; Zhou *et al.*, 2015; Cox *et al.*, 2017). Additionally, the TALE targets of African, South American and Australian *Xoo* strains as well as *Xoc* strains were evaluated to cover all rice-infecting *Xanthomonas* species.

At the start of this thesis, three target genes in rice were known to be induced by more than one TALE class (Figure 17). *OsSWEET14* is induced by TalAC and TalBH of Asian *Xoo* strains and TalDS and TalDK of African *Xoo* strains (Yang and White, 2004; Römer *et al.*, 2010; Yu *et al.*, 2011; Streubel *et al.*, 2013). *OsTFX1* is targeted by TalAR of Asian *Xoo* strains and TalDI of African *Xoo* strains (Sugio *et al.*, 2007; Tran *et al.*, 2018). *OsHEN1* is induced by TalAP of Asian *Xoo* strains and TalAK of *Xoc* (Cernadas *et al.*, 2014; Mücke *et al.*, 2019). All three target genes have been shown to influence disease severity,

Table 16. Differences in TALEs inducing *OsDOX-1*.

TALE	repeat number	RVD sequence ¹														strain of origin	
AQ3	26.5	HD	HD	NN	NN	NS	NG	HD	S*	HG	HD	NG	N*	HD	HD	HD	Xoo PX083
		N*	NN	NI	NN	HD	HI	ND	HD	HG	NN	HG	N*				
BR1	26.5	HD	HD	NN	NN	NG	N*	HD	NI	NG	HD	NG	NS	HD	HA	ND	Xoc BLS256
		N*	ND	NN	HD	NN	NN	HD	HD	N*	NN	NG	HD				

¹ differences in RVD compositions are shown in bold

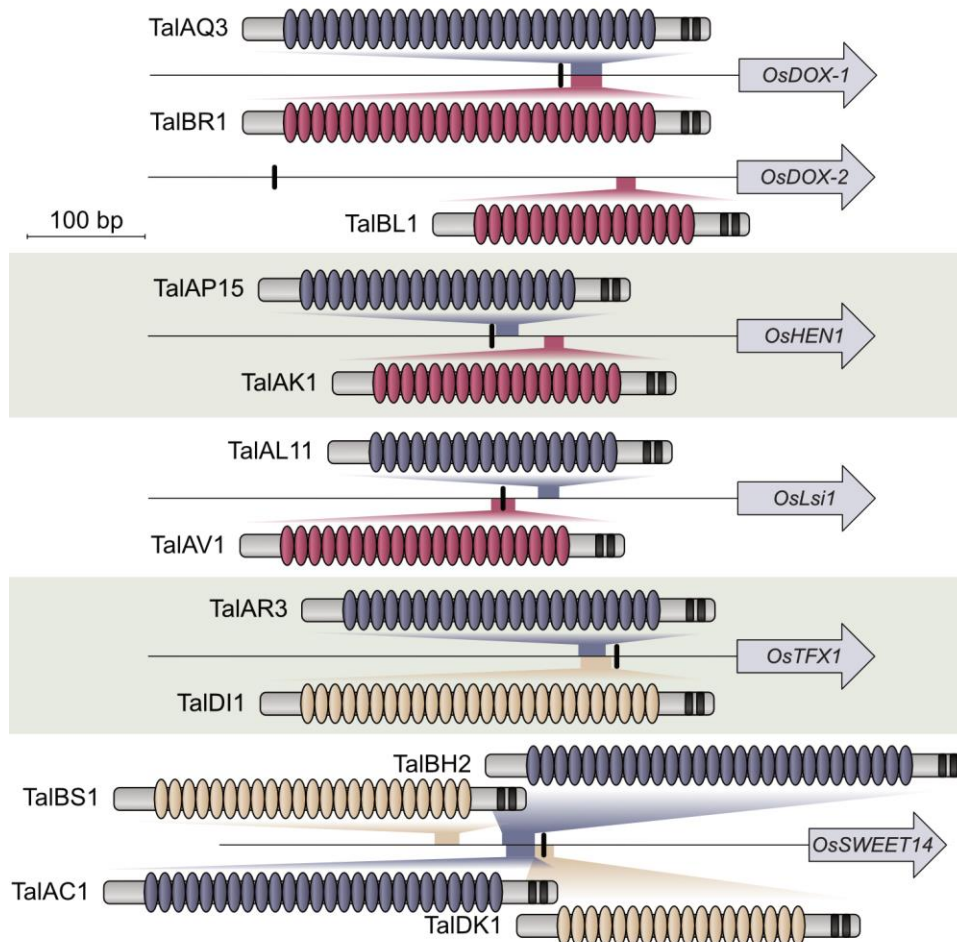


Figure 17. Overview of convergent evolution of TALEs.

A schematic overview of all known TALE target genes in rice, that are induced by more than one TALE class, is shown. Coding sequences of TALE target genes are depicted as arrows with 500 bp upstream. TALEs of Asian (blue) and African (yellow) *Xoo* strains and TALEs of *Xoc* strains (red) binding these promoters are indicated and the TALE boxes are highlighted. Natural transcriptional start sites are indicated with a black box.

indicating the importance of these target genes. TalAD and TalAF are not considered in this analysis, as these two classes are present in *Xoo* and *Xoc*.

In this thesis, two more target genes, which were induced by more than one TALE class, could be identified. The target gene *OsFNS* (Os03g03034) of TalAQ was proposed to also be induced in *Xoc* infections (Cernadas *et al.*, 2014). TalBR of *Xoc* was identified as a second TALE class addressing the same gene. Interestingly, both TALE classes have 26.5 repeats and bind the same promoter sequence, but differ in 16 RVDs (Table 16). *OsFNS* encodes a 2-oxoglutarate dioxygenase (DOX), whose substrate is highly debated in the research community (Kim *et al.*, 2008; Falcone Ferreyra *et al.*, 2015; Zeilmaker *et al.*, 2015; Zhang *et al.*, 2017b). While the debate is still ongoing, a second DOX (Os04g49194) was identified as a potential TALE target of the TALE class TalBL of *Xoc* (Cernadas *et al.*, 2014). These two DOX genes share 69.6% identity and 85.6% similarity and are described as highly related homologs (Kawai *et al.*, 2014; Falcone Ferreyra *et al.*,

2015). In order to acknowledge the uncertainty of the function of these genes and their connection in *Xanthomonas*-rice interaction, a new nomenclature was proposed to rename Os03g03034 to *OsDOX-1* and Os04g49194 to *OsDOX-2* (Mücke *et al.*, 2019). TalBR1 and TalBL1 of *Xoc* strain BLS256 as well as a GUS reporter for *OsDOX-2* were provided by Sebastian Becker to evaluate the direct interaction between the TALEs and their respective promoters as described before (Chapter 3.2.3; Figure 18A). All three TALE classes, TalAQ, TalBR and TalBL, were able to increase the measured GUS activity by directly inducing their corresponding *DOX* promoters. This data proves that three distinct TALE classes of two different *Xanthomonas oryzae* pathovars are targeting the same functional hub in rice.

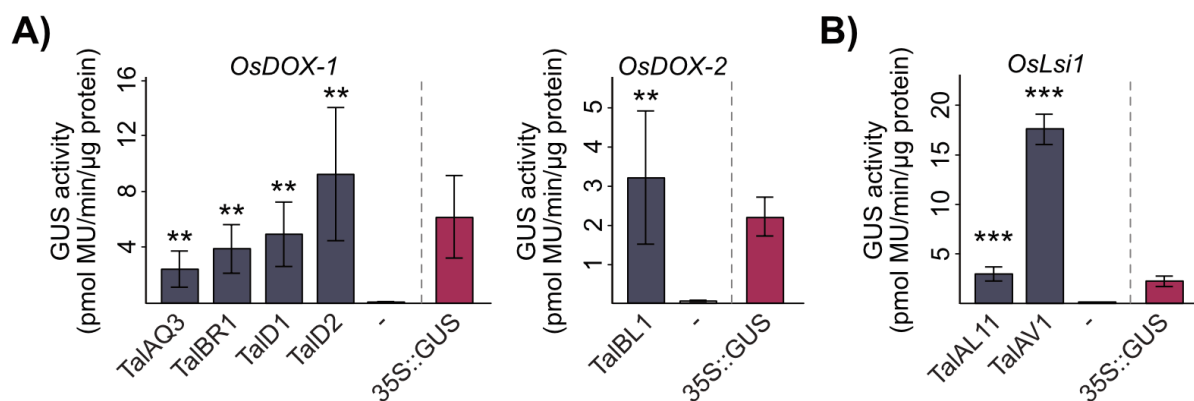


Figure 18. New shared TALE targets of *Xoo* and *Xoc*.

(A+B) 1,000 bp upstream of the ATGs of the TALE target genes were amplified from rice cultivar Nipponbare DNA and cloned in front of the coding sequence of the *uidA* reporter gene. Artificial TALEs were assembled with Hax3 N- and C-terminal regions under control of a 35S promoter. A. *tumefaciens* strains delivering the reporter constructs and strains delivering the TALE expression constructs were co-inoculated into *N. benthamiana* leaves and β -glucuronidase measurements were performed 2 dpi. Quantitative GUS activity measurements were performed three times with samples obtained as described above. Error bars represent standard deviation between triplicates. The statistical significance between samples with and without corresponding TALEs is indicated by p-values (<0.1 = *; <0.05 = **; <0.01 = ***) resulting from an unpaired t-test. The TALE Hax3 is used as a negative control in samples labeled with a dash.

Additionally, we found two TALE classes, TalAL of *Xoo* and TalAV of *Xoc*, that probably both target *OsLsi1* (Figure 17). Sebastian Becker provided an expression construct for TalAV1 and the GUS activity of an *OsLsi1* GUS reporter construct was measured in response to TalAL11 and TalAV1 (Chapter 3.2.3; Figure 18B). Both TALE classes were able to increase the measured GUS activity, indicating a direct recognition of the *OsLsi1* promoter. TalAL and TalAV bind the promoter in different positions, which suggest a convergence on this target gene. The fact that multiple Asian *Xoo* strains have two copies of this TALE underscore their potential significance (Chapter 3.1.1).

These strains might be adapted to different versions of this promoter, as the two members of TalAL always display minor differences in their RVDs (Table 17). According to the daTALbase tool, there is a known variant of the *OsLsi1* promoter with the altered

TALE box TAG[C/T]TAGCTCGATCTCCCT, but the SNP does not correspond to differences between the TalAL members (Pérez-Quintero *et al.*, 2018).

The discovery of new target genes that are addressed by multiple TALE classes from different *Xanthomonas oryzae* pathovars is an important step to understand conserved susceptibility genes. Especially in *Xoc*, the identification of potential influences of TalBR and TalBL on infection might have been obscured by their redundant function.

Table 17. Variations of TalAL in strains with more than one copy.

TALE	TALE cluster	RVD sequence ¹																strain of origin	
AL11	VIII	NI	NS	HD	NG	NS	NN	HD	N*	NN	NN	NI	NG	HD	NG	HD	HD	HD	PX0142
AL21		NS	HD	NG	NS	NN	HD	N*	NN	NN	NI	NG	HD	NG	HD	HD	HD	PX0364	
AL23		NI	NS	HD	NG	NS	NN	HD	N*	NN	NN	NI	NG	HD	NG	HD	HD	HD	PX0404
AL25		NG	NS	HD	NG	NS	NN	HD	N*	NN	NN	NI	NG	HD	NG	HD	HD	HD	PX0421
AL27		NI	NS	HD	NG	NS	NN	HD	N*	NN	NN	NI	NG	HD	NG	HD	HD	HD	PX0513
AL22	IX	NI	NS	HD	NG	NS	NN	HD	N*	NN	NN	NI	NN	HD	HG	HD	HD	NN	PX0364
AL24		NS	HD	NG	NS	NN	HD	N*	NN	NN	NI	NN	HD	HG	HD	HD	NN	PX0404	
AL26		NI	NS	HD	NG	NS	NN	HD	N*	NN	NN	NI	NN	HD	HG	HD	HD	NN	PX0421
AL28		NG	NS	HD	NG	NS	NN	HD	N*	NN	NN	NI	NN	HD	HG	HD	HD	NN	PX0513
AL12	IX	NI	NS	HD	NG	NS	NN	HD	N*	NN	NN	NS	NN	HD	HG	HD	HD	NN	PX0142
		NG	NS	HD	NG	NS	NN	HD	N*	NN	NN	NS	NN	HD	HG	HD	HD	NN	

¹ differences in RVD compositions are shown in bold

3.3. Impact of individual TALEs on virulence

TALEs were shown to induce a multitude of genes in their host plants (Tariq 2019). A lot of these genes are likely irrelevant to the pathogen-host interaction and are simply induced as a collateral target. Only the induction of a few genes, the susceptibility genes, are believed to benefit *Xanthomonas* (Kay *et al.*, 2007). Only the direct connection between the presence or absence of a TALE with a change in virulence can establish a susceptibility gene.

3.3.1. Influence of single TALEs on lesion length in rice

The most common method to quantify *Xoo* virulence is to measure the length of lesions developing on rice leaves, which were infected by cutting the leaf tip with scissors dipped in bacterial solution. In order to create long lesions, *Xoo* has to evade plant recognition, invade the xylem and establish infection to multiply.

The three *Xoo* strains PX083, PX0142 and ICMP 3125^T show very different abilities to form lesions on rice cultivar Nipponbare. PX083 is a very virulent strain and creates lesions of up to 20 cm, while PX0142 is a more moderate strain that creates lesions of about 10 cm on average (Figure 19). On the contrary, ICMP 3125^T is not able to cause lesion formation and Roth X1-8 generates little to no lesions on Nipponbare. Therefore, Roth X1-8 is the ideal tool to investigate the impact of individual TALEs on lesion length, because it does not contain natural TALEs. The Roth X1-8 derivatives created in chapter

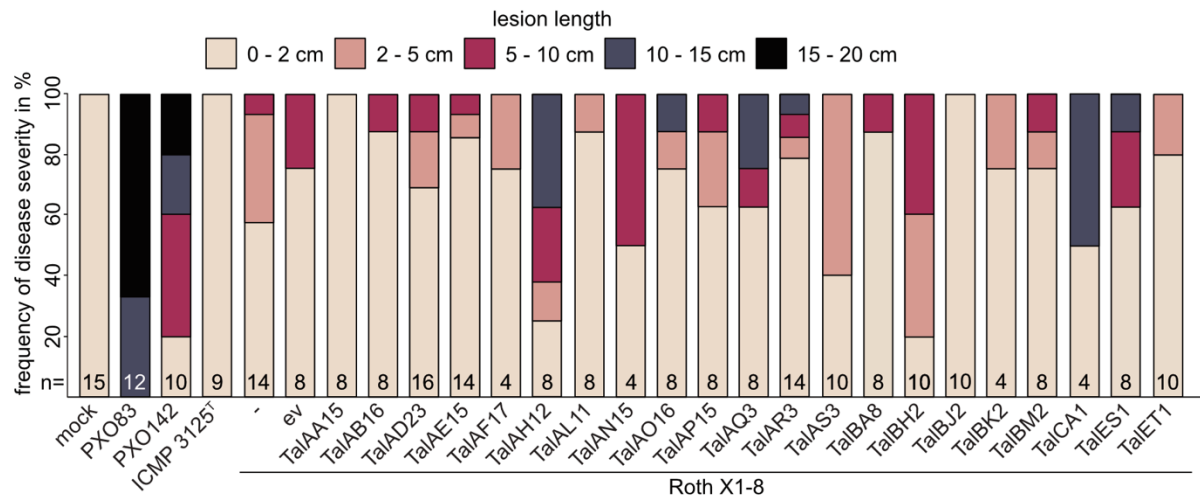


Figure 19. Impact of single TALEs on disease severity measured by lesion length.

The rice cultivar Nipponbare was infected with Xoo strains PXO83, PXO142, ICMP 3125T and Roth X1-8 as well as Roth X1-8 containing single TALE expression constructs. Infection was done by clipping the third leaf with scissors dipped in bacterial solution ($OD_{600} = 0.2$). 14 days after infection leaves were harvested and lesion length was measured. Disease severity was scored in five different categories: 0 – 2 cm, 2 – 5 cm, 5 – 10 cm, 10 – 15 cm and 15 – 20 cm. Infections were done in four independent experiments and number of infected plants (n) is shown in the bars. Depicted is the frequency of different disease severity categories observed through all experiments. ev – empty vector

3.1.2 were used to perform leaf clipping assays in order to analyze the differences in lesion length compared to Roth X1-8 without TALEs (Figure 19).

Unfortunately, the lesion lengths caused by the Roth X1-8 derivatives were very inconsistent, suggesting an external influence on the lesion formation that could not be identified. Only the lack of any lesion formation in Roth X1-8 carrying TalAA15 or TalBJ2 is very striking. This fits well with earlier observations hinting to a selection against TalAA potentially due to an as yet unknown resistance gene (Chapter 3.1.1). The known avirulence function of TalBJ (AvrXa10) in rice is probably not responsible for the lack of lesion formation, because Nipponbare does not contain the responsible resistance gene *Xa10* (Tian *et al.*, 2014). The loss of TalAR and TalBH was shown previously to cause shortening of lesion lengths in Xoo-rice interactions (Yang and White, 2004; Sugio *et al.*, 2007). Here, no clear gain-of-function can be shown for either TALE class, even though Roth X1-8 carrying TalBH was able to establish lesions more frequently and Roth X1-8 containing TalAR was able to form longer lesions occasionally. Similarly, no definitive conclusions can be drawn for the other tested TALE classes, but some TALE classes proved to be sometimes beneficial for lesion formation: TalAH, TalAN, TalAO, TalAQ, TalCA and TalES.

The measurement of lesion length was not a reliable tool to evaluate the impact of TALEs on virulence under the tested conditions. Nevertheless, some insight could be gained on which TALEs could be beneficial for infection.

3.3.2. Impact of individual TALEs on bacterial growth *in planta*

Previous studies on the influence of TALEs on virulence suggest that *SWEET*-inducing TALEs are most important for differences in disease symptom formation measured by lesion length (Streubel *et al.*, 2013). Therefore, it is possible that other TALEs can benefit infection without a visible difference in symptom formation. To test this, the bacterial growth of wild type Roth X1-8 in Nipponbare was compared to a selected group of Roth X1-8 derivatives carrying TALEs.

Nipponbare leaves, which were clipped 14 days prior with *Xoo*, were cut into two segments representing the first 5 cm after the clipping site and the following region of 5 – 10 cm (Figure 20). Leaf segments were disrupted and dilutions of the extract were plated on appropriate media to subsequently count colony forming units (CFU) of *Xoo*.

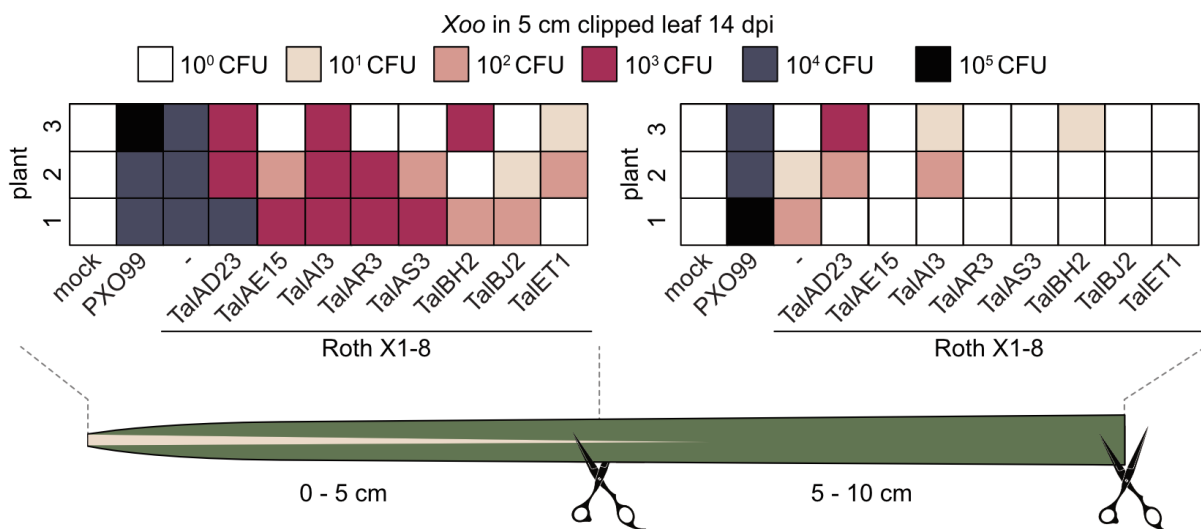


Figure 20. Influence of individual TALEs on bacterial growth *in planta*.

The rice cultivar Nipponbare was infected with *Xoo* strains PXO99 and Roth X1-8 as well as Roth X1-8 containing single TALE expression constructs. Infection was done by clipping the third leaf with bacterial solution ($OD_{600} = 0.2$). 14 days after infection leaves were harvested and separated into two 5 cm long pieces. The samples were disrupted and the extract was plated in several dilutions on PSA medium containing antibiotics selecting against fungi and other bacteria. The colony forming units (CFU) were calculated after three days.

The *Xoo* strain PXO99 was used as a positive control and displayed between 10⁴ and 10⁵ CFU for both segments. 10⁴ CFU could be counted for Roth X1-8 in the segment close to the clipping site but only 10 to 10² CFU were counted in the segment further from the site, indicating a delayed or impaired movement in the plant. Interestingly, most Roth X1-8 derivatives containing a TALE expression construct had lower CFU than the wild type Roth X1-8. Even TalAR3 and TalBH2, which are known to contribute to virulence in *Xoo*, seemed to have a negative impact on bacterial growth in this experiment (Yang and

White, 2004; Sugio *et al.*, 2007). High variation between plants could be observed, which is consistent with the high variation in lesion length in clipped leaves.

Additionally, the disruption of rice tissue proved to be difficult and the majority of *Xoo* are located in the xylem, which is further fortified. Therefore, it is possible that samples were not completely disrupted, which would lead to the observed high variability and in general, a decrease in measured CFU.

In conclusion, evaluation of bacterial growth *in planta* did not improve the quality of data output in comparison with lesion length measurements.

3.3.3. Collaborative effects of TALEs on virulence.

Inoculation of rice leaves with *Xoo* and subsequent visual assessment of lesion development after 6 days is an alternative method to evaluate the virulence of *Xoo*. Therefore, the *Xoo* strains PX083, PX0142, ICMP 3125^T and Roth X1-8 as well as the Roth X1-8 derivatives were inoculated into Nipponbare. Rice infected with PX083 showed severe disease symptoms, PX0142 caused mild symptoms and rice inoculated with ICMP 3125^T did not show any symptom formation (Figure 21). Roth X1-8 caused mild disease symptoms (Figure 21) and no difference in symptom formation could be identified for any Roth X1-8 derivatives (data not shown).

The effects of individual TALEs might be too small to be detected in this virulence assay. Therefore, the collaborative effects of TALEs were analyzed. The five core TALE classes of cluster T-IX and TalBH2, which is known to induce a susceptibility target, were selected to be analyzed (Yang and White, 2004).

In a first experiment, Roth X1-8 containing TalaQ3, TalAD23, TalBH2 or no TALE were mixed with each other in different combinations and inoculated into Nipponbare to evaluate additive effects (Figure 21). Interestingly, the mixture TalaQ3/-/-, TalBH2/-/-, TalaQ3/TalBH2/- and the TalBH2/TalAD23/- caused slightly more severe symptoms than wild type Roth X1-8. The fact that mixtures containing different combinations of the three TALEs, but not a combination of all three TALEs showed increased symptoms, suggests a high variability in the experiment. As delivery of equal amounts of inoculum is hard to achieve in rice, these fluctuations might be due to differences in inoculation of individual spots.

In a second experiment, Roth X1-8 carrying one of the five core TALEs of cluster T-IX or TalBH2 were mixed 1:5 with wild type Roth X1-8 or in equal parts with each other and inoculated into Nipponbare. None of the combinations showed a difference in disease

3.4.1. Adapting TALEs to the versatile MoClo Cloning system

In order to create new specialized assays, more flexibility in TALE expression constructs is needed. The Golden TALE Technology Cloning Kit used in this group to clone TALEs is not compatible with other modular cloning systems in regard to the use of restriction enzymes or overhangs (Geißler *et al.*, 2011). Therefore, new vectors needed to be designed to connect the Golden TALE Technology to the versatile MoClo system (Weber *et al.*, 2011; Engler *et al.*, 2014).

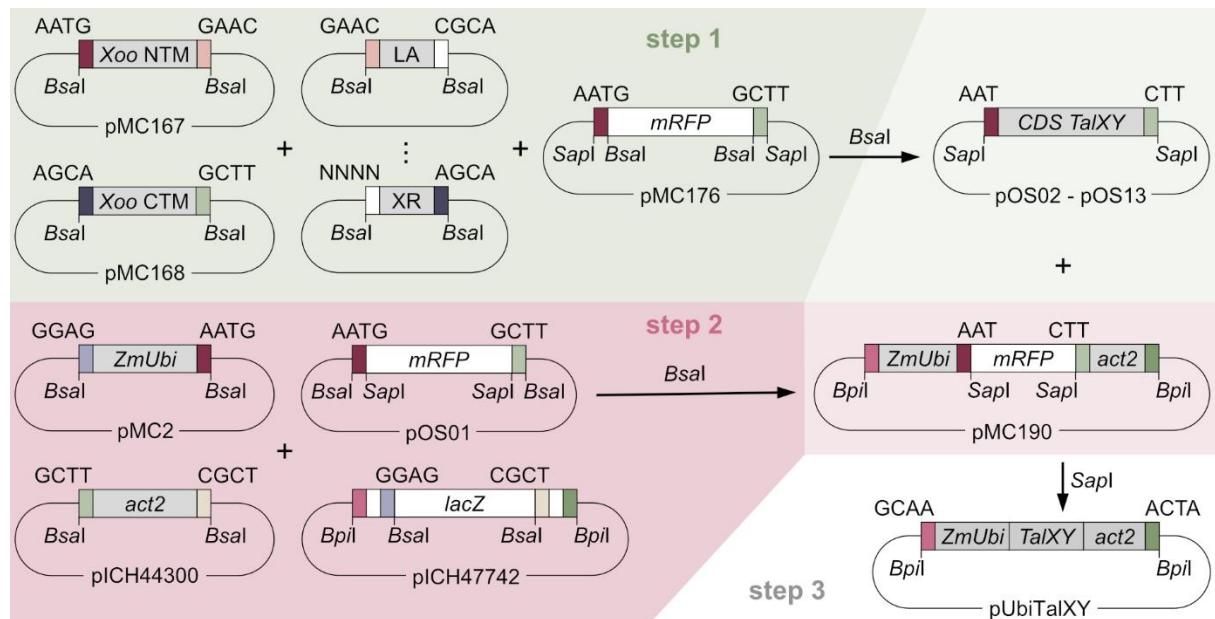


Figure 22. Adapting the Golden TALE Technology Cloning Kit to the MoClo system.

The three steps connecting the Golden TALE Technology Cloning Kit to the MoClo system are shown schematically. In the first step (green), the coding sequence (CDS) of the TALE is assembled into pMC176. In the second step (pink), a transcriptional unit is assembled into a level 1 vector using pOS01 as a dummy for the coding region. In the final step (white), the dummy in the assembled transcriptional unit is swapped with the TALE coding sequence.

The aim was to fit the complete coding sequence of TALEs into the framework of MoClo modules. The assembly of full TALEs into a destination vector in the Golden TALE system is accomplished by *BsaI*. On the contrary, coding sequences in the MoClo system are assembled into functional transcription units using *BsaI*. Thus, the TALE coding sequence is assembled using *BsaI* and in the next cloning step *BsaI* sites are needed again, which is difficult to achieve. To circumvent this problem, an intermediate cloning step was introduced (Figure 22). First, TALEs will be assembled into a new TALE receiver vector (pMC176) that adds new type IIS restriction sites to the sequence. Second, a full transcriptional unit is created in a MoClo level 1 vector according to the desired attributes (level 0 modules) with a dummy module (pOS01) instead of a coding region. Third, the dummy module in the transcriptional unit can be swapped with any TALEs cloned in the TALE receiver.

The type IIS restriction enzyme used for the final swap should be absent in the TALE sequence, all MoClo level 0 modules and the vector backbone of the level 1 vectors and the TALE receiver. *SapI*, which creates a 3 bp overhang, was deemed a suitable candidate. Next, appropriate selection markers were determined. The level 0 modules have a spectinomycin resistance, the level 1 vectors contain an ampicillin resistance and the multi repeat modules of the TALE sequence carry a kanamycin resistance. Additionally, the cloning into level 1 vectors is monitored with a blue-white screening. Therefore, a gentamycin resistance was chosen for the new TALE receiver vector and the coding sequence dummy will contain a mRFP cassette to facilitate red-white screening.

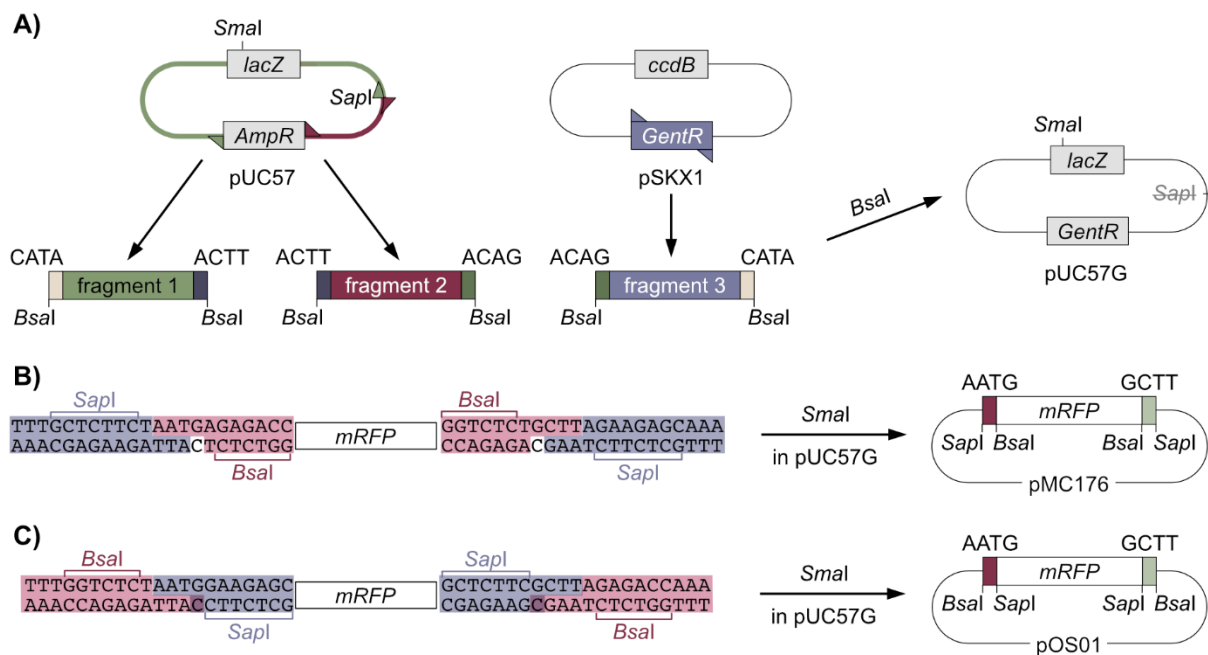


Figure 23. Cloning of pUC57G, pMC176 and pOS01.

(A) pUC57G was created out of two modules amplified from pUC57 and one module amplified from pSKX1. The modules were combined using *Bsal* in a Golden Gate reaction and the final vector is set apart from pUC57 by the missing *SapI* site and a different antibiotic resistance. (B+C) The vectors pMC176 and pOS01 were created by cloning PCR fragments blunt-end into pUC57G with *SmaI*. The flanking restriction enzyme sites for the created PCR fragments are shown in red (*Bsal*) and blue (*SapI*).

To this end, several new vectors were created. First, the pUC57 derivative pUC57G was cloned. pUC57G contains the sequence of pUC57, but a *SapI* site was mutated and the coding sequence of the ampicillin resistance was exchanged for the coding sequence of the gentamycin resistance found in pSKX1 (Figure 23A). Next, the mRFP module of pJOG107 was amplified with primers to add all needed restriction enzyme sites for the creation of pMC176 and pOS01 and the products were cloned blunt-end into pUC57G using *SmaI* (Figure 23B+C). Additionally, the N- and C-terminal TALE modules were adjusted to fit the overhangs of the MoClo coding sequence modules (AATG-GCTT) by Sebastian Becker.

Finally, the multi repeat modules created in chapter 3.1.2 were used to clone the twelve TALEs with evaluated target genes into the TALE receiver pMC176. For proof of principle, a transcriptional unit, which contained a *ZmUbi* promoter and an *act2* terminator, was created in pMC190. TalAE15, TalAL11, TalAO16 and TalBH2 were cloned into pMC190, resulting in the plasmids pUbiTalAE15, pUbiTalAL11, pUbiTalAO16 and pUbiTalBH2, respectively (Figure 22). Several of these cloning steps were performed by Olivia Sierra during her student exchange.

This new tool integrates the Golden TALE Technology cloning system into the MoClo system and can be used for all TALEs and other difficult compound coding sequences in the future.

3.4.2. TALEs and cell membrane transporters

Four of the thirteen TALE targets evaluated in this thesis are encoding membrane transporters. This is a group with high importance, as two of them, the phosphate transporter gene *OsPHO1;3* and the nitrate transporter gene *OsNPF6.3*, are targeted by the core TALE classes TalAO and TalAE, respectively. Additionally, the well-known SWEET transporters, which are described as major virulence factors, belong in this category as well (Streubel *et al.*, 2013). In order to study the TALE-dependent nutrient flow in rice, a specialized assay was developed.

3.4.2.1. Establishing rice protoplasts for TALE research

The localized nutrient flow at the infection site is difficult to analyze. Therefore, protoplasts were chosen to monitor TALE-dependent nutrient flow in single cells. Protoplasts can be transformed with expression constructs for individual TALEs and nutrient flow might subsequently be evaluated with different specialized markers.

In order to differentiate between protoplasts that were transformed with the desired construct and untransformed protoplasts, fluorescence markers were utilized. The fluorescent proteins turbo GFP (tGFP) and mCherry were cloned under the double 35S promoter into level 1 vectors of the MoClo system (Weber *et al.*, 2011; Engler *et al.*, 2014). tGFP and mCherry were chosen because they have very different excitation and emission spectra (Figure 24A). This decreases the risk that the established fluorescence markers interfere with reporter systems in the future. Before this thesis, rice protoplasts were used on occasion in our group, but no efficient protocol for protoplast isolation and transformation was established. Protoplastation and subsequent transformation with the fluorescence markers was done according to Shan *et al.* (2014).

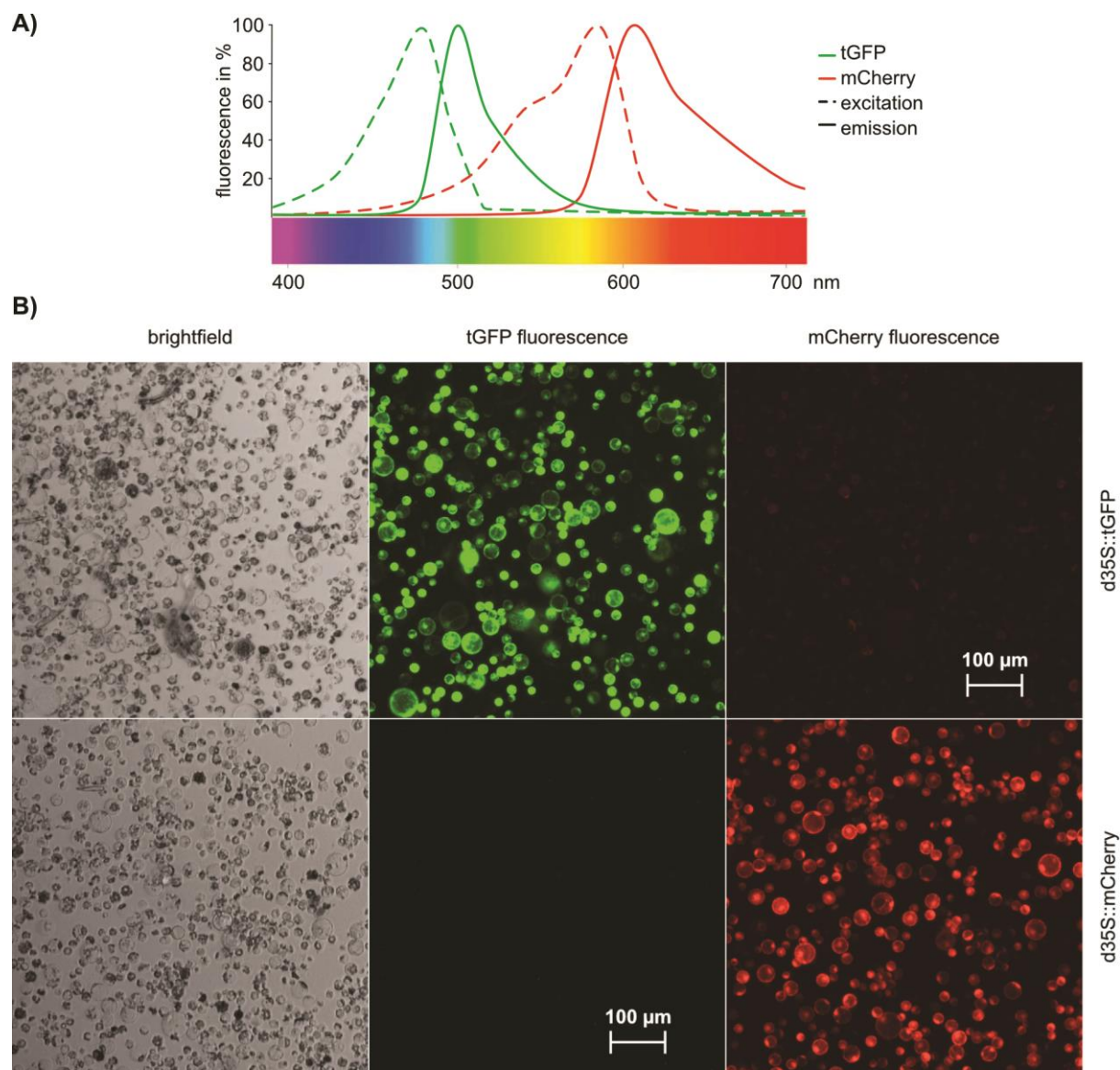


Figure 24. Establishing fluorescence markers to identify transformed rice protoplasts.

(A) The excitation and emission spectra of tGFP and mCherry are depicted. (B) Rice protoplasts were transformed with either d35S::tGFP or d35S::mCherry and fluorescence was determined after 24 h.

The stems of two-week-old rice plants were used to isolate protoplasts and the protoplasts of about 10 plants were used per transformation. Each transformation was done using 20 μ g plasmid DNA and a PEG solution. 24 h after transformation, the fluorescence of the protoplasts was evaluated with a fluorescence microscope. The analyzed protoplasts displayed strong green fluorescence with tGFP and strong red fluorescence with mCherry (Figure 24B). The protoplasts transformed with mCherry showed no green fluorescence and tGFP showed minimal red fluorescent background signal. This indicates that both fluorescence markers are functional in rice protoplasts and can be used to identify transformed protoplasts.

An area of about 0.4 mm² was used to determine the transformation efficiency for both constructs. The protoplasts were transformed with tGFP with an efficiency of 49.8% and mCherry displayed a transformation efficiency of 52.7%.

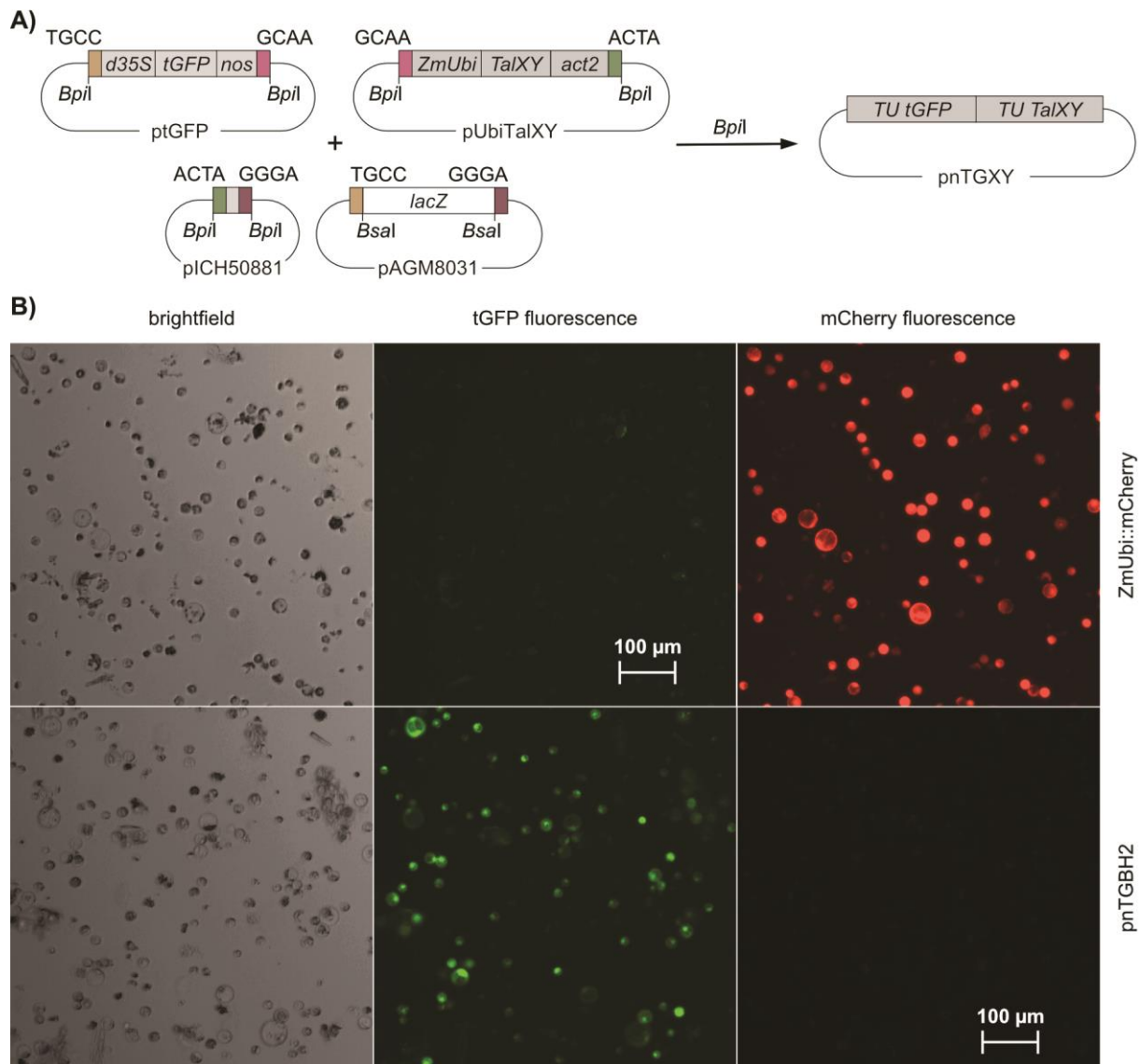


Figure 25. Visualizing protoplasts transformed with TALE expression constructs.

(A) The cloning of compound vectors containing transcriptional units for tGFP and TALEs is shown schematically. (B) Rice protoplasts were transformed with either pZmUbi::mCherry or pnTGBH2 and fluorescence was determined after 24 h.

In order to transform protoplasts with a TALE expression construct and to be able to identify the transformed cells, a compound vector needed to be created. Therefore, the level 1 construct of the fluorescence marker tGFP was combined with level 1 constructs of TALEs under ZmUbi promoters created in chapter 3.4.1, resulting in pnTGAE15, pnTGAL11, pnTGA016 and pnTGBH2 (Figure 25A). The resulting level M vector pnTGBH2, which contained TalBH2, was used to transform protoplasts to monitor changes in transformation efficiency due to the increased plasmid size of 13 kbp (Figure 25B). The transformation efficiency was determined to be 45.2%, which is slightly lower than

observed for the tGFP level 1 vector (6 kbp). Additionally, a *ZmUbi::mCherry* construct was used for transformation to verify *ZmUbi* activity in rice protoplasts (Figure 25B). *ZmUbi::mCherry* showed strong fluorescence, indicating a robust activity of the *ZmUbi* promoter.

These experiments show that rice protoplasts can be transformed with TALE expression constructs and the transformed protoplasts can be visualized. These compound vectors can subsequently be used to study TALE-dependent nutrient flow in rice cells.

3.4.2.2. SWEET-inducing TALEs and esculin uptake

The hypothesis that SWEET transporters induced by TALEs export sugars to the bacteria is based on two separate observations. First, TALEs induce the expression of *SWEET* genes and second, SWEET transporters were shown to transport sugar bidirectionally in *Xenopus* oocytes (Chen *et al.*, 2012; Streubel *et al.*, 2013). However, the direct impact of TALEs on sugar transport in rice was not evaluated. In a recent publication, the fluorescent sucrose analog esculin was utilized to visualize SWEET-mediated sucrose transport in *A. thaliana* protoplasts (Rottmann *et al.*, 2018). Therefore, esculin transporter assays were used to analyze sucrose flow in rice protoplasts.

Rottmann *et al.* (2018) reported that *A. thaliana* protoplasts of companion cells and epidermis cells naturally expressed a sucrose transporter and are able to accumulate esculin without transformation. To test this, untreated rice protoplasts were incubated with 1 mM esculin for 1 h. Afterwards, protoplasts were washed and esculin fluorescence was detected using the DAPI filter set of the fluorescence microscope (Figure 26A). Esculin fluorescence could be detected in very small protoplasts with little to no chloroplasts, which are possibly companion cells or epidermis cells. This experiment showed that the experimental conditions used in Rottmann *et al.* (2018) can also be applied for rice protoplasts.

Next, TALE-dependent changes in sucrose flow were evaluated. Rice protoplasts were transformed with *d35S::tGFP* or *pnTGBH2*, which encodes *tGFP* and *TalBH2*, to analyze the esculin uptake in the presence of *TalBH2*. Esculin uptake assays were performed 24 h after transformation (Figure 26B). Esculin fluorescence was detected in very small protoplasts as observed before, but no overlap of tGFP and esculin fluorescence could be detected. This might be due to the timing of the esculin assay. 24 h should be enough time to express the tGFP marker and *TalBH2*, but expression and synthesis of SWEET transporters might not be high enough at such an early time point. Alternatively, the

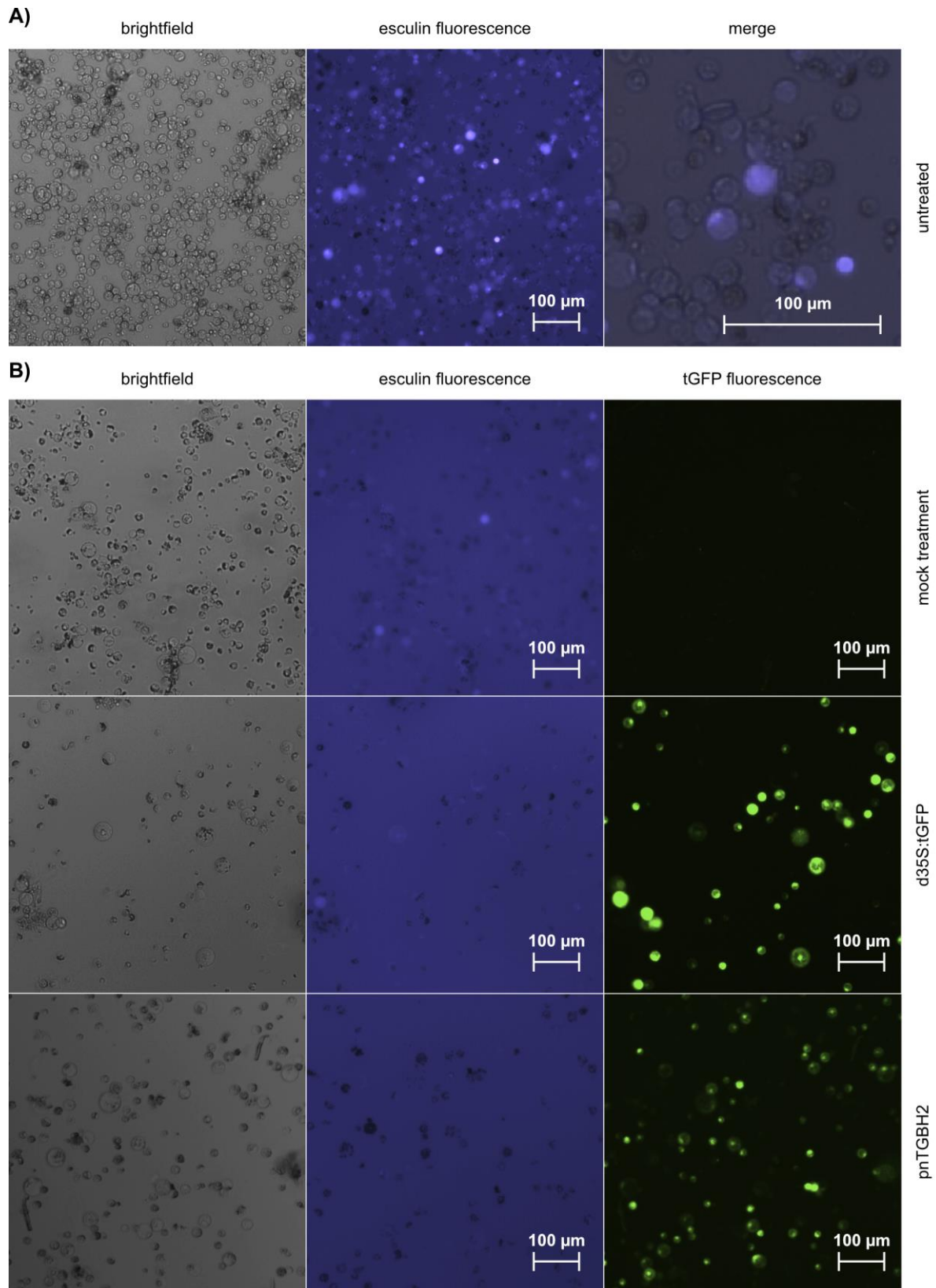


Figure 26. Esculin uptake assays in rice protoplasts.

Esculin uptake was analyzed in untreated rice protoplasts (A) and protoplasts transformed with either *d35S::tGFP* or *pnTGBH2* (B). 24 h after transformation protoplasts were incubated with 1 mM esculin for 1 h. Afterwards, protoplasts were washed and fluorescence was determined. The experiments were performed two times.

induction of SWEET transporters, which transport sucrose bidirectionally, might lead to more rapid leakage of esculin from the protoplasts.

3.4.3. TAlAQ and the OsDOX-1 phenotype

One of the most interesting TALE classes characterized in this thesis is TAlAQ, which was not only a core TALE class and part of the group of convergent TALEs targeting *DOX* genes, but also triggered slightly stronger disease symptoms (Figure 21).

The enzyme AtDMR6, which is well known to be a suppressor of immunity in *A. thaliana* and to be involved in broad-spectrum disease resistance, is closely related to the rice *DOX* genes (Figure 27A; Kawai *et al.*, 2014). The mutation of *AtDMR6* leads to an accumulation of salicylic acid in *A. thaliana*, which in turn causes resistance (van Damme *et al.*, 2008). Conflicting data have been published on how the SA accumulation occurs (Kim *et al.*, 2008; Falcone Ferreyra *et al.*, 2015; Zeilmaker *et al.*, 2015; Zhang *et al.*, 2017b). Hypothesis one describes AtDMR6 as a flavanol synthase, which uses the same substrates needed to produce SA and therefore influences SA levels (Falcone Ferreyra *et al.*, 2015). Hypothesis two proposes that AtDMR6 directly modifies SA as a substrate and is therefore influencing SA levels (Kawai *et al.*, 2014; Zeilmaker *et al.*, 2015; Zhang *et al.*, 2017b). In contrast to AtDMR6 knockouts, it is possible that inducing these *DOX* genes could decrease SA levels, which are associated with resistance against Xoo (Figure 27B; Xu *et al.*, 2013). Therefore, the most promising substrates for AtDMR6 were investigated for the TAlAQ – *OsDOX-1* interaction.

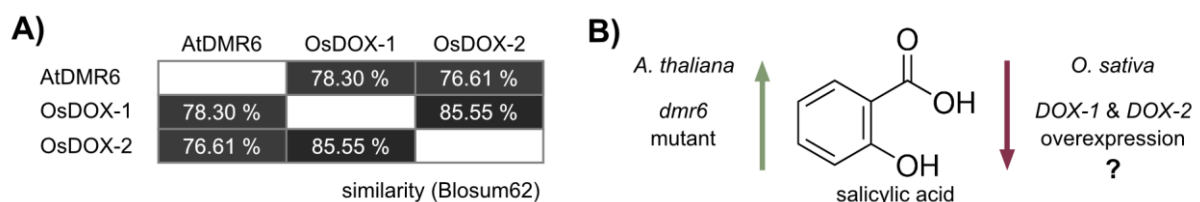


Figure 27. AtDMR6 and the rice *DOX* genes.

(A) Amino acid similarities between AtDMR6, OsDOX-1 and OsDOX-2 based on Blosum62 are listed in percent. (B) Effects of AtDMR6, OsDOX-1 and OsDOX-2 on salicylic acid are shown schematically.

3.4.3.1. Potential flavanol synthase function of OsDOX-1

Both, AtDMR6 and OsDOX-1 were described as flavanol or flavone synthases, which was underpinned by substrate conversion assays from naringenin to apigenin (Kim *et al.*, 2008; Falcone Ferreyra *et al.*, 2015). The flavonoids and SA are both produced from products of the chorismate pathway (Figure 28A). Therefore, it was hypothesized, that a decreased substrate flow in the direction of the flavonoids in *Atdmr6* mutants might increase available substrate for SA production (Falcone Ferreyra *et al.*, 2015).

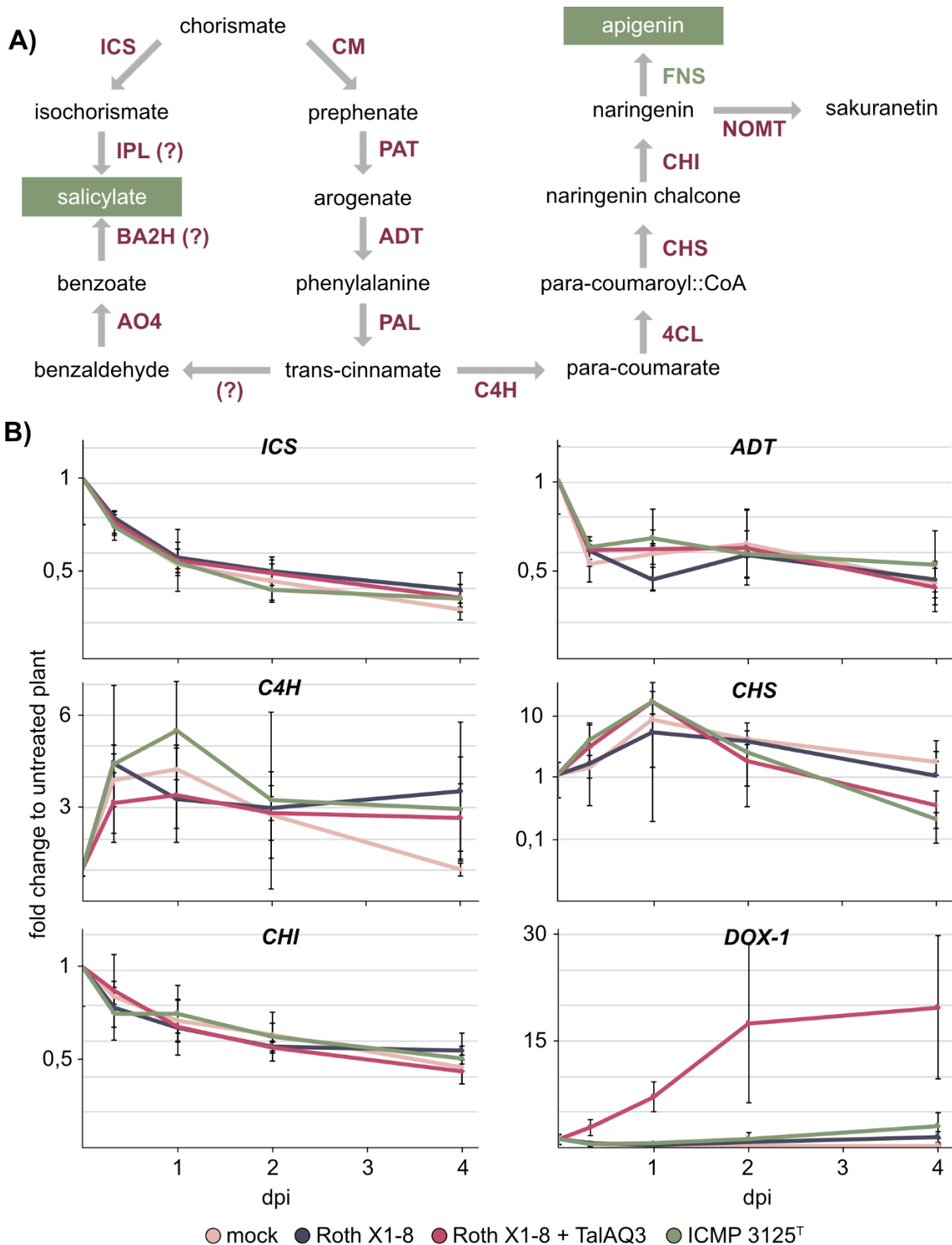


Figure 28. The apigenin biosynthesis pathway.

(A) The biosynthesis pathways of apigenin and salicylate are shown schematically starting from chorismate. The involved enzymes are shown in red and enzymes that have not been identified in rice so far are indicated by a question mark. The potential enzymatic function of OsDOX-1, apigenin and salicylate are highlighted in green. (B) Rice cultivar Nipponbare was inoculated with *Xoo* strains Roth X1-8, ICMP 3125^T and Roth X1-8 containing TalAQ3. Samples were harvested after 8, 24, 48 and 96 h and total RNA was extracted for qRT-PCR. The fold change in expression in the treated samples compared to untreated plants is shown. Error bars indicate standard deviations of three biological replicates. The experiment was performed once. ICS - isochorismate synthase, IPL - isochorismate pyruvate lyase, BA2H - benzoic acid 2-hydroxylase, AO4 - aldehyde oxidase 4, CM - chorismate mutase, PAT - prephenate aminotransferase, ADT - arogenate dehydratase, PAL - phenylalanine ammonia lyase, C4H - cinnamate 4-hydroxylase, 4CL - 4-coumaroyl:CoA-ligase, CHS - chalcone synthase, CHI - chalcone isomerase, FNS - flavanone synthase, NOMT - naringenin 7-O-methyltransferase

In order to test this in rice, Nipponbare was inoculated with ICMP 3125^T, Roth X1-8 and RothX1-8 containing TalaQ3. Samples were taken 8, 24, 48 and 96 h after inoculation for subsequent qRT-PCR. The expression of five representative enzymes involved in these pathways and the expression of *OsDOX-1* was analyzed (Figure 28B).

The isochorismate synthase (ICS), which is part of the pathway leading to SA production, and the chalcone isomerase (CHI), which is producing naringenin, were both downregulated after inoculation but showed no difference in expression between *Xoo* inoculations and mock treatment (Figure 28). The arogenate dehydratase (ADT), which can contribute to both pathways, was downregulated as well for all treatments. The cinnamate 4-hydroxylase (C4H) is the first enzyme leading into the flavonoid biosynthesis pathway. *C4H* was upregulated upon inoculation for all treatments and expression returned to levels of untreated plants after 96 h in the mock treatment. All plants inoculated with *Xoo* still showed elevated expression levels of *C4H* after 96 h, but no difference between Roth X1-8 with or without TalaQ3 was measured. The chalcone synthase (CHS), which is also involved in the flavonoid biosynthesis, also showed increased expression upon inoculation regardless of treatment. After 96 h, the expression of *CHS* was equal to untreated plants again in samples treated with wild type Roth X1-8 or mock treatment. Samples inoculated with Roth X1-8 carrying TalaQ3 or with ICMP 3125^T showed a significant downregulation of *CHS* expression. Finally, *OsDOX-1* was induced very strongly in samples treated with Roth X1-8 containing TalaQ3, but not in any other samples.

In conclusion, the differential expression of *CHS* upon infection with Roth X1-8 carrying TalaQ3 or ICMP 3125^T, might indicate that *Xoo* can influence the flavonoid biosynthesis in some capacity. ICMP 3125^T did not induce *OsDOX-1*, which could suggest that *CHS* repression is independent of TalaQ activity in this strain. Nevertheless, a clear difference between Roth X1-8 carrying TalaQ3 or not, indicates an influence of TalaQ3 on *CHS* expression.

3.4.3.2. DOX genes and suppression of immunity

Besides influencing SA content, AtDMR6 was described as a suppressor of immunity (Zeilmaker *et al.*, 2015). Several genes associated with defense were induced in the *Atdmr6* mutant. Accordingly, the influence of TalaQ on expression of defense-associated genes in rice was analyzed.

The samples of the experiments described in chapter 3.4.3.1 were used to evaluate the expression of four well characterized genes involved in the rice response to *Xoo* infection

(Song *et al.*, 2016). *OsPAT1* (*phosphoribosyl anthranilate transferase 1*) was induced 8 h after inoculation in all treatments and expression levels were equal to untreated plants again after 24 h. There was no difference between the used *Xoo* strains in *OsPAT1* expression. *OsPR1a* (*pathogenesis-related protein 1a*) was induced very strongly in all treatments and showed high variation between samples, indicating a strong reaction to wounding during inoculation. *OsPAL* (*phenylalanine ammonia lyase*) was also induced after inoculation in all samples and the mock treatment reached expression levels of untreated plants after 96 h. All samples infected with *Xoo* strains showed elevated expression of *OsPAL* throughout the whole experiment with no differences due to the presence of TalaQ3. The expression of *OsLOX* (*lipoxygenase*) showed an initial peak after 8 h for all treatments and afterwards expression returned to normal levels in samples with mock treatment. All samples infected with *Xoo* showed a second induction of *OsLOX* starting after 2 days. This induction was stronger in samples treated with Roth X1-8 regardless of TalaQ3.

This suggests that none of the tested defense associated genes were influenced by the presence of TalaQ3. Alternatively, the effects might be obscured by the strong reaction of some genes to the inoculation process itself.

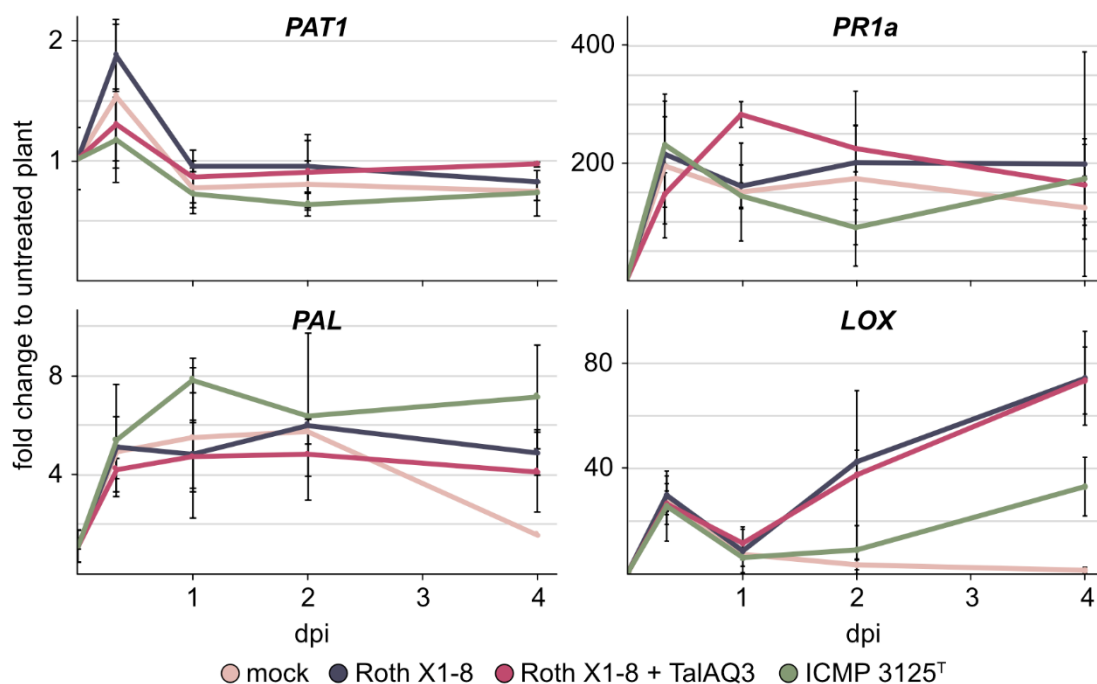


Figure 29. Influence of TalaQ3 on defense-associated gene expression in rice.

Rice cultivar Nipponbare was inoculated with the *Xoo* strains Roth X1-8, ICMP 3125^T and Roth X1-8 containing TalaQ3. Samples were harvested after 8, 24, 48 and 96 h and total RNA was extracted for qRT-PCR. The fold change in expression in the treated samples compared to untreated plants is shown. Error bars indicate standard deviations of three biological replicates. The experiment was performed once.

3.4.3.3. The influence of TalaQ on salicylic acid content in rice

Even though AtDMR6 can use flavonoids as substrates, the conversion rate is very slow (Zhang *et al.*, 2017b). On the contrary, a high conversion rate of SA was observed (Zhang *et al.*, 2017b). AtDMR6 was suggested to be a SA-5-hydroxylase, which would explain the SA accumulation in *Atdmr6*. Therefore, the direct impact of TalaQ on SA content in rice was investigated.

In parallel to the samples used for qRT-PCR in chapter 3.4.3.1, samples were taken to analyze the SA content. The SA content was determined with a spectrophotometric assay that utilizes the violet-colored complexes formed between SA and FeCl₃ (Figure 30A; Warriar *et al.*, 2013). Samples taken at early time points show high SA content, which might be in reaction to the general wounding during inoculation. The *Xoo* strains Roth X1-8, Roth X1-8 with TalaQ3, ICMP 3125^T and the mock treatment do not show significant differences, but 96 h after inoculation the SA content in rice inoculated with wild type Roth X1-8 is higher than the other treatments. This indicates that TalaQ3 may reduce SA accumulation in later stages of the infection.

Further experiments were focused on SA content after 96 h. In addition to TalaQ3, the artificial TALEs TalD1 and TalD2, which also target *OsDOX-1* and were created by Claudia Schwietzer during her master thesis, were used. TalBL1, which was provided by Sebastian Becker, is inducing *OsDOX-2* and was tested as well. TalAO16 was hypothesized to not influence SA content and was used as a negative control. To counteract high variation, an increase in sample size was chosen. Five plants per *Xoo* strain were inoculated and harvested after 96 h. The SA content was determined with the spectrophotometric assay. The experiment was repeated five times with inconsistent results.

Two out of five times, there was a strong reduction in SA content in samples treated with *Xoo* containing any TALE that induces a *DOX* gene. The other three times, no significant difference was observed. This indicated an external factor influencing the experiments. Upon further inspection, experiments with significant differences overlapped with malfunctioning in the cooling systems of the green house, which lead to elevated temperatures in the afternoon. Therefore, the results of the five experiments were split depending on greenhouse temperature (Figure 30B+C). The three experiments performed at normal temperatures showed no significant differences between tested *Xoo* strains (Figure 30C). Contrarily, the two experiments performed under elevated temperatures showed significant differences (Figure 30B).

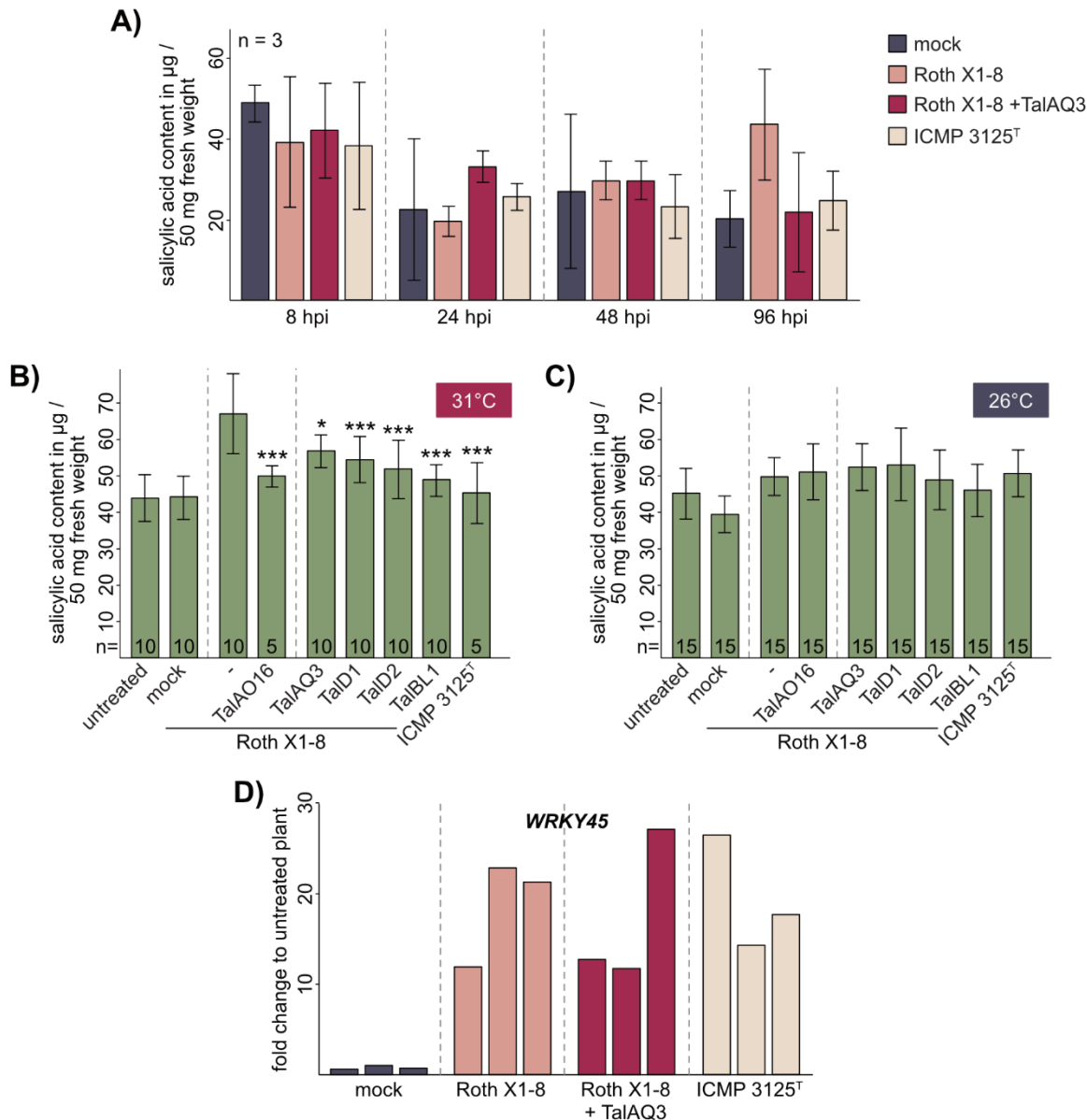


Figure 30. Changes in salicylic acid content in rice during infection with Xoo.

Rice cultivar Nipponbare was inoculated with the Xoo strains Roth X1-8, ICMP 3125^T and various Roth X1-8 derivatives containing expression constructs of individual TALEs. (A) Samples were harvested after 8, 24, 48 and 96 h and salicylic acid (SA) content was determined by a spectrophotometric assay. The bars show the average SA content of three individual plants and standard deviations are indicated by error bars. (B+C) Samples were harvested after 96 h and SA content was measured with a spectrophotometric assay. Five plants were treated with each Xoo strain or mock treatment. Experiments were performed two times at elevated greenhouse temperatures of 31°C (B) and performed three times at normal temperature of 26°C (C). The bars show the average SA content of combined repetitions and standard deviations are indicated by error bars. The statistical significance between samples treated with Roth X1-8 and all other Xoo treatments is indicated by p-values (<0.1 = *; <0.05 = **; <0.01 = ***) resulting from an unpaired t-test. (D) Samples were harvested after 96 h and total RNA was extracted for qRT-PCR. The fold change in expression of *OsWRKY45* in the samples compared to untreated plants is shown.

Interestingly, the samples inoculated with ICMP 3125^T and Roth X1-8 carrying TalAO16, TalAQ3, TalD1, TalD2 or TalBL1 all displayed significantly lower SA content compared to wild type Roth X1-8. The artificial TALE TalD2 fits the *OsDOX-1* promoter perfectly and showed the strongest activity in experiments discussed previously (Figure 18). This may explain why TalD2 had the strongest effect of all TALEs inducing *OsDOX-1*. TalBL1 caused

the lowest levels of SA in Roth X1-8 strains. Unexpectedly, Roth X1-8 carrying TalAO16 also showed significantly reduced SA content compared to Roth X1-8 wild type. It is possible that TalAO16 is able to influence defense or SA content as well as the function of TalAO16 is not completely understood.

Overall, the results suggest that both DOX genes are able to reduce SA content, but external factors have a strong influence on the subtle phenotype. Especially temperature seems to have a major impact on outcome.

It is unclear how accurately the SA content of rice can be measured using the spectrophotometric assay, because SA is conjugated with small molecules like glucose for storage purposes (Silverman *et al.*, 1995). This might limit the accuracy in SA content evaluation. Therefore, the expression of a well-known SA responsive gene in rice, *OsWRKY45*, was analyzed (Shimono *et al.*, 2007, 2012).

The samples harvested after 96 h for qRT-PCR in chapter 3.4.3.1 were utilized to evaluate expression. Interestingly, little to no change in expression of *OsWRKY45* was observed in the mock treatment, which confirms that the effects of wounding during inoculation have worn off after four days. On the contrary, all samples inoculated with *Xoo* showed elevated expression of *OsWRKY45*. The average expression of *OsWRKY45* was higher in samples inoculated with wild type Roth X1-8 than in samples treated with ICMP 3125^T and Roth X1-8 with TalAQ3 (Figure 30D). Notably, the variation in the samples was extremely high, which matches the measured SA content well. This indicates that the spectrophotometric SA assay and the expression of *OsWRKY45* are both producing similar results concerning SA content.

In summary, these experiments could not clearly confirm a link between TalAQ3, the DOX genes and SA content, because the effects are not consistent and vary strongly. Inconsistent growth conditions of the rice and varying degrees of wounding and *Xoo* delivery during inoculation might be responsible for the observed variability.

3.4.4. Rice with inducible TALEs

As subtle TALE-dependent phenotypic changes are hard to detect, a new strategy was devised to circumvent infection and study TALE-dependent changes with minimal disturbance of the rice plant. To this end, transgenic rice lines carrying inducible TALE expression constructs were established.

The dexamethasone (DEX)-inducible system was chosen because it was shown to be functional in rice and has a very low background activity (Hutin *et al.*, 2016). This system is based on the specific mode of action of the glucocorticoid receptor (GR) from rat

(Borghi, 2010). In the absence of DEX, GR binds to heat shock proteins in the cytosol. In the presence of DEX however, the interaction with cytosolic proteins is disturbed and a nuclear localization signal becomes accessible. In the DEX system, GR is combined with the activation domain VP16 of *Herpes simplex* and the GAL4 DNA-binding domain of yeast. This complex is called GVG. GVG will change localization from the cytosol to the cell nucleus upon DEX treatment and is able to bind *GAL4 upstream activation sequences* (UAS) and to activate expression of downstream genes.

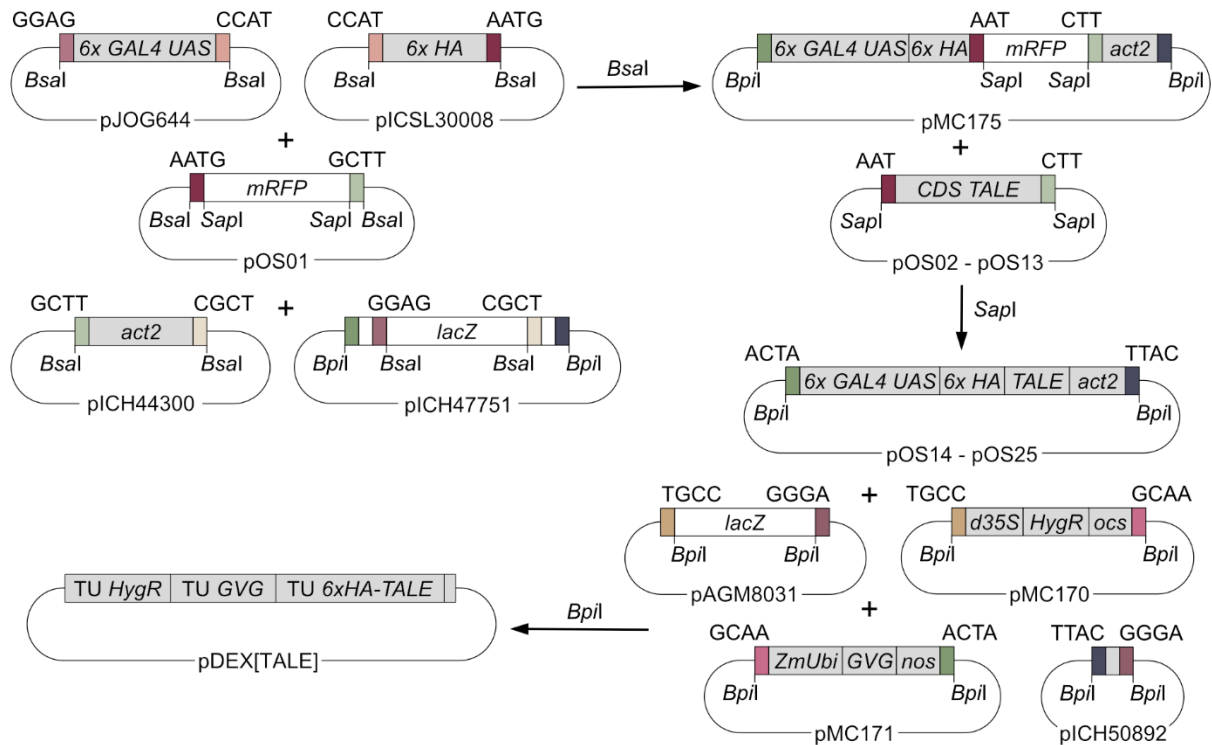


Figure 31. Cloning of DEX-inducible TALEs for rice transformation.

A schematic overview of the cloning steps is shown. First, several level 0 modules are assembled to create a transcriptional unit (TU) in pMC175. Second, the mRFP dummy module of pMC175 is switched with a TALE coding region (CDS). The resulting TALE TU is finally combined with a TU for hygromycin resistance and a TU for GVG.

Several MoClo modules containing necessary parts of the DEX system were provided by the group of Johannes Stuttmann of the Martin-Luther-Universität Halle/Wittenberg (Gantner *et al.*, 2018). These modules were utilized to create a new transcriptional unit containing a dummy module instead of the coding region as described in chapter 3.4.1. This transcriptional unit (pMC175) contained a 6x GAL4 UAS promoter, a N-terminal 6xHA tag and an *act2* terminator (Figure 31). Subsequently, the TALEs cloned into the TALE receiver in chapter 3.4.1 were swapped with the dummy module of pMC175 (Figure 31). The resulting TALE transcriptional units were combined with transcriptional units for hygromycin resistance and for expression of GVG. The final construct contained three transcriptional units that enabled selection of transformed rice and DEX-inducible

expression of individual TALEs (Figure 31). In total, twelve constructs of inducible TALEs were created containing the twelve TALEs with confirmed direct target genes (Chapter 3.2.3). Additionally, a construct for DEX-inducible tGFP expression (pMC173) was created to monitor DEX-inducibility and to function as a control for later experiments. The pMC173 plasmid is designed identical to all DEX-inducible TALE constructs, but the TALE CDS is exchanged with a tGFP CDS. Several of these cloning steps were performed by Olivia Sierra during her student exchange.

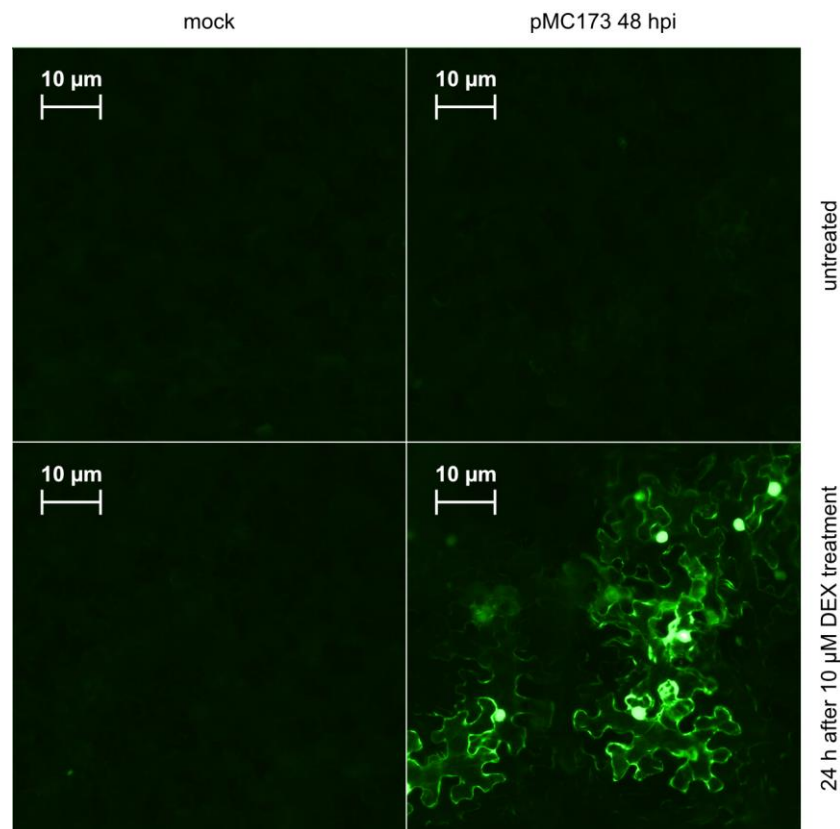


Figure 32. pMC173 enables DEX-inducible tGFP expression in *N. benthamiana*.

The fluorescent protein tGFP was cloned in the vector pMC173 to enable DEX-inducible tGFP expression. *N. benthamiana* was inoculated with *A. tumefaciens* carrying pMC173 or a mock control. 24 h after inoculation, the leaves were coated with 10 μ M DEX solution. 24 h later the tGFP fluorescence was captured with a fluorescence microscope.

In order to test the DEX-inducibility of the constructs, pMC173 was introduced into *A. tumefaciens* for inoculation into *N. benthamiana*. 24 h after inoculation, the plants were either treated with a mock treatment or coated with 10 μ M DEX solution. Fluorescence was evaluated 24 h after the DEX treatment. A strong tGFP fluorescence was detected in samples containing pMC173 that were treated with DEX (Figure 32). All other samples showed no fluorescence indicating low background activity in the system. Therefore, rice plants containing the DEX-inducible constructs were created. The delivery of the constructs was done by *A. tumefaciens* mediated transformation of rice calli derived from cultivar Kitaake. The transformations were mostly done by Beate Meyer with

help from Tjorven Ostermeier, Patricia Grabandt, Olivia Sierra, Swati Jagani and me. Plants carrying constructs for TalAB16, TalAE15, TalAL11, TalAO16, TalAP15, TalAQ3, TalBH2, TalBM2 and TalES1 as well as pMC173 could be regenerated from transformed calli. Regenerated T0 plants were tested by PCR to confirm the presence of the transgene by amplifying the *ocs* terminator of the transcriptional unit for hygromycin resistance. All tested plants carried the transgene.

Subsequently, selected T0 plants containing pMC173 were treated with 10 μ M DEX solution and fluorescence was examined after 24 h. No visible difference between treated and untreated samples could be observed. Because rice has a very hydrophobic leaf surface, experiments were repeated with 30 μ M DEX solution containing 0.01% Tween20 to facilitate leaf coating. After 24 h, no difference in fluorescence could be observed for any samples (Figure 33). In parallel, samples were taken to extract total RNA for qRT-PCR. The expression of GVG in the transgenic plants was tested and very high expression rates were detected. GVG displayed an average Ct value of 18, indicating an expression four times higher than the house keeping gene actin, which was used as a reference gene.

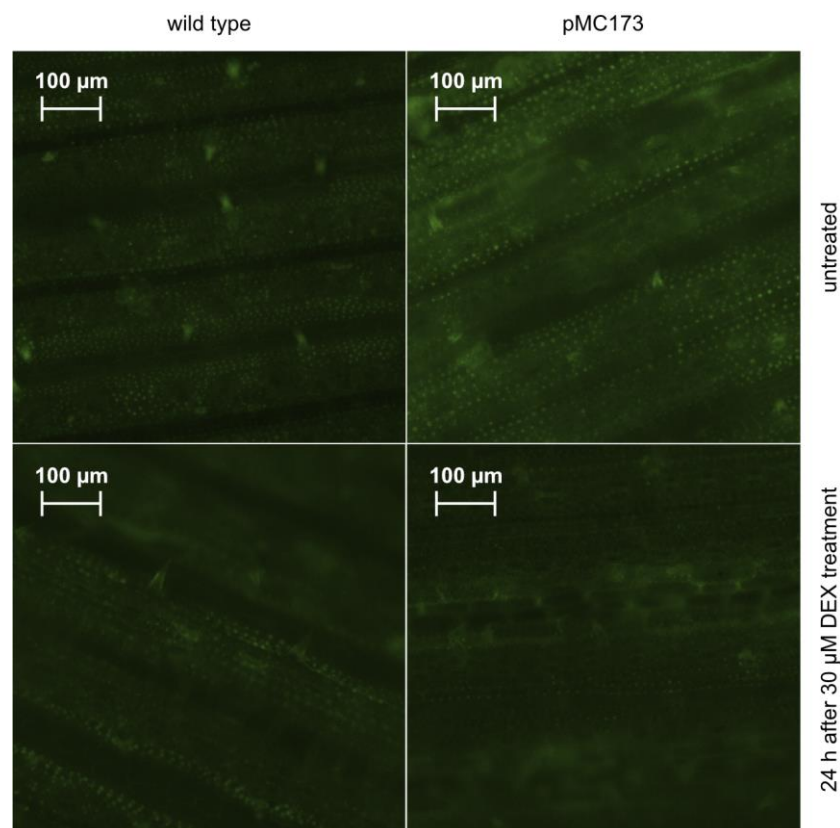


Figure 33. tGFP fluorescence in pMC173 transgenic rice leaves.

The fluorescent protein tGFP was cloned in the vector pMC173 to enable DEX-inducible tGFP expression. The rice cultivar Kitaake was transformed with *A. tumefaciens* carrying pMC173. The leaves of regenerated T0 plants were coated with 30 μ M DEX solution containing 0.01% Tween20. 24 h later the tGFP fluorescence was captured with a fluorescence microscope.

Even though these plants carried the DEX constructs and expressed the receptor GVG, no fluorescence was detected. This is possibly due to difficulties in the DEX treatment procedure, because the constructs were functional in *N. benthamiana*. DEX treatments of rice is reportedly done by adding DEX to hydroponic cultures, circumventing leaf treatment (Hutin *et al.*, 2016). At the end of this thesis, no ripe seeds of T0 plants were available to test this hypothesis.

In conclusion, rice plants containing inducible expression constructs of TALEs are possible new tools to analyze TALE function, but an improved method of DEX treatments needs to be established.

3.5. Mutating TALE target genes in rice

The impact of TALE target gene mutation on infection was investigated. Therefore, genome editing constructs were created for *A. tumefaciens*-mediated transformation of rice.

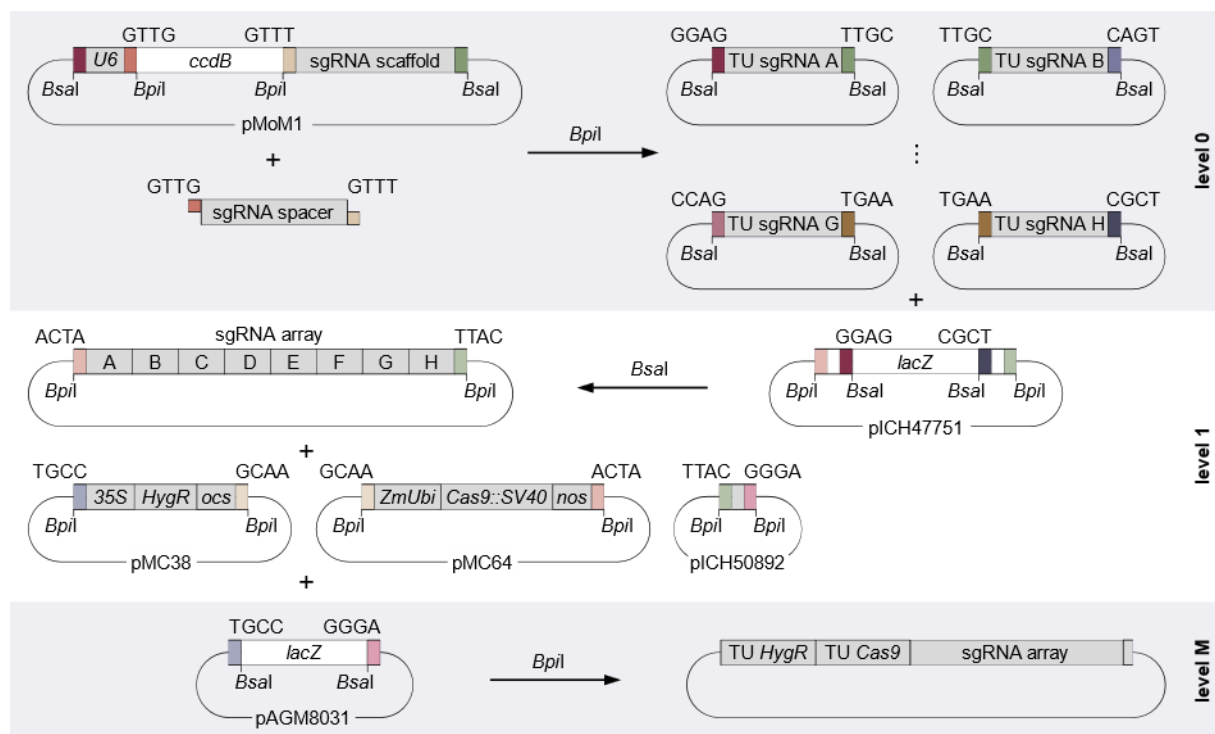


Figure 34. Cloning of CRISPR/Cas9 genome editing constructs.

The necessary cloning steps to assemble a CRISPR/Cas9 genome editing construct are shown schematically. First, annealed oligonucleotides coding the sgRNA spacer are cloned into level 0 modules to create transcriptional units (TU) of individual full length sgRNAs. Second, eight sgRNA TUs are assembled into a level 1 vector to form an sgRNA array. Finally, the sgRNA array is combined with a TU for hygromycin resistance and a TU for Cas9.

CRISPR/Cas9 was chosen as the genome editing tool, because it enables easy multiplexing approaches. The cloning of these constructs was done using the MoClo system to create compound constructs containing a selection cassette, a Cas9 transcriptional unit and the desired sgRNAs. The cloning of sgRNA transcriptional units

was based on the system published by Ordon *et al.* (2017). This system was adapted to the MoClo system by Jana Streubel, who provided the necessary cloning vectors. To create an sgRNA transcriptional unit, annealed oligonucleotides coding the sgRNA spacer are cloned into level 0 modules already containing an *U6* promoter and the sgRNA backbone (Figure 34). In the following experiments, eight sgRNAs were cloned into an sgRNA array, which was combined with the transcriptional units for hygromycin resistance and a transcriptional unit for Cas9 (Figure 34).

3.5.1. TALE target gene knockouts

The twelve TALE target genes verified in this thesis are comprised of four genes with known susceptibility association and eight genes with unknown influence on infection (Sugio *et al.*, 2007; Streubel *et al.*, 2013; Huang *et al.*, 2016). Complementary to gain-of-function assays analyzing the effect of the introduction of a single TALEs in an *Xoo* strain without TALEs, loss-of-function assays explore the effect of wild type *Xoo* strains losing the benefit of individual TALEs. As the corresponding TALE targets were verified for the TALEs in question, knockout rice lines were created to analyze the virulence of wild type strains in loss-of-function assays. Therefore, eight genome editing constructs for the knockout of each of those genes with unknown impact were created (Figure 35). For each construct, two sgRNAs were designed at the 5' end and two sgRNAs at the 3' end of the coding sequence. This was done to delete the complete CDS for a clear mutant genotype. Each of the four sgRNAs was cloned into the sgRNA array twice to increase sgRNA expression. The design of the necessary sgRNAs was done in cooperation with Sebastian Becker and cloning of the constructs was done mostly by John Connolly during his student exchange.

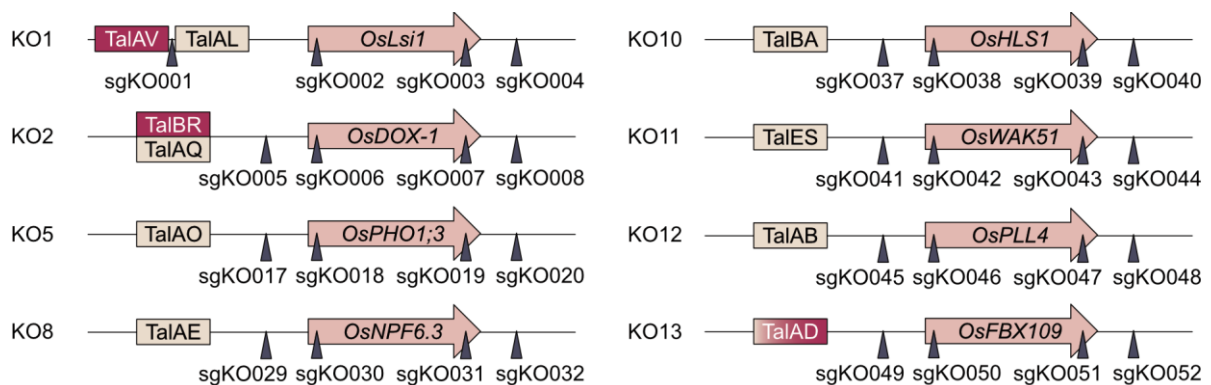


Figure 35. Overview of TALE target gene knockout constructs.

Target genes of TALEs from *Xoo* (yellow) and *Xoc* (red) were planned to be mutated in rice. The chosen genome editing tool is CRISPR/Cas9, which was cloned into knockout (KO) genome editing constructs. The location of TALE boxes, sgRNA binding sites and target gene coding sequences are shown schematically without.

The knockout (KO) constructs were delivered by *A. tumefaciens* mediated transformation of rice calli derived from cultivar Kitaake. The transformations were mostly done by Beate Meyer with help from Tjorven Ostermeier, Patricia Grabandt, Sebastian Becker, John Connolly, Swati Jagani and me. During this thesis, four KO constructs were successfully transferred into rice: KO1, KO2, KO5 and KO13. Due to the transformation process, not all regenerated lines are independent of each other and should be analyzed cautiously. If the lines are stated to be independent, they were transformed at different time points or in separate transformation reactions.

The plants containing the construct KO2 targeting *OsDOX-1* were analyzed by Sebastian Becker. Eight independent T0 lines of KO2 were regenerated, but none had mutations inside the coding sequence. The sgKO006 cutting shortly after the ATG seemed to be inactive. Therefore, a new genome editing construct with an alternative for sgKO006 needs to be created in the future. Additionally, two independent T0 lines of KO13 are regenerated so far and the targeted *OsFBX109* locus will be analyzed by Swati Jagani as part of her master thesis.

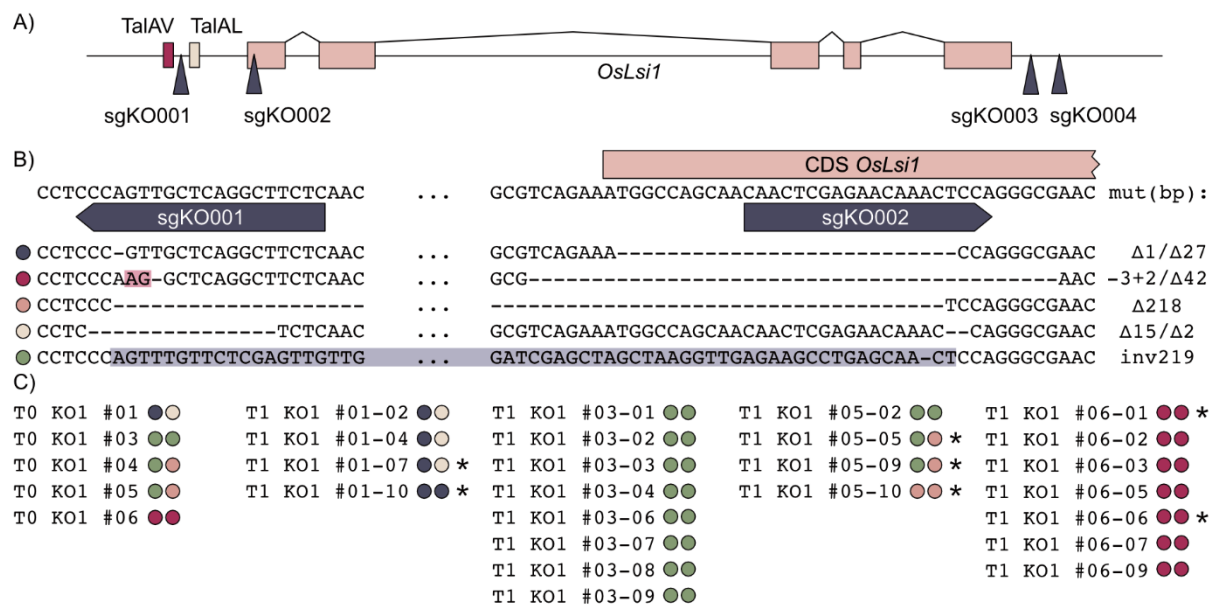


Figure 36. KO1 facilitates mutations in *OsLsi1*.

(A) *OsLsi1*, the target gene of TALEs from Xoo (yellow) and Xoc (red) was mutated in rice with CRISPR/Cas9. The location of TALE boxes, sgRNA binding sites (blue arrowhead) and target gene coding sequences are shown schematically. B) The identified alleles are aligned to the wild type sequence and the alleles are differentiated by colors. Insertions are highlighted pink and inversions are highlighted blue. C) The distribution of the mutated alleles among T0 and T1 populations is shown. T1 plants, which lost the original transgene are marked with an asterisk.

The KO1 construct targets *OsLsi1* and four independent T0 lines carrying KO1 could be regenerated. No wild type allele of *OsLsi1* could be found in any of the regenerated lines. In total, five different mutated alleles of *OsLsi1* could be identified, but no big deletions

between the sgRNAs at the 5' end and the 3' end were detected (Figure 36). Interestingly, two independent lines carried a big inversion of 211 bp between the cut sites of sgK0001 and sgK0002. The inversion might be favored due to the inverted flanking sequences: AGTT-(N)₂₀₃-AACT (Figure 36). The region around sgK0003 and sgK0004 was not sequenced. Nevertheless, all five mutated alleles have the potential to prevent production of OsLsi1, because they either create a frame shift or the annotated ATG is deleted. It should be noted that alternative in frame ATGs are present 84 bp and 93 bp downstream of the annotated start codon. Therefore, the mutant rice lines might display residual OsLsi1 activity.

Seeds of the T0 plants KO1 #01, 03, 05 and 06 representing the four independent lines were sown and the inheritability of the alleles was evaluated. The T1 lines carried the same alleles as their mother plants suggesting an effective mutation of the germ line. Additionally, the presence of the T-DNA was evaluated using PCR to amplify the ocs terminator of the hygromycin resistance cassette. 50% of KO1 #01 descendants, 75% of KO1 #05 descendants and 29% of KO1 #06 descendants had lost the KO1 transgene but contained mutations. These findings suggest that the observed *OsLsi1* mutations are stably inherited.

The construct KO5, which targets *OsPHO1;3*, could be transferred into ten independent T0 lines. None of the 47 regenerated T0 plants contained a wild type allele of *OsPHO1;3*. Instead, a total of seven different alleles was detected in all lines combined (Figure 37). Six of these alleles have deletions around the annotated ATG or small indels creating frame shifts. One allele shows a big deletion of 4773 bp spanning the cutting sites from sgK0018 to sgK0020. This allele leaves 7 bp of the coding region of *OsPHO1;3* creating a complete knockout. Interestingly, this deletion was found in two independent lines (T0 KO5 #36/37 and T0 KO5 #38-41). The most frequent allele, which was present in eight independent lines, was the perfect deletion between sgK0017 and sgK0018 missing 31 bp spanning the annotated ATG (Figure 37). The region around sgK0019 and sgK0020 was not sequenced, except for plants with big 4773 bp deletions.

As mentioned in Chapter 3.2.2, *OsPHO1;3* has three potential start codons and there is strong evidence suggesting that TalAO shifts the TSS of *OsPHO1;3* (Figure 15). If the most upstream ATG is used, many mutant alleles would still create frame shifts with the exception of the 30 bp deletion, which would result in a 10 amino acid deletion. If the most downstream ATG would be used, many mutant alleles would not impact the coding region. Nevertheless, the big deletion of 4773 bp will inactivate *OsPHO1;3* no matter which ATG is used.

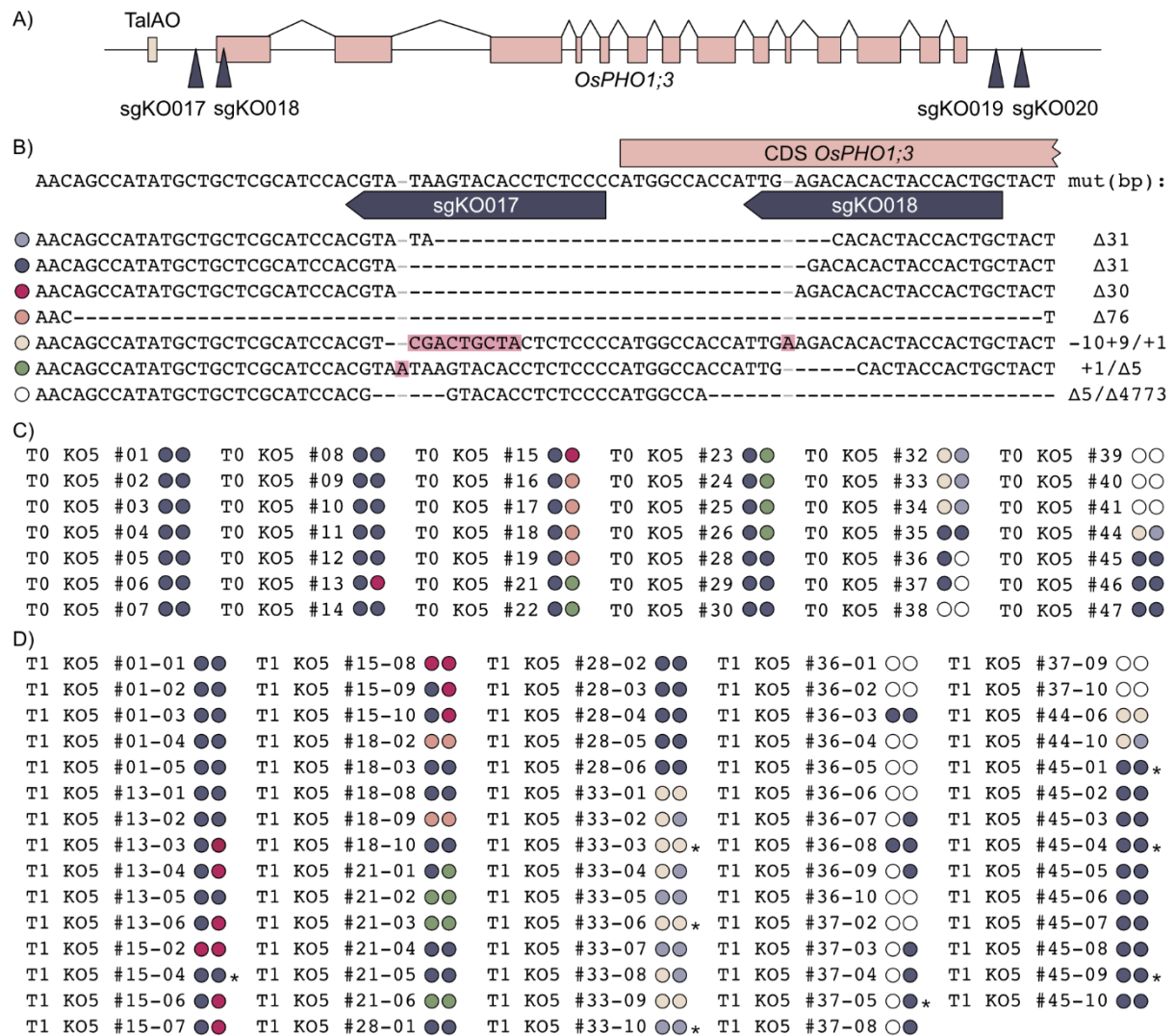


Figure 37. K05 facilitates deletion of *OsPHO1;3*.

(A) *OsPHO1;3*, the target gene of TALEO from *Xoo* was mutated in rice with CRISPR/Cas9. The location of TALE boxes, sgRNA binding sites and target gene coding sequences are shown schematically. B) The identified alleles are aligned to the wild type sequence and the alleles are differentiated by colors. Insertions are highlighted pink. C+D) The distribution of the mutated alleles among T0 and T1 populations is shown. The descendants of K05 #15, 33, 36, 37, 44 and 45 were tested for the presence of the original transgene. T1 plants, which lost the original transgene are marked with an asterisk.

The stability and inheritability of the observed alleles was assessed by testing selected T1 plants. Seeds of eleven different T0 plants representing all independent lines were sown and the *OsPHO1;3* locus was evaluated. All tested T1 plants contained alleles found in their respective mother plants. The descendants of K05 #15, 33, 36, 37, 44 and 45 were also tested for the presence of the K05 transgene using PCR to amplify the ocs terminator of the hygromycin resistance cassette. Several T1 plants originating from K05 #15, 33, 37 and 45 had lost the transgene. These findings indicate that knockout construct K05 was able to create stable, inheritable mutations in *OsPHO1;3*.

In conclusion, the designed genome editing constructs are able to create stable, inheritable mutations and the design of the sgRNAs enabled large deletions to facilitate

clean knockouts. The influence of these mutations on *Xoo* infections will be analyzed in the future.

3.5.2. Mutating TALE binding sites in rice

In order to create rice plants that are more resistant against *Xoo*, only minimal changes in the genome might be necessary. While the deletion of susceptibility target genes might have an impact on plant physiology in general, the disruption of TALE boxes in the promoter could retain normal gene expression but prevent TALE-mediated induction. Therefore, genome editing constructs were created to mutate TALE boxes in rice. CRISPR/Cas9 mutations are most often small indels that can have a big influence on TALE binding, as most TALEs cannot tolerate frame shifts in their TALE box (Richter and Boch, 2013). Additionally, the system can be easily used to multiplex and therefore target multiple TALE boxes at the same time. This multiplex approach might increase the durability of the resistance because multiple TALEs need to be adapted to regain susceptibility.

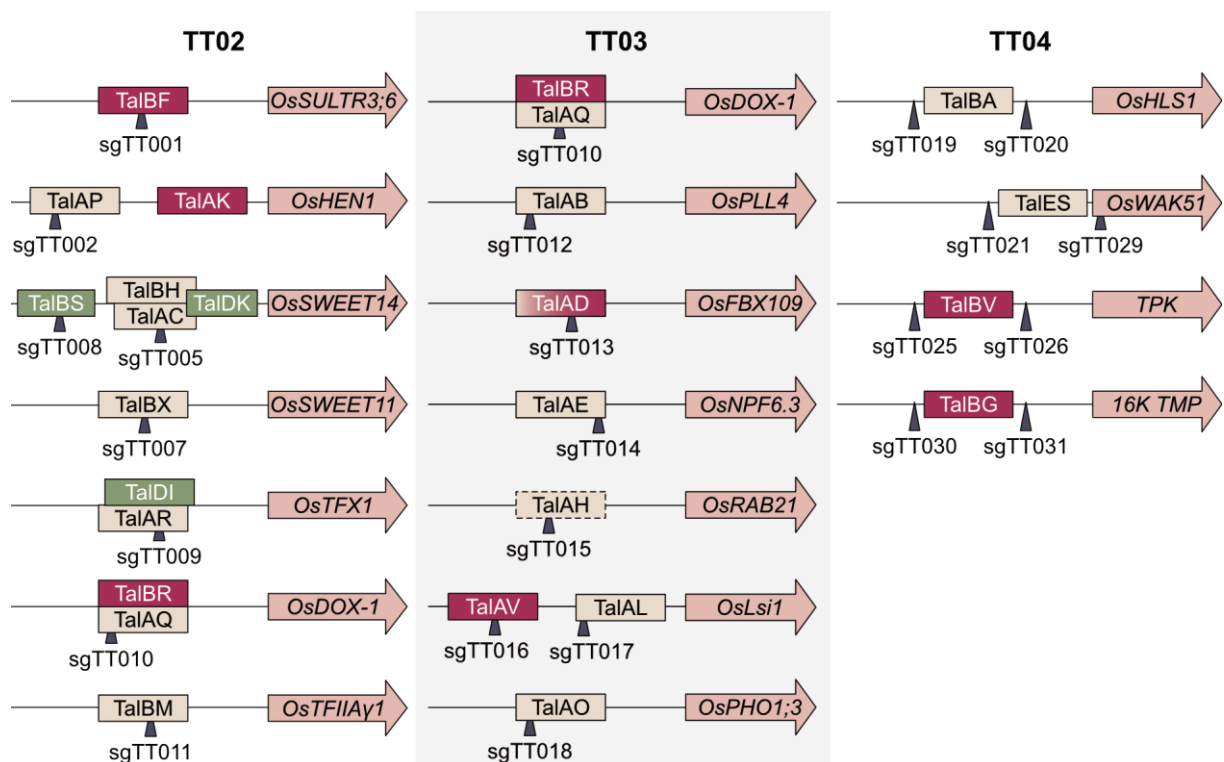


Figure 38. Overview of TALE box mutation constructs.

TALE boxes of TALEs from Asian (yellow) and African (green) *Xoo* and *Xoc* (red) were planned to be mutated in rice. The chosen genome editing tool is CRISPR/Cas9, which was cloned into TALE target box (TT) genome editing constructs containing eight sgRNAs, each. The location of TALE boxes, sgRNA binding sites and target gene coding sequences are shown schematically. TALE boxes that were disproven as direct targets in a GUS assay are marked with a dashed outline.

Three multiplexing constructs aimed at TALE target boxes (TT) were designed in cooperation with Sebastian Becker (Figure 38). TT02 targets TALE boxes of known

susceptibility genes in *Xoo* and *Xoc* infection as well as *OsDOX-1*. TT03 is targeting TALE boxes newly identified in this thesis and *OsRAB21* (Os11g26790), which was hypothesized to be a TALE target in earlier stages of the project and has been disproven by now (Chapter 3.2.2). Finally, TT04 is addressing four TALE target boxes from *Xoo* and *Xoc*, that do not have an appropriate PAM sequence in their vicinity and are therefore flanked by two sgRNAs to delete the complete box. The *Xoc* target genes of TT04 do not have established gene names and will be referred to by their annotated functions: TPK (tyrosine protein kinase) addressed by TalBV and 16K TMP (16K transmembrane protein) induced by TalBG. The constructs were cloned by John Connolly and transformed into *A. tumefaciens*. The *A. tumefaciens*-mediated transformations into rice calli derived from Kitaake were mostly done by Beate Meyer with help from Sebastian Becker, John Connolly and me. Due to the transformation process, not all regenerated lines are independent of each other and should be analyzed cautiously. If the lines are stated to be

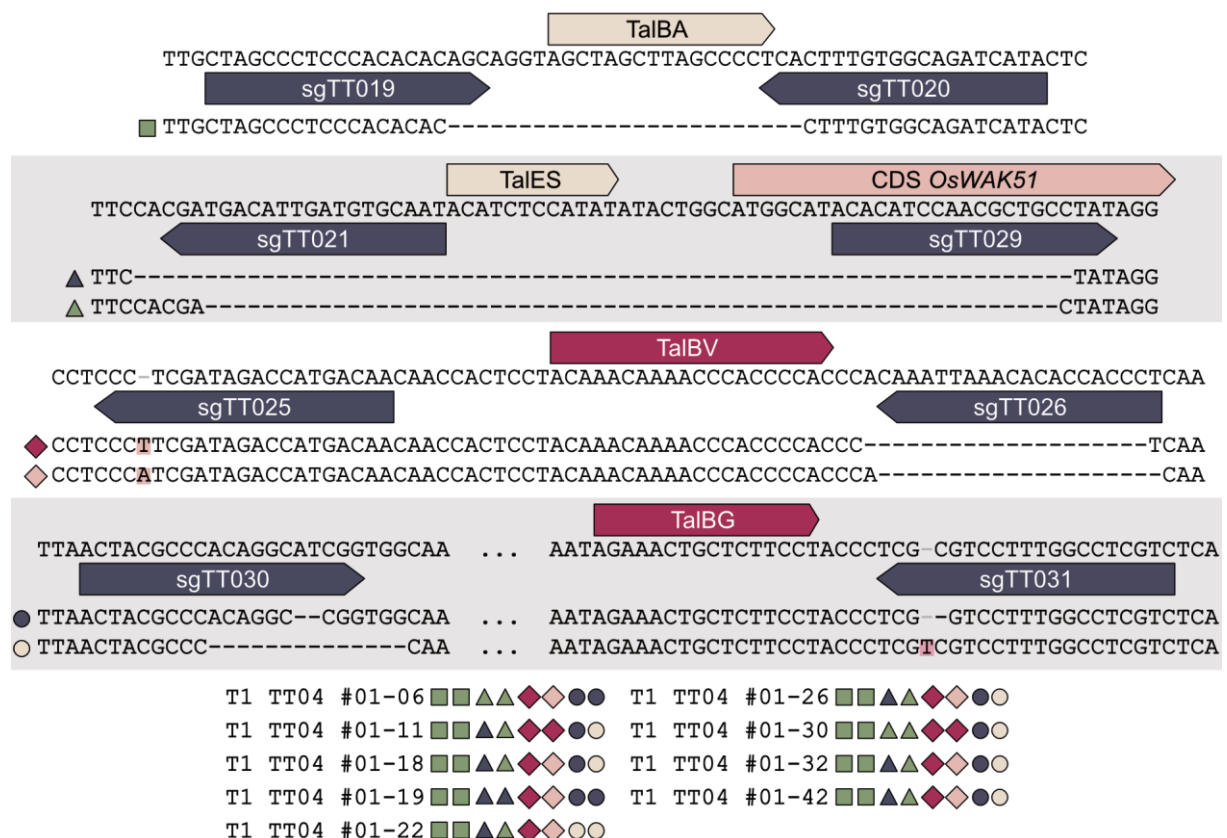


Figure 39. TT04 causes inheritable mutations.

TALE boxes of TALEs from *Xoo* (yellow) and *Xoc* (red) were mutated in rice with CRISPR/Cas9. The location of TALE boxes, sgRNA binding sites and target gene coding sequences (CDS) are shown schematically. TT04 targets four different TALE boxes and the identified alleles of the T0 plant TT04 #01 are aligned to the wild type sequences. The different loci are represented by varying shapes and the alleles are differentiated by colors. Insertions are highlighted pink. The distribution of the mutated alleles among the T1 population is shown.

independent, they were transformed at different time points or in separate transformation reactions.

So far, a single T0 plant carrying TT04 could be regenerated. The T0 plant was analyzed by Sebastian Becker and contained mutations that disrupted the TALE boxes of TalBA and TalES, but the TALE boxes of TalBG and TalBV were unaffected (Figure 39). In order to analyze the inheritability of the mutations, 50 T1 plants were sown during this thesis. The presence of the TT04 transgene was analyzed using PCR to amplify the *ocs* terminator of the hygromycin resistance cassette. Nine of these T1 plants had lost the original transgene and were subsequently sequenced at the appropriate loci. All plants inherited mutated alleles from the T0 plant (Figure 39). Even though the Cas9 cutting sites were all mutated, not all TALE boxes were disrupted. This indicates that all sgRNAs are functional and produce inheritable mutations. Therefore, additional rice transformations with TT04 should be done in the future because they might render all four TALE boxes nonfunctional.

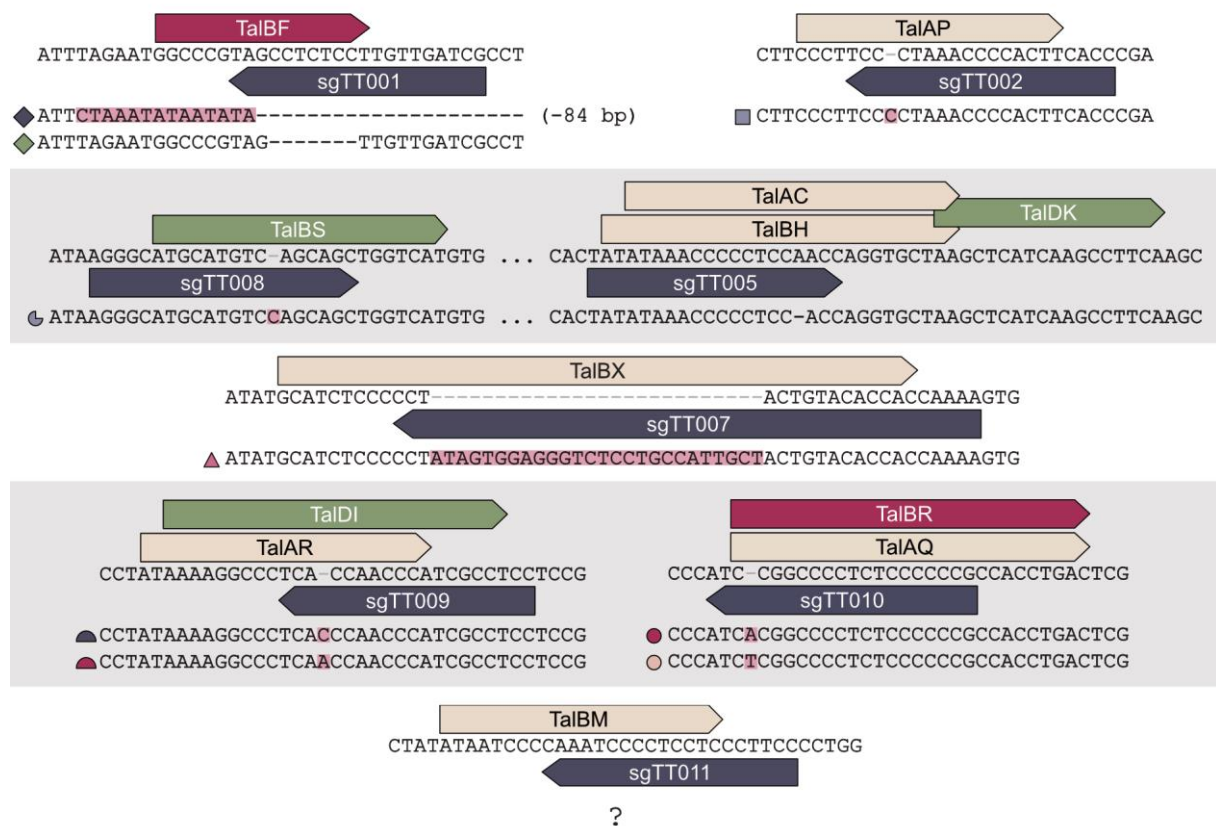


Figure 40. TT02 facilitates TALE box mutations in susceptibility genes in rice.

TALE boxes of TALEs from Asian (yellow) and African (green) Xoo and Xoc (red) were mutated in rice with CRISPR/Cas9. The location of TALE boxes and sgRNA binding sites are shown schematically. TT02 targets eight different loci with TALE boxes and the identified alleles of the T0 plant TT02 #02 are aligned to the wild type sequences. The different loci are represented by varying shapes and the alleles are differentiated by colors. Insertions are highlighted pink. Unidentified sequences are marked with a question mark.

The construct TT02 has been successfully transferred into two independent T0 plants, but only one survived the transfer into the greenhouse due to pest infestations. TT02 #02 was subsequently sequenced and showed mutations in all Cas9 cutting sites that were analyzed. The *OstFIIAy1* locus could not be amplified in TT02 #02 with any primers even though they successfully amplified a product in wild type plants. Therefore, no statements about sgTT011 or the TalBM box can be made. The TALE boxes of TalBF, TalAP, TalDI, TalAR, TalBX, TalBS, TalAC, TalBH, TalBR and TalAQ were all mutated and should no longer be bound by their respective TALEs.

Interestingly, one allele of *OsSULTR3;6* (targeted by TalBF) and the allele of *OsSWEET11* (targeted by TalBX) showed insertions of 14 bp and 26 bp, respectively, that are not part of the used vector for transformation or the reference genome of Nipponbare. Because TT02 #2 is derived from Kitaake, which is not fully sequenced, it is still possible that the inserted sequences are originating from rice. Further analysis of the T1 progeny will provide insight into the inheritability of the mutated alleles in the future.

The multiplexing construct TT03 was transformed into rice and initially, four plants representing one independent event were regenerated. These plants (T0 TT03 #01 - #04) were analyzed by Sebastian Becker (Figure 41). The plants had promising mutations but died before seeds could be formed due to pest infestations in the greenhouse. Therefore, the transformation was repeated and additional eight plants representing five independent lines could be regenerated and were analyzed in this thesis.

Nearly all loci in all regenerated T0 plants were mutated. The only exception was the CRISPR/Cas9 cutting site for sgTT015 in T0 TT03 #12, which contained a mutated allele and a wild type allele. Interestingly, identical mutations can be found in plants from independent transformations. This includes not only 1 bp insertions but also deletions of several nucleotides, indicating a preference in the repair mechanism. The Cas9 cutting site in the TalAO box is surrounded by a CTAG repetition and the most common mutation is the deletion of one CTAG block. Most loci displayed between five and nine different alleles with the TalAD box being the exception with a nearly uniform insertion of a single cytosine. All identified mutations will likely render the corresponding TALEs unable to bind the promoter. The mutations in the TalAQ box, which are very close to the 5' end, might seem likely to not completely eliminate binding, but mismatches in the 5' region were shown to have more disruptive effects than mismatches in the 3' region (Meckler *et al.*, 2013).

In conclusion, the TT constructs were able to generate rice plants with multiple edited loci efficiently. The mutations were shown to be inheritable in the case of TT04. These plants

display a lot of potential to have increased resistance due to loss of susceptibility and should be tested once progeny is available.

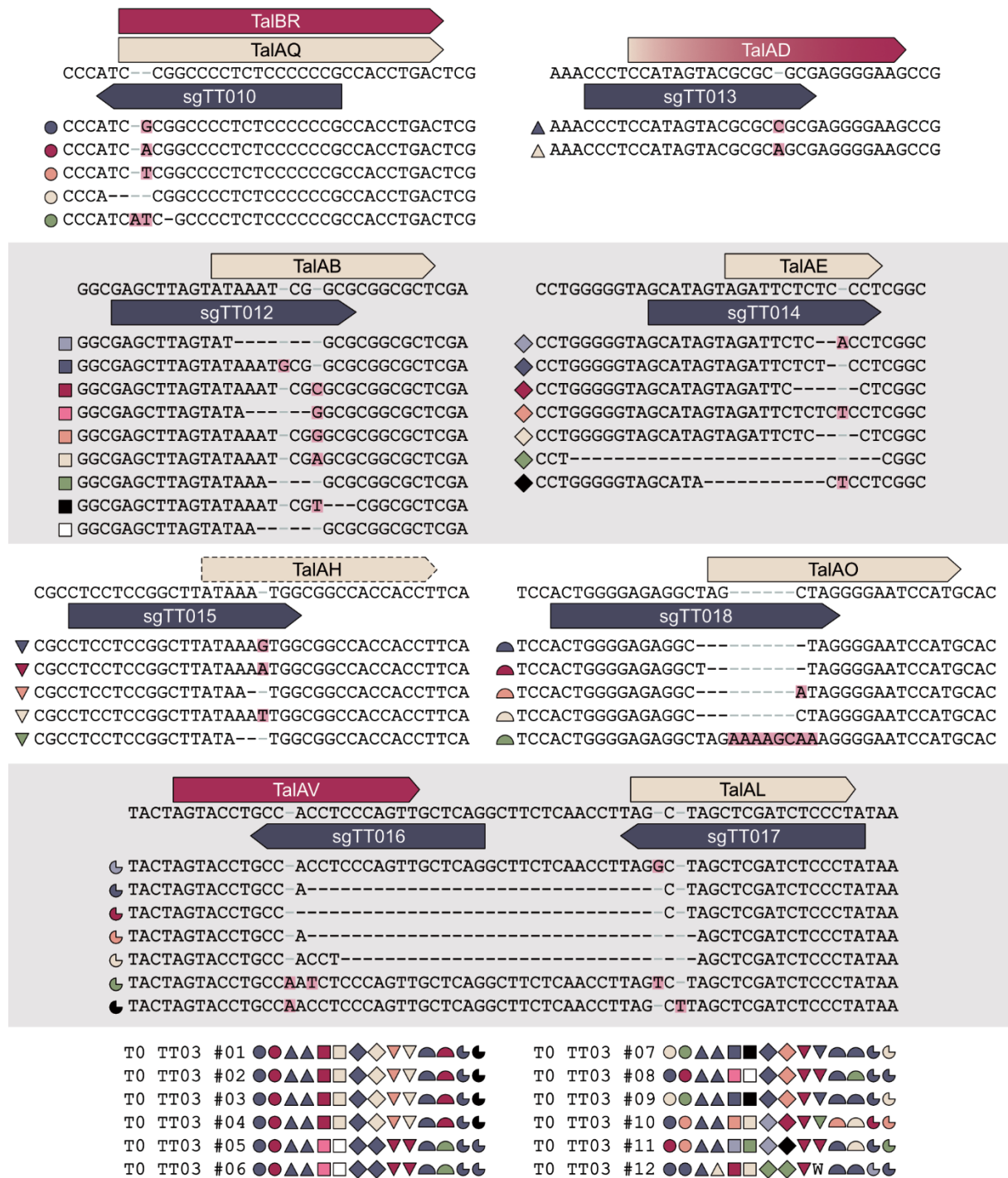


Figure 41. TT03 causes mutations in newly identified TALE boxes.

TALE boxes of TALEs from *Xoo* (yellow) and *Xoc* (red) were mutated in rice with CRISPR/Cas9. The location of TALE boxes and sgRNA binding sites are shown schematically. TT03 targets eight different loci with TALE boxes and the identified alleles of the T0 TT03 population are aligned to the wild type sequences. The different loci are represented by varying shapes and the alleles are differentiated by colors. Insertions are highlighted pink. TALE boxes that were disproven are marked with a dashed outline. The distribution of the mutated alleles among the T0 population is shown. The occurrences of wild type alleles are marked with a W.

Xoo PXO142	FBX109	TalAD23	NN HD NS NG HD NN N* NI HD NS HD NN HD NN HD NN NN NN NN NN NN NN HD NG	MM
		box WT	T C C A T A G T A C G C G C G C G C G A G G G G A A G	4
		box ▲	T C C A T A G T A C G C G C C G C G G A G G G G A A A	7
	PLL4	TalAB17	NI HG NI NI NI NN HD NS NN NS NN HD NN NI HD NN NI NG HD NG	MM
		box WT	T A T A A A T C G G C G C G G G C G C T C G	4
		box ■	A T A A A T G C G G C G C G G C G C T C G	7
	box ■	T A T A A A T C G T C G G C G C T C G A C	10	
	NPF6.3	TalAE16	NI NN NI HG HG HD NG HD HG HD HD HD NG	MM
		box WT	T A G G T T C T C T C C C T	1
		box ◆	T A G G T T C T C T C C T C	3
	box ◆	T A G G T T C T C T C T C C	3	
	PHO1.3	TalAO16	NI NN N* NG NS NN NN NN NI NN NI NG HD HD NI NG	MM
box WT		T A G C T A G G G G A A T C C A T	1	
box ◐		A G G C T A G G G G A A T C C A T	3	
Lsi1	TalAL11	NI NS HD NG NS NN HD N* NN NN NI NG HD NG HD HD HD NG	MM	
	box WT	T A G C T A G C T C G A T C T C C C T	1	
	box ☾	C C A C T A G C T C G A T C T C C C T	3	
box ☾	C A C C T A G C T C G A T C T C C C T	2		
Lsi1	TalAL12	NI NS HD NG NS NN HD N* NN NN NS NN HD HG HD HD NN NG	MM	
	box WT	T A G C T A G C T C G A T C T C C C T	3	
	box ☾	C C A C T A G C T C G A T C T C C C T	5	
box ☾	C A C C T A G C T C G A T C T C C C T	4		
DOX-1	TalAQ1	HD HD NN NN NG NG HD NS HG HD NG N* HD HD HD N* NN NI NN HD HI ND HD HG NN HG N* MM		
	box WT	T C C G G C C C C T C T C C C C C C C G C C A C C T G A C	6	
	box ○	C A C G G C C C C T C T C C C C C C C G C C A C C T G A C	8	
box ●	C A T C G C C C C T C T C C C C C C C G C C A C C T G A C	10		
Xoo PXO99	FBX109	TalAD1	NN HD NS NG HD NN N* NI HD NS HD NN HD NN HD NN NN NN NN NN NN HD NG	MM
		box WT	T C C A T A G T A C G C G C G C G C G A G G G G A A G	4
		box ▲	T C C A T A G T A C G C G C C G C G G A G G G G A A A	7
	PLL4	TalAB1	NI HG NI NI NI NN HD NS NN NS NN HD NN NI HD NN NS NG	MM
		box WT	T A T A A A T C G G C G C G G G C G C T	2
		box ■	A T A A A T G C G G C G C G G C G C T	5
	box ■	T A T A A A T C G T C G G C G C T C G	7	
	NPF6.3	TalAE1	NI NN NI HG HG NV HG HD HG HD HD HD NG	MM
		box WT	T A G G T T C T C T C C C T	1
		box ◆	T A G G T T C T C T C C T C	3
	box ◆	T A G G T T C T C T C T C C	3	
	PHO1.3	TalAO1	NI NN N* NG NS NN NN NN NI NN NI N* HD HD NI NG NG	MM
box WT		T A G C T A G G G G A A T C C A T G	2	
box ◐		A G G C T A G G G G A A T C C A T G	4	
DOX-1	TalBR5	HD HD NN NN NG N* HD NI NG HD NG NS HD HA ND N* ND NN HD NN NN HD HD N* NN NG HD	MM	
	box WT	T C C G G C C C C T C T C C C C C C C G C C A C C T G A C	4	
	box ○	C A C G G C C C C T C T C C C C C C C G C C A C C T G A C	6	
box ●	C A T C G C C C C T C T C C C C C C C G C C A C C T G A C	8		
FBX109	TalAD10	NN HD NS NG HD NN HD NI HD NN HD NN HD NN HD NN NN NN NN NN NN HD NG	MM	
	box WT	T C C A T A G T A C G C G C G C G C G A G G G G A A G	5	
	box ▲	T C C A T A G T A C G C G C G C C G C G G A G G G G A A A	8	
Lsi1	TalAV6	NN NS NG NI HD HD NG NN HD NI NG N* N* NG HD HD NS NI NN NG NG	MM	
	box WT	T A G T A C C T G C C A C C T C C C A G T T	2	
	box ☾	T A G T A C C T G C C A C T A G C T C G A T	6	
box ☾	T A G T A C C T G C C A C C T A G C T C G A	8		

Figure 42. Changes in TALE boxes of PXO142, PXO99 and CFBP2286 in T0 TT03 #09.

The T0 plant TT03 #09 is mutated in the TALE boxes of several TALEs from Xoo and Xoc using CRISPR/Cas9, as shown in Figure 41. The Xoo strains PXO142 and PXO99 and the Xoc strain CFBP2286 were chosen to challenge the progeny of TT03 #09. The affected TALEs of both strains are shown and the differences in the TALE boxes between wild type (WT) Kitaake and TT03 #09 are marked. The alleles of TT03 #09 are depicted as established in Figure 41. The cutting sites of CRISPR/Cas9 are marked with red lines and mismatches (MM) between TALEs and their TALE box are highlighted in green. TalAQ1 has a repeat with 42 amino acids, which is underlined. The corresponding TALE target genes are indicated in blue boxes.

3.5.3. TT03 rice plants have decreased TALE-mediated expression during *Xoo* and *Xoc* infection

The T0 TT03 plants developed viable seeds during this thesis and were therefore further analyzed. The progeny of T0 TT03 #09 were selected for subsequent experiments, because the critical locus around sgTT010 (TaIAQ/TaIBR) showed the biggest changes in this line and the T0 plant produced a lot of seeds. As the mutations caused by TT03 affect TALEs from *Xoo* and *Xoc*, one strain of each pathovar was selected to challenge the T0 TT03 #09 progeny.

The best candidate strains available in our group were *Xoo* PX0142 and PX099 and *Xoc* CFBP2286, which carry six, five and three affected TALEs, respectively (Figure 42). TALEs can accommodate some changes in their TALE box due to ambiguous nucleotide specificities in their RVDs. Nevertheless, each mutated TALE box increased the mismatches to the respective TALEs in PX0142, PX099 and CFBP2286.

In order to evaluate whether these changes are sufficient to prevent TALE target gene induction, T0 TT03 #09 progeny and wild type Kitaake were inoculated with PX099, CFBP2286 and a mock control. 48 h after inoculation, samples were harvested and total RNA was extracted for qRT-PCR.

Overall, gene induction of TALE target genes was low. During this experiment, the central heating of the greenhouse was disabled due to construction work and a portable heater was introduced into the chamber. These changes might have negatively affected the infection process. Nevertheless, the target genes *OsPLL4*, *OsNPF6.3* and *OsDOX-1* of PX099 were significantly less expressed in T0 TT03 #09 progeny compared to wild type Kitaake during infection. The other mutated target genes of PX099, *OsPHO1;3* and *OsFBX109*, were barely induced in wild type Kitaake and were consequently not significantly affected by the mutations in T0 TT03 #09 progeny. All three mutated TALE boxes addressed by CFBP2286 TALEs (*OsDOX-1*, *OsFBX109* and *OsLsi1*) had significantly reduced expression compared to wild type Kitaake during infection.

The expression of TALE targets that should not be affected by the TT03 mutations was tested as well to make sure that differences in affected TALE targets were not caused by differences in the progress of the infection in general. The gene induction was tested in genes that are typically moderately induced (*OsHEN1*) or strongly induced (*OsSWEET11* & *OsDOX-2*) by the tested strains. Both tested target genes for CFBP2286 were induced similarly in Kitaake and T0 TT03 #09 progeny, suggesting a comparable level of infection in all samples. PX099 was not able to induce *OsHEN1* in this experiment. *OsSWEET11*

was induced by PX099 in a similar fashion in all samples, indicating that the infection was comparable in all samples.

Overall, the results are promising, as the expression of most mutated TALE target genes was reduced.

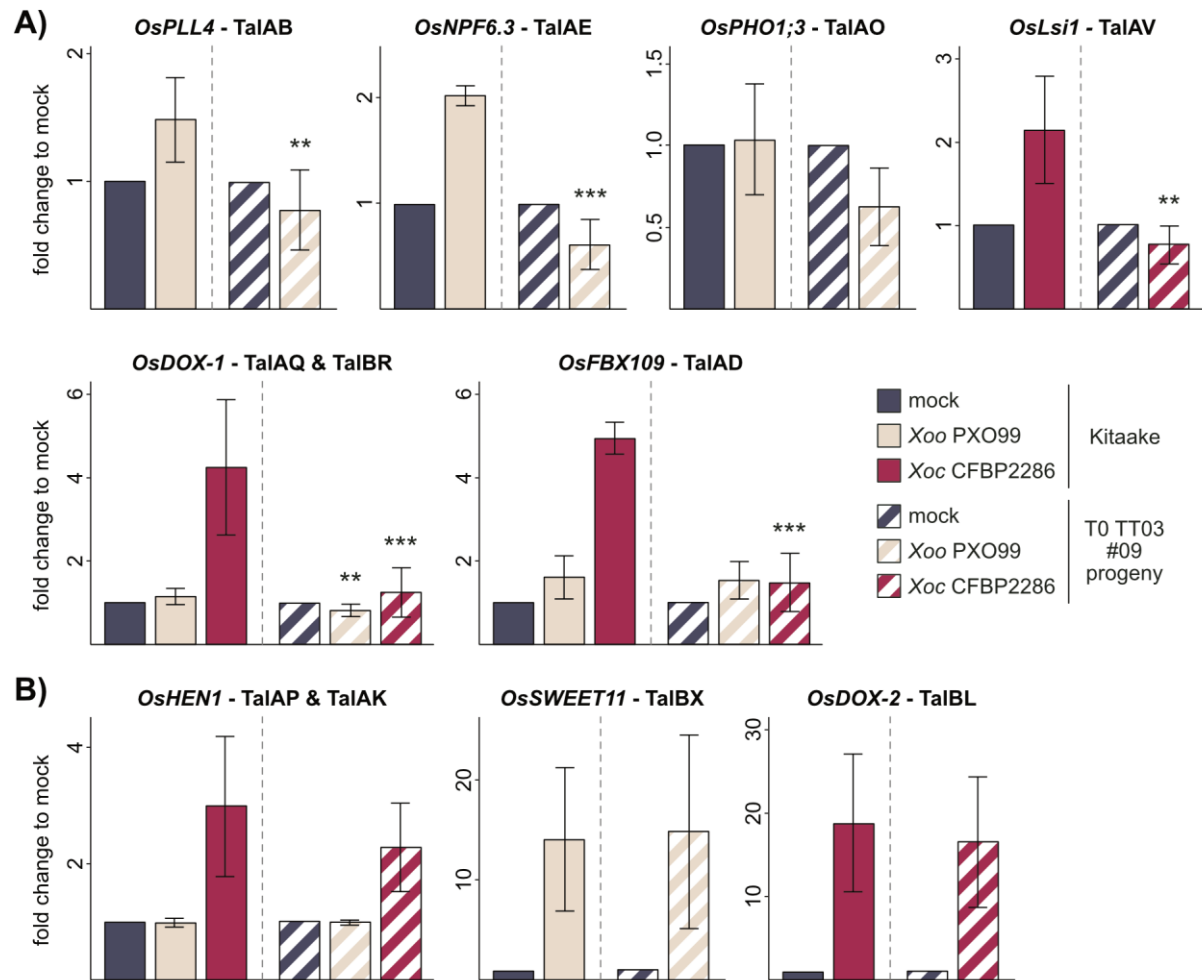


Figure 43. TT03 #09 progeny has reduced TALE-mediated expression in mutated loci.

The T0 plant TT03 #09 is mutated in the TALE boxes of several TALEs from Xoo and Xoc. T1 progeny of TT03 #09 and wild type Kitaake plants were infected with Xoo strain PX099 and Xoc strain CFBP2286. Samples were taken 48h after inoculation and gene expression levels were analyzed via qRT-PCR. Relative RNA abundance was assigned to arithmetic means of three to five biological replicates using fold changes of gene expression in samples compared to mock means of three to five biological replicates using fold changes of gene expression in samples compared to mock treatment (10 mM MgCl₂). Actin was used as a reference gene. The statistical significance between samples taken from Kitaake and T0 TT03 #09 progeny are indicated by p-values (<0.1 = *; <0.05 = **; <0.01 = ***) resulting from an unpaired t-test. A) Expression rates of TALE target genes induced by PX099 or CFBP2286 with mutated TALE boxes in TT03 #09 as shown in Figure 42. B) Expression rates of selected TALE target genes induced by PX099 or CFBP2286 that are not mutated in TT03 #09.

3.5.4. Impact of TT03 mutations on Xoo and Xoc virulence

In order to evaluate the impact of TALE box mutations in TT03 plants, infection studies were performed.

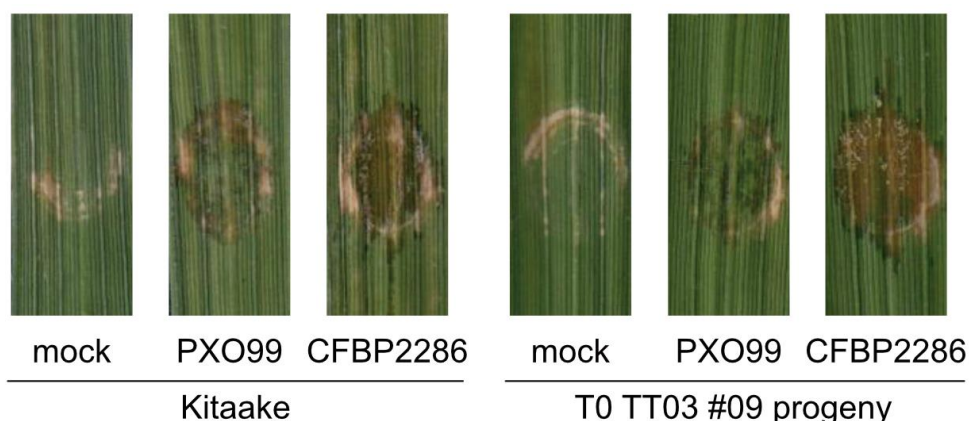


Figure 44. Xoo and Xoc symptom formation on TT03 plants.

Rice cultivar Kitaake and T0 TT03 #09 progeny were inoculated with Xoo PX099 and Xoc CFBP2286 ($OD_{600} = 0.5$) and disease symptom formation was documented after six days. Inoculations were performed on five plants each with 6 spots on the second and third leaf. One representative spot per strain is shown.

In parallel to the qRT-PCR samples taken in Chapter 3.5.3, leaves of Kitaake and T0 TT03 #09 progeny were inoculated with PX099 and CFBP2286 for phenotypic evaluation after six days. No significant changes between wild type and mutated rice could be detected (Figure 44). Notably, the symptoms of rice infected with PX099 are very faint, even in Kitaake samples, indicating non-optimal infection conditions. It is therefore not possible to draw definitive conclusions on the impact of TT03 #09 mutations on PX099 infection.

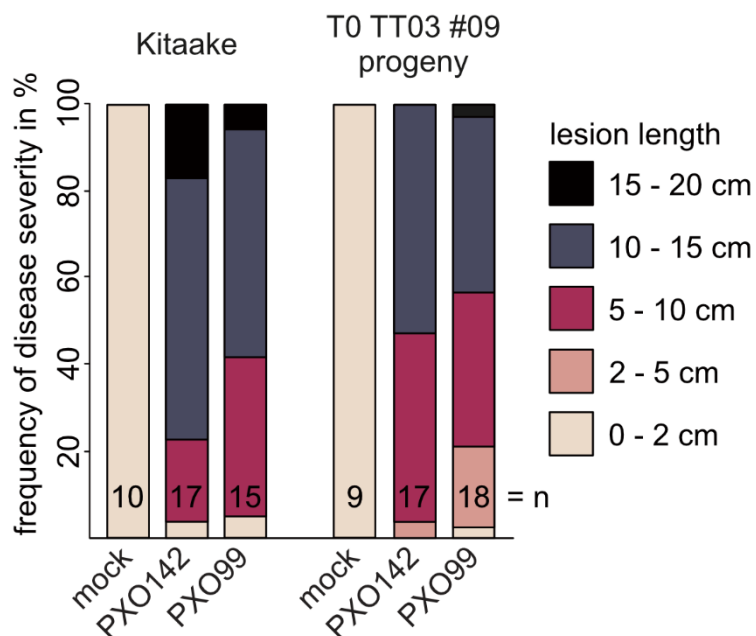


Figure 45. TT03 mutations make rice less susceptible to PX0142 and PX099.

The rice cultivar Kitaake and the progeny of T0 TT03 #09 was infected with Xoo strains PX0142 and PX099. Infection was done by clipping the second leaf with bacterial solution ($OD_{600} = 0.2$). 14 days after infection leaves were harvested and lesion length was measured. Disease severity was scored in five different categories: 0 - 2 cm, 2 - 5 cm, 5 - 10 cm, 10 - 15 cm and 15 - 20 cm. Infections were done once and number of infected plants (n) is shown in the bars. Depicted is the frequency of different disease severity categories observed through all plants.

The strain PX0142 is affected in six TALE boxes by TT03 and is only lacking a member of the TALE class TalAQ targeting *OsDOX-1* (Figure 42). PX099 is affected in five TALE boxes by TT03 and does not have a member of the TALE class TalAL targeting *OsLsi1* (Figure 42). Virulence assessment with leaf clipping was performed as described in Chapter 3.3.1 with both strains to cover all possibly affected TALE classes by at least one strain.

The lesion length of Kitaake infected with PX0142 is on average longer than in T0 TT03 #09 progeny with 11.5 and 9.3 cm, respectively (Figure 45). In rice plants carrying TT03 mutations, no lesion length of more than 15 cm can be observed and the frequency of lesions between 10 and 15 cm decreases in favor of lesions under 10 cm. Similar results can be observed in infections with PX099, which causes shorter lesions in the mutated rice compared to wild type plants with 8.3 and 10.7 cm on average, respectively (Figure 45). T0 TT03 #09 progeny shows less lesions of over 10 cm and instead displays lesions of less than 5 cm more frequently. The differences in lesion length between wildtype and mutated rice are statistically significant with p-values of 0.07 and 0.10 for PX0142 and PX099, respectively. This analysis is based on only one experiment, as repetition could not be done due to lack of time and this experiment needs to be verified with a large sample size and multiple repetitions.

The construct TT03 targets TALE boxes of TALE classes with unknown virulence functions exclusively. Based on these initial results, simultaneous mutations in the TALE boxes of TalAQ, TalAD, TalAB, TalAE, TalAO and TalAL decrease the susceptibility of rice to *Xoo* infection.

4. Discussion

In this thesis, *Xoo* genome sequences and transcriptomic data were used to categorize and analyze TALEs and identify potential target genes in rice. These target genes were confirmed and methods to determine their role during the infection were established. Finally, transgenic rice lines were created that carried mutations inside identified target genes or their respective TALE boxes to improve resistance.

4.1. The TALome of Asian *Xoo* is well understood

During this thesis, the amount of fully sequenced Asian *Xoo* strains increased from five to 34, advancing the understanding of TALome diversity drastically (Lee *et al.*, 2005; Ochiai *et al.*, 2005; Salzberg *et al.*, 2008; Booher *et al.*, 2015; Grau *et al.*, 2016; Quibod *et al.*, 2016; Carpenter *et al.*, 2018; Zheng *et al.*, 2019; Chien *et al.*, 2019; Mücke *et al.*, 2019; Oliva *et al.*, 2019). In the era of third-generation sequencing, the emerging challenge is no longer to acquire new data, but how to utilize existing genomes most effectively. Therefore, tools to categorize features and find similarities or differences are becoming more and more valuable.

The universal nomenclature of TALEs created by AnnoTALE is suitable to compare TALEs across genomes (Grau *et al.*, 2016). The assignment of TALE classes has additionally advanced our knowledge of similarities between strains (Grau *et al.*, 2016). In this thesis, the TALEs of these 34 *Xoo* strains were assigned into 45 TALE classes. This enabled the establishment of TALE abundance categories, which reflect the frequency of TALE classes in different strains. 10 core TALE classes present in over 80% of strains, 24 rare TALE classes found in fewer than 20% of strains and 11 intermittent TALE classes occurring in 20 – 80% of strains were identified. These tools enable an educated guess about the importance of certain TALEs based on how conserved they are. The concept of core effector repertoires has been a fixture in plant pathogen research and core type III effectors for *P. syringae* were established in 2012 (Lindeberg *et al.*, 2012). However, research in *X. campestris* strains revealed only three core type III effectors on the species level, but 12 to 18 core effectors on the pathovar level (Roux *et al.*, 2015). This is comparable to the 10 core TALE classes found in *Xoo*.

Among TALEs with reported virulence function, two different strategies emerge. Some TALEs with moderate impact on virulence like TalAR and TalAP are core TALE classes and highly conserved (Sugio *et al.*, 2007). In contrast, TALEs with a big impact on virulence, i.e. all SWEET-inducing TALEs, are often rare TALE classes as the *Xoo* strains have diverse TALEs with this function (Streubel *et al.*, 2013). These differences can be attributed to

the higher selection pressure on TALEs with bigger impact. TALEs with a big impact on virulence are essential to infection and the development of variants that can infect resistant rice lines is a huge selective advantage and will lead to quicker adaptation. Additionally, resistance genes against *SWEET*-inducing TALEs have been used widely in rice breeding, which increases the selection of new variants (Carpenter *et al.*, 2018; Quibod *et al.*, 2019). For example, it is advantageous for *Xoo* to evolve TALEs that only induce *OsSWEET14*, but not the resistance gene *Xa7* (Yang *et al.*, 2005). TalBH and TalAC are binding the *OsSWEET14* promoter at nearly identical positions, but TalAC is also being recognized by *Xa7* (Yang *et al.*, 2000; Antony *et al.*, 2010).

It should be noted that all assumptions on TALE abundance are based on a biased system, as the selection of strains that are sequenced is mostly based on a specific research question and might not reflect the overall population correctly. This can be observed in the large amount of strains from the Philippines (53%). Additionally, Oliva *et al.* (2019), which analyzed virulence of 105 *Xoo* strains on mutated rice plants and found only a few strains carrying the TALE class TalBK. These seven strains were sequenced and are now increasing the TALE class abundance of the intermittent TALE class TalBK, which might not be as common as the current selection of sequenced strains suggests. In parallel, Xu *et al.* (2019) found the exact same phenomenon by looking at 131 strains and identified a total of ten strains with TalBK members.

4.1.1. Spatiotemporal diversity of sequenced Asian *Xoo* strains

In general, the selection of strains that will be sequenced in the future should be chosen wisely, because the amount of new information gained with each sequenced strain is decreasing rapidly. The last 17 published genomes, which make up half of all fully sequenced Asian *Xoo* strains today, only contained three new TALEs, TalFT1, TalFM2 and TalFV1, in total (Figure 7; Table 12). All of which seem to be closely related to a well-known core TALE class (Figure 8). A multilocus sequence analysis of *Xanthomonas oryzae* strains revealed, that they are very homogeneous and show slightly lower diversity compared to *Xanthomonas campestris* strains (Hajri *et al.*, 2012). These findings indicate that the sequenced strains are already representing a large portion of TALE diversity. Additionally, the average sequenced strain was sampled in 1991 (Table 12), which suggests that the data set for TALomes that we use today might be outdated.

It is vital, that recently isolated strains are sequenced in the future to understand the mechanisms and TALEs they use. The highest potential of undiscovered TALEs lies in *Xoo* strains from regions with endemic *Xoo* infections that are not represented by other

sequenced strains, so far. For example, phylogenetic analysis of 100 Xoo strains in India identified five distinct lineages with varying levels of diversity (Midha *et al.*, 2017). A multilocus variable-number tandem-repeat analysis of Asian Xoo strains revealed comparatively high diversity in geographical locations with endemic infections, like the Philippines (Poulin *et al.*, 2015). Indonesia, which is one of the three countries most affected by Xoo, but is not represented by a sequenced strain to date, is a strong candidate for future sequencing (Table 12; OEPP/EPP, 1997). Nevertheless, geographical origin is not a failproof indicator of Xoo diversity. Strains isolated from South America were identified as closely related to strains from the Philippines, indicating a recent introduction from Asia (Triplett *et al.*, 2011; Hajri *et al.*, 2012; Poulin *et al.*, 2015). As the discoveries of new TALEs become rarer, the function of known TALEs, which were largely ignored until now, should be uncovered. The discovery of iTALE function was only managed by testing a variety of rice cultivars with a diverse Xoo mutant set (Ji *et al.*, 2016). This example shows that some TALEs might only contribute to virulence under certain conditions, but will be vital during those interactions. In the example of iTALEs, nearly all Xoo strains contain at least one TALE with this function, except KACC10331 and KX085 from Korea (Figure 7). This underlines the importance of researching core TALEs with unknown virulence function.

4.2. Solving Xoo infection mechanisms one TALE at a time

The identification of target genes of core TALEs is most important, because these genes harbor big potential as a source of resistance due to loss of susceptibility. Because the core TALEs are highly conserved, it limits available variants to break the resistance and a large number of strains might be impaired.

During this thesis, TALE target predictions were combined with transcriptomic data for the three Xoo strains PX083, PX0142 and ICMP 3125^T to identify a list of 61 promising candidate target genes in rice (Table 14). At present, 13 TALE-dependently induced rice genes were confirmed (Figure 13). This broadens our knowledge of Xoo TALE target genes significantly with now 68% of all functional Asian Xoo TALE genes having a known target. This expanded known TALE target genes for core TALE classes from 2/10 to 8/10.

4.2.1. General modes of action among phytopathogens emerge

This new data uncovered common strategies not only among *Xanthomonas* species, but also among biotrophic phytopathogens in general. Five distinct points of attack could be identified, that might play an important role in the pathogen-host interaction (Figure 46).

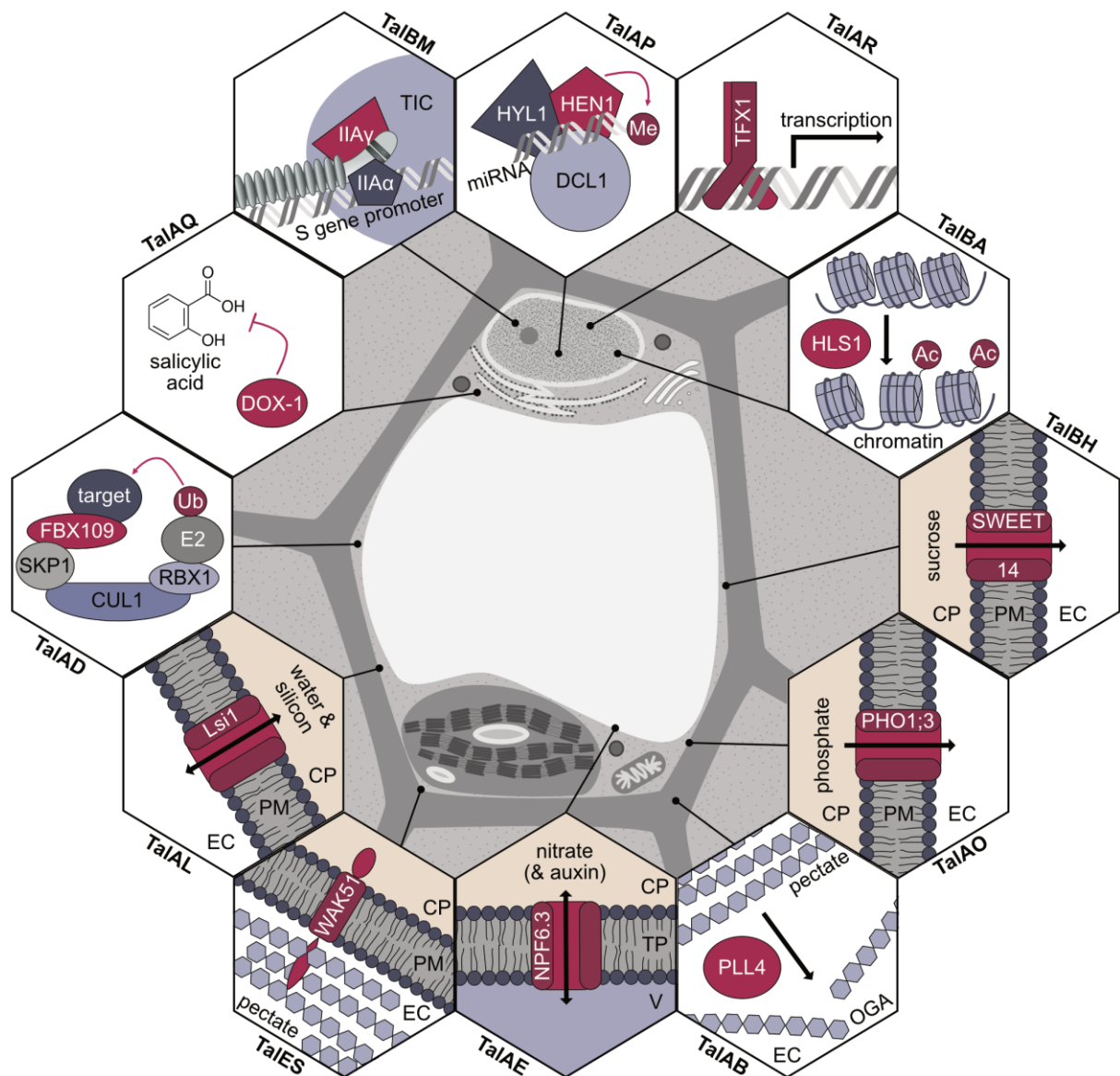


Figure 46. Modes of action for TALEs in rice.

The function for each TALE target (red) is shown in a hexagon, the subcellular location of the proteins is shown, and the corresponding TALE classes inducing the genes are noted. If the TALE target modifies a substrate, the modification is displayed in light red. TIC - transcription initiation complex; miRNA - microRNA; Me - methyl group; Ac - acetyl group; CP - cytoplasm; PM - plasma membrane; EC - extracellular space; PL - pectate lyase; OGA - oligogalacturonides; Ub - ubiquitin; TP - tonoplast; V - vacuole.

4.2.1.1. Coerced nutrient supply

Hemibiotrophic pathogens like *Xoo* need sophisticated tools to gain access to host nutrients without killing the cell prematurely. While some pathogens like *Xoc* and *P. syringae* rely on the digestion of cell wall components and other organic substances of the apoplast, *Xoo* is specialized to colonize a particularly nutrient-poor environment – the xylem (Rico and Preston, 2008; Yadeta and Thomma, 2013; Cao *et al.*, 2020). As xylem vessels are predominantly dead tissue with lignified walls, nutrient acquisition is more complicated. The results of this thesis suggest that *Xoo* has evolved a group of nutrient transporter-activating TALEs to survive in these unfavorable conditions.

4.2.1.1.1. Sugar in the xylem

One of the first identified TALE targets in rice, *OsSWEET14*, could be verified as a direct target of TalBH2 of PXO142 in this thesis. The clade III *SWEET* genes of rice are a well-described group of uniporters that are transporting sucrose bidirectionally along the concentration gradient (Chandran, 2015). They are key susceptibility genes for *Xoo* infection, but not addressed by the rice-pathogenic *Xoc* (Streubel *et al.*, 2013; Cernadas *et al.*, 2014). Similarly, *GhSWEET10* of cotton and *MeSWEET10a* of cassava are key susceptibility genes for *Xcm* and *Xam* infection, respectively (Cohn *et al.*, 2014; Cox *et al.*, 2017). In contrast, the *SWEET* genes *UPA16* of pepper and *CsSWEET1* of sweet orange were shown to be induced during infection with *Xcv* and *X. citri* *pv. citri* (*Xac*), respectively, but did not impact virulence significantly (Kay *et al.*, 2009; Hu *et al.*, 2014). This suggests that *SWEET* genes only benefit infection under certain circumstances. The common denominator of known *Xanthomonas* species that rely on *SWEET* genes is the colonization of the xylem (*Xoo*, *Xcm*, *Xam*), whereas non-vascular *Xanthomonas* species show no dependence on *SWEET* genes (*Xoc*, *Xcv*, *Xac*). Therefore, *SWEET* genes seem to particularly benefit infection in the xylem. This was supported by a study focusing on the African *Xoo* strain BAI3, which could no longer colonize the xylem without *SWEET* induction, but still multiplied locally at the infection site (Yu *et al.*, 2011). This might be due to the reduced availability of nutrients in the xylem, which increases the importance of sugar export from the host cell.

Alternatively, the importance of *SWEET*s for xylem colonizing pathogens might be based on the specific role of sucrose in the xylem. While sucrose is generally transported in the phloem, small amounts are also present in the xylem. It was shown that sucrose levels in the xylem are a major stimulus for plants detecting embolisms in the vasculature (Secchi and Zwieniecki, 2011). During the formation of embolisms, the water column of the xylem vessel is disrupted, enriching osmotic compounds near the cell wall. This provides a chemical output for the physical phenomenon that can be detected by the accompanying xylem parenchyma cells to counteract the embolism (Secchi and Zwieniecki, 2011). The accumulation of sucrose specifically was proven to induce the active export of sugars, inorganic ions and water into the xylem to increase osmotic pressure and to refill the embolism (Secchi and Zwieniecki, 2016). This could be a cascade of events to provide the pathogen with nutrients in the xylem and to support spread against xylem flow by locally increasing osmolarity.

Additionally, embolisms might even be a signal in the xylem-specific defense of plants. It is commonly believed, that if embolisms are not refilled, active vessel occlusion by the

plant will follow (De Micco *et al.*, 2016). Xylem vessel occlusion through tyloses or gums is the most effective tool in plant defense to limit the spread of vascular pathogens like *Ralstonia solanacearum* by blocking the infected xylem (Rahman *et al.*, 1999; Yadeta and Thomma, 2013; De Micco *et al.*, 2016). It was shown that xylem colonizing *Xylella fastidiosa* frequently cause embolisms in their hosts (Sabella *et al.*, 2019). It is reasonable to believe that the colonization of the rice xylem by *Xoo* might also increase embolism formation. The prevention of xylem vessel occlusion by induction of embolism refilling would be an important strategy to ensure effective colonization of the xylem and might explain the tissue specific function of *SWEET*-inducing TALEs.

4.2.1.1.2. Circumventing phosphate starvation

The core TALE class TalAO, which is present in 82% of Asian *Xoo* strains, induces the phosphate transporter *OsPHO1;3*. *OsPHO1;3* is part of the SPX-EXS domain containing transporters, that facilitate long distance phosphate transport from root to shoot (Secco *et al.*, 2012). *OsPHO1;3* is believed to be redundant to *OsPHO1;2*, which is the major xylem loading transporter for phosphate in rice (Secco *et al.*, 2010). Both transporters are close homologs to *AtPHO1*, which was shown to localize to Golgi vesicles and is hypothesized to transport phosphate by endocytosis (Młodzińska and Zboińska, 2016; Wege *et al.*, 2016).

Phosphate is one of the essential building blocks of life and is needed by all organisms to survive. Even though plants are rich in phosphate, many phytopathogens experience phosphate starvation *in planta*. *X. axonopodis* pv. *glycine* and *Xac* are reliant on very costly high-affinity phosphate uptake mechanisms for full virulence on soybean and citrus, respectively (Moreira *et al.*, 2015; Chatnaparat *et al.*, 2016). While these pathogens have problems obtaining phosphate in leaf tissue, which contains about 5-20 mM phosphate, the amount of phosphate in the xylem sap of rice is even lower at about 60 μ M (Sun *et al.*, 2012; Zheng *et al.*, 2018a). Therefore, it seems likely, that *Xoo* benefits from inducing phosphate export into the xylem. Interestingly, it was shown that *Xoo* strain PX099 is repressing the two-component system PhoBR, which is needed to induce high-affinity phosphate uptake, during infection (Zheng *et al.*, 2018a). This is in contrast to other phytopathogens even though the available phosphate in the xylem should be low. As PX099 has TalAO1 and can likely induce *OsPHO1;3*, it is possible that *Xoo* has found a way to circumvent costly high-affinity phosphate transporters by locally increasing phosphate concentrations. As the PhoBR system and TalAO might be two

alternative routes for *Xoo* to ensure sufficient phosphate uptake, a double mutant could present a severe change in virulence.

During this thesis, knockout mutants of *OsPHO1;3* were created. Future experiments with PhoBR-mutant *Xoo* strains in these knockout plants might elucidate the connection between the PhoBR system and TalAO-mediated expression of *OsPHO1;3*.

4.2.1.1.3. Manipulating the nitrogen regulon

The TALE class TalAE is a core TALE class present in 97% of Asian *Xoo* strains and induces the nitrate transporter *OsNPF6.3*. *OsNPF6.3* is a close homolog of *AtNPF6.3* (also *AtNRT1.1*; *AtCHL1*), which is a plasma membrane localized bidirectional nitrate and auxin transporter involved in root-to-shoot nitrate transport in *A. thaliana* (Guo *et al.*, 2002, 2003; Léran *et al.*, 2013, 2014). Additionally, *AtNPF6.3* is an important nitrate sensor and shapes the primary nitrate response, including transcriptional changes in nitrate uptake components and lateral root development (Bouguyon *et al.*, 2015). The phosphorylation status of Thr101 of *AtNPF6.3* is dependent on the nitrate concentration and elicits calcium-dependent downstream signaling and changes in auxin flux (Zhang *et al.*, 2019; Rashid *et al.*, 2020). The full signaling pathway is yet to be discovered.

As *OsNPF6.3* is the closest homolog to *AtNPF6.3*, it was hypothesized, that it might fulfill similar functions in rice. Instead, *OsNPF6.5* is responsible for nitrate transport from root to shoot (Léran *et al.*, 2013; Hu *et al.*, 2015). These new findings suggest that the NPF6 transporter family has undergone functional divergence in rice compared to *A. thaliana* (Wang *et al.*, 2018; Wen and Kaiser, 2018). *OsNPF6.3* localizes to the tonoplast and is responsible for intracellular nitrogen sensing and signaling (Wang *et al.*, 2018; Wen and Kaiser, 2018). *OsNPF6.3* regulates nitrogen signaling by promoting the nuclear localization of NIN-like protein (NLP) transcription factors, which play a central role in the nitrogen regulon (Guan *et al.*, 2017; Wang *et al.*, 2018). Even though the mechanism is still unclear in rice, NLPs were shown to localize to the nucleus upon phosphorylation by calcium-sensor protein kinases in *A. thaliana* (Liu *et al.*, 2017). Therefore, *OsNPF6.3* might create a calcium signal similar to *AtNPF6.3*, which in turn activates calcium-sensor protein kinases that phosphorylate NLPs. This could explain the link between *OsNPF6.3* and nuclear localization of NLPs and should be investigated in the future. It was not yet tested, if *OsNPF6.3* might also be involved in the transport of auxin or other substrates.

Overexpression lines of *OsNPF6.3* showed increased yield and shorter maturation times in rice, which makes it a very attractive feature for breeding purposes (Wang *et al.*, 2018). However, as *Xoo* is actively inducing this gene, it should be extensively tested, if

overexpression lines are more susceptible to pathogen infection, before market release. Overexpression of *OsNPF6.3* induced a range of nitrogen responsive genes including nitrate and ammonium transporters, which could provide *Xoo* with needed nitrogen sources in the xylem (Wang *et al.*, 2018).

Nitrogen assimilation was shown to be essential for virulence of the xylem colonizing pathogen *Ralstonia solanacearum* (Dalsing *et al.*, 2015). Equally, nitrogen availability is directly connected to *Xoo* virulence, as nitrogen deficiency in rice decreases symptom formation (Yu *et al.*, 2015). Yu *et al.* also described an overlap of transcriptional changes in rice due to *Xoo* PX099 infection and N deficiency, indicating PX099, which contains *TalAE1*, is inducing nitrogen responsive genes (Yu *et al.*, 2015). Additionally, nitrogen sources like ammonium nitrate were shown to be important factors in the biofilm formation of *Xoo* in the xylem (Ham *et al.*, 2018).

In the case of *OsNPF6.3*, *Xoo* is not only directly inducing a nutrient transporter, but also hijacking the plant signaling cascade to induce a multitude of nitrogen responsive genes.

4.2.1.1.4. The enigma of silicon nutrition

The transporter *OsLsi1* is induced by the intermittent TALE class *TalAL*, which is present in 76% of known Asian *Xoo* strains, and by the TALE class *TalAV*, which occurs in all known *Xoc* strains. *OsLsi1* is an aquaporin also known as *OsNIP2;1*, which has a low affinity for water and instead has a high affinity for metalloids like silicon (Si), germanium, arsenic and antimony (Ma *et al.*, 2006, 2011; Ali *et al.*, 2009). It is reported, that the physiologically important substrate of *OsLsi1* is Si(OH)_4 (silicic acid) (Ma *et al.*, 2006, 2011). *OsLsi1* is a passive channel that is localized at the distal side of both casparian bands in roots (Ma *et al.*, 2006, 2011). Together with the Si efflux transporter *OsLsi2*, *OsLsi1* enables Si uptake into the stele (Ma *et al.*, 2011). *OsLsi6*, which is a close homolog of *OsLsi1*, is responsible for xylem unloading of Si in shoots and leaves (Yamaji *et al.*, 2008). It is possible, that overexpression of *OsLsi1* at the infection site might also contribute to xylem unloading, as the functional differences between *OsLsi1* and *OsLsi6* seem to be regulated by different expression patterns, while the molecular function itself might be conserved (Ma *et al.*, 2006; Yamaji *et al.*, 2008).

Si is regarded as a “quasi-essential” mineral nutrient for higher plants (Bakhat *et al.*, 2018). Even though plants can survive without Si, they will be more susceptible to biotic and abiotic stress and they will display lower yields (Wang *et al.*, 2017c; Bakhat *et al.*, 2018). These effects are more severe in Si accumulators like rice, which can have up to 10% Si in its dry weight (Ma *et al.*, 2011). So far, no direct role of Si in biochemical or

physiological processes is known (Wang *et al.*, 2017c; Bakhat *et al.*, 2018). Until a clear molecular link between Si and observed phenotypes can be established, the correlation cannot be seen as a causation unambiguously.

Among other effects, Si is described to induce broad-spectrum disease resistance in nearly all tested plants (Wang *et al.*, 2017c). The majority of tested diseases are fungal infections that are impeded by a physical Si barrier preventing epidermal penetration. Analyzed bacterial pathogens obstructed by Si nutrition include *X. translucens* pv. *undulosa* infecting wheat, *X. campestris* pv. *musacearum* infecting banana, *Xam* infecting cassava and *Xoo* infecting rice (Silva *et al.*, 2010; Mburu *et al.*, 2016; Song *et al.*, 2016; Njenga *et al.*, 2017). Most bacterial infections are believed to be affected by Si-mediated accumulation of antibacterial compounds such as lignin and reactive oxygen species as well as induced expression of defense genes (Wang *et al.*, 2017c; Bakhat *et al.*, 2018).

In these experiments, beneficial Si nutrition is often compared to the complete absence of Si, which is known to have widespread negative effects on plant health (Wang *et al.*, 2017c). Therefore, these results should be analyzed with caution. Until direct molecular mechanisms of Si affecting defense are uncovered, it is unclear if elevated resistance is due to the general improvement of plant health and an indirect effect of Si. As long as the functional role of Si is unclear, the consequences of *Xoo*- or *Xoc*-mediated overexpression of *OsLsi1* at the infection site is speculative. If Si has a direct influence on defense, altering the Si transport might benefit the infection. In this thesis, knockout mutants of *OsLsi1* were created. In the future, virulence assays on these mutants might shed light on the role of *OsLsi1* in the *Xoo* and *Xoc* infection.

4.2.1.1.5. *Xanthomonas* and nutrient flow

Rice-pathogenic *Xanthomonas* species are reported to influence additional transporters during infection that were not studied in this thesis.

The major virulence factor of *Xoc* is the TALE class TalBF, which induces the predicted sulfate transporter gene *OsSULTR3;6* (Cernadas *et al.*, 2014). Details of *OsSULTR3;6* function are still unknown and the functions and localizations of close homologs are very diverse. *OsSULTR3;3* is localized in the endoplasmic reticulum of vascular bundles and is involved in phytic acid, sulfur and phosphorus homeostasis (Zhao *et al.*, 2016). The transported substrate and the underlying mechanisms of observed *Ossultr3;3* phenotypes are unknown. Multiple homologs in *A. thaliana* are involved in sulfate uptake by chloroplasts, which is involved in the production of antioxidants (Cao *et al.*, 2013; Cernadas *et al.*, 2014). It was therefore hypothesized, that TalBF might induce

OsSULTR3;6 to alter the antioxidant capacity of rice to hinder defense-associated oxidative bursts (Cernadas *et al.*, 2014).

On the contrary, *Xoo* was described to alter the transport of compounds that hinder *Xoo* growth. Rice infected with PX099 was shown to have altered distribution of copper, which suppresses *Xoo* growth (Yuan *et al.*, 2010). OsSWEET11, which is induced by TalBX1 of PX099, interacts with the copper transporters OsCOPT1 (Os01g56420) and OsCOPT5 (Os05g35050) to facilitate copper uptake in the shoots to decrease copper concentrations in the xylem (Yuan *et al.*, 2010).

In conclusion, *Xoo* and *Xoc* manipulate a diverse set of nutrient transporters in rice, that either directly benefit the infection by providing nutrients or indirectly benefit infection by subverting defense responses or altering plant signaling pathways.

4.2.1.2. Hormonal imbalances make plants vulnerable

Phytohormones are at the center of signaling pathways in plants and control all aspects of development and stress adaptation. Naturally, many plant pathogens exploit plant signaling by altering phytohormone balances. Two common strategies emerge for phytopathogenic bacteria. Toxins and effector proteins are either used to suppress SA, ethylene (ET) and jasmonic acid (JA), which are involved in defense signaling, or toxins and effectors are used to boost abscisic acid (ABA), auxin, cytokinin, gibberellin and brassinosteroids, that counteract defense signaling hormones and facilitate pathogen dissemination (Ma and Ma, 2016). In this thesis, two TALE targets were identified, that are likely to interfere with phytohormones in rice.

4.2.1.2.1. SA – the bane of biotrophs existence

The core TALE class TalaQ, which is present in 85% of Asian *Xoo* strains and the TALE classes TalBR and TalBL, which are found in 60% and 90% of *Xoc* strains, respectively, induce *DOX* genes. These TALE targets, OsDOX-1 and OsDOX-2, are 2-oxoglutarate dioxygenases and close homologs to AtDMR6 (Figure 27; van Damme *et al.*, 2008; Kawai *et al.*, 2014; Falcone Ferreyra *et al.*, 2015). An *Atdmr6* mutant displayed broad-spectrum disease resistance, induced defense gene expression and accumulated SA (Zeilmaker *et al.*, 2015). Similarly, the deletion of the tomato homolog *Sldmr6-1* renders plants resistant to *Xcv* (Thomazella *et al.*, 2016). AtDMR6 is described as a suppressor of immunity, but the underlying mechanism is highly contended (Zeilmaker *et al.*, 2015). Because *Atdmr6* accumulates SA, it was first believed that AtDMR6 is a SA-3-hydroxylase (Figure 47; Kawai *et al.*, 2014; Zeilmaker *et al.*, 2015). Contrarily, Falcone Ferreyra *et al.* (2015) reported that AtDMR6 was unable to convert SA in an *in vitro* enzyme activity

assay. Instead, AtDMR6 was described as a flavone synthase I, which converts the flavanone naringenin to the flavone apigenin (Figure 47; Falcone Ferreyra *et al.*, 2015). Latest reports suggest both substrates are converted, but the affinity of AtDMR6 to SA is significantly higher than flavanones *in vivo* (Zhang *et al.*, 2017b). *Atdmr6* showed severely reduced levels of 2,5-dihydroxybenzoic acid (2,5-DHBA), which suggests AtDMR6 has SA-5-hydroxylase activity (Figure 47; Zhang *et al.*, 2017b).

OsDOX-1 and OsDOX-2 were annotated in the rice genome as flavanone-3-hydroxylase and naringenin 2-oxoglutarate 3-dioxygenase, respectively (Kawahara *et al.*, 2013). OsDOX-1 was also shown to convert naringenin to apigenin *in vitro* (Kim *et al.*, 2008). Similar to AtDMR6, conflicting experimental data was reported for OsDOX-1. Lam *et al.* (2014) reported no measurable flavone synthase I function *in vivo* when *OsDOX-1* was expressed in Arabidopsis. As the connection between AtDMR6, OsDOX-1 and OsDOX-2 was widely overlooked so far, no experimental data on the influence of *DOX* genes on rice immunity is available. During this thesis, rice was transformed with genome editing tools to create an *Osdox-1* mutant, but the resulting mutations were not inside the coding region. Therefore, it remains unclear, if *Osdox-1* or *Osdox-2* have the same phenotype as *Atdmr6* or *Sldmr6-1*. Nevertheless, inducing a suppressor of immunity might easily benefit infection of *Xoo*.

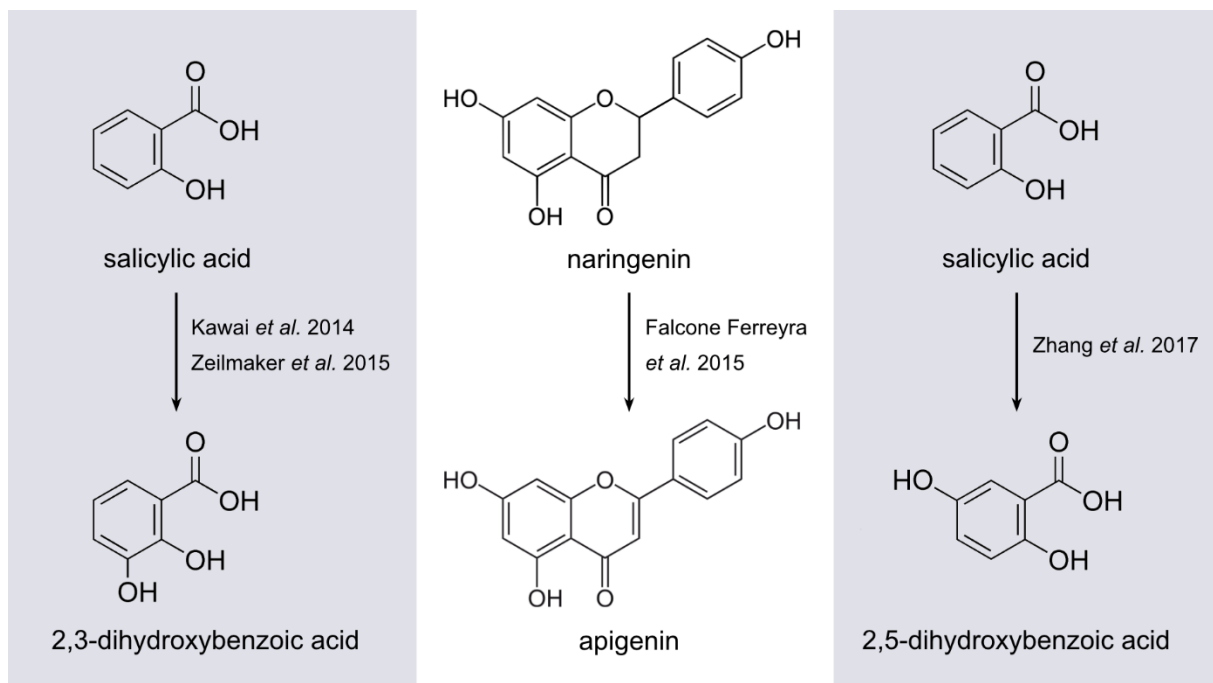


Figure 47. Postulated enzymatic functions of AtDMR6.

An overview of molecular structures of potential substrates and products of AtDMR6 is provided and corresponding references are indicated.

In this thesis, several experiments were conducted to determine the link between TALEs, *DOX* genes, flavonoid synthesis and SA. The presence or absence of TalaQ3 in *Xoo* strains could influence the expression of at least one gene of the flavonoid biosynthesis pathway in infected rice. Additionally, multiple measurements of SA contents in rice hinted at a link between *DOX* genes and reduced SA accumulation. Especially the induction of *OsDOX-2* by TaIBL1 showed significantly reduced SA levels in rice. These results suggest that rice *DOX* genes might fulfill similar functions to *AtDMR6* and influence both, flavonoid biosynthesis and SA content.

SA is a well-known phytohormone that is the primary regulator of defense against biotrophic pathogens and is accumulated during PTI and ETI (Ma and Ma, 2016; Dempsey and Klessig, 2017). Therefore, SA is a common target of pathogens, which try to prevent SA accumulation. While some fungi deplete substrates of SA biosynthesis by enzymatic conversion, bacterial pathogens interfere with SA signaling with effector proteins and toxins (Ma and Ma, 2016). *Pseudomonas syringae* uses the effector HopI1 to suppress SA accumulation and simultaneously deploys the toxin syringolin A to create SA-insensitive cells (Jelenska *et al.*, 2007; Misas-Villamil *et al.*, 2013). Interestingly, *Xac* was predicted to induce a dioxygenase gene similar to *OsDOX-1* and *OsDOX-2* with PthA4, but no experimental evidence is available at present (Pereira *et al.*, 2014). Some *Xanthomonas* species, including *Xcv*, contain the effector protein XopJ, which suppresses SA-mediated oxidative bursts (Üstün *et al.*, 2013). However, no known *Xoo* strain contains a XopJ homolog (Midha *et al.*, 2017). Nevertheless, SA interferes with *Xoo* infection and boosts defense-associated lignin production (Thanh *et al.*, 2017; Shasmita *et al.*, 2019). *Xoo* might compensate the lack of XopJ by inducing *OsDOX-1* to reduce SA accumulation. Both, the degradation of active SA i.e. by hydroxylation and the suppression of SA biosynthesis by substrate depletion are common strategies for pathogens (Ma and Ma, 2016).

4.2.1.2.2. ABA – the enemy of my enemy is my friend

The intermittent TALE class TaIBA, which is present in 32% of Asian *Xoo* strains, induces the putative histone N-acetyltransferase *HOOKLESS1* (*OsHLS1*). *OsHLS1* is a homolog of *AtHLS1*, which acetylates histone 3 to induce expression of specific target loci (Liao *et al.*, 2016). *AtHLS1* and homologs in tomato and peas were shown to be ethylene responsive genes that influence apical hook formation of the hypocotyl (Du and Kende, 2001; Chaabouni *et al.*, 2016; Liao *et al.*, 2016). Recently, *AtHLS1* was shown to induce the

expression of ABA signaling regulators and overexpression of AtHLS1 resulted in ABA hypersensitivity (Liao *et al.*, 2016).

OsHLS1 was not included in previous studies on histone acetyltransferases in rice and little is known about its expression patterns or function (Liu *et al.*, 2012). Nevertheless, GCC-boxes (GCCGCC) that are ethylene responsive elements can be found in the promoter of *OsHLS1* with the help of the New PLACE database tool (Higo *et al.*, 1999). These findings suggest that OsHLS1 might share the ethylene responsiveness with other HLS1 homologs. During this thesis, efforts were made to create inducible overexpression lines of individual TALEs. Even though no rice plants carrying a DEX-inducible TaIBA could be generated yet, this will be a vital tool in the future to determine if *OsHLS1* overexpression leads to ABA hypersensitivity as well.

ABA acts as a negative regulator of defense against biotrophic pathogens because of its antagonistic role against SA (Xu *et al.*, 2013; Ma and Ma, 2016). To this end, many biotrophic bacterial pathogens boost ABA synthesis or signaling. *P. syringae* uses AvrPtoB to indirectly induce the ABA biosynthetic gene *NCED3* and HopAM1 to induce ABA hypersensitivity in an unknown manner in *A. thaliana* (Ma and Ma, 2016; Peng *et al.*, 2019). This method is also deployed by *Xcc*, which elevates ABA levels in *A. thaliana* using AvrXccC to induce the ABA biosynthetic gene *NCED5*, and by *X translucens* pv. *undulosa*, which induces ABA synthesis with Tal8 by targeting a *NCED5* homolog in wheat (Ho *et al.*, 2013; Peng *et al.*, 2019). ABA was further shown to promote susceptibility to *Xoo* in rice and can be perceived by *Xoo* to modulate virulence functions (Xu *et al.*, 2013, 2015).

If the induction of *OsHLS1* leads to ABA hypersensitivity, this would be an attractive target for *Xoo* to promote infection. Additionally, overexpression of a histone acetyltransferase might loosen the chromatin and might facilitate access to the genome by TALEs in general (Görisch *et al.*, 2005).

4.2.1.2.1. Other hormonal manipulations

In addition to TALE-mediated changes, the phytohormone homeostasis in the rice-*Xoo* interaction is influenced by other elements. The effector XopAA is highly conserved among Asian *Xoo* strains and is suppressing rice immunity by inhibiting OsSERK1 (Yamaguchi *et al.*, 2013). This leads to an insensitivity to brassinosteroids and blocks the recognition of PAMPs like flg22 (Yamaguchi *et al.*, 2013). Similarly, the *Xoo* effector XopK is facilitating the degradation of OsSERK2, which is a functional homolog of OsSERK1 (Qin *et al.*, 2018). Additionally, other *Xanthomonas* species contain the effector XopD,

which desumoylates the ET responsive transcription factor SIERF4 to suppress ET signaling and immunity (Kim *et al.*, 2013).

Nevertheless, the host plant can still use phytohormone signals to its advantage. Upon infection with *Xoo*, the suppressor of immunity OsFD1 is repressed and JA responsive genes are activated (Ke *et al.*, 2019). JA- and SA-mediated defense have some common pathways and it was shown that JA can negatively affect *Xoo* infection (Tamaoki *et al.*, 2013; Ranjan *et al.*, 2015; Hui *et al.*, 2019a).

In conclusion, the very complex system of phytohormones is used by the plant and exploited by the pathogens to gain advantages during the infection. The two major players in *Xoo* infection of rice are SA and ABA, which have antagonistic effects and might both be manipulated by TALEs.

4.2.1.3. TALEs specialize in transcription manipulation

It is common knowledge that TALEs modulate transcription by gene induction, but *Xoo* has different means to affect transcription on a larger scale. Cernadas *et al.* (2014) reported 94 upregulated genes in rice specifically due to infection by PX099, which contains only 19 TALE genes. Therefore, transcriptional changes might be secondary effects of TALEs or due to other non-TALE effectors. Several TALE targets studied in this thesis have a direct impact on transcription, which are good access points for far reaching manipulations.

4.2.1.3.1. Nested transcription factors

The core TALE class TalAR, which is present in 88% of Asian *Xoo* strains and TalDI, which is present in 96% of African *Xoo* strains induce the bZIP transcription factor *OsTFX1*, which is a major susceptibility target for Asian *Xoo* strains (Sugio *et al.*, 2007; Tran *et al.*, 2018). TalDI additionally induces the IXC AP2/ERF transcription factor *OsERF#123*, which is a susceptibility target for African *Xoo* strains (Tran *et al.*, 2018). Coincidentally, *OsERF#123* is also induced by TalBI of *Xoc* (Wilkins *et al.*, 2015; Tran *et al.*, 2018). Even though both, *OsTFX1* and *OsERF#123*, are major susceptibility targets and induced by multiple TALEs from *Xanthomonas* strains of different pathovars or regions, their downstream effects are unknown.

Other *Xanthomonas* species also induce transcription factors as major susceptibility targets. *Xcv* induces the bHLH transcription factor *UPA20* in pepper with the TALE AvrBs3 to promote cell hypertrophy (Kay *et al.*, 2007). AvrHah1 of *X. gardneri* induces the two bHLH transcription factors bHLH3 and bHLH6 of tomato, which in turn activate the expression of a pectate lyase to facilitate water soaking (Schwartz *et al.*, 2017). *Xac* and

Xca use PthA4, PthAw, PthA*, PthB or PthC to induce the LOB domain family transcription factor *OsLOB1*, which promotes pustule formation in citrus (Hu *et al.*, 2014).

Similar to induced transcription factors in rice, the downstream activity of these targets is unknown in most cases. During this thesis, the first steps for inducible overexpression of heterologous genes in rice were taken. Creating DEX-inducible rice lines containing either TalAR or OstFX1 might enable future analysis of the transcriptome. Potential targets of OstFX1 would be induced in both rice lines but should not contain a TalAR box.

4.2.1.3.2. Modulating transcription machinery and transcripts

The rare TALE class TalBM, which is present in 15% of Asian Xoo strains, is known to induce the transcription initiation factor *OsTFIIA γ 1* (Sugio *et al.*, 2007). The TFIIA γ subunit of the transcription initiation complex was recently shown to directly interact with the C-terminal part of TALEs and forms a tertiary complex with TFIIA α and TALEs to initiate transcription (Ma *et al.*, 2018; Hui *et al.*, 2019b). The interaction between TALEs and a TFIIA γ subunit is essential for TALE-mediated gene induction and virulence (Ma *et al.*, 2018; Hui *et al.*, 2019b). Usually, *OsTFIIA γ 5* is expressed in rice to form transcription initiation complexes (Huang *et al.*, 2017; Hui *et al.*, 2019b). In rice carrying the *xa5* recessive resistance gene, the binding of TALEs to *OsTFIIA γ 5* is compromised and TALE function is severely reduced (Sugio *et al.*, 2007; Yuan *et al.*, 2016; Huang *et al.*, 2017). The induction of *OsTFIIA γ 1* by TalBM can partially restore TALE function and is used to overcome the *xa5* resistance (Sugio *et al.*, 2007; Huang *et al.*, 2017). It was widely believed that *OsTFIIA γ 1* can replace *OsTFIIA γ 5* in the tertiary transcription initiation complex formed by TALEs, but no direct interaction between *OsTFIIA γ 1* and TALEs could be observed *in planta* (Yuan *et al.*, 2016). Further, reduced *OsTFIIA γ 1* expression lead to enhanced resistance regardless of normal *OsTFIIA γ 5* expression (Yuan *et al.*, 2016). Therefore, the true mechanism of *OsTFIIA γ 1*-mediated virulence is still unknown. Nevertheless, manipulating the transcription initiation complex itself could have far reaching effects in the host plant.

The core TALE class TalAP, which is found in 91% of Asian Xoo strains, and the TALE class TalAK, which occurs in 60% of Xoc strains, induce the RNA methyltransferase *OsHEN1* (also called *OsWAF1*). *OsHEN1* methylates the 3' end of small RNA duplexes and stabilizes micro RNAs and trans-acting small interfering RNAs in rice (Abe *et al.*, 2010; Achkar *et al.*, 2016). Both micro RNAs and small interfering RNAs are specialized in post-transcriptional regulation by mRNA cleavage or translation repression (Zhang *et al.*, 2006). Especially micro RNAs require HEN1-dependent methylation to be integrated into

RNA- induced silencing complexes (Baranauskė *et al.*, 2015). Plant micro RNAs regulate a plethora of different plant processes making the effects on disease development difficult to identify (Zhang *et al.*, 2006; Samad *et al.*, 2017). A mutation of *OshEN1* lead to pleiotropic effects including severely reduced shoot development and abnormal leaf morphology in rice (Abe *et al.*, 2010). *OshEN1* influenced the expression of micro RNA targets including several transcription factor families (Abe *et al.*, 2010). During this thesis, rice plants carrying a putatively DEX-inducible TalAP15 were created. Analyzing phenotypic changes upon *OshEN1* overexpression might elucidate the role of *OshEN1* in *Xoo* and *Xoc* infection in the future.

Post-transcriptional regulation is also manipulated by *Ralstonia solanacearum*, which deploys the TALE-like effector Brg11 to induce an arginine decarboxylase (Wu *et al.*, 2019). Brg11 shifts the transcriptional start site and produces a 5' truncated transcript that has lost a regulatory element and bypasses translational control (Wu *et al.*, 2019).

In conclusion, TALEs manipulate regulatory circuits of their hosts by inducing transcription factors and they are able to change fundamental steps of post-transcriptional regulation. While it is likely, that many of these TALEs contribute to virulence, the responsible mechanisms are not well understood.

4.2.1.4. Tearing down walls

The cell wall of plant cells is one of the physical barriers that need to be overcome to infect the plant effectively. Therefore, pathogens have evolved a multitude of tools to degrade cell wall components for easier access to the host (Bacete *et al.*, 2018). In turn, the plant monitors the cell wall closely for any changes that indicate a pathogen attack. In this thesis, two TALE targets were identified, which take part in cell wall alterations and cell wall monitoring.

4.2.1.4.1. Getting rid of pectin

The core TALE class TalAB, which is found in 94% of Asian *Xoo* strains, induces the pectate lyase *OsPLL4*. Pectate lyases degrade pectin, one of the main components of primary cell walls (Uluisek and Seymour, 2020). Therefore, pectate lyases are involved in various developmental processes that require modulation of the cell wall (Uluisek and Seymour, 2020). Knockdown of *OsPLL4* caused impaired pollen development and partial male sterility (Zheng *et al.*, 2018b). Pathogen-mediated overexpression of pectate lyases might lead to morphological changes at the infection site. Overexpression of pectate lyase *PtPL1-18* in poplar disrupted xylem formation and caused thinner secondary walls in vascular tissue (Bai *et al.*, 2017). Similar results might be found in TalAB-mediated

overexpression of *OsPLL4* in the xylem. Additionally, pectin-rich gels are deployed by the plant to prevent the spread of xylem-colonizing pathogens (Yadeta and Thomma, 2013). The induction of pectin degrading enzymes might help *Xoo* to conquer these defense mechanisms.

Most phytopathogens possess their own set of cell wall degrading enzymes that are used to break down cell wall components. *Xoo* has a variety of type II secreted cell wall degrading enzymes including cellulases, a xylanase, a polygalacturonase, an esterase and two pectate lyases (Tayi *et al.*, 2016a, 2016b). In this context, the manipulation of host pectate lyases might seem unnecessary, but it is commonly found in different pathogen systems. *P. syringae* was shown to rely on a polygalacturonase of *A. thaliana* for virulence (Wang *et al.*, 2017d). Similarly, *X. gardneri* depends on the activity of a pectate lyase in tomato for symptom formation and *Xoc* was reported to increase the expression of several cell wall loosening genes in rice (Schwartz *et al.*, 2017; Liao *et al.*, 2019). This indicates that the degradation of pectin is a common strategy in plant colonizing pathogens.

4.2.1.4.2. Confusing the guards

TalES1, at present unique for *Xoo* strain ICMP 3125^T, induces the cell wall-associated kinase (WAK) receptor-like protein *OsWAK51*. WAKs are pectin receptors that integrate into the cell membrane and have a cytosolic kinase domain (Kohorn and Kohorn, 2012). WAKs can bind both, pectin polymers and their fragments, and generate different regulatory responses dependent on pectin status (Kohorn and Kohorn, 2012; Kohorn, 2016). These diverse signals are presumably achieved by different co-receptors and ligands (Kohorn, 2016). WAKs are especially important for cell expansion and stress responses upon cell wall degradation (Kohorn, 2016). In rice, the WAK family is expanded to about 125 members and it was hypothesized that functional diversification had occurred (Zhang *et al.*, 2005; de Oliveira *et al.*, 2014). *OsWAKs* display very diverse responses to pathogens. The virulence of rice blast fungus was positively and negatively affected by different *OsWAKs* (Delteil *et al.*, 2016). Overexpression of *OsWAK25* increased resistance against biotrophic pathogens like *Xoo*, but decreased resistance against necrotrophic pathogens (Harkenrider *et al.*, 2016). Finally, *OsWAK18* was identified as the *Xoo* resistance gene *Xa4* in rice variety IRBB4 (Hu *et al.*, 2017). *OsWAK51* has not been studied in any detail and subsequently no known regulatory pathways of the *OsWAK51* regulon are available. If *OsWAK51* regulates defense against biotrophic pathogens negatively, this might be an attractive target for *Xoo*.

In conclusion, *Xoo* hijacks host cell wall degrading enzymes and manipulates cell wall degradation perception regulators with TALEs. Additionally, the type III effectors XopN, XopQ, XopX and XopZ of *Xoo* were shown to additively suppress immune responses triggered by cell wall degradation (Sinha *et al.*, 2013). This underlines the importance of cell wall degradation and evasion of detection by the host plant for successful infection.

4.2.1.5. Waste management

Alongside transcriptional control, posttranslational regulations are one of the main factors that can influence the metabolism and signaling inside the plant cell. The most drastic changes can be achieved by manipulating protein degradation. This is a common hub for pathogens to manipulate their hosts.

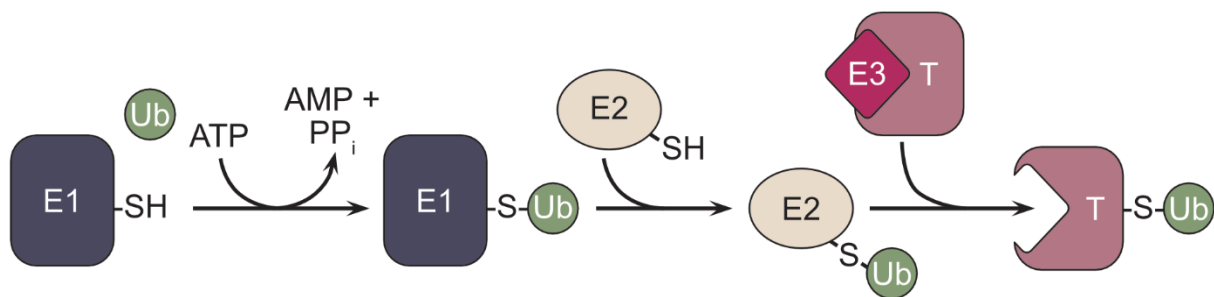


Figure 48. Schematic overview of the ubiquitination machinery.

The ubiquitination machinery activates Ubiquitin (Ub) using ATP. Next, the ubiquitin-activating enzyme (E1) transfers Ub to the ubiquitin-conjugating enzyme (E2). Last, the ubiquitin ligase (E3) recruits the target protein (T) and facilitates the transfer of Ub from E2 to T. This overview is based on Bhogaraju and Dikic (2016).

The core TALE class TalAD, which occurs in 97% of Asian *Xoo* strains and 70% of *Xoc* strains, induces the F-box protein *OsFBX109*. F-box proteins are part of the ubiquitination machinery (Jain *et al.*, 2007). Ubiquitin is activated by Ubiquitin-activating enzymes (E1) and transferred to Ubiquitin-conjugating enzymes (E2) (Figure 48). The ubiquitin ligase (E3) recruits loaded E2s, brings it into close proximity to the target protein and facilitates the actual ubiquitination of the target (Figure 48; Zhou and Zeng, 2016). F-box proteins are part of the E3 and are responsible for target protein binding (Zhou and Zeng, 2016). Ubiquitination can lead to a variety of fates for the protein, but the most common consequence of ubiquitination is protein degradation by the proteasome (Zhou and Zeng, 2016). There are 687 known F-box proteins in rice with a diverse set of target proteins (Jain *et al.*, 2007). However, the targets of *OsFBX109* are still unknown and the target binding domain of the protein does not contain a known protein motif (Jain *et al.*, 2007). *Xanthomonas* species are known to hijack the plant ubiquitination machinery to benefit infection. The type III effector XopI, also present in *Xoo*, mimics a plant F-box protein and was hypothesized to manipulate stomatal opening to facilitate colonization of pepper by

Xcv (Schulze *et al.*, 2012; Midha *et al.*, 2017). The type III effector XopL, which is present in most *Xanthomonas* species including *Xoo*, has E3 activity and can suppress PTI in *A. thaliana* during *Xcc* infection (Midha *et al.*, 2017; Erickson *et al.*, 2018; Yan *et al.*, 2019). XopK is a type III effector of *Xoo* with E3 activity and was shown to suppress PTI by targeting OsSERK2 for degradation (Qin *et al.*, 2018). Similarly, XopAE of *Xcv*, which also occurs in *Xoo*, can suppress PTI with its E3 activity in *A. thaliana* (Popov *et al.*, 2018). Additionally, the *Xoo* effector XopP inhibits the E3 activity of OsPUB44 to suppress PTI in rice (Ishikawa *et al.*, 2014).

In summary, *Xoo* has a plethora of type III effectors that utilize the rice ubiquitination machinery to suppress PTI and promote disease. The induction of a F-box protein by TalAD is therefore not an unknown strategy in the rice-*Xoo* interaction. In the future, interaction studies might elucidate the direct target of OsFBX109 to reveal the function of TalAD.

4.2.2. Convergent evolution – connections are unveiled

The identification of TALE target genes is an important step in deciphering the complicated crosstalk between rice and *Xoo* and this thesis has made significant advances in this field. Among the identified TALE targets, more and more examples of functional convergence emerge. The classification into five distinct functional hubs for TALEs, Xops and other virulence factors shows functional redundancies among effectors. Weßling *et al.* (2014) observed functional redundancy of effector proteins in different *A. thaliana*-infecting species and theorized this might buffer against a loss or rapid selection against specific effectors due to host recognition. Similarly, *Xoo* might have several Xops and TALEs to manipulate different nodes of the same network as backups.

Additional to functional convergence of effectors in single strains, convergent evolution between different pathovars and species can be observed. It was hypothesized before, that biotrophic pathogens might need to manipulate a shared set of physiological networks for successful infection (Mukhtar *et al.*, 2011; Pérez-Quintero *et al.*, 2013; Weßling *et al.*, 2014; Hutin *et al.*, 2015a). The convergence is probably achieved by addressing mainly unrelated primary targets, which converge on a common physiological process (Pérez-Quintero *et al.*, 2013). In this thesis, the new functional hubs around *DOX* genes and *OsLsi1* were uncovered. These genes are induced by *Xoo* and *Xoc*, which were previously thought to share very little common targets (Cernadas *et al.*, 2014). The TALE repertoire was initially thought to be responsible for tissue specificity between both pathovars, but new data suggests a common strategy (Cernadas *et al.*, 2014; Hutin *et al.*,

2015a). The more is known about virulence targets, the easier it is to find connections and overlapping strategies. At present, five genes or gene families are known to be addressed by more than one TALE class in rice.

This is in accordance with recent studies that unveiled a common host-pathogen interaction pattern in *A. thaliana*, which is supplemented with individual patterns for different infection strategies (Li *et al.*, 2017). Similarly, *Xoo* and *Xoc* probably share a common set of targets that are necessary to undermine plant immunity and a set of divergent effectors that are probably specialized for different tissues.

4.2.3. Temporal hierarchy of type III effectors

In this thesis, several TALE targets were verified that were not significantly induced in the RNA-seq data after 24 h. Especially *OsLsi1* and *OsNPF6.3* were significantly induced after 48 h in the qRT-PCR but showed less than 1.5-fold induction in the RNA-seq. This might indicate that TALE fulfill time-dependent roles in different stages of the infection. This phenomenon is well described in hemibiotrophic fungi *Colletotrichum* ssp., which express their effector repertoire in three distinct waves – biotrophic stage, transition stage, necrotrophic stage (Toruño *et al.*, 2016). *Salmonella enterica*, which infects humans, possess two type III secretion systems that are expressed at different stages of infection and allow the translocation of distinct effector repertoires (Galán, 2009). The expression of effector proteins in general is not well researched in *Xoo*. TALE gene clusters have no clear PIP boxes and no data is available suggesting they belong to the HrpX regulon, which coordinates Hrp and Xop gene expression (Furutani *et al.*, 2006). Different TALEs might be expressed at different times or in different tissues during infection.

An alternative reason for different induction times for certain TALEs might be a secretion hierarchy. Enteropathogenic *E. coli* have several type III secretion chaperones that bind effector proteins and determine an order of secretion (Runte *et al.*, 2018). The phytopathogenic *Erwinia amylovora* also has chaperones that determine the hierarchy of its four effector proteins (Castiblanco *et al.*, 2018). In *Xoo*, two chaperones involved in effector secretion are known: HpaB and HpaP (also known as HpaC). These chaperones are involved in the secretion hierarchy of different secreted protein groups. HpaP coordinates the switch from type III secretion system components to translocon proteins and effectors, while HpaB switches from translocon proteins to effector proteins only (Prochaska *et al.*, 2018). Both chaperones are required for the efficient secretion of non-TAL effectors in *Xoo*, but are not indispensable for secretion (Furutani *et al.*, 2009). This

could suggest that additional chaperones that have yet to be identified might also be involved in effector secretion.

Liao *et al.* (2019) recently published a method to observe the transcriptome of both, pathogen and host, at the same time using dual RNA-seq in the *Xoc*-rice interaction. A time resolved dual RNA-seq might unveil possible expression waves of effectors or delayed activity of some effectors due to other factors.

4.2.4. TALEs with no known target gene

At present, several TALE classes have no known target gene. There are multiple possible explanations for the lack of induced genes with TALE boxes for these classes in their promoters. On one hand, the TALE might be adapted to a different rice cultivar, which possesses divergent promoters. This would hinder the identification of potential target genes, as the appropriate rice cultivar needs to be used in the research. On the other hand, the TALE might induce transcription of a target, which has not been identified with the used experimental parameters. Our current definition of the applied promoterome is considering only a certain region around the transcriptional start sites of coding RNAs and would therefore exclude TALE boxes further away from the start codon, TALE boxes in front of non-coding RNAs or TALE boxes in front of not annotated genes (Grau *et al.*, 2013). Additionally, the RNA-Seq experiments are excluding small RNAs due to RNA isolation methods and enrichment treatments. Therefore, induced small RNAs cannot be identified in our current data sets.

In the future, the TALE box prediction of TALE classes with unknown target genes should be expanded to the whole genome and an additional RNA-Seq experiment focusing on small RNAs should be conducted.

4.3. A new approach to TALE research

Even before the code of TALEs was solved, it was already known that TALEs contribute very differently to *Xoo* virulence in the tested conditions (Bai *et al.*, 2000). Similar observations were also reported for *Xoc* (Cernadas *et al.*, 2014). Until today, the results remain the same: only one or two out of many strains are classified as major virulence factors. Cernadas *et al.* (2014) reported three possible reasons that might explain this phenomenon. First, some TALEs might be specialized for different rice varieties or are only needed to infect rice plants of specific growth stages that were not tested (Cernadas *et al.*, 2014). New advances like the daTALbase tool will enable researchers in the future to scan the promoters of many rice varieties to find potential target genes (Pérez-Quintero *et al.*, 2018). Second, many of the TALEs might solely exist as a repository to increase the

potential for recombination to adapt to new genotypes (Cernadas *et al.*, 2014). In recent years, the amount of sequenced strains has greatly increased and most TALEs are highly conserved in a spatiotemporal scale. It seems very unlikely, that these TALEs are mainly used as genetic backups, but recombination can seldom be observed. Third, TALEs might be redundant or have very subtle phenotypes, as was reported for most non-TALE type III effectors (Cernadas *et al.*, 2014). As more and more functional convergence between effectors is uncovered, this theory might very well be true. Additionally, TALEs might not show any virulence contribution, because they are needed in different stages of infection, which were not analyzed. Faced with these difficulties, how should the impact of TALEs on virulence be assessed in the future?

4.3.1. Growth phenotypes – an outdated system?

Classic assessments of virulence contributions of TALEs in *Xoo* involve the monitoring of symptom formation for a defined period of time in rice plants of a certain age. These rigid criteria select for a specific kind of virulence contribution in effectors. Only TALEs that are actively promoting symptom formation or bacterial migration along the xylem will have a noticeable effect on lesion length. Additionally, the TALE must fit the selected rice variety, the plant age, it must be active in the defined infection time and cannot be redundant (Cernadas *et al.*, 2014). This leaves a lot of room for missing important functions.

In this thesis, no definitive change in growth phenotypes could be observed in gain-of-function assays in Roth X1-8 for any TALEs. This strain alone does not elicit PTI or ETI and is able to partially infect the tested rice varieties. Therefore, all TALEs that are contributing to suppression of immunity might be redundant to the non-TALE effector repertoire of Roth X1-8 and might not show significant changes. The lack of nutrient transporter-inducing TALEs might be compensated by inducing high-affinity transporters in Roth X1-8 that render the benefit of these TALEs minimal. Similarly, type II secreted enzymes that degrade the cell wall might be redundant to TALEs that manipulate cell wall components.

Growth phenotype assays will always be useful to assess the resistance capabilities of rice and to track accomplishments in resistance breeding. However, they should not be exclusively used to characterize virulence contributions of individual effectors.

4.3.2. Tailored phenotype assays

Traditional virulence assays should be supplemented with experiments that are specialized for the individual effector. TALE research has the great advantage that the identified target gene already reveals a lot about potential molecular functions of the

TALEs in the infection. In this thesis, two different approaches were pursued to analyze the impact of individual TALEs on virulence.

4.3.2.1. Observing molecular functions

First, the consequences of inducing TALE targets for plant cell physiology can be observed. Therefore, rice protoplastation and transformation was optimized in this thesis. The transformation of protoplast with TALE expression constructs enables a quick assessment of resultant changes on the cellular level. Especially TALEs that induce cell membrane transporters can be studied *in vivo* to verify if TALEs influence nutrient flow. During this thesis, initial experiments concerning the sucrose flow in cells expressing TalBH2 were conducted. Surprisingly, protoplasts expressing TalBH2 did not contain visible amounts of the sucrose analog esculin. As TalBH2 induces *OsSWEET14*, a bidirectional sucrose transporter, it is possible that accumulated esculin will be exported with increased speed after the protoplasts are washed. To test this, protoplasts should be incubated with esculin overnight and esculin export should be measured by loss of esculin fluorescence in transformed protoplasts.

While sucrose transport can be monitored with the fluorescent analog esculin, similar substrates are not known for most transporters (Rottmann *et al.*, 2018). Luckily, radioactive labeling of protoplasts by uptake of labeled substrates has been established for a long time (Lewis and Patel, 1978). In future experiments, the uptake of several labeled substrates in the presence of TALEs can be analyzed with such a method. Additionally, fusion proteins of TALE targets and fluorescent proteins can be introduced into protoplasts to verify the subcellular localization of targets and to observe possible changes due to TALE-mediated overexpression.

Furthermore, specialized measurements for certain metabolites might elucidate TALE-mediated changes in the plant cell. In this thesis, experiments concerning the SA content in infected rice plants were conducted. The TALE-mediated induction of *DOX* genes might lead to reduced SA content in rice to benefit infection. The results show TalBL-dependent changes in SA content in spectrophotometric assays and inconclusive data for other tested TALE classes. In the future, these results should be analyzed further by using the established harvest times of this thesis to measure the most important phytohormones SA and ABA in response to different TALE classes using mass spectrometry. During this thesis, several qRT-PCRs were established to monitor the expression of defense-associated genes. The influence of TALEs on defense gene expression might indicate functions in suppression of immunity.

4.3.2.2. Altered target gene expression

Second, knockout mutants of TALE targets were created to observe their impact on *Xoo* virulence. These mutations will block the function of individual TALEs during infections with wild type strains. While gain-of-function assays based on complementation of *Xoo* Roth X1-8 with individual TALEs were inconclusive for most TALEs in this thesis, loss-of-function assay might yield better results. At present, the knockout lines KO1 and KO5 for *OsLsi1* and *OsPHO1;3*, respectively, are available for virulence assays. In the future, the remaining KO constructs need to be transferred into rice to create the required mutant lines.

On the contrary, inducible overexpression lines of TALEs will mimic the induced target gene expression during infection. The controlled overexpression of a single TALE inside the plant can isolate the effects of the TALE from background activity triggered by non-TALE effectors, inoculation wounds or pathogen detection. This might produce a clearer output on molecular functions and physiological roles of individual TALE targets. The overexpression was designed to be inducible to limit silencing effects and circumvent possible problems with plant development. At this time, nine TALEs can be analyzed in DEX-inducible rice lines. Even though the constructs were shown to be functional in *N. benthamiana*, DEX induction was compromised in rice. In the future, various methods of DEX delivery, including hydroponically, should be explored to solve this problem.

In summary, this thesis has expanded the toolbox to analyze the impact of TALEs on virulence and laid the foundation for future work to elucidate the roles of TALE targets during infection and normal physiological development.

4.4. Resistance breeding – hopes and limits

Preventing colonization by pathogens is one of the major challenges in plant breeding today. The advanced knowledge of TALE target genes and infection mechanisms of *Xoo* should ultimately lead to new approaches for breeding of resistant rice lines. Especially the control of *Xoo*, which is hard to reach with pesticides inside the xylem, has largely relied on resistance breeding (Yadeta and Thomma, 2013).

The classic resistance genes of the NB-LRR class like *Xo1* and *Xa1*, which identify TALEs by their structure, have long been overcome by truncated TALEs that are present in all *Xoo* strains to block detection (Ji *et al.*, 2016; Read *et al.*, 2016). Today, the resistance to *Xoo* is often atypical to other pathogens, as the fight against TALEs requires special types of resistance genes. The two most common specialized groups include executor R genes that trigger defense upon TALE-mediated induction and recessive resistance alleles due

to loss of inducibility by mutated promoters of susceptibility genes (Iyer-Pascuzzi and McCouch, 2007; Zhang *et al.*, 2015). A lot of these sources of resistance were found in natural varieties and subsequently used in resistance breeding for high-yielding crops (Quibod *et al.*, 2019). In the past, many deployed resistant rice varieties were conquered by new *Xoo* lineages (Carpenter *et al.*, 2018). How these resistances were broken and what can be learned for future application, will be discussed below.

4.4.1. Durable resistance and trade-off

The green revolution and the deployment of genotypically uniform rice varieties over large areas has been beneficial for pathogen spread. Once a strain has become virulent on a host variety, it has a strong selective advantage and will become the dominant lineage in all areas using the same resistance genes. Thus, the host population selects pathogen genotypes (Brown, 2015). Therefore, the selection of used resistance genes should be based on increased durability to circumvent repeated cycles of broken resistance.

4.4.1.1. Cost of virulence and executor R genes

Gene-for-gene resistance genes, like executor R genes, are specialized to detect a specific effector protein to induce ETI. They are by default not very durable, because the mutation or deletion of the detected virulence factor will result in the resistance gene being void (van Schie and Takken, 2014). This effect can be counteracted, if the addressed virulence factor is important for the infection and its loss will come at great cost (Brown, 2015). One prominent example is the rice executor R gene *Xa7*, which recognizes the *Xoo* TALE *AvrXa7* (TaIAC) that is a major virulence factor inducing a *SWEET* gene (Yang *et al.*, 2000, 2005; Zhang *et al.*, 2015). The cost of losing *AvrXa7* was high and *Xa7* was effective for at least a decade (Brown, 2015).

Effector proteins are often redundant and especially TALE effectors with their high sequence similarity are prone to rearrangements. In experimental setups, *AvrXa7* could lose its induction of *Xa7* but retain the ability to induce the susceptibility gene via rearrangements with a different TALE (Yang *et al.*, 2005). In nature, the *Xa7* resistance can be overcome by *Xoo* strains carrying different *SWEET* inducing TALEs that do not trigger *Xa7*-mediated resistance (Streubel *et al.*, 2013; van Schie and Takken, 2014).

4.4.1.2. Partial resistance and the cost of durability

The most durable resistance genes deployed to date were not gene-for-gene resistance genes but instead display nonspecific effects against all pathogen genotypes and are most likely not involved in pathogen detection (Brown, 2015). Instead, they are most often involved in adjusting defense responses downstream (van Schie and Takken, 2014;

Brown, 2015). These alterations can come at a cost. The constitutive alteration of defense gene expression might influence plant growth and development (Van Hulten *et al.*, 2006; Vos *et al.*, 2013). Additionally, strong defenses against biotrophic pathogens can make plants more vulnerable to necrotrophic pathogens and vice versa (Vos *et al.*, 2013). Changing the delicate balance of resistance against biotrophic and necrotrophic pathogens might lead to increased susceptibility for other pathogens. Resistance at the cost of yield will not be an attractive option for farmers and will therefore not be used in the field.

Instead, crops should maintain yield at the cost of low levels of disease. It was shown that resistance genes that are not completely effective are more durable, because they decrease selection pressure on the pathogens (Brown, 2015). The *Xa4* resistance gene is a good example of durable, nonspecific partial resistance (Quibod *et al.*, 2019). *Xa4* is encoded by *OsWAK18* and promotes cellulase synthesis to reinforce cell walls (Hu *et al.*, 2017). The thicker cell wall compromises *Xoo* infection in a nonspecific manner and cannot be overcome easily (Brown, 2015; Hu *et al.*, 2017; Quibod *et al.*, 2019). In this rare example, *Xa4* additionally improves other agronomic traits by stabilizing the plant and preventing lodging (Hu *et al.*, 2017).

4.4.1.3. Novel ideas and technologies

The discovery of potentially durable resistance genes in rice varieties is rare and suitable guidelines in creating new resistance genes are needed. An emerging idea is the stacking of multiple available resistance genes, which would create a more durable resistance because the pathogen has to overcome several resistance genes at the same time (Brown, 2015). This will be more effective, if the resistance genes cause a synergistic cost for virulence i.e. the adaptation to one resistance genes prevents the adaptation to the second gene without losing virulence completely (Brown, 2015).

The durability of resistance can be increased further by growing mixtures of rice lines to provide more genetic diversity and therefore less selective advantage for overcoming a specific resistance gene (Mundt, 2002). The used resistance genes should have had little to no exposure to the pathogen in the past, because it is probable that part of the pathogen population would already possess virulence factors that can conquer resistance genes exposed to them before.

With the help of new genome editing tools that create double strand breaks, a variety of new resistance alleles can be created. The nature of NHEJ results in a diverse set of

mutations that are potentially unknown to the pathogen population and simultaneously provide a level of diversity that is harder to adapt to (Gorbunova and Levy, 1997).

4.4.2. Sustainability and loss of susceptibility

The recessive resistance due to loss of susceptibility is an interesting target for resistance breeding, as loss-of-function mutations are generated easily with modern genome editing tools. Loss of susceptibility can lead to increased resistance or even non-host resistance and is harder to overcome, because often a gain-of-function is needed to counter the lost susceptibility gene (Humphry *et al.*, 2006; van Schie and Takken, 2014). Especially biotrophic pathogens like *Xoo* are reliant on host factors to provide nutrients. The knockout of susceptibility genes might lead to significant health costs for the plant, because these genes fulfill important tasks in normal plant physiology. Similarly, mutations in *OsSWEET14* lead to resistance against *Xoo*, but also resulted in yield loss and reduced plant fitness (Antony *et al.*, 2010). The mutation of TALE boxes in susceptibility gene promoters is an exception, because this might have less health costs as normal gene function should be undisturbed. Many resistance genes against *Xoo* belong to this category. The *xa13* resistance has mutations in the *OsSWEET11* promoter, *xa41* affects TALE boxes in the *OsSWEET14* promoter and *xa25* is caused by changes in the *OsSWEET13* promoter (Yang *et al.*, 2006; Hutin *et al.*, 2015b; Zhou *et al.*, 2015). This emphasizes that the best strategy for creating new *Xoo*-resistant alleles without health costs is to mutate TALE boxes.

4.4.2.1. Creating less susceptible rice lines based on identified TALE boxes

Creating *Xanthomonas*-resistant plants by mutating TALE boxes has been pursued for a few years. First, the *OsSWEET14* promoter was edited using TALEN to disrupt TALE boxes (Li *et al.*, 2012; Blanvillain-Baufumé *et al.*, 2017). Second, *CsLOB1* promoters were edited in grapefruit using Cas9 to suppress *Xac* infection (Jia *et al.*, 2016). Finally, rice mutant lines with edited TALE boxes in *OsSWEET14* and *OsSWEET11* promoters plus a natural *xa25* mutation in the *OsSWEET13* promoter were combined (Oliva *et al.*, 2019; Xu *et al.*, 2019). These rice plants displayed a broad-spectrum resistance to *Xoo* and were created using Cas9 multiplexing, but could still be infected with strains breaking the *xa25* resistance using the TALE class TaIBK.

Rice lines with multiple mutated TALE boxes might show altered susceptibility more drastically, if the TALEs act in an additive manner. In case of redundancy, several mutated TALE boxes would be the best method to unveil the impact on virulence for these TALEs. Therefore, rice lines with mutations in multiple TALE boxes were created in

this thesis. In contrast to other approaches published before, the TT03 lines only targeted TALE boxes of TALE classes with no known virulence function. Nevertheless, initial results suggest, that progeny of TO TT03 #09 is less susceptible to *Xoo* strains PX0142 and PX099. This in turn leads to the hypothesis, that at least one TALE target identified in this thesis has an effect on virulence. In the future, experiments should elucidate whether the observed phenotypic changes are due to additive effects of the affected TALE classes or if the simultaneous targeting of redundant TALE classes is responsible. This can be tested by introducing artificial TALEs, which bind to the mutated TALE boxes, into PX0142 and PX099. After the contributions of the affected TALE classes are unveiled, the durability of these mutations should be assessed. Multiple mutated TALE boxes of TO TT03 #09 contain very few changes that might be easily overcome in the future.

4.4.2.2. TALE evolution and the arms race of breeding

Since the deployment of resistant rice lines in the 1980's, the infections with *Xoo* were widely reduced, until the first strains breaking the resistance were emerging in the early 2000's (Zheng *et al.*, 2019). Sugio *et al.* (2007) describe that rice lines containing *xa5*, which reduces TALE activity in general, can be partially overcome by *Xoo* with TalBM (Sugio *et al.*, 2007). New reports suggest however, that TalBX can also facilitate infection of *xa5* plants because of the strong induction of *OsSWEET11*, which is not reduced efficiently by *xa5* (Carpenter *et al.*, 2018). Recently, several reports described *Xoo* strains breaking the *xa13*, *xa41* or *xa25* resistances (Carpenter *et al.*, 2018; Doucouré *et al.*, 2018; Oliva *et al.*, 2019; Xu *et al.*, 2019). While *xa41* can be overcome by TALEs binding a different promoter region of *OsSWEET14* and *xa13* is broken by other *SWEET*-inducing TALEs, *xa25* is overcome by TALEs that have adapted to the 1 bp deletion in the TALE box (Carpenter *et al.*, 2018; Doucouré *et al.*, 2018; Oliva *et al.*, 2019; Xu *et al.*, 2019). Oliva *et al.* (2019) hypothesized that adaptation to a new binding site is getting harder the more nucleotides in the target sequence are new.

The research on TALE evolution similarly suggests that some mutations are easier to adapt to than others, based on specific evolving mechanisms. TALEs can change the coding of RVDs by base substitution, recombine with other TALEs to form new TALEs or delete individual repeats from the repeat array (Erkes *et al.*, 2017). Additionally, repeats might be duplicated inside the repeat array (Schandry *et al.*, 2016). Most of these mechanisms enable the adaptation to small changes in the TALE box, which leads to the assumption, that larger deletions or insertions might be the most durable choice. These changes can probably be overcome by rearrangements and recombination between

TALEs. These changes are less predictable and the immense potential of TALE recombination to overcome resistance genes was shown in the past. Spontaneous recombination between TALEs created the new virulence factors PthXo5, which could still induce a *SWEET* gene, but was no longer recognized by *Xa7* (Yang *et al.*, 2005). It should be noted that *Xa7*-adaptations were based on the loss of *Xa7* induction, which is likely easier to achieve than the adaptation to a new sequence. As the examples of *xa13* and *xa41* demonstrate, the availability of closely related family members of the susceptibility genes should be considered as well (van Schie and Takken, 2014; Carpenter *et al.*, 2018; Doucouré *et al.*, 2018).

While durability is hard to predict, bigger changes to the TALE box seem advisable. If the mutation of many TALE boxes as in the TT03 plants will be a durable in nature, will be one of the next big questions in resistance breeding.

References

- Abe, M., Yoshikawa, T., Nosaka, M., Sakakibara, H., and Sato, Y. (2010). *WAVY LEAF1*, an ortholog of Arabidopsis *HEN1*, regulates shoot development by maintaining microRNA and trans-acting small interfering RNA accumulation in rice. *Plant Physiol.* 154, 1335–1346.
- Achkar, N. P., Cambiagno, D. A., and Manavella, P. A. (2016). miRNA biogenesis: A dynamic pathway. *Trends Plant Sci.* 21, 1034–1044.
- Ali, W., Isayenkov, S. V., Zhao, F. J., and Maathuis, F. J. M. (2009). Arsenite transport in plants. *Cell. Mol. Life Sci.* 66, 2329–2339.
- Ali, Z., Abulfaraj, A., Idris, A., Ali, S., Tashkandi, M., and Mahfouz, M. M. (2015). CRISPR/Cas9-mediated viral interference in plants. *Genome Biol.* 16, 238.
- Anders, C., Niewoehner, O., Duerst, A., and Jinek, M. (2014). Structural basis of PAM-dependent target DNA recognition by the Cas9 endonuclease. *Nature* 513, 569–573.
- Antony, G., Zhou, J., Huang, S., Li, T., Liu, B., White, F., et al. (2010). Rice *xa13* recessive resistance to bacterial blight is defeated by induction of the disease susceptibility gene *Os-11N3*. *Plant Cell* 22, 3864–3876.
- Bacete, L., Mélida, H., Miedes, E., and Molina, A. (2018). Plant cell wall-mediated immunity: cell wall changes trigger disease resistance responses. *Plant J.* 93, 614–636.
- Bai, J., Choi, S.-H., Ponciano, G., Leung, H., and Leach, J. E. (2000). *Xanthomonas oryzae* pv. *oryzae* avirulence genes contribute differently and specifically to pathogen aggressiveness. *Mol. Plant-Microbe Interact.* 13, 1322–1329.
- Bai, Y., Wu, D., Liu, F., Li, Y., Chen, P., Lu, M., et al. (2017). Characterization and functional analysis of the poplar pectate lyase-like gene *PtPL1-18* reveal its role in the development of vascular tissues. *Front. Plant Sci.* 8, 1–17.
- Bakhat, H. F., Bibi, N., Zia, Z., Abbas, S., Hammad, H. M., Fahad, S., et al. (2018). Silicon mitigates biotic stresses in crop plants: A review. *Crop Prot.* 104, 21–34.
- Balint-Kurti, P. (2019). The plant hypersensitive response: concepts, control and consequences. *Mol. Plant Pathol.* 20, 1163–1178.
- Baranauskė, S., Mickutė, M., Plotnikova, A., Finke, A., Venclovas, Č., Klimašauskas, S., et al. (2015). Functional mapping of the plant small RNA methyltransferase: HEN1 physically interacts with HYL1 and DICER-LIKE 1 proteins. *Nucleic Acids Res.* 43, 2802–2812.
- Berman, H. M., Westbrook, J., Feng, Z., Gilliland, G., Bhat, T. N., Weissig, H., et al. (2000). The Protein Data Bank. *Nucleic Acids Res.* 28, 235–242.
- Bhaya, D., Davison, M., and Barrangou, R. (2011). CRISPR-Cas systems in bacteria and archaea: Versatile small RNAs for adaptive defense and regulation. *Annu. Rev. Genet.* 45, 273–297.

- Bhogaraju, S., and Dikic, I. (2016). Cell biology: Ubiquitination without E1 and E2 enzymes. *Nature* 533, 43–44.
- Bitinaite, J., Wah, D. A., Aggarwal, A. K., and Schildkraut, I. (1998). FokI dimerization is required for DNA cleavage. *Proc. Natl. Acad. Sci. U. S. A.* 95, 10570–10575.
- Blanvillain-Baufumé, S., Reschke, M., Solé, M., Auguy, F., Doucoure, H., Szurek, B., et al. (2017). Targeted promoter editing for rice resistance to *Xanthomonas oryzae* pv. *oryzae* reveals differential activities for SWEET14-inducing TAL effectors. *Plant Biotechnol. J.* 15, 306–317.
- Boch, J., and Bonas, U. (2010). *Xanthomonas* AvrBs3 family-type III effectors: discovery and function. *Annu. Rev. Phytopathol.* 48, 419–436.
- Boch, J., Scholze, H., Schornack, S., Landgraf, A., Hahn, S., Kay, S., et al. (2009). Breaking the code of DNA binding specificity of TAL-type III effectors. *Science* 326, 1509–12.
- Booher, N. J., Carpenter, S. C. D., Sebra, R. P., Wang, L., Salzberg, S. L., Leach, J. E., et al. (2015). Single molecule real-time sequencing of *Xanthomonas oryzae* genomes reveals a dynamic structure and complex TAL (transcription activator-like) effector gene relationships. *Microb. Genomics* 1, e000032.
- Borghini, L. (2010). “Inducible gene expression systems for plants,” in *Plant Developmental Biology: Methods and Protocols*, eds. L. Hennig and C. Köhler (Totowa, NJ: Humana Press), 65–75.
- Bouguyon, E., Brun, F., Meynard, D., Kubeš, M., Pervent, M., Leran, S., et al. (2015). Multiple mechanisms of nitrate sensing by Arabidopsis nitrate transceptor NRT1.1. *Nat. Plants* 1, 15015.
- Brinkman, E. K., Chen, T., de Haas, M., Holland, H. A., Akhtar, W., and van Steensel, B. (2018). Kinetics and fidelity of the repair of Cas9-induced double-strand DNA breaks. *Mol. Cell* 70, 801-813.e6.
- Brouns, S. J. J., Jore, M. M., Lundgren, M., Westra, E. R., Slijkhuis, R. J. H., Snijders, A. P. L., et al. (2008). Small CRISPR RNAs Guide Antiviral Defense in Prokaryotes. *Science* 321, 960 LP – 964.
- Brown, J. K. M. (2015). Durable resistance of crops to disease: A Darwinian perspective. *Annu. Rev. Phytopathol.* 53, 513–539.
- Büttner, D. (2016). Behind the lines-actions of bacterial type III effector proteins in plant cells. *FEMS Microbiol. Rev.* 40, 894–937.
- Büttner, D., Nennstiel, D., Klüsener, B., and Bonas, U. (2002). Functional analysis of HrpF, a putative type III translocon protein from *Xanthomonas campestris* pv. *vesicatoria*. *J. Bacteriol.* 184, 2389 LP – 2398.
- Cao, J., Chu, C., Zhang, M., He, L., Qin, L., Li, X., et al. (2020). Different cell wall-degradation ability leads to tissue-specificity between *Xanthomonas oryzae* pv. *oryzae* and *Xanthomonas oryzae* pv. *oryzicola*. *Pathogens* 9, 187.

- Cao, M. J., Wang, Z., Wirtz, M., Hell, R., Oliver, D. J., and Xiang, C. B. (2013). SULTR3;1 is a chloroplast-localized sulfate transporter in *Arabidopsis thaliana*. *Plant J.* 73, 607–616.
- Carpenter, S. C. D., Mishra, P., Ghoshal, C., Dash, P. K., Wang, L., Midha, S., et al. (2018). A strain of an emerging Indian *Xanthomonas oryzae* pv. *oryzae* pathotype defeats the rice bacterial blight resistance gene *xa13* without inducing a clade III SWEET gene and is nearly identical to a recent Thai isolate. *Front. Microbiol.* 9, 2703.
- Castiblanco, L. F., Triplett, L. R., and Sundin, G. W. (2018). Regulation of effector delivery by type III secretion chaperone proteins in *Erwinia amylovora*. *Front. Microbiol.* 9, 1–10.
- Ceccaldi, R., Rondinelli, B., and D'Andrea, A. D. (2016). Repair pathway choices and consequences at the double-strand break. *Trends Cell Biol.* 26, 52–64.
- Cermak, T., Doyle, E. L., Christian, M., Wang, L., Zhang, Y., Schmidt, C., et al. (2011). Efficient design and assembly of custom TALEN and other TAL effector-based constructs for DNA targeting. *Nucleic Acids Res.* 39, 1–11.
- Cernadas, R. A., Doyle, E. L., Niño-Liu, D. O., Wilkins, K. E., Bancroft, T., Wang, L., et al. (2014). Code-assisted discovery of TAL effector targets in bacterial leaf streak of rice reveals contrast with bacterial blight and a novel susceptibility gene. *PLoS Pathog.* 10, e1003972.
- Chaabouni, S., Pirrello, J., Liu, M., El-Sharkawy, I., Roustan, J. P., and Bouzayen, M. (2016). Identification and functional characterization of two HOOKLESS genes in tomato (*Solanum lycopersicum*). *J. Plant Physiol.* 200, 76–81.
- Chandran, D. (2015). Co-option of developmentally regulated plant SWEET transporters for pathogen nutrition and abiotic stress tolerance. *IUBMB Life* 67, 461–471.
- Chatnaparat, T., Prathuangwong, S., and Lindow, S. E. (2016). Global pattern of gene expression of *Xanthomonas axonopodis* pv. *glycines* within soybean leaves. *Mol. Plant-Microbe Interact.* 29, 508–522.
- Chen, L.-Q., Hou, B.-H., Lalonde, S., Takanaga, H., Hartung, M. L., Qu, X.-Q., et al. (2010). Sugar transporters for intercellular exchange and nutrition of pathogens. *Nature* 468, 527–532.
- Chen, L.-Q., Qu, X.-Q., Hou, B.-H., Sosso, D., Osorio, S., Fernie, A. R., et al. (2012). Sucrose efflux mediated by SWEET proteins as a key step for phloem transport. *Science* 335, 207–11.
- Chien, C.-C., Chou, M.-Y., Chen, C.-Y., and Shih, M.-C. (2019). Analysis of genetic diversity of *Xanthomonas oryzae* pv. *oryzae* populations in Taiwan. *Sci. Rep.* 9, 316.
- Christian, M., Cermak, T., Doyle, E. L., Schmidt, C., Zhang, F., Hummel, A., et al. (2010). Targeting DNA double-strand breaks with TAL effector nucleases. *Genetics* 186, 756–761.

- Cohn, M., Bart, R. S., Shybut, M., Dahlbeck, D., Gomez, M., Morbitzer, R., *et al.* (2014). *Xanthomonas axonopodis* virulence is promoted by a transcription activator-like effector-mediated induction of a SWEET sugar transporter in cassava. *Mol. Plant-Microbe Interact.* 27, 1186–1198.
- Cox, K. L., Meng, F., Wilkins, K. E., Li, F., Wang, P., Booher, N. J., *et al.* (2017). TAL effector driven induction of a SWEET gene confers susceptibility to bacterial blight of cotton. *Nat. Commun.* 8, 15588.
- Cuculis, L., Abil, Z., Zhao, H., and Schroeder, C. M. (2015). Direct observation of TALE protein dynamics reveals a two-state search mechanism. *Nat. Commun.* 6, 7277.
- Dalsing, B. L., Truchon, A. N., Gonzalez-Orta, E. T., Milling, A. S., and Allen, C. (2015). *Ralstonia solanacearum* uses inorganic nitrogen metabolism for virulence, ATP production, and detoxification in the oxygen-limited host xylem environment. *MBio* 6, e02471.
- Dangl, J. L., and Jones, J. D. G. (2001). Plant pathogens and integrated defence responses to infection. *Nature* 411, 826–833.
- De Micco, V., Balzano, A., Wheeler, E. A., and Baas, P. (2016). Tyloses and gums: A review of structure, function and occurrence of vessel occlusions. *IAWA J.* 37, 186–205.
- de Oliveira, L. F. V., Christoff, A. P., de Lima, J. C., de Ross, B. C. F., Sachetto-Martins, G., Margis-Pinheiro, M., *et al.* (2014). The wall-associated kinase gene family in rice genomes. *Plant Sci.* 229, 181–192.
- Delteil, A., Gobbato, E., Cayrol, B., Estevan, J., Michel-Romiti, C., Dievart, A., *et al.* (2016). Several wall-associated kinases participate positively and negatively in basal defense against rice blast fungus. *BMC Plant Biol.* 16, 17.
- Dempsey, D. A., and Klessig, D. F. (2017). How does the multifaceted plant hormone salicylic acid combat disease in plants and are similar mechanisms utilized in humans? *BMC Biol.* 15, 1–11.
- Deng, D., Yan, C., Pan, X., Mahfouz, M., Wang, J., Zhu, J.-K., *et al.* (2012). Structural basis for sequence-specific recognition of DNA by TAL effectors. *Science* 335, 720.
- Ding, X., Cao, Y., Huang, L., Zhao, J., Xu, C., Li, X., *et al.* (2008). Activation of the indole-3-acetic acid-amido synthetase GH3-8 suppresses expansin expression and promotes salicylate- and jasmonate-independent basal immunity in rice. *Plant Cell* 20, 228–240.
- Doench, J. G., Fusi, N., Sullender, M., Hegde, M., Vaimberg, E. W., Donovan, K. F., *et al.* (2016). Optimized sgRNA design to maximize activity and minimize off-target effects of CRISPR-Cas9. *Nat. Biotechnol.* 34, 184–191.
- Doench, J. G., Hartenian, E., Graham, D. B., Tothova, Z., Hegde, M., Smith, I., *et al.* (2014). Rational design of highly active sgRNAs for CRISPR-Cas9-mediated gene inactivation. *Nat. Biotechnol.* 32, 1262–1267.

- Doucouré, H., Pérez-Quintero, A. L., Reshetnyak, G., Tekete, C., Auguy, F., Thomas, E., et al. (2018). Functional and genome sequence-driven characterization of *tal* effector gene repertoires reveals novel variants with altered specificities in closely related malian *Xanthomonas oryzae* pv. *oryzae* strains. *Front. Microbiol.* 9, 1657.
- Doyle, E. L., Booher, N. J., Standage, D. S., Voytas, D. F., Brendel, V. P., VanDyk, J. K., et al. (2012). TAL effector-nucleotide targeter (TALE-NT) 2.0: tools for TAL effector design and target prediction. *Nucleic Acids Res.* 40, W117–W122.
- Du, Q., and Kende, H. (2001). Expression of two *HOOKLESS* genes in peas (*Pisum sativum* L.). *Plant Cell Physiol.* 42, 374–378.
- Engler, C., Kandzia, R., and Marillonnet, S. (2008). A one pot, one step, precision cloning method with high throughput capability. *PLoS One* 3, e3647.
- Engler, C., Youles, M., Gruetzner, R., Ehnert, T.-M., Werner, S., Jones, J. D. G., et al. (2014). A Golden Gate modular cloning toolbox for plants. *ACS Synth. Biol.* 3, 839–843.
- Erickson, J. L., Adlung, N., Lampe, C., Bonas, U., and Schattat, M. H. (2018). The *Xanthomonas* effector XopL uncovers the role of microtubules in stromule extension and dynamics in *Nicotiana benthamiana*. *Plant J.* 93, 856–870.
- Erkes, A., Mücke, S., Reschke, M., Boch, J., and Grau, J. (2019). PrediTAL: A novel model learned from quantitative data allows for new perspectives on TALE targeting. *PLOS Comput. Biol.* 15, e1007206.
- Erkes, A., Reschke, M., Boch, J., and Grau, J. (2017). Evolution of transcription activator-like effectors in *Xanthomonas oryzae*. *Genome Biol. Evol.* 9, 1599–1615.
- Falcone Ferreyra, M. L., Emiliani, J., Rodriguez, E. J., Campos-Bermudez, V. A., Grotewold, E., and Casati, P. (2015). The identification of maize and *Arabidopsis* type I flavone synthases links flavones with hormones and biotic interactions. *Plant Physiol.* 169, 1090–107.
- Fu, Y., Foden, J. a, Khayter, C., Maeder, M. L., Reyon, D., Joung, J. K., et al. (2013). High-frequency off-target mutagenesis induced by CRISPR-Cas nucleases in human cells. *Nat. Biotechnol.* 31, 822–6.
- Furutani, A., Nakayama, T., Ochiai, H., Kaku, H., Kubo, Y., and Tsuge, S. (2006). Identification of novel HrpXo regulons preceded by two cis-acting elements, a plant-inducible promoter box and a –10 box-like sequence, from the genome database of *Xanthomonas oryzae* pv. *oryzae*. *FEMS Microbiol. Lett.* 259, 133–141.
- Furutani, A., Takaoka, M., Sanada, H., Noguchi, Y., Oku, T., Tsuno, K., et al. (2009). Identification of novel type III secretion effectors in *Xanthomonas oryzae* pv. *oryzae*. *Mol. Plant-Microbe Interact.* 22, 96–106.
- Galán, J. E. (2009). Common Themes in the Design and Function of Bacterial Effectors. *Cell Host Microbe* 5, 571–579.

- Gantner, J., Ordon, J., Ilse, T., Kretschmer, C., Gruetzner, R., Löffke, C., et al. (2018). Peripheral infrastructure vectors and an extended set of plant parts for the Modular Cloning system. *PLoS One* 13, e0197185.
- Gao, H., Wu, X., Chai, J., and Han, Z. (2012). Crystal structure of a TALE protein reveals an extended N-terminal DNA binding region. *Cell Res.* 22, 1716–1720.
- Geissler, R., Hauber, I., Funk, N., Richter, A., Behrens, M., Renner, I., et al. (2015). Patient-adapted, specific activation of HIV-1 by customized TAL effectors (TALEs), a proof of principle study. *Virology* 486, 248–254.
- Geißler, R., Scholze, H., Hahn, S., Streubel, J., Bonas, U., Behrens, S.-E., et al. (2011). Transcriptional activators of human genes with programmable DNA-specificity. *PLoS One* 6, e19509.
- Gorbunova, V., and Levy, A. A. (1997). Non-homologous DNA end joining in plant cells is associated with deletions and filler DNA insertions. *Nucleic Acids Res.* 25, 4650–4657.
- Görisch, S. M., Wachsmuth, M., Tóth, K. F., Lichter, P., and Rippe, K. (2005). Histone acetylation increases chromatin accessibility. *J. Cell Sci.* 118, 5825–34.
- Grau, J., Reschke, M., Erkes, A., Streubel, J., Morgan, R. D., Wilson, G. G., et al. (2016). AnnoTALE: bioinformatics tools for identification, annotation and nomenclature of TALEs from *Xanthomonas* genomic sequences. *Sci. Rep.* 6, 21077.
- Grau, J., Wolf, A., Reschke, M., Bonas, U., Posch, S., and Boch, J. (2013). Computational predictions provide insights into the biology of TAL effector target sites. *PLoS Comput. Biol.* 9, e1002962.
- Gu, K., Yang, B., Tian, D., Wu, L., Wang, D., Sreekala, C., et al. (2005). *R* gene expression induced by a type-III effector triggers disease resistance in rice. *Nature* 435, 1122–1125.
- Guan, P., Ripoll, J. J., Wang, R., Vuong, L., Bailey-Steinitz, L. J., Ye, D., et al. (2017). Interacting TCP and NLP transcription factors control plant responses to nitrate availability. *Proc. Natl. Acad. Sci. U. S. A.* 114, 2419–2424.
- Guo, F.-Q., Young, J., and Crawford, N. M. (2003). The nitrate transporter AtNRT1.1 (CHL1) functions in stomatal opening and contributes to drought susceptibility in *Arabidopsis*. *Plant Cell* 15, 107–17.
- Guo, F., Wang, R., and Crawford, N. M. (2002). The *Arabidopsis* dual-affinity nitrate transporter gene AtNRT1.1 (CHL1) is regulated by auxin in both shoots and roots. *J. Exp. Bot.* 53, 835–844.
- Hajri, A., Brin, C., Zhao, S., David, P., Feng, J.-X., Koebnik, R., et al. (2012). Multilocus sequence analysis and type III effector repertoire mining provide new insights into the evolutionary history and virulence of *Xanthomonas oryzae*. *Mol. Plant Pathol.* 13, 288–302.
- Ham, B.-K., Chen, J., Yan, Y., and Lucas, W. J. (2018). Insights into plant phosphate sensing and signaling. *Curr. Opin. Biotechnol.* 49, 1–9.

- Harkenrider, M., Sharma, R., Vleeschauwer, D. De, and Tsao, L. (2016). Overexpression of rice wall-associated kinase 25 (OsWAK25) alters resistance to bacterial and fungal pathogens. *25*, 1–16.
- Herbers, K., Conrads-Strauch, J., and Bonas, U. (1992). Race-specificity of plant resistance to bacterial spot disease determined by repetitive motifs in a bacterial avirulence protein. *Nature* 356, 172–174.
- Higo, K., Ugawa, Y., Iwamoto, M., and Korenaga, T. (1999). Plant cis-acting regulatory DNA elements (PLACE) database: 1999. *Nucleic Acids Res.* 27, 297–300.
- Ho, Y. P., Tan, C. M., Li, M. Y., Lin, H., Deng, W. L., and Yang, J. Y. (2013). The AvrB-AvrC domain of AvrXccC of *Xanthomonas campestris* pv. *campestris* is required to elicit plant defense responses and manipulate ABA homeostasis. *Mol. Plant-Microbe Interact.* 26, 419–430.
- Holmes, G. (2010). Black rot of crucifers (*Xanthomonas campestris* pv. *campestris*). *Calif. Polytech. State Univ. San Luis Obispo, Bugwood.com*. Available at: <https://www.forestryimages.org/browse/detail.cfm?&imgnum=1574933> [Accessed November 20, 2019].
- Hood, E. E., Gelvin, S. B., Melchers, L. S., and Hoekema, A. (1993). New *Agrobacterium* helper plasmids for gene transfer to plants. *Transgenic Res.* 2, 208–218.
- Hu, B., Wang, W., Ou, S., Tang, J., Li, H., Che, R., et al. (2015). Variation in NRT1.1B contributes to nitrate-use divergence between rice subspecies. *Nat. Genet.* 47, 834–838.
- Hu, K., Cao, J., Zhang, J., Xia, F., Ke, Y., Zhang, H., et al. (2017). Improvement of multiple agronomic traits by a disease resistance gene via cell wall reinforcement. *Nat. Plants* 3, 17009.
- Hu, Y., Zhang, J., Jia, H., Sosso, D., Li, T., Frommer, W. B., et al. (2014). *Lateral organ boundaries 1* is a disease susceptibility gene for citrus bacterial canker disease. *Proc. Natl. Acad. Sci. U. S. A.* 111, E521-9.
- Huang, R., Hui, S., Zhang, M., Li, P., Xiao, J., Li, X., et al. (2017). A conserved basal transcription factor is required for the function of diverse TAL effectors in multiple plant hosts. *Front. Plant Sci.* 8, 1919.
- Huang, S., Antony, G., Li, T., Liu, B., Obasa, K., Yang, B., et al. (2016). The broadly effective recessive resistance gene *xa5* of rice is a virulence effector-dependent quantitative trait for bacterial blight. *Plant J.* 86, 186–194.
- Hui, S., Hao, M., Liu, H., Xiao, J., Li, X., Yuan, M., et al. (2019a). The group I GH3 family genes encoding JA-Ile synthetase act as positive regulator in the resistance of rice to *Xanthomonas oryzae* pv. *oryzae*. *Biochem. Biophys. Res. Commun.* 508, 1062–1066.
- Hui, S., Liu, H., Zhang, M., Chen, D., Li, Q., Tian, J., et al. (2019b). The host basal transcription factor IIA subunits coordinate for facilitating infection of TALEs-carrying bacterial pathogens in rice. *Plant Sci.* 284, 48–56.

- Hummel, A. W., Doyle, E. L., and Bogdanove, A. J. (2012). Addition of transcription activator-like effector binding sites to a pathogen strain-specific rice bacterial blight resistance gene makes it effective against additional strains and against bacterial leaf streak. *New Phytol.* 195, 883–893.
- Humphry, M., Consonni, C., and Panstruga, R. (2006). *mlo*-based powdery mildew immunity: silver bullet or simply non-host resistance? *Mol. Plant Pathol.* 7, 605–10.
- Hutin, M., Césari, S., Chalvon, V., Michel, C., Tran, T. T., Boch, J., et al. (2016). Ectopic activation of the rice NLR heteropair RGA4/RGA5 confers resistance to bacterial blight and bacterial leaf streak diseases. *Plant J.* 88, 43–55.
- Hutin, M., Pérez-Quintero, A. L., Lopez, C., and Szurek, B. (2015a). MorTAL Kombat: The story of defense against TAL effectors through loss-of-susceptibility. *Front. Plant Sci.* 6, 535.
- Hutin, M., Sabot, F., Ghesquière, A., Koebnik, R., and Szurek, B. (2015b). A knowledge-based molecular screen uncovers a broad-spectrum OsSWEET14 resistance allele to bacterial blight from wild rice. *Plant J.* 84, 694–703.
- Ishikawa, K., Yamaguchi, K., Sakamoto, K., Yoshimura, S., Inoue, K., Tsuge, S., et al. (2014). Bacterial effector modulation of host E3 ligase activity suppresses PAMP-triggered immunity in rice. *Nat. Commun.* 5, 5430.
- Iyer-Pascuzzi, A. S., and McCouch, S. R. (2007). Recessive resistance genes and the *Oryza sativa* - *Xanthomonas oryzae* pv. *oryzae* pathosystem. *Mol. Plant-Microbe Interact.* 20, 731–739.
- Iyer, A. S., and McCouch, S. R. (2004). The rice bacterial blight resistance gene *xa5* encodes a novel form of disease resistance. *Mol. Plant-Microbe Interact.* 17, 1348–1354.
- Jain, M., Nijhawan, A., Arora, R., Agarwal, P., Ray, S., Sharma, P., et al. (2007). F-Box proteins in rice. Genome-wide analysis, classification, temporal and spatial gene expression during panicle and seed development, and regulation by light and abiotic stress. *Plant Physiol.* 143, 1467–1483.
- Jeena, G. S., Kumar, S., and Shukla, R. K. (2019). Structure, evolution and diverse physiological roles of SWEET sugar transporters in plants. *Plant Mol. Biol.* 100, 351–365.
- Jelenska, J., Yao, N., Vinatzer, B. A., Wright, C. M., Brodsky, J. L., and Greenberg, J. T. (2007). A J domain virulence effector of *Pseudomonas syringae* remodels host chloroplasts and suppresses defenses. *Curr. Biol.* 17, 499–508.
- Ji, Z., Ji, C., Liu, B., Zou, L., Chen, G., and Yang, B. (2016). Interfering TAL effectors of *Xanthomonas oryzae* neutralize *R*-gene-mediated plant disease resistance. *Nat. Commun.* 7, 13435.
- Jia, H., Orbovic, V., Jones, J. B., and Wang, N. (2016). Modification of the PthA4 effector binding elements in Type I *CsLOB1* promoter using Cas9/sgRNA to produce transgenic Duncan grapefruit alleviating XccΔpthA4:dCsLOB1.3 infection. *Plant Biotechnol. J.* 14, 1291–1301.

- Jiang, W., Zhou, H., Bi, H., Fromm, M., Yang, B., and Weeks, D. P. (2013). Demonstration of CRISPR/Cas9/sgRNA-mediated targeted gene modification in *Arabidopsis*, tobacco, sorghum and rice. *Nucleic Acids Res.* 41, 1–12.
- Jinek, M., Chylinski, K., Fonfara, I., Hauer, M., Doudna, J. A., and Charpentier, E. (2012). A programmable dual-RNA-guided DNA endonuclease in adaptive bacterial immunity. *Science* (80-). 337, 816–821.
- Jones, J. D. G., and Dangl, J. L. (2006). The plant immune system. *Nature* 444, 323–329.
- Juillerat, A., Pessereau, C., Dubois, G., Guyot, V., Maréchal, A., Valton, J., et al. (2015). Optimized tuning of TALEN specificity using non-conventional RVDs. *Sci. Rep.* 5, 8150.
- Kawahara, Y., de la Bastide, M., Hamilton, J. P., Kanamori, H., McCombie, W. R., Ouyang, S., et al. (2013). Improvement of the *Oryza sativa* Nipponbare reference genome using next generation sequence and optical map data. *Rice* 6, 1–10.
- Kawai, Y., Ono, E., and Mizutani, M. (2014). Evolution and diversity of the 2-oxoglutarate-dependent dioxygenase superfamily in plants. *Plant J.* 78, 328–343.
- Kay, S., Boch, J., and Bonas, U. (2005). Characterization of AvrBs3-like effectors from a *Brassicaceae* pathogen reveals virulence and avirulence activities and a protein with a novel repeat architecture. *Mol. Plant-Microbe Interact.* 18, 838–848.
- Kay, S., Hahn, S., Marois, E., Hause, G., and Bonas, U. (2007). A bacterial effector acts as a plant transcription factor and induces a cell size regulator. *Science* 318, 648–51.
- Kay, S., Hahn, S., Marois, E., Wieduwild, R., and Bonas, U. (2009). Detailed analysis of the DNA recognition motifs of the *Xanthomonas* type III effectors AvrBs3 and AvrBs3 Δ rep16. *Plant J.* 59, 859–871.
- Ke, Y., Wu, M., Zhang, Q., Li, X., Xiao, J., and Wang, S. (2019). Hd3a and OsFD1 negatively regulate rice resistance to *Xanthomonas oryzae* pv. *oryzae* and *Xanthomonas oryzae* pv. *oryzicola*. *Biochem. Biophys. Res. Commun.* 513, 775–780.
- Khan, M., Subramaniam, R., and Desveaux, D. (2016). Of guards, decoys, baits and traps: Pathogen perception in plants by type III effector sensors. *Curr. Opin. Microbiol.* 29, 49–55.
- Kim, J.-G., Stork, W., and Mudgett, M. B. (2013). *Xanthomonas* Type III Effector XopD desumoylates tomato transcription factor SIERF4 to suppress ethylene responses and promote pathogen growth. *Cell Host Microbe* 13, 143–154.
- Kim, J. H., Cheon, Y. M., Kim, B.-G., and Ahn, J.-H. (2008). Analysis of flavonoids and characterization of the *OsFNS* gene involved in flavone biosynthesis in rice. *J. Plant Biol.* 51, 97–101.
- Kim, Y. G., Cha, J., and Chandrasegaran, S. (1996). Hybrid restriction enzymes: zinc finger fusions to FokI cleavage domain. *Proc. Natl. Acad. Sci. U. S. A.* 93, 1156–1160.

- Klessig, D. F., Choi, H. W., and Dempsey, D. A. (2018). Systemic acquired resistance and salicylic acid: Past, present, and future. *Mol. Plant-Microbe Interact.* 31, 871–888.
- Koebnik, R., Krüger, A., Thieme, F., Urban, A., and Bonas, U. (2006). Specific binding of the *Xanthomonas campestris* pv. *vesicatoria* AraC-type transcriptional activator HrpX to plant-inducible promoter boxes. *J. Bacteriol.* 188, 7652–7660.
- Kohorn, B. D. (2016). Cell wall-associated kinases and pectin perception. *J. Exp. Bot.* 67, 489–494.
- Kohorn, B. D., and Kohorn, S. L. (2012). The cell wall-associated kinases, WAKs, as pectin receptors. *Front. Plant Sci.* 3, 88.
- Koncz, C., and Schell, J. (1986). The promoter of TL-DNA gene 5 controls the tissue-specific expression of chimaeric genes carried by a novel type of *Agrobacterium* binary vector. *Mol. Gen. Genet. MGG* 204, 383–396.
- Lam, P. Y., Zhu, F.-Y., Chan, W. L., Liu, H., and Lo, C. (2014). Cytochrome P450 93G1 is a flavone synthase II that channels flavanones to the biosynthesis of tricin O-linked conjugates in rice. *Plant Physiol.* 165, 1315–1327.
- Lee, B.-M., Park, Y.-J., Park, D.-S., Kang, H.-W., Kim, J.-G., Song, E.-S., et al. (2005). The genome sequence of *Xanthomonas oryzae* pathovar *oryzae* KACC10331, the bacterial blight pathogen of rice. *Nucleic Acids Res.* 33, 577–586.
- Léran, S., Muñoz, S., Brachet, C., Tillard, P., Gojon, A., and Lacombe, B. (2013). Arabidopsis NRT1.1 is a bidirectional transporter involved in root-to-shoot nitrate translocation. *Mol. Plant* 6, 1984–1987.
- Léran, S., Varala, K., Boyer, J.-C., Chiurazzi, M., Crawford, N., Daniel-Vedele, F., et al. (2014). A unified nomenclature of NITRATE TRANSPORTER 1/PEPTIDE TRANSPORTER family members in plants. *Trends Plant Sci.* 19, 5–9.
- Letunic, I., and Bork, P. (2019). Interactive Tree Of Life (iTOL) v4: recent updates and new developments. *Nucleic Acids Res.* 47, W256–W259.
- Lewis, M. J., and Patel, P. C. (1978). Isolation and identification of the cytoplasmic membrane from *Saccharomyces carlsbergensis* by radioactive labeling. *Appl. Environ. Microbiol.* 36, 851–856.
- Lex, A., Gehlenborg, N., Strobelt, H., Vuillemot, R., and Pfister, H. (2014). UpSet: Visualization of intersecting sets. *IEEE Trans. Vis. Comput. Graph.* 20, 1983–1992.
- Li, H., Zhou, Y., and Zhang, Z. (2017). Network analysis reveals a common host–pathogen interaction pattern in Arabidopsis immune responses. *Front. Plant Sci.* 8, 1–13.
- Li, L., Wu, L. P., and Chandrasegaran, S. (1992). Functional domains in *FokI* restriction endonuclease. *Proc. Natl. Acad. Sci. U. S. A.* 89, 4275–4279.
- Li, R. F., Lu, G. T., Li, L., Su, H. Z., Feng, G. fang, Chen, Y., et al. (2014). Identification of a putative cognate sensor kinase for the two-component response regulator HrpG, a key regulator controlling the expression of the hrp genes in *Xanthomonas campestris* pv. *campestris*. *Environ. Microbiol.* 16, 2053–2071.

- Li, T., Huang, S., Jiang, W. Z., Wright, D., Spalding, M. H., Weeks, D. P., *et al.* (2011). TAL nucleases (TALNs): Hybrid proteins composed of TAL effectors and *FokI* DNA-cleavage domain. *Nucleic Acids Res.* 39, 359–372.
- Li, T., Liu, B., Spalding, M. H., Weeks, D. P., and Yang, B. (2012). High-efficiency TALEN-based gene editing produces disease-resistant rice. *Nat. Biotechnol.* 30, 390–392.
- Li, T., Yang, X., Yu, Y., Si, X., Zhai, X., Zhang, H., *et al.* (2018). Domestication of wild tomato is accelerated by genome editing. *Nat. Biotechnol.* 36, 1160–1163.
- Liao, C. J., Lai, Z., Lee, S., Yun, D. J., and Mengiste, T. (2016). *Arabidopsis* HOOKLESS1 regulates responses to pathogens and abscisic acid through interaction with MED18 and acetylation of *WRKY33* and *ABI5* chromatin. *Plant Cell* 28, 1662–1681.
- Liao, Z.-X., Ni, Z., Wei, X.-L., Chen, L., Li, J.-Y., Yu, Y.-H., *et al.* (2019). Dual RNA-seq of *Xanthomonas oryzae* pv. *oryzicola* infecting rice reveals novel insights into bacterial-plant interaction. *PLoS One* 14, e0215039.
- Lindeberg, M., Cunnac, S., and Collmer, A. (2012). *Pseudomonas syringae* type III effector repertoires: last words in endless arguments. *Trends Microbiol.* 20, 199–208.
- Liu, J., Liu, X., Dai, L., and Wang, G. (2007). Recent progress in elucidating the structure, function and evolution of disease resistance genes in plants. *J. Genet. Genomics* 34, 765–776.
- Liu, K.-H., Niu, Y., Konishi, M., Wu, Y., Du, H., Sun Chung, H., *et al.* (2017). Discovery of nitrate-CPK-NLP signalling in central nutrient-growth networks. *Nature* 545, 311–316.
- Liu, W., Liu, J., Triplett, L., Leach, J. E., and Wang, G.-L. (2014). Novel insights into rice innate immunity against bacterial and fungal pathogens. *Annu. Rev. Phytopathol.* 52, 213–241.
- Liu, X., Luo, M., Zhang, W., Zhao, J., Zhang, J., Wu, K., *et al.* (2012). Histone acetyltransferases in rice (*Oryza sativa* L.): phylogenetic analysis, subcellular localization and expression. *BMC Plant Biol.* 12, 1–17.
- Livak, K. J., and Schmittgen, T. D. (2001). Analysis of Relative Gene Expression Data Using Real-Time Quantitative PCR and the 2- $\Delta\Delta$ CT Method. *Methods* 25, 402–408.
- Ma, J. F., Tamai, K., Yamaji, N., Mitani, N., Konishi, S., Katsuhara, M., *et al.* (2006). A silicon transporter in rice. *Nature* 440, 688–691.
- Ma, J. F., Yamaji, N., and Mitani-Ueno, N. (2011). Transport of silicon from roots to panicles in plants. *Proc. Japan Acad. Ser. B* 87, 377–385.
- Ma, K. W., and Ma, W. (2016). Phytohormone pathways as targets of pathogens to facilitate infection. *Plant Mol. Biol.* 91, 713–725.
- Ma, L., Wang, Q., Yuan, M., Zou, T., Yin, P., and Wang, S. (2018). *Xanthomonas* TAL effectors hijack host basal transcription factor IIA α and γ subunits for invasion. *Biochem. Biophys. Res. Commun.* 496, 608–613.

- Madeira, F., Park, Y. M., Lee, J., Buso, N., Gur, T., Madhusoodanan, N., et al. (2019). The EMBL-EBI search and sequence analysis tools APIs in 2019. *Nucleic Acids Res.* 47, W636–W641.
- Mak, A. N.-S., Bradley, P., Cernadas, R. A., Bogdanove, A. J., and Stoddard, B. L. (2012). The crystal structure of TAL effector PthXo1 bound to its DNA target. *Science* 335, 716–9.
- Martins, P. M. M., Merfa, M. V., Takita, M. A., and De Souza, A. A. (2018). Persistence in phytopathogenic bacteria: Do we know enough? *Front. Microbiol.* 9, 1–14.
- Mburu, K., Oduor, R., Mgtutu, A., and Tripathi, L. (2016). Silicon application enhances resistance to *Xanthomonas* wilt disease in banana. *Plant Pathol.* 65, 807–818.
- McVey, M., and Lee, S. E. (2008). MMEJ repair of double-strand breaks (director's cut): deleted sequences and alternative endings. *Trends Genet.* 24, 529–538.
- Meckler, J. F., Bhakta, M. S., Kim, M.-S., Ovadia, R., Habrian, C. H., Zykovich, A., et al. (2013). Quantitative analysis of TALE-DNA interactions suggests polarity effects. *Nucleic Acids Res.* 41, 4118–4128.
- Midha, S., Bansal, K., Kumar, S., Girija, A. M., Mishra, D., Brahma, K., et al. (2017). Population genomic insights into variation and evolution of *Xanthomonas oryzae* pv. *oryzae*. *Sci. Rep.* 7, 40694.
- Miller, J. C., Tan, S., Qiao, G., Barlow, K. A., Wang, J., Xia, D. F., et al. (2011). A TALE nuclease architecture for efficient genome editing. *Nat. Biotechnol.* 29, 143–148.
- Miller, J. C., Zhang, L., Xia, D. F., Campo, J. J., Ankoudinova, I. V., Guschin, D. Y., et al. (2015). Improved specificity of TALE-based genome editing using an expanded RVD repertoire. *Nat. Methods* 12, 465–471.
- Miller, J., McLachlan, A. D., and Klug, A. (1985). Repetitive zinc-binding domains in the protein transcription factor IIIA from *Xenopus* oocytes. *EMBO J.* 4, 1609–1614.
- Misas-Villamil, J. C., Kolodziejek, I., Crabill, E., Kaschani, F., Niessen, S., Shindo, T., et al. (2013). *Pseudomonas syringae* pv. *syringae* uses proteasome inhibitor syringolin A to colonize from wound infection sites. *PLoS Pathog.* 9, 10–16.
- Młodzińska, E., and Zboińska, M. (2016). Phosphate uptake and allocation – A closer look at *Arabidopsis thaliana* L. and *Oryza sativa* L. *Front. Plant Sci.* 7, 1198.
- Moreira, L. M., Facincani, A. P., Ferreira, C. B., Ferreira, R. M., Ferro, M. I. T., Gozzo, F. C., et al. (2015). Chemotactic signal transduction and phosphate metabolism as adaptive strategies during citrus canker induction by *Xanthomonas citri*. *Funct. Integr. Genomics* 15, 197–210.
- Morel, J.-B., and Dangl, J. L. (1997). The hypersensitive response and the induction of cell death in plants. *Cell Death Differ.* 4, 671–683.
- Moscou, M. J., and Bogdanove, A. J. (2009). A simple cipher governs DNA recognition by TAL effectors. *Science* (80-.). 326, 1501.

- Mücke, S., Reschke, M., Erkes, A., Schwietzer, C.-A., Becker, S., Streubel, J., et al. (2019). Transcriptional reprogramming of rice cells by *Xanthomonas oryzae* TALEs. *Front. Plant Sci.* 10, 162.
- Mukhtar, M. S., Carvunis, A., Dreze, M., Epple, P., Steinbrenner, J., Moore, J., et al. (2011). Independently evolved virulence effectors converge onto hubs in a plant immune system network. *Science* 333, 596–601.
- Mundt, C. C. (2002). Use of multiline cultivars and cultivar mixtures for disease management. *Annu. Rev. Phytopathol.* 40, 381–410.
- Nakagawa, T., Kurose, T., Hino, T., Tanaka, K., Kawamukai, M., Niwa, Y., et al. (2007). Development of series of gateway binary vectors, pGWBs, for realizing efficient construction of fusion genes for plant transformation. *J. Biosci. Bioeng.* 104, 34–41.
- Nancy Castilla Bacterial blight. *Rice Knowl. Bank, Int. Rice Res. Inst.* Available at: <http://www.knowledgebank.irri.org/decision-tools/rice-doctor/rice-doctor-fact-sheets/item/bacterial-blight> [Accessed November 20, 2019].
- Niño-Liu, D. O., Ronald, P. C., and Bogdanove, A. J. (2006). *Xanthomonas oryzae* pathovars: model pathogens of a model crop. *Mol. Plant Pathol.* 7, 303–324.
- Nishimasu, H., Ran, F. A., Hsu, P. D., Konermann, S., Shehata, S. I., Dohmae, N., et al. (2014). Crystal structure of Cas9 in complex with guide RNA and target DNA. *Cell* 156, 935–949.
- Njenga, K. W., Nyaboga, E., Wagacha, J. M., and Mwaura, F. B. (2017). Silicon induces resistance to bacterial blight by altering the physiology and antioxidant enzyme activities in cassava. *World J. Agric. Res.* 5, 42–51.
- Noda, T., and Kaku, H. (1999). Growth of *Xanthomonas oryzae* pv. *oryzae* in planta and in guttation fluid of rice. *Japanese J. Phytopathol.* 65, 9–14.
- Ochiai, H., Inoue, Y., Takeya, M., Sasaki, A., and Kaku, H. (2005). Genome sequence of *Xanthomonas oryzae* pv. *oryzae* suggests contribution of large numbers of effector genes and insertion sequences to its race diversity. *Japan Agric. Res. Q.* 39, 275–287.
- OEPP/EPPPO (1997). Data Sheets on Quarantine Pests: *Xanthomonas oryzae*. *EPPPO Glob. database*. Available at: <https://gd.eppo.int/taxon/XANTOR/documents> [Accessed December 11, 2019].
- Oliva, R., Ji, C., Atienza-Grande, G., Huguet-Tapia, J. C., Perez-Quintero, A., Li, T., et al. (2019). Broad-spectrum resistance to bacterial blight in rice using genome editing. *Nat. Biotechnol.* 37, 1344–1350.
- Ordon, J., Gantner, J., Kemna, J., Schwalgun, L., Reschke, M., Streubel, J., et al. (2017). Generation of chromosomal deletions in dicotyledonous plants employing a user-friendly genome editing toolkit. *Plant J.* 89, 155–168.
- Ou, S. H. (1985). *Rice Diseases*. Commonwealth Mycological Institute.

- Peng, Z., Hu, Y., Zhang, J., Huguet-Tapia, J. C., Block, A. K., Park, S., *et al.* (2019). *Xanthomonas translucens* commandeers the host rate-limiting step in ABA biosynthesis for disease susceptibility. *Proc. Natl. Acad. Sci.*, 201911660.
- Pereira, A. L. A., Carazzolle, M. F., Abe, V. Y., de Oliveira, M. L. P., Domingues, M. N., Silva, J. C., *et al.* (2014). Identification of putative TAL effector targets of the citrus canker pathogens shows functional convergence underlying disease development and defense response. *BMC Genomics* 15, 1–15.
- Pérez-Quintero, A. L., Lamy, L., Zarate, C. A., Cunnac, S., Doyle, E., Bogdanove, A., *et al.* (2018). daTALbase: A database for genomic and transcriptomic data related to TAL effectors. *Mol. Plant-Microbe Interact.* 31, 471–480.
- Pérez-Quintero, A. L., Rodríguez-R, L. M., Dereeper, A., López, C., Koebnik, R., Szurek, B., *et al.* (2013). An improved method for TAL effectors DNA-binding sites prediction reveals functional convergence in TAL repertoires of *Xanthomonas oryzae* strains. *PLoS One* 8, e68464.
- Popov, G., Majhi, B. B., and Sessa, G. (2018). Effector gene *xopAE* of *Xanthomonas euvesicatoria* 85-10 is part of an operon and encodes an E3 ubiquitin ligase. *J. Bacteriol.* 200, e00104-18.
- Portaliou, A. G., Tsolis, K. C., Loos, M. S., Zorzini, V., and Economou, A. (2016). Type III secretion: building and operating a remarkable nanomachine. *Trends Biochem. Sci.* 41, 175–189.
- Poulin, L., Grygiel, P., Magne, M., Gagnevin, L., Rodríguez-R, L. M., Forero Serna, N., *et al.* (2015). New multilocus variable-number tandem-repeat analysis tool for surveillance and local epidemiology of bacterial leaf blight and bacterial leaf streak of rice caused by *Xanthomonas oryzae*. *Appl. Environ. Microbiol.* 81, 688–698.
- Prochaska, H., Thieme, S., Daum, S., Grau, J., Schmidtke, C., Hallensleben, M., *et al.* (2018). A conserved motif promotes HpaB-regulated export of type III effectors from *Xanthomonas*. *Mol. Plant Pathol.* 19, 2473–2487.
- Puchta, H. (2005). The repair of double-strand breaks in plants: Mechanisms and consequences for genome evolution. *J. Exp. Bot.* 56, 1–14.
- Qin, J., Zhou, X., Sun, L., Wang, K., Yang, F., Liao, H., *et al.* (2018). The *Xanthomonas* effector XopK harbours E3 ubiquitin-ligase activity that is required for virulence. *New Phytol.* 220, 219–231.
- Quibod, I. L., Atieza-Grande, G., Oreiro, E. G., Palmos, D., Nguyen, M. H., Coronejo, S. T., *et al.* (2019). The Green Revolution shaped the population structure of the rice pathogen *Xanthomonas oryzae* pv. *oryzae*. *ISME J.* 14, 492-505.
- Quibod, I. L., Perez-Quintero, A., Booher, N. J., Dossa, G. S., Grande, G., Szurek, B., *et al.* (2016). Effector diversification contributes to *Xanthomonas oryzae* pv. *oryzae* phenotypic adaptation in a semi-isolated environment. *Sci. Rep.* 6, 34137.

- Rahman, M. A., Abdullah, H., and Vanhaecke, M. (1999). Histopathology of susceptible and resistant *Capsicum annuum* cultivars infected with *Ralstonia solanacearum*. *J. Phytopathol.* 147, 129–140.
- Ranjan, A., Vadassery, J., Patel, H. K., Pandey, A., Palaparathi, R., Mithöfer, A., et al. (2015). Upregulation of jasmonate biosynthesis and jasmonate-responsive genes in rice leaves in response to a bacterial pathogen mimic. *Funct. Integr. Genomics* 15, 363–373.
- Rashid, M., Bera, S., Banerjee, M., Medvinsky, A. B., Sun, G.-Q., Li, B.-L., et al. (2020). Feedforward control of plant nitrate transporter NRT1.1 biphasic adaptive activity. *Biophys. J.* 118, 898–908.
- Read, A. C., Rinaldi, F. C., Hutin, M., He, Y.-Q., Triplett, L. R., and Bogdanove, A. J. (2016). Suppression of *Xo1*-mediated disease resistance in rice by a truncated, non-DNA-binding TAL effector of *Xanthomonas oryzae*. *Front. Plant Sci.* 7, 1516.
- Richter, A., and Boch, J. (2013). Designer TALEs team up for highly efficient gene induction. *Nat. Methods* 10, 207–8.
- Richter, A., Streubel, J., Blücher, C., Szurek, B., Reschke, M., Grau, J., et al. (2014). A TAL effector repeat architecture for frameshift binding. *Nat. Commun.* 5, 3447.
- Rico, A., and Preston, G. M. (2008). *Pseudomonas syringae* pv. *tomato* DC3000 uses constitutive and apoplast-induced nutrient assimilation pathways to catabolize nutrients that are abundant in the tomato apoplast. *Mol. Plant-Microbe Interact.* 21, 269–282.
- Rinaldi, F. C., Doyle, L. A., Stoddard, B. L., and Bogdanove, A. J. (2017). The effect of increasing numbers of repeats on TAL effector DNA binding specificity. *Nucleic Acids Res.* 45, 6960–6970.
- Ritchie, D. F., and Dittapongpitch, V. (1991). Copper- and streptomycin-resistant strains and host differentiated races of *Xanthomonas campestris* pv. *vesicatoria* in North Carolina. *Plant Dis.* 75, 733–736.
- Römer, P., Hahn, S., Jordan, T., Strauß, T., Bonas, U., and Lahaye, T. (2007). Plant pathogen recognition mediated by promoter activation of the pepper *Bs3* resistance gene. *Science* 318, 645 LP – 648.
- Römer, P., Recht, S., Strauß, T., Elsaesser, J., Schornack, S., Boch, J., et al. (2010). Promoter elements of rice susceptibility genes are bound and activated by specific TAL effectors from the bacterial blight pathogen, *Xanthomonas oryzae* pv. *oryzae*. *New Phytol.* 187, 1048–1057.
- Rottmann, T. M., Fritz, C., Lauter, A., Schneider, S., Fischer, C., Danzberger, N., et al. (2018). Protoplast-esculin assay as a new method to assay plant sucrose transporters: Characterization of AtSUC6 and AtSUC7 sucrose uptake activity in *Arabidopsis* Col-0 ecotype. *Front. Plant Sci.* 9, 1–22.
- Roux, B., Bolot, S., Guy, E., Denancé, N., Lautier, M., Jardinaud, M.-F., et al. (2015). Genomics and transcriptomics of *Xanthomonas campestris* species challenge the concept of core type III effectome. *BMC Genomics* 16, 975.

- Runte, C. S., Jain, U., Getz, L. J., Secord, S., Kuwae, A., Abe, A., et al. (2018). Tandem tyrosine phosphosites in the enteropathogenic *Escherichia coli* chaperone CseT are required for differential type III effector translocation and virulence. *Mol. Microbiol.* 108, 536–550.
- Ryan, R. P., Vorhölter, F. J., Potnis, N., Jones, J. B., Van Sluys, M. A., Bogdanove, A. J., et al. (2011). Pathogenomics of *Xanthomonas*: Understanding bacterium-plant interactions. *Nat. Rev. Microbiol.* 9, 344–355.
- Sabella, E., Aprile, A., Genga, A., Siciliano, T., Nutricati, E., Nicolì, F., et al. (2019). Xylem cavitation susceptibility and refilling mechanisms in olive trees infected by *Xylella fastidiosa*. *Sci. Rep.* 9, 9602.
- Saiki, R. K., Gelfand, D. H., Stoffel, S., Scharf, S. J., Higuchi, R., Horn, G. T., et al. (1988). Primer-directed enzymatic amplification of DNA with a thermostable DNA polymerase. *Science* 39, 487 LP – 491.
- Sakuma, T., Hosoi, S., Woltjen, K., Suzuki, K. I., Kashiwagi, K., Wada, H., et al. (2013). Efficient TALEN construction and evaluation methods for human cell and animal applications. *Genes to Cells* 18, 315–326.
- Salinas, M. (2017). Citrus canker in Northwest Florida. *Univ. Florida Blogs*. Available at: <http://blogs.ifas.ufl.edu/santarosaco/2017/09/08/citrus-canker-in-northwest-florida/> [Accessed November 20, 2019].
- Sallaud, C., Meynard, D., Van Boxtel, J., Gay, C., Bès, M., Brizard, J. P., et al. (2003). Highly efficient production and characterization of T-DNA plants for rice (*Oryza sativa* L.) functional genomics. *Theor. Appl. Genet.* 106, 1396–1408.
- Salzberg, S. L., Sommer, D. D., Schatz, M. C., Phillippy, A. M., Rabinowicz, P. D., Tsuge, S., et al. (2008). Genome sequence and rapid evolution of the rice pathogen *Xanthomonas oryzae* pv. *oryzae* PXO99A. *BMC Genomics* 9, 204.
- Samad, A. F. A., Sajad, M., Nazaruddin, N., Fauzi, I. A., Murad, A. M. A., Zainal, Z., et al. (2017). MicroRNA and transcription factor: key players in plant regulatory network. *Front. Plant Sci.* 8, 565.
- Sánchez-León, S., Gil-Humanes, J., Ozuna, C. V, Giménez, M. J., Sousa, C., Voytas, D. F., et al. (2018). Low-gluten, nontransgenic wheat engineered with CRISPR/Cas9. *Plant Biotechnol. J.* 16, 902–910.
- Sander, J. D., Cade, L., Khayter, C., Reyon, D., Peterson, R. T., Joung, J. K., et al. (2011). Targeted gene disruption in somatic zebrafish cells using engineered TALENs. *Nat. Biotechnol.* 29, 697–698.
- Sanjana, N. E., Cong, L., Zhou, Y., Cunniff, M. M., Feng, G., and Zhang, F. (2012). A transcription activator-like effector toolbox for genome engineering. *Nat. Protoc.* 7, 171–192.
- Schandry, N., de Lange, O., Prior, P., and Lahaye, T. (2016). TALE-like effectors are an ancestral feature of the *Ralstonia solanacearum* species complex and converge in DNA targeting specificity. *Front. Plant Sci.* 7, 1225.

- Schmid-Burgk, J. L., Schmidt, T., Kaiser, V., Höning, K., and Hornung, V. (2013). A ligation-independent cloning technique for high-throughput assembly of transcription activator-like effector genes. *Nat. Biotechnol.* 31, 76–81.
- Schmidt, C., Pacher, M., and Puchta, H. (2019). DNA break repair in plants and its application for genome engineering. *Methods Mol. Biol.* 1864, 237–266.
- Schornack, S., Ballvora, A., Gürlebeck, D., Peart, J., Ganal, M., Baker, B., et al. (2004). The tomato resistance protein Bs4 is a predicted non-nuclear TIR-NB-LRR protein that mediates defense responses to severely truncated derivatives of AvrBs4 and overexpressed AvrBs3. *Plant J.* 37, 46–60.
- Schornack, S., Minsavage, G. V., Stall, R. E., Jones, J. B., and Lahaye, T. (2008). Characterization of AvrHah1, a novel AvrBs3-like effector from *Xanthomonas gardneri* with virulence and avirulence activity. *New Phytol.* 179, 546–556.
- Schornack, S., Peter, K., Bonas, U., and Lahaye, T. (2005). Expression levels of *avrBs3*-like genes affect recognition specificity in tomato *Bs4*- but not in pepper *Bs3*-Mediated Perception. *Mol. Plant-Microbe Interact.* 18, 1215–1225.
- Schreiber, T., Sorgatz, A., List, F., Blüher, D., Thieme, S., Wilmanns, M., et al. (2015). Refined requirements for protein regions important for activity of the TALE AvrBs3. *PLoS One* 10, 1–21.
- Schulze, S., Kay, S., Büttner, D., Egler, M., Eschen-Lippold, L., Hause, G., et al. (2012). Analysis of new type III effectors from *Xanthomonas* uncovers XopB and XopS as suppressors of plant immunity. *New Phytol.* 195, 894–911.
- Schwartz, A. R., Morbitzer, R., Lahaye, T., and Staskawicz, B. J. (2017). TALE-induced bHLH transcription factors that activate a pectate lyase contribute to water soaking in bacterial spot of tomato. *Proc. Natl. Acad. Sci. U. S. A.* 114, E897–E903.
- Secchi, F., and Zwieniecki, M. A. (2011). Sensing embolism in xylem vessels: the role of sucrose as a trigger for refilling. *Plant. Cell Environ.* 34, 514–524.
- Secchi, F., and Zwieniecki, M. A. (2016). Accumulation of sugars in the xylem apoplast observed under water stress conditions is controlled by xylem pH. *Plant. Cell Environ.* 39, 2350–2360.
- Secco, D., Baumann, A., and Poirier, Y. (2010). Characterization of the rice *PHO1* gene family reveals a key role for *OsPHO1;2* in phosphate homeostasis and the evolution of a distinct clade in dicotyledons. *Plant Physiol.* 152, 1693–704.
- Secco, D., Wang, C., Arpat, B. A., Wang, Z., Poirier, Y., Tyerman, S. D., et al. (2012). The emerging importance of the SPX domain-containing proteins in phosphate homeostasis. *New Phytol.* 193, 842–851.
- Sehnal, D., Rose, A. S., Koča, J., Burley, S. K., and Velankar, S. (2018). Mol*: Towards a Common Library and Tools for Web Molecular Graphics. in *Proceedings of the Workshop on Molecular Graphics and Visual Analysis of Molecular Data MolVA '18*. (Goslar, DEU: Eurographics Association), 29–33.

- Shan, Q., Wang, Y., Li, J., and Gao, C. (2014). Genome editing in rice and wheat using the CRISPR/Cas system. *Nat. Protoc.* 9, 2395.
- Shasmita, Mohapatra, D., Mohapatra, P. K., Naik, S. K., and Mukherjee, A. K. (2019). Priming with salicylic acid induces defense against bacterial blight disease by modulating rice plant photosystem II and antioxidant enzymes activity. *Physiol. Mol. Plant Pathol.* 108, 101427.
- Shimono, M., Koga, H., Akagi, A., Hayashi, N., Goto, S., Sawada, M., et al. (2012). Rice WRKY45 plays important roles in fungal and bacterial disease resistance. *Mol. Plant Pathol.* 13, 83–94.
- Shimono, M., Sugano, S., Nakayama, A., Jiang, C.-J., Ono, K., Toki, S., et al. (2007). Rice WRKY45 Plays a Crucial Role in Benzothiadiazole-Inducible Blast Resistance. *Plant Cell* 19, 2064 LP – 2076.
- Silva, I. T., Rodrigues, F. Á., Oliveira, J. R., Pereira, S. C., Andrade, C. C. L., Silveira, P. R., et al. (2010). Wheat resistance to bacterial leaf streak mediated by silicon. *J. Phytopathol.* 158, 253–262.
- Silverman, P., Seskar, M., Kanter, D., Schweizer, P., Metraux, J. P., and Raskin, I. (1995). Salicylic acid in rice (biosynthesis, conjugation, and possible role). *Plant Physiol.* 108, 633 LP – 639.
- Sinha, D., Gupta, M. K., Patel, H. K., Ranjan, A., and Sonti, R. V (2013). Cell wall degrading enzyme induced rice innate immune responses are suppressed by the type 3 secretion system effectors XopN, XopQ, XopX and XopZ of *Xanthomonas oryzae* pv. *oryzae*. *PLoS One* 8, e75867.
- Song, A., Xue, G., Cui, P., Fan, F., Liu, H., Yin, C., et al. (2016). The role of silicon in enhancing resistance to bacterial blight of hydroponic- and soil-cultured rice. *Sci. Rep.* 6, 24640.
- Sparks, A., Castilla, N. P., and Vera Cruz, C. Bacterial leaf streak. *Rice Knowl. Bank, Int. Rice Res. Inst.* Available at: <http://www.knowledgebank.irri.org/decision-tools/rice-doctor/rice-doctor-fact-sheets/item/bacterial-leaf-streak> [Accessed November 20, 2019].
- Sternberg, S. H., Redding, S., Jinek, M., Greene, E. C., and Doudna, J. A. (2014). DNA interrogation by the CRISPR RNA-guided endonuclease Cas9. *Nature* 507, 62–67.
- Streubel, J., Baum, H., Grau, J., Stuttman, J., and Boch, J. (2017). Dissection of TALE-dependent gene activation reveals that they induce transcription cooperatively and in both orientations. *PLoS One* 12, e0173580.
- Streubel, J., Blücher, C., Landgraf, A., and Boch, J. (2012). TAL effector RVD specificities and efficiencies. *Nat. Biotechnol.* 30, 593–595.
- Streubel, J., Pesce, C., Hutin, M., Koebnik, R., Boch, J., and Szurek, B. (2013). Five phylogenetically close rice *SWEET* genes confer TAL effector-mediated susceptibility to *Xanthomonas oryzae* pv. *oryzae*. *New Phytol.* 200, 808–819.

- Sugio, A., Yang, B., Zhu, T., and White, F. F. (2007). Two type III effector genes of *Xanthomonas oryzae* pv. *oryzae* control the induction of the host genes *OsTFIIAgamma1* and *OsTFX1* during bacterial blight of rice. *Proc. Natl. Acad. Sci. U. S. A.* 104, 10720–5.
- Sun, S., Gu, M., Cao, Y., Huang, X., Zhang, X., Ai, P., et al. (2012). A constitutive expressed phosphate transporter, *OsPht1;1*, modulates phosphate uptake and translocation in phosphate-replete rice. *Plant Physiol.* 159, 1571 LP – 1581.
- Szurek, B., Marois, E., Bonas, U., and Van Ackerveken, G. Den (2001). Eukaryotic features of the *Xanthomonas* type III effector *AvrBs3*: Protein domains involved in transcriptional activation and the interaction with nuclear import receptors from pepper. *Plant J.* 26, 523–534.
- Szurek, B., Rossier, O., Hause, G., and Bonas, U. (2002). Type III-dependent translocation of the *Xanthomonas* *AvrBs3* protein into the plant cell. *Mol. Microbiol.* 46, 13–23.
- Tamaoki, D., Seo, S., Yamada, S., Kano, A., Miyamoto, A., Shishido, H., et al. (2013). Jasmonic acid and salicylic acid activate a common defense system in rice. *Plant Signal. Behav.* 8, e24260.
- Tang, L., Mao, B., Li, Y., Lv, Q., Zhang, L., Chen, C., et al. (2017). Knockout of *OsNramp5* using the CRISPR/Cas9 system produces low Cd-accumulating indica rice without compromising yield. *Sci. Rep.* 7, 14438.
- Tayi, L., Maku, R., Patel, H. K., and Sonti, R. V. (2016a). Action of multiple cell wall-degrading enzymes is required for elicitation of innate immune responses during *Xanthomonas oryzae* pv. *oryzae* infection in rice. *Mol. Plant-Microbe Interact.* 29, 599–608.
- Tayi, L., Maku, R. V., Patel, H. K., and Sonti, R. V. (2016b). Identification of pectin degrading enzymes secreted by *Xanthomonas oryzae* pv. *oryzae* and determination of their role in virulence on rice. *PLoS One* 11, e0166396.
- Thanh, T. Le, Thumanu, K., Wongkaew, S., Boonkerd, N., Teaumroong, N., Phansak, P., et al. (2017). Salicylic acid-induced accumulation of biochemical components associated with resistance against *Xanthomonas oryzae* pv. *oryzae* in rice. *J. Plant Interact.* 12, 108–120.
- Thomazella, D. P. de T., Brail, Q., Dahlbeck, D., and Staskawicz, B. J. (2016). CRISPR-Cas9 mediated mutagenesis of a *DMR6* ortholog in tomato confers broad-spectrum disease resistance. *bioRxiv*, 064824.
- Tian, D., Wang, J., Zeng, X., Gu, K., Qiu, C., Yang, X., et al. (2014). The rice TAL effector-dependent resistance protein *XA10* triggers cell death and calcium depletion in the endoplasmic reticulum. *Plant Cell* 26, 497–515.
- Toruño, T. Y., Stergiopoulos, I., and Coaker, G. (2016). Plant-pathogen effectors: Cellular probes interfering with plant defenses in spatial and temporal manners. *Annu. Rev. Phytopathol.* 54, 419–441.

- Tran, T. T., Pérez-Quintero, A. L., Wonni, I., Carpenter, S. C. D., Yu, Y., Wang, L., et al. (2018). Functional analysis of African *Xanthomonas oryzae* pv. *oryzae* TALomes reveals a new susceptibility gene in bacterial leaf blight of rice. *PLoS Pathog.* 14, e1007092.
- Triplett, L. R., Hamilton, J. P., Buell, C. R., Tisserat, N. A., Verdier, V., Zink, F., et al. (2011). Genomic analysis of *Xanthomonas oryzae* isolates from rice grown in the United States reveals substantial divergence from known *X. oryzae* pathovars. *Appl. Environ. Microbiol.* 77, 3930–7.
- Uluşık, S., and Seymour, G. B. (2020). Pectate lyases: Their role in plants and importance in fruit ripening. *Food Chem.* 309, 125559.
- Urnov, F. D., Rebar, E. J., Holmes, M. C., Zhang, H. S., and Gregory, P. D. (2010). Genome editing with engineered zinc finger nucleases. *Nat. Rev. Genet.* 11, 636–646.
- Üstün, S., Bartetzko, V., and Börnke, F. (2013). The *Xanthomonas campestris* type III effector XopJ targets the host cell proteasome to suppress salicylic-acid mediated plant defence. *PLoS Pathog.* 9, e1003427.
- Valton, J., Dupuy, A., Daboussi, F., Thomas, S., Maréchal, A., Macmaster, R., et al. (2012). Overcoming transcription activator-like effector (TALE) DNA binding domain sensitivity to cytosine methylation. *J. Biol. Chem.* 287, 38427–38432.
- van Damme, M., Huibers, R. P., Elberse, J., and Van den Ackerveken, G. (2008). *Arabidopsis* DMR6 encodes a putative 2OG-Fe(II) oxygenase that is defense-associated but required for susceptibility to downy mildew. *Plant J.* 54, 785–793.
- Van den Ackerveken, G., Marois, E., and Bonas, U. (1996). Recognition of the bacterial avirulence protein AvrBs3 occurs inside the host plant cell. *Cell* 87, 1307–1316.
- van der Oost, J., Westra, E. R., Jackson, R. N., and Wiedenheft, B. (2014). Unravelling the structural and mechanistic basis of CRISPR–Cas systems. *Nat. Rev. Microbiol.* 12, 479–492.
- Van Hulten, M., Pelsler, M., Van Loon, L. C., Pieterse, C. M. J., and Ton, J. (2006). Costs and benefits of priming for defense in *Arabidopsis*. *Proc. Natl. Acad. Sci. U. S. A.* 103, 5602–5607.
- Van Larebeke, N., Engler, G., Holsters, M., Van den Elsacker, S., Zaenen, I., Schilperoort, R. A., et al. (1974). Large plasmid in *Agrobacterium tumefaciens* essential for crown gall-inducing ability. *Nature* 252, 169–170.
- van Schie, C. C. N., and Takken, F. L. W. (2014). Susceptibility genes 101: How to be a good host. *Annu. Rev. Phytopathol.* 52, 551–581.
- Vos, I. A., Pieterse, C. M. J., and Van Wees, S. C. M. (2013). Costs and benefits of hormone-regulated plant defences. *Plant Pathol.* 62, 43–55.
- Waltz, E. (2016). CRISPR-edited crops free to enter market, skip regulation. *Nat. Biotechnol.* 34, 582.

- Wang, C., Zhang, X., Fan, Y., Gao, Y., Zhu, Q., Zheng, C., et al. (2015). XA23 is an executor R protein and confers broad-spectrum disease resistance in rice. *Mol. Plant* 8, 290–302.
- Wang, D., Pajerowska-Mukhtar, K., Culler, A. H., and Dong, X. (2007). Salicylic acid inhibits pathogen growth in plants through repression of the auxin signaling pathway. *Curr. Biol.* 17, 1784–1790.
- Wang, F.-Z., Chen, M.-X., Yu, L.-J., Xie, L.-J., Yuan, L.-B., Qi, H., et al. (2017a). OsARM1, an R2R3 MYB transcription factor, is involved in regulation of the response to arsenic stress in rice. *Front. Plant Sci.* 8, 1868.
- Wang, J., Tian, D., Gu, K., Yang, X., Wang, L., Zeng, X., et al. (2017b). Induction of Xa10-like genes in rice cultivar Nipponbare confers disease resistance to rice bacterial blight. *Mol. Plant-Microbe Interact.* 30, 466–477.
- Wang, M., Gao, L., Dong, S., Sun, Y., Shen, Q., and Guo, S. (2017c). Role of silicon on plant–pathogen interactions. *Front. Plant Sci.* 8, 1–14.
- Wang, T., Wei, J. J., Sabatini, D. M., and Lander, E. S. (2014a). Genetic screens in human cells using the CRISPR-Cas9 system. *Science* 343, 80 LP – 84.
- Wang, W., Hu, B., Yuan, D., Liu, Y., Che, R., Hu, Y., et al. (2018). Expression of the nitrate transporter gene *OsNRT1.1A/OsNPF6.3* confers high yield and early maturation in rice. *Plant Cell* 30, 638–651.
- Wang, X., Hou, S., Wu, Q., Lin, M., Acharya, B. R., Wu, D., et al. (2017d). IDL6-HAE/HSL2 impacts pectin degradation and resistance to *Pseudomonas syringae* pv *tomato* DC3000 in *Arabidopsis* leaves. *Plant J.* 89, 250–263.
- Wang, Y., Cheng, X., Shan, Q., Zhang, Y., Liu, J., Gao, C., et al. (2014b). Simultaneous editing of three homoeoalleles in hexaploid bread wheat confers heritable resistance to powdery mildew. *Nat. Biotechnol.* 32, 947–951.
- Warrier, R., Paul, M., and V. Vineetha, M. (2013). Estimation of salicylic acid in eucalyptus leaves using spectrophotometric methods. *Genet. Plant Physiol* 3, 90-97.
- Weber, E., Engler, C., Gruetzner, R., Werner, S., and Marillonnet, S. (2011). A modular cloning system for standardized assembly of multigene constructs. *PLoS One* 6, e16765.
- Weber, E., Ojanen-Reuhs, T., Huguet, E., Hause, G., Romantschuk, M., Korhonen, T. K., et al. (2005). The type III-dependent Hrp pilus is required for productive interaction of *Xanthomonas campestris* pv. *vesicatoria* with pepper host plants. *J. Bacteriol.* 187, 2458 LP – 2468.
- Wege, S., Khan, G. A., Jung, J. Y., Vogiatzaki, E., Pradervand, S., Aller, I., et al. (2016). The EXS domain of PHO1 participates in the response of shoots to phosphate deficiency via a root-to-shoot signal. *Plant Physiol.* 170, 385–400.
- Wen, Z., and Kaiser, B. N. (2018). Unraveling the functional role of NPF6 transporters. *Front. Plant Sci.* 9, 1–8.

- Wengelnik, K., Van Den Ackerveken, G., and Bonas, U. (1996). HrpG, a key *hrp* regulatory protein of *Xanthomonas campestris* pv. *vesicatoria* is homologous to two-component response regulators. *Mol. Plant-Microbe Interact.* 9, 704–712.
- Werner, S., Engler, C., Weber, E., Gruetzner, R., and Marillonnet, S. (2012). Fast track assembly of multigene constructs using Golden Gate cloning and the MoClo system. *Bioengineered* 3, 38–43.
- Weßling, R., Epple, P., Altmann, S., He, Y., Yang, L., Henz, S. R., et al. (2014). Convergent targeting of a common host protein-network by pathogen effectors from three kingdoms of life. *Cell Host Microbe* 16, 364–375.
- White, F. F., and Yang, B. (2009). Host and pathogen factors controlling the rice-*Xanthomonas oryzae* interaction. *Plant Physiol.* 150, 1677–1686.
- Wilkins, K., Booher, N., Wang, L., and Bogdanove, A. (2015). TAL effectors and activation of predicted host targets distinguish Asian from African strains of the rice pathogen *Xanthomonas oryzae* pv. *oryzicola* while strict conservation suggests universal importance of five TAL effectors. *Front. Plant Sci.* 6, 536.
- Wolfe, S. A., Nekludova, L., and Pabo, C. O. (2000). DNA Recognition by Cys2His2 Zinc Finger Proteins. *Annu. Rev. Biophys. Biomol. Struct.* 29, 183–212.
- Wu, D., von Roepenack-Lahaye, E., Buntru, M., de Lange, O., Schandry, N., Pérez-Quintero, A. L., et al. (2019). A plant pathogen type III effector protein subverts translational regulation to boost host polyamine levels. *Cell Host Microbe* 26, 638-649.e5.
- Wu, L., Goh, M. L., Sreekala, C., and Yin, Z. (2008a). XA27 depends on an amino-terminal signal-anchor-like sequence to localize to the apoplast for resistance to *Xanthomonas oryzae* pv *oryzae*. *Plant Physiol.* 148, 1497–509.
- Wu, S., Shan, L., and He, P. (2014). Microbial signature-triggered plant defense responses and early signaling mechanisms. *Plant Sci.* 228, 118–126.
- Wu, W., Wang, M., Wu, W., Singh, S. K., Mussfeldt, T., and Iliakis, G. (2008b). Repair of radiation induced DNA double strand breaks by backup NHEJ is enhanced in G2. *DNA Repair* 7, 329–338.
- Xu, J., Audenaert, K., Hofte, M., and De Vleeschauwer, D. (2013). Abscisic acid promotes susceptibility to the rice leaf blight pathogen *Xanthomonas oryzae* pv *oryzae* by suppressing salicylic acid-mediated defenses. *PLoS One* 8, e67413.
- Xu, J., Zhou, L., Venturi, V., He, Y.-W., Kojima, M., Sakakibari, H., et al. (2015). Phytohormone-mediated interkingdom signaling shapes the outcome of rice-*Xanthomonas oryzae* pv. *oryzae* interactions. *BMC Plant Biol.* 15, 10.
- Xu, R., Yang, Y., Qin, R., Li, H., Qiu, C., Li, L., et al. (2016). Rapid improvement of grain weight via highly efficient CRISPR/Cas9-mediated multiplex genome editing in rice. *J. Genet. Genomics* 43, 529–532.

- Xu, Z., Xu, X., Gong, Q., Li, Z., Li, Y., Wang, S., et al. (2019). Engineering broad-spectrum bacterial blight resistance by simultaneously disrupting variable TALE-binding elements of multiple susceptibility genes in rice. *Mol. Plant* 12, 1434–1446.
- Yadeta, K., and Thomma, B. (2013). The xylem as battleground for plant hosts and vascular wilt pathogens. *Front. Plant Sci.* 4, 97.
- Yamaguchi, K., Yamada, K., Ishikawa, K., Yoshimura, S., Hayashi, N., Uchihashi, K., et al. (2013). A receptor-like cytoplasmic kinase targeted by a plant pathogen effector is directly phosphorylated by the chitin receptor and mediates rice immunity. *Cell Host Microbe* 13, 347–357.
- Yamaji, N., Mitatni, N., and Ma, J. F. (2008). A transporter regulating silicon distribution in rice shoots. *Plant Cell* 20, 1381–9.
- Yan, X., Tao, J., Luo, H.-L., Tan, L.-T., Rong, W., Li, H.-P., et al. (2019). A type III effector XopL Xcc8004 is vital for *Xanthomonas campestris* pathovar *campestris* to regulate plant immunity. *Res. Microbiol.* 170, 138–146.
- Yang, B., Sugio, A., and White, F. F. (2005). Avoidance of host recognition by alterations in the repetitive and C-terminal regions of AvrXa7, a type III effector of *Xanthomonas oryzae* pv. *oryzae*. *Mol. Plant-Microbe Interact.* 18, 142–149.
- Yang, B., Sugio, A., and White, F. F. (2006). Os8N3 is a host disease-susceptibility gene for bacterial blight of rice. *Proc. Natl. Acad. Sci. U. S. A.* 103, 10503–10508.
- Yang, B., and White, F. F. (2004). Diverse members of the AvrBs3/PthA family of type III effectors are major virulence determinants in bacterial blight disease of rice. *Mol. Plant-Microbe Interact.* 17, 1192–1200.
- Yang, B., Zhu, W., Johnson, L. B., and White, F. F. (2000). The virulence factor AvrXa7 of *Xanthomonas oryzae* pv. *oryzae* is a type III secretion pathway-dependent nuclear-localized double-stranded DNA-binding protein. *Proc. Natl. Acad. Sci. U. S. A.* 97, 9807–9812.
- Yang, J., Zhang, Y., Yuan, P., Zhou, Y., Cai, C., Ren, Q., et al. (2014). Complete decoding of TAL effectors for DNA recognition. *Cell Res.* 24, 628–31.
- Yanisch-Perron, C., Vieira, J., and Messing, J. (1985). Improved M13 phage cloning vectors and host strains: nucleotide sequences of the M13mpl8 and pUC19 vectors. *Gene* 33, 103–119.
- Yu, C., Chen, H. M., Tian, F., Bi, Y. M., Steven, R. J., Jan, L. E., et al. (2015). Identification of differentially-expressed genes of rice in overlapping responses to bacterial infection by *Xanthomonas oryzae* pv. *oryzae* and nitrogen deficiency. *J. Integr. Agric.* 14, 888–899.
- Yu, Y., Streubel, J., Balzergue, S., Champion, A., Boch, J., Koebnik, R., et al. (2011). Colonization of rice leaf blades by an African strain of *Xanthomonas oryzae* pv. *oryzae* depends on a new TAL effector that induces the rice nodulin-3 Os11N3 gene. *Mol. Plant-Microbe Interact.* 24, 1102–1113.

- Yuan, M., Ke, Y., Huang, R., Ma, L., Yang, Z., and Chu, Z. (2016). A host basal transcription factor is a key component for infection of rice by TALE-carrying bacteria. *Elife* 5, 1–16.
- Yuan, M., Wang, S., Chu, Z., Li, X., and Xu, C. (2010). The bacterial pathogen *Xanthomonas oryzae* overcomes rice defenses by regulating host copper redistribution. *Plant Cell* 22, 3164–3176.
- Zeilmaker, T., Ludwig, N. R., Elberse, J., Seidl, M. F., Berke, L., Van Doorn, A., et al. (2015). DOWNY MILDEW RESISTANT 6 and DMR6-LIKE OXYGENASE 1 are partially redundant but distinct suppressors of immunity in *Arabidopsis*. *Plant J.* 81, 210–222.
- Zhang, B., Pan, X., Cobb, G. P., and Anderson, T. A. (2006). Plant microRNA: A small regulatory molecule with big impact. *Dev. Biol.* 289, 3–16.
- Zhang, F., Cong, L., Lodato, S., Kosuri, S., Church, G., and Arlotta, P. (2011). Programmable sequence-specific transcriptional regulation of mammalian genome using designer TAL effectors. *Nat. Biotechnol.* 29, 149–153.
- Zhang, J., Yin, Z., and White, F. (2015). TAL effectors and the executor *R* genes. *Front. Plant Sci.* 6, 1–9.
- Zhang, S., Chen, C., Li, L., Meng, L., Singh, J., Jiang, N., et al. (2005). Evolutionary expansion, gene structure, and expression of the rice wall-associated kinase gene family. *Plant Physiol.* 139, 1107–24.
- Zhang, X., Cui, Y., Yu, M., Su, B., Gong, W., Baluška, F., et al. (2019). Phosphorylation-mediated dynamics of nitrate transceptor NRT1.1 regulate auxin flux and nitrate signaling in lateral root growth. *Plant Physiol.* 181, 480 LP – 498.
- Zhang, Y., Liu, L., Guo, S., Song, J., Zhu, C., Yue, Z., et al. (2017a). Deciphering TAL effectors for 5-methylcytosine and 5-hydroxymethylcytosine recognition. *Nat. Commun.* 8, 901.
- Zhang, Y., Zhao, L., Zhao, J., Li, Y., Wang, J., Guo, R., et al. (2017b). S5H/DMR6 encodes a salicylic acid 5-hydroxylase that fine-tunes salicylic acid homeostasis. *Plant Physiol.* 175, 1082–1093.
- Zhao, H., Frank, T., Tan, Y., Zhou, C., Jabnourne, M., Arpat, A. B., et al. (2016). Disruption of *OsSULTR3;3* reduces phytate and phosphorus concentrations and alters the metabolite profile in rice grains. *New Phytol.* 211, 926–939.
- Zheng, D., Xue, B., Shao, Y., Yu, H., Yao, X., and Ruan, L. (2018a). Activation of PhoBR under phosphate-rich conditions reduces the virulence of *Xanthomonas oryzae* pv. *oryzae*. *Mol. Plant Pathol.* 19, 2066–2076.
- Zheng, J., Song, Z., Zheng, D., Hu, H., Yu, H., Liu, H., et al. (2019). Population genomics and pathotypic evaluation of the bacterial leaf blight pathogen of rice. *bioRxiv*, 704221.

- Zheng, Y., Yan, J., Wang, S., Xu, M., Huang, K., Chen, G., et al. (2018b). Genome-wide identification of the *pectate lyase-like (PLL)* gene family and functional analysis of two *PLL* genes in rice. *Mol. Genet. Genomics* 293, 1317–1331.
- Zhou, B., and Zeng, L. (2016). Conventional and unconventional ubiquitination in plant immunity. *Mol. Plant Pathol.* 8, 1313–1330.
- Zhou, J., Peng, Z., Long, J., Sosso, D., Liu, B., Eom, J.-S. S., et al. (2015). Gene targeting by the TAL effector PthXo2 reveals cryptic resistance gene for bacterial blight of rice. *Plant J.* 82, 632–643.
- Zhu, W., Yang, B., Chittoor, J. M., Johnson, L. B., and White, F. F. (1998). AvrXa10 contains an acidic transcriptional activation domain in the functionally conserved C terminus. *Mol. Plant-Microbe Interact.* 11, 824–832.
- Zipfel, C. (2014). Plant pattern-recognition receptors. *Trends Immunol.* 35, 345–351.

Curriculum vitae

Name: Stefanie Mücke
Address: Buddeweg 2
30419 Hannover
Birth: 24.04.1992 in Lutherstadt Eisleben (Germany)

Education

- 03/2016 – 09/2020 **Doctorate at the Leibniz Universität Hannover**
in the department for plant genetics, division plant biotechnology, Prof. Dr. J. Boch
doctoral thesis: „Identification of susceptibility targets of bacterial leaf blight and development of genome edited rice lines with increased resistance“
- 10/2013 – 01/2016 **Master of Science Biologie at the Martin-Luther-Universität Halle/Wittenberg**
master thesis: „Funktionelle Analyse möglicher *cis*-regulatorischer Elemente des Typ-III-Effektorgens *xopB* aus *Xanthomonas*“; Prof. Dr. U. Bonas
- 10/2010 – 09/2013 **Bachelor of Science Biologie at the Martin-Luther-Universität Halle/Wittenberg**
bachelor thesis: „Identifizierung neuer pflanzlicher Interaktoren des Typ-III-Effektorproteins Xopl aus *Xanthomonas campestris* pv. *vesicatoria*“; Prof. Dr. U. Bonas
- 07/2004 – 07/2010 **Higher education entrance qualification at "Gymnasium am Markt" Hettstedt**

Scientific talks

- 07/2018 2nd Annual Conference of the EuroXanth COST CA16107 Halle (Germany)
Talk: „Functional convergence of TALEs addressing susceptibility hubs“
- 12/2017 1st Annual Conference of the EuroXanth COST CA16107 Coimbra (Portugal)
Talk: „*Xanthomonas* redirects host defense metabolism to benefit infection“

List of publications

Mücke, S., Reschke, M., Erkes, A., Schwietzer, C.-A., Becker, S., Streubel, J., et al. (2019). Transcriptional reprogramming of rice cells by *Xanthomonas oryzae* TALEs. *Front. Plant Sci.* 10, 162.

Mücke, S., and Boch, J. (2019). TALEs - 10 Jahre nach Entschlüsselung des Codes. *BIOspektrum* 25, 375–377.

Erkes, A., **Mücke, S.**, Reschke, M., Boch, J., and Grau, J. (2019). PrediTALE: A novel model learned from quantitative data allows for new perspectives on TALE targeting. *PLOS Comput. Biol.* 15, e1007206.

Mücke, S. (2018) Phytopathogen attackiert Phytat und beeinflusst Hormon-Signalwege. *BIOspektrum* 24, 413.